MITOCHONDRIAL DYSFUNCTION IN STROKE

EDITED BY: Feng Yan, Lin Wang, John Zhang, Hailiang Tang and Lei Huang
PUBLISHED IN: Frontiers in Aging Neuroscience

frontiers Research Topics

ISSN 1664-8714
ISBN 978-2-88974-980-5
DOI 10.3389/978-2-88974-980-5

About Frontiers

Frontiers is more than just an open-access publisher of scholarly articles: it is a pioneering approach to the world of academia, radically improving the way scholarly research is managed. The grand vision of Frontiers is a world where all people have an equal opportunity to seek, share and generate knowledge. Frontiers provides immediate and permanent online open access to all its publications, but this alone is not enough to realize our grand goals.

Frontiers Journal Series

The Frontiers Journal Series is a multi-tier and interdisciplinary set of open-access, online journals, promising a paradigm shift from the current review, selection and dissemination processes in academic publishing. All Frontiers journals are driven by researchers for researchers; therefore, they constitute a service to the scholarly community. At the same time, the Frontiers Journal Series operates on a revolutionary invention, the tiered publishing system, initially addressing specific communities of scholars, and gradually climbing up to broader public understanding, thus serving the interests of the lay society, too.

Dedication to Quality

Each Frontiers article is a landmark of the highest quality, thanks to genuinely collaborative interactions between authors and review editors, who include some of the world's best academicians. Research must be certified by peers before entering a stream of knowledge that may eventually reach the public - and shape society; therefore, Frontiers only applies the most rigorous and unbiased reviews.
Frontiers revolutionizes research publishing by freely delivering the most outstanding research, evaluated with no bias from both the academic and social point of view. By applying the most advanced information technologies, Frontiers is catapulting scholarly publishing into a new generation.

What are Frontiers Research Topics?

Frontiers Research Topics are very popular trademarks of the Frontiers Journals Series: they are collections of at least ten articles, all centered on a particular subject. With their unique mix of varied contributions from Original Research to Review Articles, Frontiers Research Topics unify the most influential researchers, the latest key findings and historical advances in a hot research area! Find out more on how to host your own Frontiers Research Topic or contribute to one as an author by contacting the Frontiers Editorial Office: frontiersin.org/about/contact

MITOCHONDRIAL DYSFUNCTION IN STROKE

Topic Editors:
Feng Yan, Zhejiang University, China
Lin Wang, Zhejiang University, China
John Zhang, Loma Linda University, United States
Hailiang Tang, Fudan University, China
Lei Huang, Loma Linda University, United States

Citation: Yan, F., Wang, L., Zhang, J., Tang, H., Huang, L., eds. (2022). Mitochondrial Dysfunction in Stroke. Lausanne: Frontiers Media SA. doi: 10.3389/978-2-88974-980-5

Table of Contents

frontiers in Aging Neuroscience

EDITORIAL
published: 29 March 2022
doi: 10.3389/fnagi.2022.888952

Editorial: Mitochondrial Dysfunction in Stroke

Feng Yan[1†], *Hailiang Tang*[2†], *Lin Wang*[1], *Lei Huang*[3,4*] and *John Zhang*[3,4*]

[1] Second Affiliated Hospital, School of Medicine, Zhejiang University, Hangzhou, China, [2] Department of Neurosurgery, Huashan Hospital, Fudan University, Shanghai, China, [3] Department of Neurosurgery, Loma Linda University, Loma Linda, CA, United States, [4] Department of Physiology and Pharmacology, Loma Linda University, Loma Linda, CA, United States

Keywords: mitochondrial dysfunction, stroke, mitochondrial dynamics, mitophagy and apoptosis, mitochondrial transfer

Editorial on the Research Topic

Editorial: Mitochondrial Dysfunction in Stroke

INTRODUCTION

Stroke is one of the main causes of mortality and remains the second leading cause of death worldwide (Chen et al., 2020). The current therapies of tissue plasminogen activator (tPA) thrombosis and mechanical thrombectomy for ischemic stroke are limited by the narrow therapeutic time window (Zhao et al., 2022). Effective pharmacologic treatments for hemorrhagic stroke are lacking. Emerging evidences demonstrate the importance of mitochondria hemostasis in cell survival and the critical role of mitochondrial dysfunction in the stroke pathogenesis (Kaur and Sharma, 2022). The calcium overload, opening of mitochondrial permeability transition pore (mPTP), and excessive generation of reactive oxygen species (ROS) are mitochondrial pathology contributing to neuronal death after stroke (**Figure 1**). A better understanding of mitochondrial self-regulation mechanisms and its interaction with other intracellular organelles may reveal novel molecular targets of neuroprotection against stroke (Jia et al., 2021).

In this Research Topic of **"mitochondrial dysfunction in stroke,"** we totally collected 11 articles, majority of which are focusing on the pathophysiology and molecular mechanisms of mitochondrial dysfunction after stroke, as well as potential stroke therapeutics from the mitochondrial perspective.

MITOCHONDRIAL DYNAMICS AND MITOCHONDRIAL DYSFUNCTION IN STROKE

Mitochondrial dynamics including fusion, fission, selective degradation, and transport processes are important for immunity, apoptosis, and the cell cycle (An et al., 2021; Carinci et al., 2021; Wu et al., 2021; Yang et al., 2022). Zhou et al. reviewed the molecular mechanisms of mitochondrial dynamics and its role in ischemic stroke. The inhibition of excessive mitochondrial fission and preservation of mitochondrial hemostasis are suggested to be potential strategies of neural repair after ischemic stroke.

Mitophagy is a kind of autophagy by specific wipe out of damaged or dysfunctional mitochondria, in order to prevent excessive generation of ROS and neural cell death (He et al., 2021). Mitochondrial fission and mitophagy are two cellular mechanisms that coordinately control mitochondrial quality. In another review article, Shen et al. discussed the involvement of mitochondria dynamics and mitophagy regulation in the pathophysiology of ischemic stroke and ischemic/reperfusion (I/R) injury in particular. The mitophagy-targeted interventions may be potentially applied as an adjunctive therapeutic to extend neuroprotective time window after ischemic stroke. Lei et al.

OPEN ACCESS

Edited and reviewed by:
Jorge Busciglio,
University of California, Irvine, United States

***Correspondence:**
Lei Huang
lhuang@llu.edu
John Zhang
johnzhang3910@yahoo.com

[†] *These authors have contributed equally to this work*

Specialty section:
This article was submitted to Cellular and Molecular Mechanisms of Brain-aging, a section of the journal Frontiers in Aging Neuroscience

Received: *03 March 2022*
Accepted: *07 March 2022*
Published: *29 March 2022*

Citation:
Yan F, Tang H, Wang L, Huang L and Zhang J (2022) Editorial: Mitochondrial Dysfunction in Stroke. Front. Aging Neurosci. 14:888952. doi: 10.3389/fnagi.2022.888952

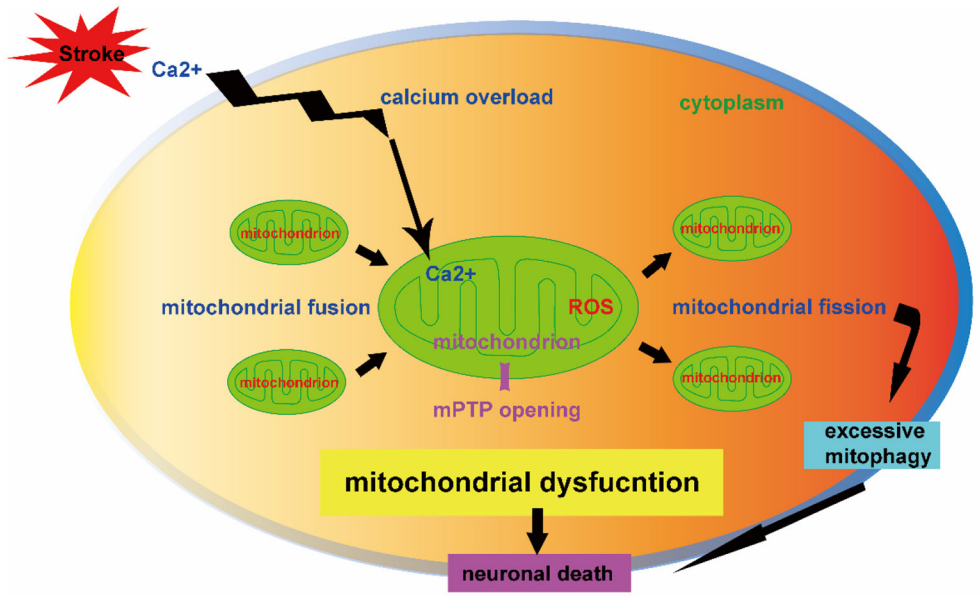

FIGURE 1 | Mitochondrial dysfunction contributing to neuronal death after stroke. The mitochondrial dynamics (fission and fusion) and mitophagy-mediated mitochondrial quality control are key mechanisms in regulation of neuron fate after stroke. The mitochondrial calcium overload, opening of mitochondrial permeability transition pore (mPTP) and over production of reactive oxygen species (ROS) impair mitochondrial dynamics. The effect of mitophagy depends on its injury severity in which overactive mitophagy is detrimental to neuronal survival. The dysregulation of mitochondrial dynamics and excessive mitophagy result in neuronal death.

further reviewed the current research advances of mitophagy regulatory mechanisms after ischemic and hemorrhagic stroke. However, they stressed that the cytoprotective effects of mitophagy modulation in cerebral stroke need further validation by clarifying its possible side effects.

Mitochondrial dynamics can affect energy metabolism and post-stroke neuronal function by regulating the number, morphology, and function of mitochondria. Irisin, a cleaved version of fibronectin domain-containing protein 5 (FNDC5), has been shown to regulate mitochondrial homeostasis. In a mouse model of subarachnoid hemorrhage (SAH), Tu et al. explored the protective effects of irisin and the underlying mechanisms related to mitochondrial biogenesis. The administration of exogenous irisin conserved the mitochondrial morphology and promoted mitochondrial biogenesis, partly through mitochondrial uncoupling protein-2.

Given that early surgical clearance of hematomas does not improve the prognosis in intracerebral hemorrhage (ICH) patients, interventions that attenuate ICH-induced secondary brain injury (SBI) are critical. Chen W et al. summarized the mitochondrial mechanisms in ICH pathology. Abnormal regulation of mitochondrial dynamics that shifts to excessive fission is involved in the pathological process of SBI. Therefore, mitochondrial protection could be a therapeutic target for SBI following ICH.

INTERCELLULAR MITOCHONDRIAL TRANSFER IN STROKE

Damaged cells can produce phosphatidylserine, inducing the tunneling nanotubes (TNTs) formation promoting mitochondrial transfer. Intercellular mitochondrial transfer between different cell types as a potential therapeutic approach has been widely studied (Norat et al., 2020; Gomzikova et al., 2021; Lu et al., 2021). Transient focal cerebral ischemia in mice induced astrocytic mitochondria entry to adjacent neurons that amplified cell survival signals (Hayakawa et al., 2016). Mitochondrial transfer improves functional neuron damage after stroke. Gao et al. evaluated the mitochondria transfer and underlying mechanism involved in the neuron-glia crosstalk in primary cultured mouse cortical neurons subjected to a variety of ischemic related insults. They found that the neuron-derived mitochondria may serve as a "help-me" signal and mediate the neuron-astrocyte crosstalk. Promoting the intercellular mitochondrial transfer by accelerating the neuronal releasing or astrocytic engulfing may serve as a potential therapeutic strategy for the treatment of ischemic stroke in the future.

CONCLUSION

Mitochondrial dynamics and mitophagy are of great importance in the mitochondrial quantity and quality control. This Research Topic discusses the role of mitochondria in the process of neuronal injury and protection in stroke, aiming to provide valuable insights in aspect of mitochondrial-targeted stroke therapy. Mitochondrial hemostasis preservation, and intracellular mitochondrial transport have a key function in the protection of neuronal injury after experimental stroke, which need future clinical validation in stroke patients. Basic science research is warranted regarding exact interaction mechanism of mitophagy and mitochondria

quality control in contribution to pathological or/and protective effect in stroke. The detailed mechanisms of mitochondria release and receptor recognition in donor cells are also needs further investigation in the setting of stroke.

AUTHOR CONTRIBUTIONS

FY and HT wrote the editorial equally. LW draw the picture. LH and JZ revised the editorial. All authors contributed to the article and approved the submitted version.

ACKNOWLEDGMENTS

The guest editors sincerely thank the journal of *Frontiers in Aging Neuroscience* for providing us the chance to organize the Research Topic. We would like to thank all the authors who contribute to the topic collection and all the reviewers who participate in the review process. Finally, we are very grateful to all the editors for assisting us in manuscripts handling.

REFERENCES

An H, Zhou B, Ji X. Mitochondrial quality control in acute ischemic stroke. *J Cereb Blood Flow Metab.* (2021) 41:3157–70. doi: 10.1177/0271678X211046992

Carinci M, Vezzani B, Patergnani S, Ludewig P, Lessmann K, Magnus T, et al. Different roles of mitochondria in cell death and inflammation: focusing on mitochondrial quality control in ischemic stroke and reperfusion. *Biomedicines.* (2021) 9:169. doi: 10.3390/biomedicines9020169

Chen W, Huang J, Hu Y, Khoshnam SE, Sarkaki A. Mitochondrial transfer as a therapeutic strategy against ischemic stroke. *Transl Stroke Res.* (2020) 11:1214–28. doi: 10.1007/s12975-020-00828-7

Gomzikova MO, James V, Rizvanov AA. Mitochondria donation by mesenchymal stem cells: current understanding and mitochondria transplantation strategies. *Front Cell Dev Biol.* (2021) 9:653322. doi: 10.3389/fcell.2021.653322

Hayakawa K, Esposito E, Wang X, Terasaki Y, Liu Y, Xing C, et al. Transfer of mitochondria from astrocytes to neurons after stroke. *Nature.* (2016) 535:551–5. doi: 10.1038/nature18928

He J, Liu J, Huang Y, Tang X, Xiao H, Hu Z. Oxidative stress, inflammation, and autophagy: potential targets of mesenchymal stem cells-based therapies in ischemic stroke. *Front Neurosci.* (2021) 15:641157. doi: 10.3389/fnins.2021.641157

Jia J, Jin H, Nan D, Yu W, Huang Y. New insights into targeting mitochondria in ischemic injury. *Apoptosis.* (2021) 26:163–83. doi: 10.1007/s10495-021-01661-5

Kaur MM, Sharma DS. Mitochondrial repair as potential pharmacological target in cerebral ischemia. *Mitochondrion.* (2022) 63:23–31. doi: 10.1016/j.mito.2022.01.001

Lu M, Guo J, Wu B, Zhou Y, Wu M, Farzaneh M, et al. Mesenchymal stem cell-mediated mitochondrial transfer: a therapeutic approach for ischemic stroke. *Transl Stroke Res.* (2021) 12:212–29. doi: 10.1007/s12975-020-00853-6

Norat P, Soldozy S, Sokolowski JD, Gorick CM, Kumar JS, Chae Y, et al. Mitochondrial dysfunction in neurological disorders: Exploring mitochondrial transplantation. *NPJ Regen Med.* (2020) 5:22. doi: 10.1038/s41536-020-00107-x

Wu M, Gu X, Ma Z. Mitochondrial quality control in cerebral ischemia-reperfusion injury. *Mol Neurobiol.* (2021) 58:5253–71. doi: 10.1007/s12035-021-02494-8

Yang M, He Y, Deng S, Xiao L, Tian M, Xin Y, et al. Mitochondrial quality control: a pathophysiological mechanism and therapeutic target for stroke. *Front Mol Neurosci.* (2022) 14:78 6099. doi: 10.3389/fnmol.2021.786099

Zhao T, Zhu T, Xie L, Li Y, Xie R, Xu F, et al. Neural stem cells therapy for ischemic stroke: progress and challenges. *Transl Stroke Res.* (2022) 2022:1–11. doi: 10.1007/s12975-022-00984-y

Conflict of Interest: The authors declare that the research was conducted in the absence of any commercial or financial relationships that could be construed as a potential conflict of interest.

frontiers in Aging Neuroscience

REVIEW
published: 27 January 2021
doi: 10.3389/fnagi.2020.615451

Mitochondria: Novel Mechanisms and Therapeutic Targets for Secondary Brain Injury After Intracerebral Hemorrhage

Weixiang Chen[1,2,3,4†], *Chao Guo*[1,2,3,4†], *Hua Feng*[1,2,3,4] *and Yujie Chen*[1,2,3,4*]

[1] Department of Neurosurgery, Southwest Hospital, Third Military Medical University (Army Medical University), Chongqing, China, [2] State Key Laboratory of Trauma, Burn and Combined Injury, Third Military Medical University (Army Medical University), Chongqing, China, [3] Chongqing Key Laboratory of Precision Neuromedicine and Neuroregenaration, Third Military Medical University (Army Medical University), Chongqing, China, [4] Collaborative Innovation Center for Brain Science, Third Military Medical University (Army Medical University), Chongqing, China

Intracerebral hemorrhage (ICH) is a destructive form of stroke that often results in death or disability. However, the survivors usually experience sequelae of neurological impairments and psychiatric disorders, which affect their daily functionality and working capacity. The recent MISTIE III and STICH II trials have confirmed that early surgical clearance of hematomas does not improve the prognosis of survivors of ICH, so it is vital to find the intervention target of secondary brain injury (SBI) after ICH. Mitochondrial dysfunction, which may be induced by oxidative stress, neuroinflammation, and autophagy, among others, is considered to be a novel pathological mechanism of ICH. Moreover, mitochondria play an important role in promoting neuronal survival and improving neurological function after a hemorrhagic stroke. This review summarizes the mitochondrial mechanism involved in cell death, reactive oxygen species (ROS) production, inflammatory activation, blood–brain barrier (BBB) disruption, and brain edema underlying ICH. We emphasize the potential of mitochondrial protection as a potential therapeutic target for SBI after stroke and provide valuable insight into clinical strategies.

Keywords: intracerebral hemorrhage, mitochondrial protection, secondary brain injury, mitochondrial membrane potential, stroke

OPEN ACCESS

Edited by:
Feng Yan,
Zhejiang University, China

Reviewed by:
Zhen-Ni Guo,
First Affiliated Hospital of Jilin University, China
Anatol Manaenko,
University Hospital Erlangen, Germany

***Correspondence:**
Yujie Chen
yujiechen6886@foxmail.com
orcid.org/0000-0002-9905-9138

†These authors have contributed equally to this work

Received: *09 October 2020*
Accepted: *28 December 2020*
Published: *27 January 2021*

Citation:
Chen W, Guo C, Feng H and Chen Y (2021) Mitochondria: Novel Mechanisms and Therapeutic Targets for Secondary Brain Injury After Intracerebral Hemorrhage. Front. Aging Neurosci. 12:615451. doi: 10.3389/fnagi.2020.615451

INTRODUCTION

Hemorrhagic stroke, which is less common but far more likely to be fatal, makes up about 13% of stroke cases. Indeed, two-thirds of stroke survivors will experience moderate or severe disability (Balami and Buchan, 2012). The high incidence and mortality of intracerebral hemorrhage (ICH) are due to both primary brain injury (mainly caused by a mass effect) and secondary brain injury (SBI; mainly caused by hemoglobin degradation products), including neuronal death, oxidative stress injury, and cerebral edema (Wang et al., 2002; Cordonnier et al., 2018). Recently, the MISTIE III and STICH II trials confirmed that early surgical clearance of hematomas does not improve the prognosis of patients with ICH (Mendelow et al., 2013; Hanley et al., 2019), and the lack of evidence-based surgical treatment strategies has prompted researchers to seek effective intervention targets and therapies for secondary injuries after ICH.

The prevalence of ICH is ∼120 per 100,000; 58% of patients die within 1 year, with two-thirds of the survivors being moderately or severely disabled (Balami and Buchan, 2012; Kumar et al., 2016). Furthermore, the 30-days mortality rate is ∼30–55% (Feigin et al., 2015). ICH is associated with high morbidity and mortality from severe SBI, including white matter damage, neuronal death (apoptosis and necrosis), and inflammatory changes (Bobinger et al., 2018).

As the powerhouse of cells, mitochondria play a crucial role in cell energy homeostasis; thus, they are inevitably associated with the pathophysiology of ICH (Georgieva et al., 2017; Chen et al., 2020b). Mitochondrial injury in patients with ICH was first reported in 2006, suggesting that the damage is not caused by hypoxia and ischemia but rather by mitochondrial dysfunction (Kim-Han et al., 2006). Based on the knowledge gained by the greater attention paid to the development of methods for mitochondrial research, it is currently believed that the function of mitochondria involves both supplying energy for the cell and regulating cell death and inflammation (Dawson and Dawson, 2017; Gong et al., 2018). Metformin, a mitochondrion-related treatment drug, has been shown to reduce apoptosis, inflammation, oxidative stress, DNA damage, and mitochondrial damage after cerebral hemorrhage (Wang et al., 2018). Additionally, mitoquinone (MitoQ), a mitochondrial reactive oxygen-scavenging agent, improves mitochondrial function and motor function after ICH, reduces the hematoma volume, and alleviates cerebral edema (Chen et al., 2020a,b).

In this review, we discuss the latest perspectives on the role of mitochondria in cell death and survival and highlight the pathogenesis and treatment of mitochondrion-associated ICH.

PATHOPHYSIOLOGY OF ICH

Intracerebral hemorrhage is a subtype of stroke that is associated with high rates of mortality and disability (Feigin et al., 2015). There are two million cases of ICH worldwide each year, and those who survive often have severe neurological deficits (Kumar et al., 2016). At present, the mainstream view is that nerve injury after ICH can be divided into primary brain injury and SBI (**Figure 1**; Aronowski and Zhao, 2011). The former is mainly caused by mechanical disruption after initial bleeding, whereas the latter is caused by a series of mechanisms including oxidative stress, inflammation, mitochondrial dysfunction, and neuronal death (including apoptosis and necrosis; Yu et al., 2019).

Although most researchers believe that these mechanisms are related to SBI after ICH, effective interventions are still lacking (Cordonnier et al., 2018). Therefore, it is important to explore ways of promoting the recovery of nerve function by reducing secondary injury in the treatment of ICH.

STRUCTURE AND FUNCTION OF MITOCHONDRIA

Mitochondria are ovoid or rod-shaped organelles with double-membrane structures comprising four distinct compartments: the outer membrane, the intermembrane space, the inner membrane, and the matrix (**Figure 2**; Giacomello et al., 2020). These organelles perform a variety of key functions in different cellular processes (Cunnane et al., 2020). The human nervous system consumes a great amount of energy, and by providing ATP through oxidative phosphorylation, mitochondria are the main source of energy for normal neuronal homeostasis and function (Area-Gomez et al., 2019).

Indeed, mitochondria are pivotal regulators of cell survival, and their crucial role in cell survival is mainly reflected in three aspects (Bock and Tait, 2020). Mitochondria are the hubs of cellular calcium signaling, and they provide an important mechanism for regulating calcium concentration during signal transduction, which is particularly important for excitable cells, such as neurons (Giorgi et al., 2018). The enzyme complexes located in the mitochondrial inner membrane are essential for maintaining cellular energy requirements and metabolic homeostasis (Fricker et al., 2018). The survival of neuronal cells depends largely on the integrity and function of mitochondria. Therefore, mitochondrial defects have severe destructive effects on the central nervous system (CNS; Zsurka and Kunz, 2015).

MITOCHONDRIAL QUALITY CONTROL SYSTEMS AND ICH

Mitochondria control almost every aspect of cellular function, including managing REDOX status, modulating Ca^{2+} homeostasis, generating ATP, and regulating responses to cellular and environmental stresses (Liu et al., 2018). The function of mitochondria is also important for the health of neurons, and the activities of axons and dendritic neuron fibers are highly dependent on mitochondria, which are highly dynamic and exhibit an activity-induced interval distribution (Eisner et al., 2018; Bock and Tait, 2020). For example, mitochondrial transport to the remote synapse provides sufficient energy for local synaptic activity in the maintenance of ion channels, transporters, and synaptic transmission (Licznerski et al., 2020).

Moreover, abundant evidence supports the importance of maintaining normal clearance of damaged mitochondria for neuron survival after ICH (Huang and Jiang, 2019; Li et al., 2020). Mitochondrial dysfunction in SBI after ICH has been well-described, and mitochondrial quality and transport have a key function in the protection of neuronal injury. In fact, maintaining mitochondrial integrity and removing damaged mitochondria are important ways to prevent extensive mitochondrial dysfunction, oxidative stress, and cell death caused by hemorrhagic injury (Huang and Jiang, 2019). Therefore, mitochondrial dynamics and mitophagy are vital for maintaining cellular homeostasis and function after ICH. Here, we systematically review the critical roles of mitochondrial integrity and function in neuronal survival after ICH.

Mitochondrial ROS and ICH

Reactive oxygen species (ROS) are the causes of SBI after ICH (Duan et al., 2016; Qu et al., 2016). Excessive accumulation of ROS can lead to macromolecular damage, cellular signal

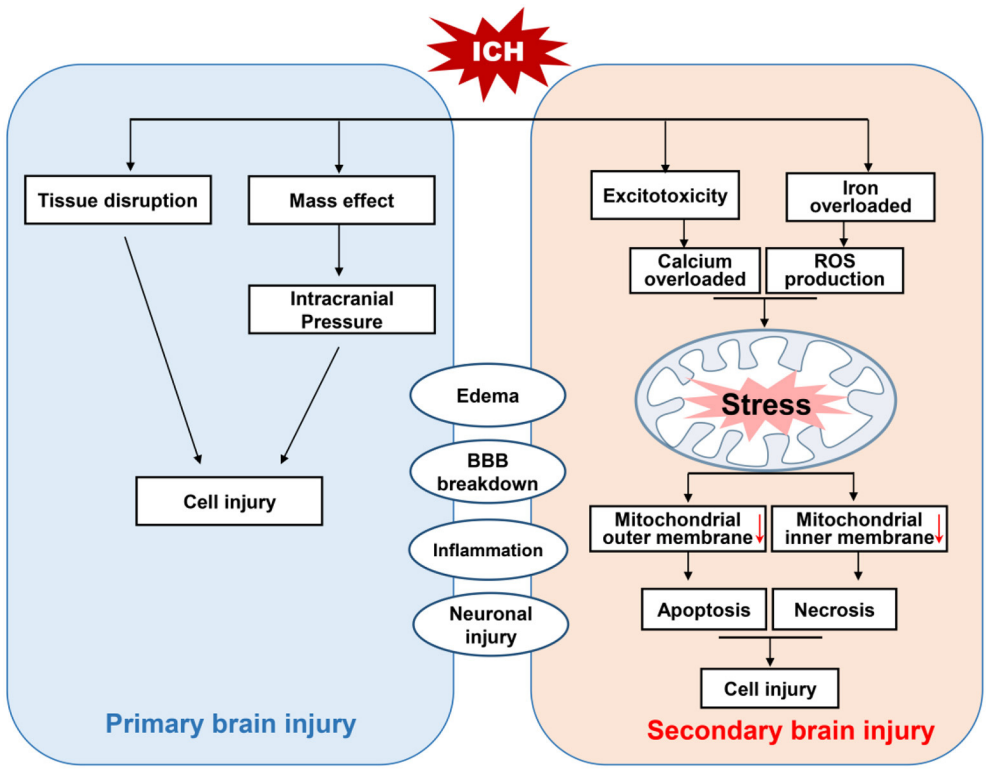

FIGURE 1 | Schematic diagram of brain injury after intracerebral hemorrhage (ICH). Brain injury after ICH can be divided into primary and secondary brain injury (SBI). The primary brain injury is caused by tissue disruption and mass effect after initial bleeding. Whereas, SBI is induced by oxidative stress, the activation of TRP channels and excitotoxicity due to the accumulation of reactive oxygen species (ROS) triggered by iron overload and calcium. This excessive ROS and calcium cause mitochondrial dysfunction, and the activation of apoptotic factors leads to apoptotic and necrotic cell death.

transduction disorder, cell death, and tissue damage (Forrester et al., 2018).

After ICH, hematoma and perihematomal regions are rich with RBC lysis products, especially hemin. In addition, intracellular hemin is degraded into Fe^{2+}. Fenton reaction caused by Fe^{2+} can generate a hydroxyl radical, which is the most reactive of all oxygen radicals, and leads to oxidative stress (Zille et al., 2017; Bertero and Maack, 2018). The initial bleed leads to an influx of glutamate from the bloodstream, and excessive glutamate is one of the most important damaging factors in the nervous system (Cheng et al., 2016). Excessive glutamate in the brain parenchyma can induce Ca^{2+} overload, which leads to membrane depolarization and ROS release (Joshi et al., 2015). Activation of inflammatory cells also contributes to the pathogenesis of brain injury in ICH, and granulocytes can be a source of ROS after ICH. They can cause the release of ROS *via* nicotine adenine dinucleotide phosphate (NADPH) oxidase and myeloperoxidase (Zia et al., 2009).

The blood–brain barrier (BBB) is a dynamic interface between the peripheral circulation and the CNS that prevents toxic substances from the CNS and contributes to the maintenance of brain homeostasis (Tschoe et al., 2020). Disruption of the BBB can cause brain edema, which is also an important secondary injury after ICH (**Figure 3**). Many researchers have demonstrated that mitochondrial membrane potential (MMP)-9 are upregulated after ICH, which is associated with oxidative stress and BBB disruption (Katsu et al., 2010). Inhibition of oxidative stress can decrease MMP-9 levels (Katsu et al., 2010). Therefore, ROS can trigger the activation of MMPs, leading to BBB disruption.

As mitochondria are the main sites of ROS production, mitochondrial accumulation and high oxygen consumption in the CNS render nerve tissue vulnerable to oxidative stress (Mariani et al., 2005; Sidlauskaite et al., 2018; Zheng et al., 2018).

Oligodendrocytes are rich in sphingomyelins, which are prone to injury from oxidative stress, leading to white matter damage (Zhuo et al., 2016). Some non-selective antioxidants, such as edaravone, have been shown to be effective in animal studies but have failed in clinical trials for use in a patient of ICH (Nakamura et al., 2008; Yang et al., 2011, 2015). Recent studies report that selective mitochondrial ROS (mROS) scavengers are superior to non-selective ROS scavengers in the treatment of many REDOX diseases involving mitochondrial dysfunction (Hu et al., 2016; Georgieva et al., 2017; Dey et al., 2018). Our group found that the MitoQ, a mitochondrial reactive oxygen-scavenging agent, can improve mitochondrial function and outcome of mice after ICH (Chen et al., 2020a,b).

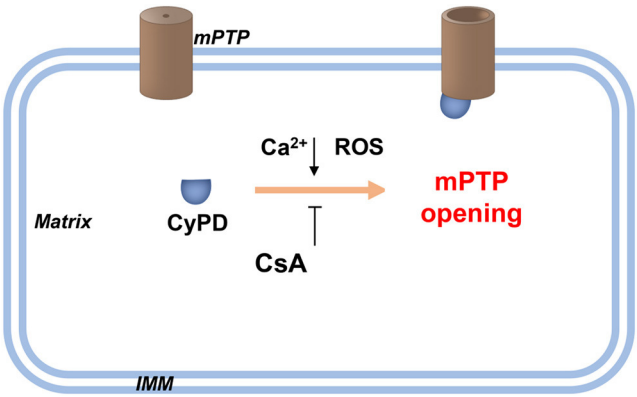

FIGURE 2 | Schematic diagram of the PTP opening hypothesis. As illustrated in the figure above, an increasing level of Ca^{2+} and/or ROS in the mitochondrial matrix promotes the opening of high conductance of the PTP. This process is achieved by combining CyPD with PTP. Therefore, drugs targeting CypD, such as CsA, or genetic interventions for CyPD reduction can be applied without affecting PTP opening. Recently, Ca^{2+}-induced PTP opening *via* small conductance PTP has been reported, and this process inhibits CsA. However, the same protein with different conformations may form pores of increasing size. CsA, cyclosporin A; CyPD, cyclophylin D; IMM, inner mitochondrial membrane; ROS, reactive oxygen species.

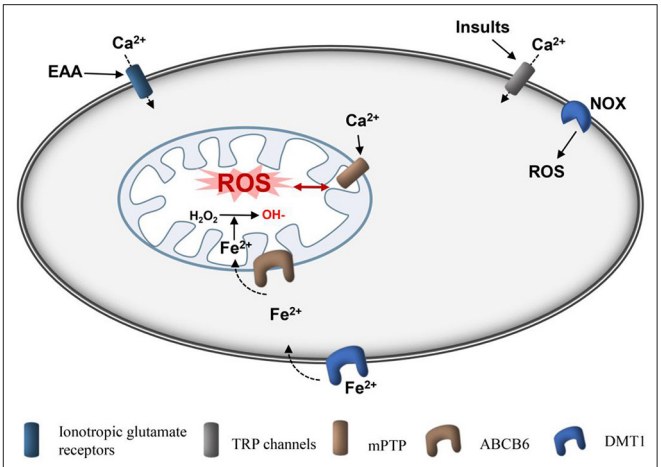

FIGURE 3 | Schematic diagram of production of mitochondrial ROS after ICH. Ionotropic glutamate receptors, such as NMDA receptor and APMA receptor, are activated by glutamate, causing cellular Ca^{2+} overload in cells and mitochondria, respectively. Insults, such as ROS and pressure can induce cellular Ca^{2+} overload directly through TRP channels. Ferrous iron can be transported into cells by DMT1 and then loaded into mitochondria by ABCB6. Ferrous is used to convert H_2O_2 to hydroxyl radicals, which are the active radicals causing severe oxidative damage. mPTPs are activated by Ca^{2+} and ROS to open, and ROS are subsequently released. In addition, NOX can produce ROS. ROS, reactive oxygen species; Fe^{2+}, ferrous iron; AMPA, amino-3-hydroxy-5-methyl-4-isoxazole-propionic acid receptor; NMDA, N-methyl-D-aspartic acid receptor; fer-1, ferrostatin-1; DMT1, divalent metal transporter 1; mPTP, mitochondrial permeability transition pore; NADPH, nicotinamide adenine dinucleotide phosphate; NOX, nicotinamide adenine dinucleotide phosphate oxidase.

Adaptive and non-adaptive responses to REDOX stress may involve mitochondrial channels, such as mitochondrial permeability transition pore (mPTP) and intimal anion channels (IMACs), and activation of these channels leads to an imbalance of REDOX homeostasis in cells and mitochondria, inducing ROS release (Augustynek et al., 2014; Bernardi et al., 2015). The regeneration cycle of the formation and release of mROS is termed as ROS-induced ROS release (Zorov et al., 2014). The mPTP is a multiprotein complex consisting of cyclophilin D (CyPD), mitochondrial peptide proline trans isomerase, voltage-dependent anion channel (VDAC), adenine nucleotide transporter (ANT), and other molecules that form channels in the mitochondrial inner membrane (Li et al., 2014; Bernardi et al., 2015; Chinopoulos, 2018). Regular mPTP opening plays a key physiological role in maintaining a healthy internal mitochondrial environment (Chinopoulos, 2018). At high ROS levels, continuous mPTP opening will trigger ROS release, leading to mitochondrial dysfunction; moreover, the transmission of ROS from damaged mitochondria to neighboring mitochondria results in uncontrollable damage (Zandalinas and Mittler, 2018). In addition, activation of the mPTP, a pore channel in the mitochondrial membrane, may also be a potential mechanism for necrosis and apoptosis (Porter and Beutner, 2018). Overall, mitochondria are the main sites of ROS production and participate in the amplification of ROS (Sies et al., 2017). The increase in mROS that occurs after ICH can be partially reversed by the VDAC inhibitor TRO-19622 or the mROS-specific-scavenging agent Mito-tempo (Ma et al., 2014).

In general, it is vital to explore the protective effect of selective mROS scavengers for treating ICH-induced SBI.

Mitochondria-Related Neuronal Apoptosis Pathway After ICH

Mitochondria are associated with a variety of apoptotic mechanisms. Apoptosis is a process by which early tissue injury around hematoma occurs after ICH (Lu et al., 2015; Bobinger et al., 2018). There are many factors influencing apoptosis after ICH, such as free-radical cascade reactions, inflammation, cytokines, thrombin, and erythrocyte lysis (Salihu et al., 2016). Apoptosis-related genes are involved in neuronal apoptosis after ICH, including BCL-2 associated x protein (Bax), which promotes apoptosis, and Bcl-2, which inhibits apoptosis (Song et al., 2019; Tang et al., 2020). Bcl-2 and Bax are located in the outer mitochondrial membrane, and the Bcl-2/Bax ratio can reflect the tendency of cells to undergo apoptosis or to survive after stimulation: When the Bcl-2 level increases and the Bax decreases, the ratio increases and cells tended to survive (Chen et al., 2015; Luo et al., 2020). The Bcl-2/Bax ratio in cerebral tissue decreases after ICH, which can be inhibited by melatonin (Wang et al., 2018).

Mitochondria directly participate in the pre-apoptotic signaling pathway by releasing cytochrome C (CytoC) and apoptosis induction factor (AIF), which play a central role in the survival or death of neurons (Sabirzhanov et al., 2016). The latter induces apoptosis by activating caspases, whereas AIF is not related to caspase-mediated apoptosis (Hangen et al., 2010). Changes in mitochondrial outer membrane permeability

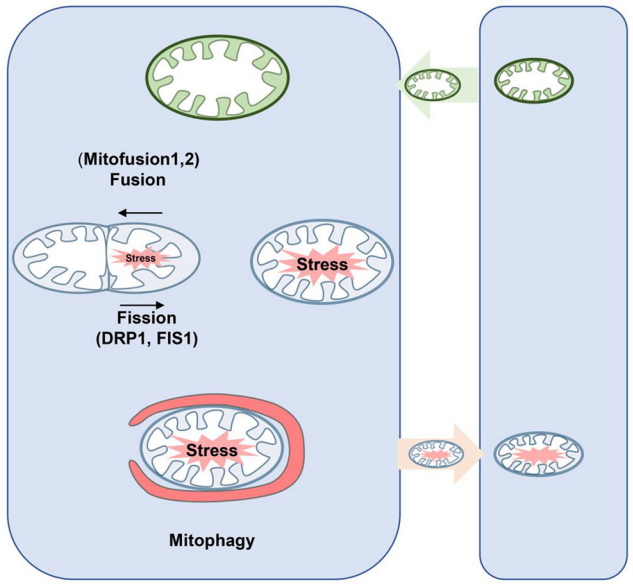

FIGURE 4 | Schematic diagram of mitochondrial dynamics and mitophagy. Fusion is regulated by Mfn1/2 and Opa1, which mediate fusion of the outer and inner mitochondrial membrane, respectively. In the process of fission, Drp1 is recruited from the cytoplasm to the outer membrane of mitochondria and interacts with its receptor protein and Fis1 to form the fission complex in the outer membrane. Thus, damaged mitochondria can be repaired through fusion with healthy mitochondria; mitochondrial fission allows damaged mitochondria to be separated and eliminated by mitophagy. Neurons may secrete mitochondria, and these mitochondria may be unhealthy but may accept healthy mitochondria at the same time to maintain normal neuronal function. Drp, dynamin-related proteins; Mfn1/2, mitofusins; Opa1, optic atrophy 1.

lead to mitochondrial metabolic failure and the release of caspase-activating molecules as well as caspase-dependent death effectors, inducing mitochondrial swelling and neuron death (Augustynek et al., 2014). Previous studies have reported reduced mitochondrial respiratory function and CytoC release around the hematoma after ICH, suggesting that mitochondrial dysfunction is associated with brain injury (Lu et al., 2015; Ding et al., 2017). Moreover, based on double-labeled immunofluorescence, CytoC mainly colocalizes with CNPase, suggesting that the apoptosis of oligodendrocytes after intracapsular hemorrhage may be mediated by the mitochondrial pathway (Zhuo et al., 2016). CytoC levels reflect whether apoptosis in oligodendrocytes induced by ICH is mediated by the mitochondrial pathway (You et al., 2016). Recent studies have found that the expression of CytoC is upregulated in rats with ICH, which is consistent with the apoptosis trend of oligodendrocytes (Lu et al., 2015). Cell death after ICH can be induced by brain edema, inflammatory reaction, and BBB disruption, which are the results of secondary injury.

Mitochondrial Dynamics and ICH

Abnormal regulation of mitochondrial dynamics, which shifts the balance of fusion and fission to fission, is involved in the pathological process of hemorrhagic SBI (Wu et al., 2020a). Mitochondria are highly dynamic organelles that constantly undergo fission and fusion to maintain normal morphology and function (Fenton et al., 2020), as characterized by highly coordinated fission (the separation of a single mitochondria into two or more daughter organelles), fusion (an opposing reaction), and transport to a specific location in the cell (Giacomello et al., 2020) (**Figure 4**). These dynamic processes are accompanied by changes in mitochondrion size and shape (Pekkurnaz et al., 2014).

Under physiological conditions, mitochondrial fission is crucial for removing damaged mitochondria to maintain mitochondrial stability (Weir et al., 2017). However, excessive fission damages mitochondrial structure, leading to impaired respiratory function, increased mROS production, ATP deficiency, and apoptotic pathway activation (Nakamura and Lipton, 2011; Zhou et al., 2019; Rong et al., 2020).

In turn, mitochondrial division is mainly regulated by dynamic protein-related protein 1 (Drp1), a membrane protein, which is recruited into the mitochondrial outer membrane and triggers mitochondrial division (Montessuit et al., 2010). Phosphorylation is a key step in regulating Drp1 recruitment under different conditions (Kashatus et al., 2011). Phosphorylation at Ser616 (S616) is generally believed to accelerate its recruitment to the mitochondrial membrane, whereas phosphorylation at S637 inhibits this process (Xu et al., 2016; Ma et al., 2020). Mitochondrial quality control mediated by Drp1 and mfn1/2 has been shown to play a crucial role in preventing ICH injury, such as neural apoptosis, brain edema, and inflammatory response (Wu et al., 2020a,b).

Previous studies have shown that the Drp1 inhibitor mdivi-1 can attenuate oxidative stress and neuronal apoptosis after subarachnoid hemorrhage (Fan et al., 2017). Furthermore, recent studies have shown that Drp1 inhibitors exert neuroprotective effects in the ICH models (Wu et al., 2020a,b), suggesting that excessive Drp1 activity may be an important risk factor for ICH-induced brain injury. In fact, mitochondrial injury induced by acrolein around the hematoma after ICH is associated with increased Drp1 translocation and excessive mitochondrial fission, and acrolein-scavenging agents can significantly inhibit Drp1-mediated nuclear fission after ICH and reduce mitochondrial morphological damage (Wu et al., 2020a). Most importantly, inhibition of mitochondrial fission significantly alleviates neuronal apoptosis, cerebral edema, and neurological deficits after ICH (Wu et al., 2020c).

Mitophagy and Its Role in ICH

Mitophagy was first described by Lemasters (2005), who determined that mitophagy is an autophagic response that is responsible for the specific removal of damaged mitochondria to maintain mitochondrial homeostasis and is an important mechanism for maintaining mitochondrial health (Lemasters, 2014) (**Figure 4**). Recently, it has been found that the inhibition of mitophagy is beneficial in the pathogenesis of various neurological diseases, such as subarachnoid hemorrhage (Li et al., 2014; Zhang et al., 2019). Mechanically, PINK1/Parkin-mediated fission is the most characteristic mitophagy pathway (Geisler et al., 2010). Moreover, other E3 ubiquitin-protein ligases,

TABLE 1 | Registered drugs targeting mitochondrial dysfunction on ClinicalTrials.gov.

Condition/Disease	Status	Phase	Treatment	Trial number
Parkinson's disease	Completed	2	Mitoquinone	NCT00329056
Stroke	Completed	2	Cyclosporin A	NCT01527240
Glucose metabolism disorders	Active, not recruiting	Not applicable	NMN	NCT03151239
Progressive supranuclear palsy Neurological disorders	Completed	2 and 3	CoQ_{10}	NCT00532571
Sleep disorder Traumatic brain injury	Withdrawn	2	Tesamorelin	NCT02931474
Mild cognitive impairment	Recruiting	1	Niagen®	NCT03482167
Friedreich's ataxia	Completed	3	Idebenone	NCT01303406
Brain tumor treated with cranial or cranial-spinal radiation	Completed	3	Metformin	NCT02040376
Cerebral infarction	Completed	4	Edaravone	NCT00200356

such as SMURF1, SIAH1, MUL1, Gp78, ARIH1, and HUWE1, are involved in the regulation of PINK1-Parkin independent mitophagy (Li et al., 2014).

In various pathological environments, "alternative" activation pathways of mitophagy are also involved in mitophagy (Ma et al., 2019). As an example, it has been demonstrated that FUNDC1, an OMM protein, is able to activate mitophagy. Indeed, FUNDC1 can directly recruit LC3 through its LIR domain [36]. Bcl-2-like 13 (BCL2 L13), another OMM protein and a homolog of Atg32, is a mitochondrial autophagy receptor in yeast that can also directly bind to LC3 and promote mitochondrial autophagy through its LIR motif (Jing et al., 2012). Recently, it has been found that mitophagy is involved in the pathogenesis of various neurological diseases, such as subarachnoid hemorrhage (Li et al., 2014; Zhang et al., 2019).

In general, it appears that the effect of mitophagy depends on its severity. Under physiological conditions, mitophagy prevents accelerated cellular senescence and programmed cell death (Kang, 2020; Zhou and Tan, 2020). However, excessive mitophagy plays a lethal role when overactivated by severe pathological stress like ischemia (Huang et al., 2020). NIX primarily regulates the basal level of mitophagy in physiological conditions, whereas BNIP3 exclusively activates excessive mitophagy, leading to cell death (Shi et al., 2014), although the role of mitophagy in ICH has not been fully appreciated to date. Further research is needed to understand whether mitophagy is beneficial after ICH.

Mitochondrial Membrane Potential

In cells, the MMP is typically maintained between 80 and 140 mV (Cloonan et al., 2016) and is regulated by mPTP. Although the structure and composition of mPTP remain controversial, CyPD has long been recognized as a pivotal regulator of the pore openness (Baines and Gutierrez-Aguilar, 2018; Porter and Beutner, 2018). The activity of CyPD is mainly regulated by post-translational modifications, including acetylation, S-glutathione, glycosylation, and S-nitrification (Hafner et al., 2010).

The mitochondrial injury induced by ICH is the result of mPTP opening, whereby various proteins, such as CytoC, are released into the cytoplasm, constituting important events that lead to apoptosis (Tomasello et al., 2009; Bock and Tait, 2020). Melatonin inhibits mPTP opening by upregulating antioxidants to reduce mitochondrial dysfunction therefore inhibiting SBI after ICH (Wang et al., 2018). It has been shown that melatonin treatment significantly inhibits apoptosis and mitochondrial damage, findings verified *in vivo* and *in vitro*, and some researchers have found that melatonin can significantly inhibit apoptosis and mitochondrial damage *in vivo* and *in vitro* (Wang et al., 2018). Our group found that selective mROS antioxidants MitoQ, but not the non-selective antioxidants, almost completely attenuated the iron-induced membrane potential decrease and cell death (Chen et al., 2020b). Additionally, Honokiol (HKL, a pharmacological agonist of sirt3) protects against hyperglycemic ICH-induced neuronal injury *via* the inhibition of mitochondrial depolarization (Zheng et al., 2018).

In addition, Miro1 is a glutamate receptor-dependent calcium sensor that targets the mitochondria of neurons, connecting mitochondria with motor proteins (Macaskill et al., 2009). The Miro1 protein is rapidly ubiquitinated and exhausted in damaged mitochondria to block microtubule-dependent transport of damaged mitochondria, thus promoting mitophagy in mitochondria with decreased membrane potential (Hsieh et al., 2019). Chen et al. reported that the upregulation of Miro1 significantly alleviated pathological symptoms on SBI *in vivo* and *in vitro* (Li et al., 2020). Miro1 may also be involved in a key mechanism for mitochondrial quality control after ICH.

Mitochondrial Transfer

Hayakawa et al. (2016) demonstrated for the first time in 2016 that astrocytes can transfer functional mitochondria to neighboring neurons and promote the survival of receptor neurons (**Figure 4**). These transferred mitochondria are involved in many important functions that benefit the recipient cells. In addition, these groups suggested that mitochondrial transfer improves functional neuron damage after stroke (Hayakawa et al., 2016).

Astrocytic release of extracellular mitochondria particles was mediated by a calcium-dependent mechanism involving CD38/cyclic ADP ribose signaling. Transient focal cerebral ischemia in mice induced astrocytic mitochondria entry to adjacent neurons that amplified cell survival signals (Hayakawa et al., 2016). In addition, damaged cells can produce phosphatidylserine, inducing the tunneling nanotubes (TNTs) formation promoting mitochondrial transfer (Liu et al., 2014). Similarly, TNT mitochondrial transfer from mesenchymal

stem cells to cardiomyocytes improved survival and reduced cellular damage in an *in vitro* ischemia/reperfusion model (Han et al., 2016).

Studies have shown that the main function of transferred mitochondria is to enhance the capacity of recipient cells to metabolize energy (Picca et al., 2019). It has also been reported that mitochondria-derived humanin (HN), a cross-cellular signaling molecule, promotes neuron recovery after ICH: Mitochondrial transfer and the microglia phenotype regulate the function of "reparative" microglia after astrocytes are secreted as peptides or transferred among mitochondria (Chou et al., 2017). Additionally, neurons may secrete mitochondria, but these mitochondria may be unhealthy and may be considered cellular waste (Chou et al., 2017).

PERSPECTIVES AND CONCLUSIONS

Mitochondrial dysfunction is an early initiating event in the pathophysiology of ICH. Bioenergy genetic defects, structural abnormalities and mitochondrial morphology, and aberrant mitochondrial dynamics play an important role in the activation of neuronal death signaling pathways. In preclinical studies, interventions aimed at mitochondrial quality control and mitochondrial dynamics have been shown to have neuroprotective effects (Chimeh et al., 2018).

Recent evidence of mitochondrial transfer has provided a new perspective for intercellular communication. The latest research suggests that mitochondria themselves can act as "help me" signals to respond to different extracellular stimuli and recruit adjacent cells to rescue those injured in stroke and those affected by aging, and disease (Heyck et al., 2019; Gollihue and Norris, 2020). Clearance of damaged mitochondria and replacement with healthy organelles is another promising treatment for CNS diseases, where mitochondria are abundant in distal axonal synapses and dendrites (He et al., 2020). The detailed mechanisms of mitochondrial release and receptor recognition in donor cells, the generalizability of beneficial results, and the ethical implications associated with the artificial transfer of mitochondria remain to be further studied.

Here, **Table 1** lists the potential translational and clinical strategies targeting mitochondria in CNS disease. We have listed mitochondrial protectants that were used to protect neuronal injury from diseases occurring due to damage in the nervous system. Some of them, such as edaravone, are effective to improve prognosis in the studies of ischemic stroke (Shinohara et al., 2009). However, Cyclosporine was generally not effective in reducing infarct size after stroke (Nighoghossian et al., 2015). Regrettably, these drugs have not yet been tested in ICH.

The clinical trials using mitochondrial protectants or antioxidants have not been successful or fulfilled yet. ROS and mitochondrial damage are produced rapidly and have a cascade amplification effect (Qu et al., 2016). This time window of administration may be a problem for patients. In future clinical research, researchers should pay attention to the time window of antioxidant drugs to improve the therapeutic effect of ICH. In addition, a more comprehensive study of the mechanism of mitochondrial damage can also provide a more perfect strategy for the treatment of ICH.

AUTHOR CONTRIBUTIONS

WC, CG, and YC drafted the manuscript and figures. HF and YC proofread and revised the manuscript. YC gave the final proof for this submission. All authors contributed to the article and approved the submitted version.

FUNDING

This work was supported by the National Natural Science Foundation of China (82001263 to WC), State Key Laboratory of Trauma, Burn and Combined Injury (SKLYQ202002 to YC), Southwest Hospital (SWH2018BJKJ-05 to YC), and Chongqing Talent Program (4139Z2391 to HF). The funders are not involved in the commissioning, conception, planning, design, conduct, or analysis of the work, the preparation or editing of the manuscript, or the decision to publish.

REFERENCES

Area-Gomez, E., Guardia-Laguarta, C., Schon, E. A., and Przedborski, S. (2019). Mitochondria, OxPhos, and neurodegeneration: cells are not just running out of gas. *J. Clin. Invest.* 129, 34–45. doi: 10.1172/JCI120848

Aronowski, J., and Zhao, X. (2011). Molecular pathophysiology of cerebral hemorrhage: secondary brain injury. *Stroke* 42, 1781–1786. doi: 10.1161/STROKEAHA.110.596718

Augustynek, B., Kudin, A. P., Bednarczyk, P., Szewczyk, A., and Kunz, W. S. (2014). Hemin inhibits the large conductance potassium channel in brain mitochondria: a putative novel mechanism of neurodegeneration. *Exp. Neurol.* 257, 70–75. doi: 10.1016/j.expneurol.2014.04.022

Baines, C. P., and Gutierrez-Aguilar, M. (2018). The still uncertain identity of the channel-forming unit(s) of the mitochondrial permeability transition pore. *Cell Calcium* 73, 121–130. doi: 10.1016/j.ceca.2018.05.003

Balami, J. S., and Buchan, A. M. (2012). Complications of intracerebral haemorrhage. *Lancet Neurol.* 11, 101–118. doi: 10.1016/S1474-4422(11)70264-2

Bernardi, P., Rasola, A., Forte, M., and Lippe, G. (2015). The mitochondrial permeability transition pore: channel formation by F-ATP synthase, integration in signal transduction, and role in pathophysiology. *Physiol. Rev.* 95, 1111–1155. doi: 10.1152/physrev.00001.2015

Bertero, E., and Maack, C. (2018). Calcium signaling and reactive oxygen species in mitochondria. *Circ. Res.* 122, 1460–1478. doi: 10.1161/CIRCRESAHA.118.310082

Bobinger, T., Burkardt, P., Huttner, B. H., and Manaenko, A. (2018). Programmed cell death after intracerebral hemorrhage. *Curr. Neuropharmacol.* 16, 1267–1281. doi: 10.2174/1570159X15666170602112851

Bock, F. J., and Tait, S. W.G. (2020). Mitochondria as multifaceted regulators of cell death. *Nat. Rev. Mol. Cell Biol.* 21, 85–100. doi: 10.1038/s41580-019-0173-8

Chen, H. C., Kanai, M., Inoue-Yamauchi, A., Tu, H. C., Huang, Y., Ren, D., et al. (2015). An interconnected hierarchical model of cell death regulation by the BCL-2 family. *Nat. Cell Biol.* 17, 1270–1281. doi: 10.1038/ncb3236

Chen, W., Guo, C., Huang, S., Jia, Z., Wang, J., Zhong, J., et al. (2020a). MitoQ attenuates brain damage by polarizing microglia towards the M2 phenotype

through inhibition of the NLRP3 inflammasome after ICH. *Pharmacol. Res.* 161:105122. doi: 10.1016/j.phrs.2020.105122

Chen, W., Guo, C., Jia, Z., Wang, J., Xia, M., Li, C., et al. (2020b). Inhibition of mitochondrial ROS by MitoQ alleviates white matter injury and improves outcomes after intracerebral haemorrhage in mice. *Oxid. Med. Cell Longev.* 2020:8285065. doi: 10.1155/2020/8285065

Cheng, A., Yang, Y., Zhou, Y., Maharana, C., Lu, D., Peng, W., et al. (2016). Mitochondrial SIRT3 mediates adaptive responses of neurons to exercise and metabolic and excitatory challenges. *Cell Metab.* 23, 128–142. doi: 10.1016/j.cmet.2015.10.013

Chimeh, U., Zimmerman, M. A., Gilyazova, N., and Li, P. A. (2018). B355252, a novel small molecule, confers neuroprotection against cobalt chloride toxicity in mouse hippocampal cells through altering mitochondrial dynamics and limiting autophagy induction. *Int. J. Med. Sci.* 15, 1384–1396. doi: 10.7150/ijms.24702

Chinopoulos, C. (2018). Mitochondrial permeability transition pore: back to the drawing board. *Neurochem. Int.* 117, 49–54. doi: 10.1016/j.neuint.2017.06.010

Chou, S. H., Lan, J., Esposito, E., Ning, M., Balaj, L., Ji, X., et al. (2017). Extracellular mitochondria in cerebrospinal fluid and neurological recovery after subarachnoid hemorrhage. *Stroke* 48, 2231–2237. doi: 10.1161/STROKEAHA.117.017758

Cloonan, S. M., Glass, K., Laucho-Contreras, M. E., Bhashyam, A. R., Cervo, M., Pabon, M. A., et al. (2016). Mitochondrial iron chelation ameliorates cigarette smoke-induced bronchitis and emphysema in mice. *Nat. Med.* 22, 163–174. doi: 10.1038/nm.4021

Cordonnier, C., Demchuk, A., Ziai, W., and Anderson, C. S. (2018). Intracerebral haemorrhage: current approaches to acute management. *Lancet* 392, 1257–1268. doi: 10.1016/S0140-6736(18)31878-6

Cunnane, S. C., Trushina, E., Morland, C., Prigione, A., Casadesus, G., Andrews, Z. B., et al. (2020). Brain energy rescue: an emerging therapeutic concept for neurodegenerative disorders of ageing. *Nat. Rev. Drug Discov.* 19, 609–633. doi: 10.1038/s41573-020-0072-x

Dawson, T. M., and Dawson, V. L. (2017). Mitochondrial mechanisms of neuronal cell death: potential therapeutics. *Annu. Rev. Pharmacol. Toxicol.* 57, 437–454. doi: 10.1146/annurev-pharmtox-010716-105001

Dey, S., Demazumder, D., Sidor, A., Foster, D. B., and O'rourke, B. (2018). Mitochondrial ROS drive sudden cardiac death and chronic proteome remodeling in heart failure. *Circ. Res.* 123, 356–371. doi: 10.1161/CIRCRESAHA.118.312708

Ding, W., Chen, R., Wu, C., Chen, W., Zhang, H., Fan, X., et al. (2017). Increased expression of HERPUD1 involves in neuronal apoptosis after intracerebral hemorrhage. *Brain Res. Bull.* 128, 40–47. doi: 10.1016/j.brainresbull.2016.11.006

Duan, X., Wen, Z., Shen, H., Shen, M., and Chen, G. (2016). Intracerebral hemorrhage, oxidative stress, and antioxidant therapy. *Oxid. Med. Cell Longev.* 2016:1203285. doi: 10.1155/2016/1203285

Eisner, V., Picard, M., and Hajnoczky, G. (2018). Mitochondrial dynamics in adaptive and maladaptive cellular stress responses. *Nat. Cell Biol.* 20, 755–765. doi: 10.1038/s41556-018-0133-0

Fan, L. F., He, P. Y., Peng, Y. C., Du, Q. H., Ma, Y. J., Jin, J. X., et al. (2017). Mdivi-1 ameliorates early brain injury after subarachnoid hemorrhage via the suppression of inflammation-related blood-brain barrier disruption and endoplasmic reticulum stress-based apoptosis. *Free Radic. Biol. Med.* 112, 336–349. doi: 10.1016/j.freeradbiomed.2017.08.003

Feigin, V. L., Krishnamurthi, R. V., Parmar, P., Norrving, B., Mensah, G. A., Bennett, D. A., et al. (2015). Update on the global burden of ischemic and hemorrhagic stroke in 1990–2013: the GBD 2013 study. *Neuroepidemiology* 45, 161–176. doi: 10.1159/000441085

Fenton, A. R., Jongens, T. A., and Holzbaur, E. L.F. (2020). Mitochondrial dynamics: shaping and remodeling an organelle network. *Curr. Opin. Cell Biol.* 68, 28–36. doi: 10.1016/j.ceb.2020.08.014

Forrester, S. J., Kikuchi, D. S., Hernandes, M. S., Xu, Q., and Griendling, K. K. (2018). Reactive oxygen species in metabolic and inflammatory signaling. *Circ. Res.* 122, 877–902. doi: 10.1161/CIRCRESAHA.117.311401

Fricker, M., Tolkovsky, A. M., Borutaite, V., Coleman, M., and Brown, G. C. (2018). Neuronal cell death. *Physiol. Rev.* 98, 813–880. doi: 10.1152/physrev.00011.2017

Geisler, S., Holmstrom, K. M., Skujat, D., Fiesel, F. C., Rothfuss, O. C., Kahle, P. J., et al. (2010). PINK1/Parkin-mediated mitophagy is dependent on VDAC1 and p62/SQSTM1. *Nat. Cell Biol.* 12, 119–131. doi: 10.1038/ncb2012

Georgieva, E., Ivanova, D., Zhelev, Z., Bakalova, R., Gulubova, M., and Aoki, I. (2017). Mitochondrial dysfunction and redox imbalance as a diagnostic marker of "free radical diseases". *Anticancer Res.* 37, 5373–5381. doi: 10.21873/anticanres.11963

Giacomello, M., Pyakurel, A., Glytsou, C., and Scorrano, L. (2020). The cell biology of mitochondrial membrane dynamics. *Nat. Rev. Mol. Cell Biol.* 21, 204–224. doi: 10.1038/s41580-020-0210-7

Giorgi, C., Marchi, S., and Pinton, P. (2018). The machineries, regulation and cellular functions of mitochondrial calcium. *Nat. Rev. Mol. Cell Biol.* 19, 713–730. doi: 10.1038/s41580-018-0052-8

Gollihue, J. L., and Norris, C. M. (2020). Astrocyte mitochondria: Central players and potential therapeutic targets for neurodegenerative diseases and injury. *Ageing Res. Rev.* 59:101039. doi: 10.1016/j.arr.2020.101039

Gong, Z., Pan, J., Shen, Q., Li, M., and Peng, Y. (2018). Mitochondrial dysfunction induces NLRP3 inflammasome activation during cerebral ischemia/reperfusion injury. *J. Neuroinflamm.* 15:242. doi: 10.1186/s12974-018-1282-6

Hafner, A. V., Dai, J., Gomes, A. P., Xiao, C. Y., Palmeira, C. M., Rosenzweig, A., et al. (2010). Regulation of the mPTP by SIRT3-mediated deacetylation of CypD at lysine 166 suppresses age-related cardiac hypertrophy. *Aging* 2, 914–923. doi: 10.18632/aging.100252

Han, H., Hu, J., Yan, Q., Zhu, J., Zhu, Z., Chen, Y., et al. (2016). Bone marrow-derived mesenchymal stem cells rescue injured H9c2 cells via transferring intact mitochondria through tunneling nanotubes in an *in vitro* simulated ischemia/reperfusion model. *Mol. Med. Rep.* 13, 1517–1524. doi: 10.3892/mmr.2015.4726

Hangen, E., Blomgren, K., Benit, P., Kroemer, G., and Modjtahedi, N. (2010). Life with or without AIF. *Trends Biochem. Sci.* 35, 278–287. doi: 10.1016/j.tibs.2009.12.008

Hanley, D. F., Thompson, R. E., Rosenblum, M., Yenokyan, G., Lane, K., Mcbee, N., et al. (2019). Efficacy and safety of minimally invasive surgery with thrombolysis in intracerebral haemorrhage evacuation (MISTIE III): a randomised, controlled, open-label, blinded endpoint phase 3 trial. *Lancet* 393, 1021–1032. doi: 10.1016/S0140-6736(19)30195-3

Hayakawa, K., Esposito, E., Wang, X., Terasaki, Y., Liu, Y., Xing, C., et al. (2016). Transfer of mitochondria from astrocytes to neurons after stroke. *Nature* 535, 551–555. doi: 10.1038/nature18928

He, Z., Ning, N., Zhou, Q., Khoshnam, S. E., and Farzaneh, M. (2020). Mitochondria as a therapeutic target for ischemic stroke. *Free Radic. Biol. Med.* 146, 45–58. doi: 10.1016/j.freeradbiomed.2019.11.005

Heyck, M., Bonsack, B., Zhang, H., Sadanandan, N., Cozene, B., Kingsbury, C., et al. (2019). The brain and eye: treating cerebral and retinal ischemia through mitochondrial transfer. *Exp. Biol. Med.* 244, 1485–1492. doi: 10.1177/1535370219881623

Hsieh, C. H., Li, L., Vanhauwaert, R., Nguyen, K. T., Davis, M. D., Bu, G., et al. (2019). Miro1 Marks Parkinson's disease subset and Miro1 reducer rescues neuron loss in Parkinson's models. *Cell Metab.* 30, 1131–1140 e1137. doi: 10.1016/j.cmet.2019.08.023

Hu, X., Tao, C., Gan, Q., Zheng, J., Li, H., and You, C. (2016). Oxidative stress in intracerebral hemorrhage: sources, mechanisms, and therapeutic targets. *Oxid. Med. Cell Longev.* 2016:3215391. doi: 10.1155/2016/3215391

Huang, J., and Jiang, Q. (2019). Dexmedetomidine protects against neurological dysfunction in a mouse intracerebral hemorrhage model by inhibiting mitochondrial dysfunction-derived oxidative stress. *J. Stroke Cerebrovasc. Dis.* 28, 1281–1289. doi: 10.1016/j.jstrokecerebrovasdis.2019.01.016

Huang, Y., Gao, X., Zhou, X., Xie, B., Zhang, Y., Zhu, J., et al. (2020). Mitophagy in the hippocampus is excessive activated after cardiac arrest and cardiopulmonary resuscitation. *Neurochem. Res.* 45, 322–330. doi: 10.1007/s11064-019-02916-z

Jing, C. H., Wang, L., Liu, P. P., Wu, C., Ruan, D., and Chen, G. (2012). Autophagy activation is associated with neuroprotection against apoptosis via a mitochondrial pathway in a rat model of subarachnoid hemorrhage. *Neuroscience* 213, 144–153. doi: 10.1016/j.neuroscience.2012.03.055

Joshi, D. C., Tewari, B. P., Singh, M., Joshi, P. G., and Joshi, N. B. (2015). AMPA receptor activation causes preferential mitochondrial Ca(2)(+)

load and oxidative stress in motor neurons. *Brain Res.* 1616, 1–9. doi: 10.1016/j.brainres.2015.04.042

Kang, T. C. (2020). Nuclear factor-erythroid 2-related factor 2 (Nrf2) and mitochondrial dynamics/mitophagy in neurological diseases. *Antioxidants (Basel)* 9:617. doi: 10.3390/antiox9070617

Kashatus, D. F., Lim, K. H., Brady, D. C., Pershing, N. L., Cox, A. D., and Counter, C. M. (2011). RALA and RALBP1 regulate mitochondrial fission at mitosis. *Nat. Cell Biol.* 13, 1108–1115. doi: 10.1038/ncb2310

Katsu, M., Niizuma, K., Yoshioka, H., Okami, N., Sakata, H., and Chan, P. H. (2010). Hemoglobin-induced oxidative stress contributes to matrix metalloproteinase activation and blood-brain barrier dysfunction *in vivo*. *J. Cereb. Blood Flow Metab.* 30, 1939–1950. doi: 10.1038/jcbfm.2010.45

Kim-Han, J. S., Kopp, S. J., Dugan, L. L., and Diringer, M. N. (2006). Perihematomal mitochondrial dysfunction after intracerebral hemorrhage. *Stroke* 37, 2457–2462. doi: 10.1161/01.STR.0000240674.99945.4e

Kumar, S., Selim, M., Marchina, S., and Caplan, L. R. (2016). Transient neurological symptoms in patients with intracerebral hemorrhage. *JAMA Neurol.* 73, 316–320. doi: 10.1001/jamaneurol.2015.4202

Lemasters, J. J. (2005). Selective mitochondrial autophagy, or mitophagy, as a targeted defense against oxidative stress, mitochondrial dysfunction, and aging. *Rejuv. Res.* 8, 3–5. doi: 10.1089/rej.2005.8.3

Lemasters, J. J. (2014). Variants of mitochondrial autophagy: types 1 and 2 mitophagy and micromitophagy (Type 3). *Redox. Biol.* 2, 749–754. doi: 10.1016/j.redox.2014.06.004

Li, B., Zhang, Y., Li, H., Shen, H., Wang, Y., Li, X., et al. (2020). Miro1 regulates neuronal mitochondrial transport and distribution to alleviate neuronal damage in secondary brain injury after intracerebral hemorrhage in rats. *Cell Mol. Neurobiol.* 40. doi: 10.1007/s10571-020-00887-2. [Epub ahead of print].

Li, J., Lu, J., Mi, Y., Shi, Z., Chen, C., Riley, J., et al. (2014). Voltage-dependent anion channels (VDACs) promote mitophagy to protect neuron from death in an early brain injury following a subarachnoid hemorrhage in rats. *Brain Res.* 1573, 74–83. doi: 10.1016/j.brainres.2014.05.021

Licznerski, P., Park, H. A., Rolyan, H., Chen, R., Mnatsakanyan, N., Miranda, P., et al. (2020). ATP synthase c-subunit leak causes aberrant cellular metabolism in fragile X syndrome. *Cell* 182, 1170–1185 e1179. doi: 10.1016/j.cell.2020.07.008

Liu, F., Lu, J., Manaenko, A., Tang, J., and Hu, Q. (2018). Mitochondria in ischemic stroke: new insight and implications. *Aging Dis.* 9, 924–937. doi: 10.14336/AD.2017.1126

Liu, K., Ji, K., Guo, L., Wu, W., Lu, H., Shan, P., et al. (2014). Mesenchymal stem cells rescue injured endothelial cells in an *in vitro* ischemia-reperfusion model via tunneling nanotube like structure-mediated mitochondrial transfer. *Microvasc. Res.* 92, 10–18. doi: 10.1016/j.mvr.2014.01.008

Lu, H., Jiang, M., Lu, L., Zheng, G., and Dong, Q. (2015). Ultrastructural mitochondria changes in perihematomal brain and neuroprotective effects of Huperzine A after acute intracerebral hemorrhage. *Neuropsychiatr. Dis. Treat.* 11, 2649–2657. doi: 10.2147/NDT.S92158

Luo, X., O'neill, K. L., and Huang, K. (2020). The third model of Bax/Bak activation: a Bcl-2 family feud finally resolved? *F1000Research* 9:F1000 Faculty Rev-935. doi: 10.12688/f1000research.25607.1

Ma, J., Ni, H., Rui, Q., Liu, H., Jiang, F., Gao, R., et al. (2019). Potential roles of NIX/BNIP3L pathway in rat traumatic brain injury. *Cell Transplant.* 28, 585–595. doi: 10.1177/0963689719840353

Ma, Q., Chen, S., Hu, Q., Feng, H., Zhang, J. H., and Tang, J. (2014). NLRP3 inflammasome contributes to inflammation after intracerebral hemorrhage. *Ann. Neurol.* 75, 209–219. doi: 10.1002/ana.24070

Ma, R., Ma, L., Weng, W., Wang, Y., Liu, H., Guo, R., et al. (2020). DUSP6 SUMOylation protects cells from oxidative damage via direct regulation of Drp1 dephosphorylation. *Sci. Adv.* 6:eaaz0361. doi: 10.1126/sciadv.aaz0361

Macaskill, A. F., Rinholm, J. E., Twelvetrees, A. E., Arancibia-Carcamo, I. L., Muir, J., Fransson, A., et al. (2009). Miro1 is a calcium sensor for glutamate receptor-dependent localization of mitochondria at synapses. *Neuron* 61, 541–555. doi: 10.1016/j.neuron.2009.01.030

Mariani, E., Polidori, M. C., Cherubini, A., and Mecocci, P. (2005). Oxidative stress in brain aging, neurodegenerative and vascular diseases: an overview. *J. Chromatogr. B Analyt. Technol. Biomed. Life Sci.* 827, 65–75. doi: 10.1016/j.jchromb.2005.04.023

Mendelow, A. D., Gregson, B. A., Rowan, E. N., Murray, G. D., Gholkar, A., Mitchell, P. M., et al. (2013). Early surgery versus initial conservative treatment in patients with spontaneous supratentorial lobar intracerebral haematomas (STICH II): a randomised trial. *Lancet* 382, 397–408. doi: 10.1016/S0140-6736(13)60986-1

Montessuit, S., Somasekharan, S. P., Terrones, O., Lucken-Ardjomande, S., Herzig, S., Schwarzenbacher, R., et al. (2010). Membrane remodeling induced by the dynamin-related protein Drp1 stimulates Bax oligomerization. *Cell* 142, 889–901. doi: 10.1016/j.cell.2010.08.017

Nakamura, T., Kuroda, Y., Yamashita, S., Zhang, X., Miyamoto, O., Tamiya, T., et al. (2008). Edaravone attenuates brain edema and neurologic deficits in a rat model of acute intracerebral hemorrhage. *Stroke* 39, 463–469. doi: 10.1161/STROKEAHA.107.486654

Nakamura, T., and Lipton, S. A. (2011). Redox modulation by S-nitrosylation contributes to protein misfolding, mitochondrial dynamics, and neuronal synaptic damage in neurodegenerative diseases. *Cell Death Differ.* 18, 1478–1486. doi: 10.1038/cdd.2011.65

Nighoghossian, N., Berthezene, Y., Mechtouff, L., Derex, L., Cho, T. H., Ritzenthaler, T., et al. (2015). Cyclosporine in acute ischemic stroke. *Neurology* 84, 2216–2223. doi: 10.1212/WNL.0000000000001639

Pekkurnaz, G., Trinidad, J. C., Wang, X., Kong, D., and Schwarz, T. L. (2014). Glucose regulates mitochondrial motility via Milton modification by O-GlcNAc transferase. *Cell* 158, 54–68. doi: 10.1016/j.cell.2014.06.007

Picca, A., Guerra, F., Calvani, R., Bucci, C., Lo Monaco, M. R., Bentivoglio, A. R., et al. (2019). Mitochondrial dysfunction and aging: insights from the analysis of extracellular vesicles. *Int. J. Mol. Sci.* 20:805. doi: 10.3390/ijms20040805

Porter, G. A., and Beutner, G. (2018). Cyclophilin D, somehow a master regulator of mitochondrial function. *Biomolecules* 8:176. doi: 10.3390/biom8040176

Qu, J., Chen, W., Hu, R., and Feng, H. (2016). The injury and therapy of reactive oxygen species in intracerebral hemorrhage looking at mitochondria. *Oxid. Med. Cell Longev.* 2016:2592935. doi: 10.1155/2016/2592935

Rong, R., Xia, X., Peng, H., Li, H., You, M., Liang, Z., et al. (2020). Cdk5-mediated Drp1 phosphorylation drives mitochondrial defects and neuronal apoptosis in radiation-induced optic neuropathy. *Cell Death Dis.* 11:720. doi: 10.1038/s41419-020-02922-y

Sabirzhanov, B., Stoica, B. A., Zhao, Z., Loane, D. J., Wu, J., Dorsey, S. G., et al. (2016). miR-711 upregulation induces neuronal cell death after traumatic brain injury. *Cell Death Differ.* 23, 654–668. doi: 10.1038/cdd.2015.132

Salihu, A. T., Muthuraju, S., Idris, Z., Izaini Ghani, A. R., and Abdullah, J. M. (2016). Functional outcome after intracerebral haemorrhage–a review of the potential role of antiapoptotic agents. *Rev. Neurosci.* 27, 317–327. doi: 10.1515/revneuro-2015-0046

Shi, R. Y., Zhu, S. H., Li, V., Gibson, S. B., Xu, X. S., and Kong, J. M. (2014). BNIP3 interacting with LC3 triggers excessive mitophagy in delayed neuronal death in stroke. *CNS Neurosci. Ther.* 20, 1045–1055. doi: 10.1111/cns.12325

Shinohara, Y., Saito, I., Kobayashi, S., and Uchiyama, S. (2009). Edaravone (radical scavenger) versus sodium ozagrel (antiplatelet agent) in acute noncardioembolic ischemic stroke (EDO trial). *Cerebrovasc. Dis.* 27, 485–492. doi: 10.1159/000210190

Sidlauskaite, E., Gibson, J. W., Megson, I. L., Whitfield, P. D., Tovmasyan, A., Batinic-Haberle, I., et al. (2018). Mitochondrial ROS cause motor deficits induced by synaptic inactivity: implications for synapse pruning. *Redox Biol.* 16, 344–351. doi: 10.1016/j.redox.2018.03.012

Sies, H., Berndt, C., and Jones, D. P. (2017). Oxidative stress. *Annu. Rev. Biochem.* 86, 715–748. doi: 10.1146/annurev-biochem-061516-045037

Song, L., Xu, L. F., Pu, Z. X., and Wang, H. H. (2019). IL-10 inhibits apoptosis in brain tissue around the hematoma after ICH by inhibiting proNGF. *Eur. Rev. Med. Pharmacol. Sci.* 23, 3005–3011. doi: 10.26355/eurrev_201904_17582

Tang, X., Yan, K., Wang, Y., Wang, Y., Chen, H., Xu, J., et al. (2020). Activation of PPAR-beta/delta attenuates brain injury by suppressing inflammation and apoptosis in a collagenase-induced intracerebral hemorrhage mouse model. *Neurochem. Res.* 45, 837–850. doi: 10.1007/s11064-020-02956-w

Tomasello, F., Messina, A., Lartigue, L., Schembri, L., Medina, C., Reina, S., et al. (2009). Outer membrane VDAC1 controls permeability transition of the inner mitochondrial membrane in cellulo during stress-induced apoptosis. *Cell Res.* 19, 1363–1376. doi: 10.1038/cr.2009.98

Tschoe, C., Bushnell, C. D., Duncan, P. W., Alexander-Miller, M. A., and Wolfe, S. Q. (2020). Neuroinflammation after intracerebral hemorrhage and potential therapeutic targets. *J. Stroke* 22, 29–46. doi: 10.5853/jos.2019.02236

Wang, X., Mori, T., Sumii, T., and Lo, E. H. (2002). Hemoglobin-induced cytotoxicity in rat cerebral cortical neurons: caspase activation and oxidative stress. *Stroke* 33, 1882–1888. doi: 10.1161/01.STR.0000020121.41527.5D

Wang, Z., Zhou, F., Dou, Y., Tian, X., Liu, C., Li, H., et al. (2018). Melatonin alleviates intracerebral hemorrhage-induced secondary brain injury in rats via suppressing apoptosis, inflammation oxidative stress, DNA damage, and mitochondria injury. *Transl. Stroke Res.* 9, 74–91. doi: 10.1007/s12975-017-0559-x

Weir, H. J., Yao, P., Huynh, F. K., Escoubas, C. C., Goncalves, R. L., Burkewitz, K., et al. (2017). Dietary restriction and AMPK increase lifespan via mitochondrial network and peroxisome remodeling. *Cell Metab.* 26, 884–896 e885. doi: 10.1016/j.cmet.2017.09.024

Wu, X., Cui, W., Guo, W., Liu, H., Luo, J., Zhao, L., et al. (2020a). Acrolein aggravates secondary brain injury after intracerebral hemorrhage through Drp1-mediated mitochondrial oxidative damage in mice. *Neurosci. Bull.* 36, 1158–1170. doi: 10.1007/s12264-020-00505-7

Wu, X., Luo, J., Liu, H., Cui, W., Guo, K., Zhao, L., et al. (2020b). Recombinant adiponectin peptide ameliorates brain injury following intracerebral hemorrhage by suppressing astrocyte-derived inflammation via the inhibition of Drp1-mediated mitochondrial fission. *Transl. Stroke Res.* 11, 924–939. doi: 10.1007/s12975-019-00768-x

Wu, X., Luo, J., Liu, H., Cui, W., Guo, W., Zhao, L., et al. (2020c). Recombinant adiponectin peptide promotes neuronal survival after intracerebral haemorrhage by suppressing mitochondrial and ATF4-CHOP apoptosis pathways in diabetic mice via Smad3 signalling inhibition. *Cell Prolif.* 53:e12759. doi: 10.1111/cpr.12759

Xu, S., Wang, P., Zhang, H., Gong, G., Gutierrez Cortes, N., Zhu, W., et al. (2016). CaMKII induces permeability transition through Drp1 phosphorylation during chronic beta-AR stimulation. *Nat. Commun.* 7:13189. doi: 10.1038/ncomms13189

Yang, J., Cui, X., Li, J., Zhang, C., Zhang, J., and Liu, M. (2015). Edaravone for acute stroke: meta-analyses of data from randomized controlled trials. *Dev. Neurorehabil.* 18, 330–335. doi: 10.3109/17518423.2013.830153

Yang, J., Liu, M., Zhou, J., Zhang, S., Lin, S., and Zhao, H. (2011). Edaravone for acute intracerebral haemorrhage. *Cochrane Database Syst. Rev.* CD007755. doi: 10.1002/14651858.CD007755.pub2

You, Y., Hou, Y., Zhai, X., Li, Z., Li, L., Zhao, Y., et al. (2016). Protective effects of PGC-1alpha via the mitochondrial pathway in rat brains after intracerebral hemorrhage. *Brain Res.* 1646, 34–43. doi: 10.1016/j.brainres.2016.04.076

Yu, J., Zheng, J., Lu, J., Sun, Z., Wang, Z., and Zhang, J. (2019). AdipoRon protects against secondary brain injury after intracerebral hemorrhage via alleviating mitochondrial dysfunction: possible involvement of AdipoR1-AMPK-PGC1alpha pathway. *Neurochem. Res.* 44, 1678–1689. doi: 10.1007/s11064-019-02794-5

Zandalinas, S. I., and Mittler, R. (2018). ROS-induced ROS release in plant and animal cells. *Free Radic. Biol. Med.* 122, 21–27. doi: 10.1016/j.freeradbiomed.2017.11.028

Zhang, T., Wu, P., Budbazar, E., Zhu, Q., Sun, C., Mo, J., et al. (2019). Mitophagy reduces oxidative stress via Keap1 (kelch-like epichlorohydrin-associated protein 1)/Nrf2 (nuclear factor-E2-related factor 2)/PHB2 (prohibitin 2) pathway after subarachnoid hemorrhage in rats. *Stroke* 50, 978–988. doi: 10.1161/STROKEAHA.118.021590

Zheng, J., Shi, L., Liang, F., Xu, W., Li, T., Gao, L., et al. (2018). Sirt3 ameliorates oxidative stress and mitochondrial dysfunction after intracerebral hemorrhage in diabetic rats. *Front. Neurosci.* 12:414. doi: 10.3389/fnins.2018.00414

Zhou, H., Zhu, P., Wang, J., Toan, S., and Ren, J. (2019). DNA-PKcs promotes alcohol-related liver disease by activating Drp1-related mitochondrial fission and repressing FUNDC1-required mitophagy. *Signal Transduct. Target Ther.* 4:56. doi: 10.1038/s41392-019-0094-1

Zhou, Z. D., and Tan, E. K. (2020). Oxidized nicotinamide adenine dinucleotide-dependent mitochondrial deacetylase sirtuin-3 as a potential therapeutic target of Parkinson's disease. *Ageing Res. Rev.* 62:101107. doi: 10.1016/j.arr.2020.101107

Zhuo, F., Qiu, G., Xu, J., Yang, M., Wang, K., Liu, H., et al. (2016). Both endoplasmic reticulum and mitochondrial pathways are involved in oligodendrocyte apoptosis induced by capsular hemorrhage. *Mol. Cell Neurosci.* 72, 64–71. doi: 10.1016/j.mcn.2016.01.009

Zia, M. T., Csiszar, A., Labinskyy, N., Hu, F., Vinukonda, G., Lagamma, E. F., et al. (2009). Oxidative-nitrosative stress in a rabbit pup model of germinal matrix hemorrhage: role of NAD(P)H oxidase. *Stroke* 40, 2191–2198. doi: 10.1161/STROKEAHA.108.544759

Zille, M., Karuppagounder, S. S., Chen, Y., Gough, P. J., Bertin, J., Finger, J., et al. (2017). Neuronal death after hemorrhagic stroke *in vitro* and *in vivo* shares features of ferroptosis and necroptosis. *Stroke* 48, 1033–1043. doi: 10.1161/STROKEAHA.116.015609

Zorov, D. B., Juhaszova, M., and Sollott, S. J. (2014). Mitochondrial reactive oxygen species (ROS) and ROS-induced ROS release. *Physiol. Rev.* 94, 909–950. doi: 10.1152/physrev.00026.2013

Zsurka, G., and Kunz, W. S. (2015). Mitochondrial dysfunction and seizures: the neuronal energy crisis. *Lancet Neurol.* 14, 956–966. doi: 10.1016/S1474-4422(15)00148-9

Conflict of Interest: The authors declare that the research was conducted in the absence of any commercial or financial relationships that could be construed as a potential conflict of interest.

frontiers in Aging Neuroscience

ORIGINAL RESEARCH
published: 03 February 2021
doi: 10.3389/fnagi.2021.640215

Irisin Contributes to Neuroprotection by Promoting Mitochondrial Biogenesis After Experimental Subarachnoid Hemorrhage

Tianqi Tu[1], *Shigang Yin*[2,3], *Jinwei Pang*[1,3,4], *Xianhui Zhang*[4], *Lifang Zhang*[4], *Yuxuan Zhang*[1], *Yuke Xie*[2], *Kecheng Guo*[2], *Ligang Chen*[1,3,4], *Jianhua Peng*[1,2,4*] and *Yong Jiang*[1,2,3,4*]

[1] *Department of Neurosurgery, The Affiliated Hospital of Southwest Medical University, Luzhou, China,* [2] *Luzhou Key Laboratory of Neurological Diseases and Brain Function, The Affiliated Hospital of Southwest Medical University, Luzhou, China,* [3] *Academician (Expert) Workstation of Sichuan Province, The Affiliated Hospital of Southwest Medical University, Luzhou, China,* [4] *Sichuan Clinical Research Center for Neurosurgery, The Affiliated Hospital of Southwest Medical University, Luzhou, China*

Subarachnoid hemorrhage (SAH) is a devastating form of stroke, which poses a series of intractable challenges to clinical practice. Imbalance of mitochondrial homeostasis has been thought to be the crucial pathomechanism in early brain injury (EBI) cascade after SAH. Irisin, a protein related to metabolism and mitochondrial homeostasis, has been reported to play pivotal roles in post-stroke neuroprotection. However, whether this myokine can exert neuroprotection effects after SAH remains unknown. In the present study, we explored the protective effects of irisin and the underlying mechanisms related to mitochondrial biogenesis in a SAH animal model. Endovascular perforation was used to induce SAH, and recombinant irisin was administered intracerebroventricularly. Neurobehavioral assessments, TdT-UTP nick end labeling (TUNEL) staining, dihydroethidium (DHE) staining, immunofluorescence, western blot, and transmission electron microscopy (TEM) were performed for post-SAH assessments. We demonstrated that irisin treatment improved neurobehavioral scores, reduced neuronal apoptosis, and alleviated oxidative stress in EBI after SAH. More importantly, the administration of exogenous irisin conserved the mitochondrial morphology and promoted mitochondrial biogenesis. The protective effects of irisin were partially reversed by the mitochondrial uncoupling protein-2 (UCP-2) inhibitor. Taken together, irisin may have neuroprotective effects against SAH *via* improving the mitochondrial biogenesis, at least in part, through UCP-2 related targets.

Keywords: FNDC5/irisin, subarachnoid hemorrhage, mitochondrial homeostasis, oxidative stress, neuronal apoptosis

OPEN ACCESS

Edited by:
Hailiang Tang,
Fudan University, China

Reviewed by:
Yinghua Jiang,
Tulane University, United States
Hualin Sun,
Nantong University, China

***Correspondence:**
Jianhua Peng
pengjianhua@swmu.edu.cn
Yong Jiang
jiangyong@swmu.edu.cn

Received: *10 December 2020*
Accepted: *12 January 2021*
Published: *03 February 2021*

Citation:
Tu T, Yin S, Pang J, Zhang X, Zhang L, Zhang Y, Xie Y, Guo K, Chen L, Peng J and Jiang Y (2021) Irisin Contributes to Neuroprotection by Promoting Mitochondrial Biogenesis After Experimental Subarachnoid Hemorrhage. Front. Aging Neurosci. 13:640215. doi: 10.3389/fnagi.2021.640215

INTRODUCTION

Subarachnoid hemorrhage (SAH) accounts for 5–10% in all stroke events (Lawton and Vates, 2017). With extremely high mortality (nearly 50%) and disability rate (over 30%), this form of stroke causes a severe health problem worldwide. For decades, studies have focused on the processes of early brain injury (EBI) after SAH, which was widely attributed to be one of the primary

causes of the poor outcomes (Cahill et al., 2006; Cahill and Zhang, 2009). Recently, mitochondrial homeostasis during the EBI process has gradually become the focus of studies (Hagberg et al., 2014).

Mitochondria, as the core of energy metabolism, are strongly associated with the homeostasis of cell metabolism. Previous studies have emphasized on the necessity of improving mitochondrial dysregulation when it comes to neuroprotection (Hagberg et al., 2014). The brain is an important organ with high metabolic rates, and the imbalance of energy metabolism, which is caused by the dysfunction of mitochondria after brain injury, would lead to pathological cascades in EBI (Sims and Muyderman, 2010; Hayakawa et al., 2016). Considering the significant role of mitochondria, the exploration of innovative mitochondria-targeted therapeutic strategies of brain injury is prospective (Bolanos et al., 2009).

Irisin is a cleaved version of fibronectin domain-containing protein 5 (FNDC5), a membrane protein comprising a short cytoplasmic domain (Lourenco et al., 2019). Recently, the actual existence of irisin has been verified in myocytes, plasma, and brain tissues (Dun et al., 2013; Piya et al., 2014; Ruan et al., 2018). Meanwhile, the outstanding effects of irisin in metabolism regulation, especially in lipid metabolism and mitochondrial homeostasis, make this cytokine to attract much attention in the research field (Bostrom et al., 2012; Hocking et al., 2013; Farmer, 2019). More importantly, irisin has been proved to be an effective intervention for reducing damage, promoting recovery, and improving prognosis in acute brain injury studies (Li et al., 2017; Tu et al., 2020).

In the current study, we focused on the role of irisin in neuroprotective effects and the underlying mitochondria-related mechanisms, shedding light on the influence of irisin after SAH.

MATERIALS AND METHODS

Animals

All experimental procedures were approved by the Care and Use of Laboratory Animals of China and were following the guidelines of the Animal Committee of the Ethics Committee of Southwest Medical University. Male C57BL/6J mice (aged 8–12 weeks with an average weight of 18–22 g) were obtained from Chengdu Dashuo Experimental Animal Co., Ltd. All mice were housed in a room with a 12-h light/dark cycle and with controlled humidity and temperature. All of the animals could freely access fresh food and clean water.

SAH Model

The endovascular perforation model of SAH was performed as previously described (Peng et al., 2019b). Briefly, mice were inductively anesthetized in a hermetic box with 3–4% isoflurane, and then mice were masked and ventilated with 1–1.5% isoflurane throughout the operation. In a supine position, the skin of the neck was opened with a sharp scalpel in the midline. Then, the common carotid artery (CCA), external carotid artery (ECA), and internal carotid artery (ICA) of the right side were exposed. A 5.0 filament was inserted into the right ICA through the isolated right ECA. After a resistance was felt at the bifurcation of the anterior and middle cerebral arteries, the suture was advanced 2 mm further to perforate the vessel during immediate withdrawal. We monitored the occurrence of the typical Cushing response as a secondary judgment of the success of the SAH model. The mice in the sham group underwent the same procedures without vessel perforation. After the filament was removed and the stump of the ICA was ligated, the skin incision was sutured and disinfected with diluted iodophor. The mice were monitored at 25°C with warm sets of cage every 15 min until they recovered from anesthesia, and then they were transferred back to their home cages.

SAH Grading and Mortality Analysis

The assessment of the SAH grading score was performed by two independent investigators blinded to the experimental design at 24 h after SAH, as previously described (Wu Y. et al., 2019). The basal cistern of the mouse brain was divided into six regions, and according to the amount of blood clotting, each region was assigned a grade ranging from 0 to 3. The total score for the six regions was defined as the mouse SAH grade. Briefly, total grades of 0–7, 8–12, and 13–18 indicated mild, moderate, and severe SAH, respectively. In this study, mice with the SAH grade < 8 were excluded. Mortality was calculated as the number of dead mice divided by the total number of mice used after SAH in the experiment.

Study Design

Four experiments were conducted as follows.

Experiment 1

Typical time points in the EBI process were chosen to detect the temporal expression of endogenous irisin within the ipsilateral hemisphere of the brain after SAH. A total of 36 mice were randomly divided into six groups for Western blotting: Sham ($n = 6$), SAH-6 h ($n = 6$), SAH-12 h ($n = 6$), SAH-24 h ($n = 6$), SAH-48 h ($n = 6$), and SAH-72 h ($n = 6$). Additionally, six mice in the Sham ($n = 3$) and the SAH-24 h ($n = 3$) group were used for FNDC5/irisin spatial co-localization *via* immunofluorescence.

Experiment 2

To optimize the concentration of exogenous irisin used in the experiments, three concentration gradients of exogenous irisin were designed, and 30 mice were divided into five groups: Sham ($n = 6$), SAH+vehicle (0.9% NaCl, $n = 6$), SAH+irisin (150 μg/kg, $n = 6$), SAH+irisin (300 μg/kg, $n = 6$), and SAH+irisin (600 μg/kg, $n = 6$). Neurological scores and SAH grades were evaluated 24 h after SAH. To reduce any subjective bias, all mice were marked with a marker pen on their tails by an experimenter to distinguish between groups, and another two investigators who were blinded to the groups' information performed the tests. Based on the results of the above tests, irisin-treated mice (300 μg/kg) were used for future experiments.

Experiment 3

A total of 36 mice were divided into three groups randomly: Sham ($n = 12$), SAH+vehicle (0.9% NaCl $n = 12$), and SAH+irisin (300 μg/kg, $n = 12$). Western blotting,

immunofluorescence, TdT-UTP nick end labeling (TUNEL) staining, dihydroethidium (DHE) staining, and assay kits were implemented to evaluate neuronal apoptosis and oxidative stress at 24 h after SAH. Meanwhile, transmission electron microscopy (TEM) was performed to measure the change of the number, morphology, and function of mitochondria. Western blotting and immunofluorescence were also used to analyze the expression of proteins related to mitochondrial biogenesis at 24 h after SAH.

Experiment 4

To explore the mechanism of the neuroprotective role of irisin, a total of 36 mice were randomly assigned into four groups: Sham ($n = 9$), SAH+vehicle (0.9% NaCl, $n = 9$), SAH+irisin+vehicle (300 μg/kg-irisin, 0.9% NaCl, $n = 9$), and SAH+irisin+Genipin (300 μg/kg-irisin, 30 mg/kg-Genipin, $n = 9$). Western blotting, TUNEL staining, and immunofluorescence were used to analyze the effects of genipin, the inhibitor of uncoupling protein-2 (UCP-2), on the protective roles of exogenous irisin at 24 h after SAH. Additionally, to estimate the influence of genipin, four groups were added: naive+vehicle, naive+genipin, SAH+vehicle, and SAH+genipin.

Neurological Performance Evaluation

Two independent investigators who were blinded to the experimental design information evaluated the neurological performance to avoid any bias. The modified Garcia scale and the beam balance tests were used to evaluate neurological scores as previously described (Xie et al., 2020). The modified Garcia scale (maximum score = 18) included the tests of spontaneous activity (0–3), the spontaneous movement of the four limbs (0–3), forelimbs outstretching (0–3), climbing capacity (1–3), response to vibrissae touch (1–3), and trunk touch (1–3). The ability of mice to walk on a round wooden beam within 1 min was evaluated using the beam balance test (0–4), and the mean score was calculated based on three consecutive trials scored from 0 to 4 according to the walking ability.

Drug Administration

Intracerebroventricular administration was performed as previously described (Xie et al., 2020). Briefly, after mice were anesthetized, the scalps were opened through the midline, and a burr hole was drilled with a needle of a 50 ml syringe (0.3 mm anterior and 1 mm lateral to the bregma). Then, the needle of a 10-μl microsyringe was inserted into the hole (3 mm in depth) to enter the lateral ventricle. Exogenous irisin diluted in a normal saline solution (067-29A, Phoenix Pharmaceuticals, USA) was injected intracerebroventricularly 30 min after SAH induction. Similarly, the normal saline (vehicle), which does not contain irisin, was injected into the vehicle groups as controls.

To explore whether the effects of irisin is associated with the upregulation of UCP-2, genipin, a specific UCP-2 inhibitor, was injected intravenously before the administration of irisin in experimental animals with SAH. Briefly, at 30 min before SAH, the animals were injected with genipin diluted in a normal saline solution (30 mg/kg body weight; Solarbio, China) *via* the caudal vein. After 30 min of SAH, irisin administration was performed as previously described. Similarly, the animals in the vehicle group were treated intravenously with an equivalent amount of the normal saline solution without genipin 30 min before SAH, and then, an equivalent amount of the normal saline solution without irisin was treated intracerebroventricularly 30 min after SAH.

Immunofluorescence Staining

Double fluorescence staining was performed as previously described (Pang et al., 2018). The slices were rewarmed at room temperature for 10 min and permeabilized with 0.1% Triton X-100 (diluted in PBS) for 5 min. After being washed with PBS three times (5 min per time), the slices were blocked with 10% goat serum (diluted in PBS) for 2 h at room temperature. Then, the slices were incubated overnight (about 12 h) at 4°C with primary antibodies, including anti-irisin (ab131390, Abcam, USA, 1:100) and anti-NeuN (ab104224, Abcam, USA, 1:100).

Next, the slices were washed with PBS and incubated with the appropriate secondary antibody (1:200) at room temperature for 2 h. Finally, 4',6-diamidino-2-phenylindole (DAPI; C0060, Solarbio, China, 1:200) were used to stain the cell nucleus for 5 min at room temperature. After dropping the anti-fluorescence attenuation agents (20 μl per tissue) and covering the cover slides, the slices were observed and recorded with a fluorescence microscope. Next, three random coronal sections per brain were selected, and the defined regions around the puncture point were observed in the right hemisphere for analysis. Photographs and fluorescence intensity were analyzed with Image-Pro Plus 6.0 software (MediaCybernetics, USA).

DHE Staining

To assess the oxidative stress level in the brain, double staining of neurons and DHE (D7008, Sigma-Aldrich, USA) was used to stain the frozen brain slices at 24 h after SAH. Neurons were stained by a neuron marker, the neuronal nuclear protein (NeuN; ab104224, Abcam, USA, 1:100). Freshly prepared slices were incubated with 3 μmol/l DHE in a humidified chamber and protected from light (at 37°C incubator for 45 min). Photographs and the fluorescence intensity were analyzed with Image Image-Pro Plus 6.0 software (MediaCybernetics, USA).

TUNEL Staining

To quantify the neuronal apoptosis level, double staining of neurons and TUNEL-positive cells was performed at 24 h after SAH. Neurons were stained by the neuron marker NeuN (ab104224, Abcam, USA, 1:100), and TUNEL staining was done according to the manufacturer's instructions of *in situ* Cell Death Detection Kit, TMR red (Roche, USA). Three microscopic fields of each slice were observed and recorded by a fluorescence microscope, and the TUNEL-positive neurons around the puncture point were counted. Data were presented as the apoptotic index, TUNEL-positive neurons/total neurons in %.

Western Blotting

Western blotting analysis was performed as previously described (Peng et al., 2019a). The total proteins were extracted from the right brain hemisphere tissues, and bicinchoninic acid (BCA)

assay kits (Beyotime, China) were used to determine protein concentration. Equal amounts of a sample protein were loaded onto an SDS-PAGE gel for protein separation. Then, samples were transferred onto a nitrocellulose membrane (0.20 μm, Millipore) by using a wet transfer system. After the membrane transfer was finished, the membrane was blocked in 5% non-fat dry milk (diluted in Tris-Buffered Saline and Tween 20, TBST) for 2 h at room temperature. Next, the membrane was washed three times with TBST (5 min per time) and incubated with the following primary antibodies at 4°C overnight: anti-irisin (ab131390, Abcam, USA, 1:1,000), anti-TFAM (ab131607, Cell Signaling Technology, USA, 1:1,000), anti-PGC-1α (ab2178s, Cell Signaling Technology, USA, 1:1,000), anti-Cleaved caspase-3 (9661, Cell Signaling Technology, USA, 1:1,000), anti-Bcl-2 (1:1,000, Proteintech, China, 1:1,000), anti-Bcl-2-associated X protein (Bax; 1:1,000, Cell Signaling Technology, USA, 1:1500), anti-SOD-2 (24127-1-AP, Proteintech, China, 1:2,000), anti-UCP-2 (11081-1-AP, Proteintech, China, 1:1500), and anti-β-actin (20536-1-AP, Proteintech, China, 1:6,000).

Then, the membrane was washed five times with TBST (5 min per time), and the secondary antibody of SA00001-2 (Proteintech, China, 1:6,000) was incubated for 1 h at room temperature. The membranes were washed five times with TBST (5 min per time) before the immunoblots were taken for visualization. The bands were displayed by using enhanced electrogenerated chemiluminescence (ECL; Fdbio Science) and photographed by the ChemiDoc Imaging System (Bio-Rad, Hercules, USA). Immunoblot band images were analyzed by Image Pro-Plus 6.0 software (MediaCybernetics, USA).

Assay Kits of Oxidative Stress

For detecting the change of the levels of oxidative stress in mice brain at 24 h after SAH, fresh brain tissues were collected, and samples were prepared as per the manufacturer's instructions. Superoxide dismutase (SOD) Assay Kit (S0103, Beyotime, China), Malonaldehyde (MDA) Assay Kit (S0131, Beyotime, China), and Glutathione Peroxidase Activity (GSH-PX) Assay Kit (S0052, Beyotime, China) were used as the instructions illustrated.

Transmission Electron Microscopy

Transmission electron microscopy was performed as previously reported (Gao et al., 2017). Briefly, under deep anesthesia, the mice were perfused transcardially with pre-cooled PBS (40 ml per mouse). Then, the right brain tissues around the puncture point in the SAH groups and their corresponding areas in the sham group of the mice were collected and fixed in 2.5% glutaraldehyde (diluted in PBS) at 4°C overnight. After the tissues were washed four times with PBS (5 min per time) and stayed for 15 min, these brain tissues were fixed in 1% Osmium acid (diluted in PBS) at 4°C for 2 h. Next, the brain tissues were dehydrated in different concentrations of ethanol. Then, these samples were buried into the embedding medium and cut into 70-nm-thick slices by using an ultramicrotome (EM UC7, Leica, Germany). The slices were then stained with 4% uranyl acetate (10 min) and 0.5% lead citrate (10 min) at room temperature. Finally, the ultrathin sections were visualized and photographed by using the TEM (Tecnai G2 Spirit, FEI, Holland).

Statistical Analysis

Statistical evaluation of the data was performed using data statistics software GraphPad Prism 8 (GraphPad Software Inc., San Diego, CA, USA) and SPSS 24.0 software (SPSS, Inc., Chicago, IL, USA). All of the measurement data in this article were tested for normality first. Median (interquartile range) percentiles were used to express data that were not consistent with normal distribution, and Mann-Whitney *U*-tests were used to analyze the difference between groups. The normally distributed data were presented as the mean ± SD. The ANOVA followed by Tukey's *post-hoc* analysis was applied to analyze the difference between multiple groups. The value of $p < 0.05$ was considered as a significant difference.

RESULTS

Animal Mortality and SAH Grade

A total of 165 animals were used in this study, of which 8 were used in the naive group, 30 were used in the sham group, and 127 were subjected to induce the SAH model (**Figure 1A**). There was no mortality in the naive group and the sham group, while 20 (15.74%) mice died after SAH. Three mice were excluded from the study due to mild SAH (SAH grade < 8). No significant difference in SAH grades was observed among all SAH groups at 24 h after SAH (**Figures 1B,C**).

Time Course and Spatial Change of Endogenous FNDC5/Irisin Levels in Ipsilateral Hemisphere at 24 h After SAH

Western blotting results displayed that endogenous FNDC5/irisin protein decreased at 6 h after SAH and increased at 12 h and decreased again at 24 h after SAH when compared to the sham group (**Figure 2A**). Double immunofluorescence staining showed that FNDC5/irisin could be co-localized with neurons in the mouse brain. Meanwhile, the number of FNDC5/irisin-positive neurons decreased at 24 h after SAH when compared with that in the sham group (**Figure 2B**).

Short-Term Neurological Functions Were Improved by Exogenous Irisin Treatments After SAH

At 24 h after SAH, worse neurobehavioral performances of animals in the vehicle group were observed in the modified Garcia scale and the beam balance test when compared to the sham group. Compared with animals in the vehicle group, exogenous irisin treatment at a middle dose (300 μg/kg) and a high dose (600 μg/kg) significantly improved the neurological performance of those animals at 24 h after SAH (**Figures 3A,B**). Based on the results, the dosage of 300 μg/kg was chosen for subsequent experiments.

A

Groups	Number	Motality	Excluded
Experiment 1			
Sham	9	0%（0/9）	0
SAH(6h/12h/24h/48h/72h)	39	17.95%（7/39）	2
SAH(24h)	4	25%（1/4）	0
Experiment 2			
Sham *	6	0%（0/6）	0
SAH+Vehicle *	6	0%（0/6）	0
SAH+irisin 150μg/kg	6	0%（0/6）	0
SAH+irisin 300μg/kg *	6	0%（0/6）	0
SAH+irisin 600μg/kg	8	25%（2/8）	0
Experiment 3			
Sham	12	0%	0
SAH+Vehicle	14	14.28%（2/14）	0
SAH+irisin 300μg/kg	15	20%（3/15）	0
Experiment 4			
Sham	9	0%	0
SAH+Vehicle	10	10%（1/10）	0
SAH+irisin 300μg/kg+Vehicle	11	18.18%（2/11）	0
SAH+irisin 300μg/kg+Genipin	11	9.09%（1/11）	1
naive+Vehicle	4	0%（0/4）	0
naive+Genipin	4	0%（0/4）	0
SAH+Vehicle	5	20%（1/5）	0
SAH+Genipin	4	0%（0/4）	0
Total			
naive	8	0%（0/8）	0
Sham	30	0%（0/8）	0
SAH	127	15.74%（20/127）	3

***Shared with experiment 3**

B

C

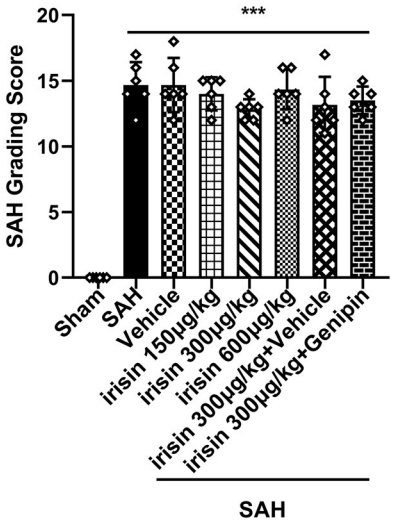

FIGURE 1 | Animal usage and SAH grade. **(A)** The record of the animal used in this experiment. **(B)** Representative pictures of brains in the sham and SAH groups. **(C)** SAH grade scores in each group. Data were represented with mean ± SD, $n = 6$ per group; the one-way ANOVA was used followed by the Tukey's HSD *post-hoc* test and the Holm–Bonferroni correction method. ***$P < 0.001$ vs. sham group. Vehicle group, sterile 0.9% of NaCl; SAH, subarachnoid hemorrhage.

Neuronal Apoptosis Was Ameliorated by Exogenous Irisin Treatment After SAH

The pathological change of neuronal apoptosis was caused by SAH stroke. Co-staining of neurons and TUNEL-positive cells were performed to detect the effects of exogenous irisin. Evident neuronal apoptosis was observed in the vehicle group after SAH, while the number of TUNEL-positive neurons decreased after irisin administration (**Figures 4A,B**). Western blotting was used to semi-quantify the protein levels related to apoptosis (**Figures 4C–F**). By the evident elevation of the cleaved caspase-3 protein level, apoptosis in the brain tissue was confirmed (**Figures 4C,D**). Irisin treatment alleviated this injury, for decreasing the protein level of the cleaved caspase-3, when compared to the vehicle group. Bax and Bcl-2, the pro-apoptotic marker and the anti-apoptotic marker, were also assessed to confirm these results. Evidently, the level of the Bax protein was increased and the Bcl-2 protein was decreased after SAH, when compared to the sham group. However, irisin treatment reversed these changes. Immunoblot data showed that the Bax protein decreased in the irisin-treated group while the Bcl-2 protein increased in the irisin-treated group, when compared to the vehicle group (**Figures 4C,E,F**).

Oxidative Stress Insults Were Alleviated by Exogenous Irisin Treatment After SAH

After SAH stroke, the oxidative stress reaction was presented in the cascade insults. ROS, as a crucial factor in the oxidative stress reaction, was evaluated by DHE staining (**Figures 5A,B**). Our data revealed a significantly high red fluorescence intensity in the vehicle group when compared to the sham group. However, irisin

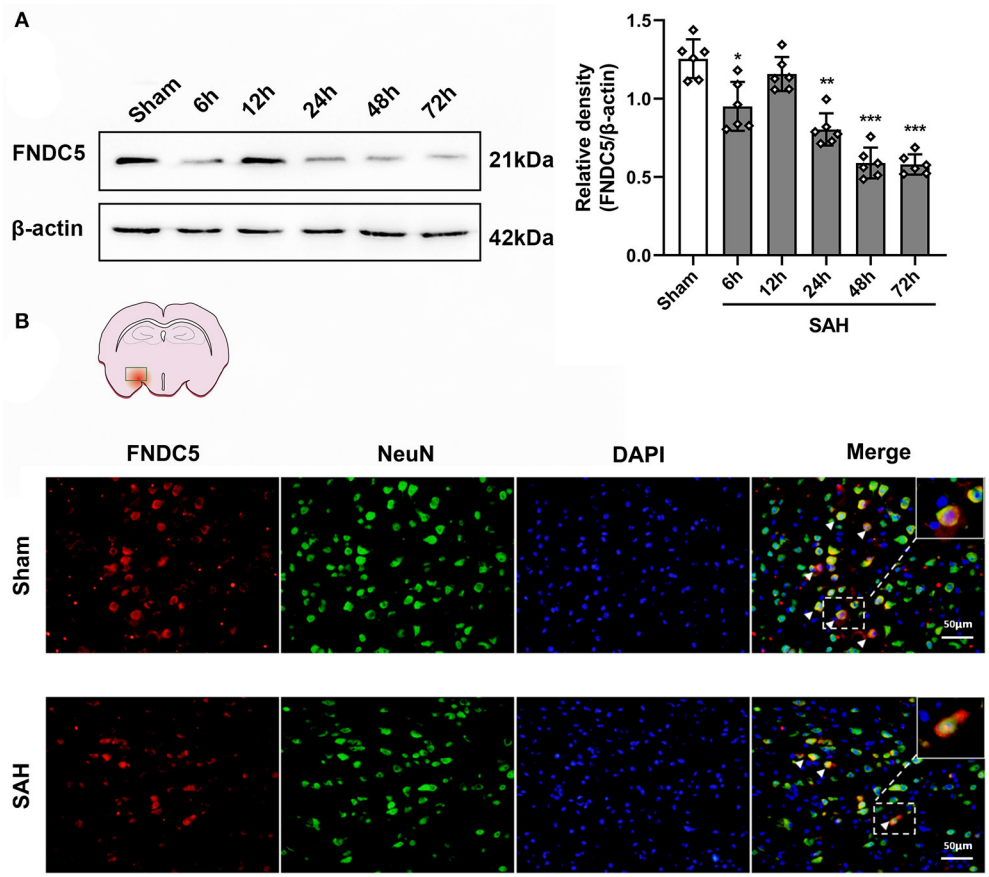

FIGURE 2 | Time course of FNDC5/irisin expression after SAH. **(A)** Representative western blotting images and relative density analysis of FNDC5/irisin at 6, 12, 24, 48, and 72 h after SAH. Endogenous FNDC5/irisin protein decreased at 6 h while it increased at 12 h and decreased again from 24 to 72 h after SAH. Data were represented as mean ± SD, $n = 6$ per group; the one-way ANOVA was used followed by the Tukey's HSD *post-hoc* test and the Holm–Bonferroni correction method. $^{*}P < 0.05$, $^{**}P < 0.01$, $^{***}P < 0.001$ vs. sham group. **(B)** FNDC5/irisin could be co-localized with neurons, and the number of FNDC5/irisin-positive neurons was decreased at 24 h after SAH. Scale bar = 50 μm, n = 3 per group; FNDC5, fibronectin domain-containing protein 5; SAH, subarachnoid hemorrhage.

administration ameliorated the oxidative stress insult, as lower red fluorescence intensity and lower number of DHE-positive cells were observed in the irisin-intervened group than those in the vehicle group. Other markers of oxidative stress, involving MDA, SOD, and GSH-PX, were examined to confirm the above results (**Figures 5C–E**). As our data showed, the activity of SOD and GSH-PX decreased after irisin treatment, while the level of MDA was increased, when compared with the vehicle group.

The Mitochondrial Morphology and Mitochondrial Biogenesis Were Maintained by Exogenous Irisin Treatment After SAH

Transmission electron microscopy was conducted to observe the mitochondrial dysfunction after SAH around hemorrhage regions. Images captured by TEM suggested the imbalance of mitochondrial dynamics, which is the initial process of cell apoptosis after SAH. In the irisin-treated group, these changes were relieved, and the number of swelling mitochondria and vacuoles were decreased (**Figure 6A**). Mitochondrial biogenesis is essential for maintaining normal mitochondrial function. Markedly, this kind of self-regulation was disturbed after SAH. TFAM and PGC-1α, two key proteins related to mitochondrial biogenesis, were significantly decreased after SAH cascade insults when compared with those in the sham group. However, there was an evident upregulation of these two proteins observed after the treatment of irisin (**Figures 6B–D**). Furthermore, although the SAH stroke may stimulate the UCP-2 increase by a feedback regulation mechanism, the irisin treatment enhanced this promotion of UCP-2 in the SAH + irisin group (**Figures 6B,E**).

The Neuroprotective Effects of Irisin Were Reversed by the Inhibition of UCP-2

Our data showed that genipin significantly reversed the neuroprotective effects of irisin after SAH. Firstly, in the preliminary experiment, genipin was confirmed to have no effect on neurological scores (**Supplementary Figures 1A,B**). Then, lower neurological scores of the modified Garcia scale and the beam balance test in the SAH+irisin+genipin group were obtained when compared to the SAH+irisin+vehicle group (**Figures 7A,B**). Similarly, co-immunofluorescence

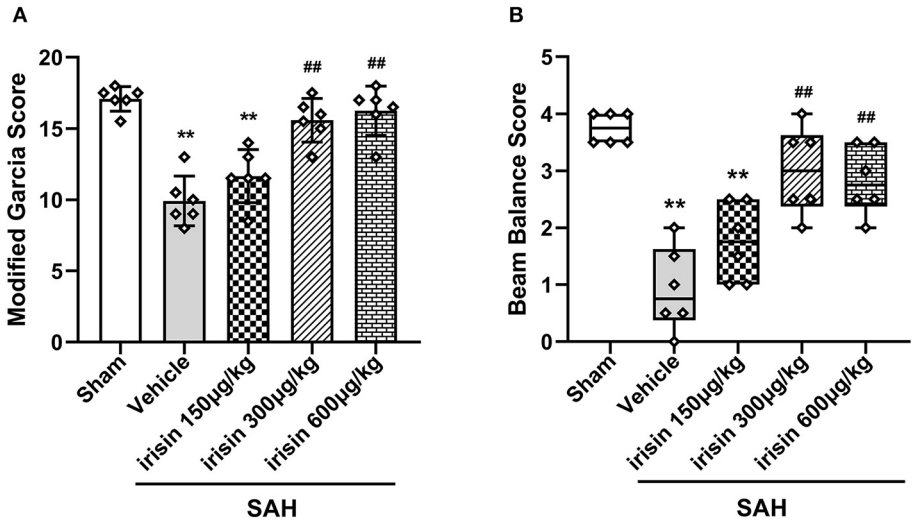

FIGURE 3 | Beneficial effects of irisin on neuronal function 24 h after SAH. **(A,B)** Treatment with irisin significantly improved neurological deficits at 24 h after SAH and 300 μg/kg irisin was selected as the effective dose, $n = 6$ per group. The modified Garcia scores were represented as mean ± SD; the one-way ANOVA was used followed by the Tukey's HSD *post-hoc* test and the Holm–Bonferroni correction method. The beam balance test scores were represented as median 25–75th percentiles, and the Mann–Whitney *U*-test and the Kruskal–Wallis test followed by the Steel–Dwass test for multiple comparisons were used to analyze the difference between groups. $^{**}P < 0.01$, $^{\#\#}P < 0.01$ vs. SAH + Vehicle group. Vehicle group, sterile 0.9% of NaCl; SAH, subarachnoid hemorrhage.

staining of neurons and apoptosis cells were applied to explore the relationship between the effects of irisin and the UCP-2 antagonist, genipin. A higher number of TUNEL-positive neurons were calculated in the SAH+irisin+Genipin group when compared to the SAH+irisin+vehicle group (**Figures 8A,B**). Semi-quantitative methods of proteins reconfirmed these results. Levels of apoptotic-related protein cleaved caspase-3, Bcl-2 and Bax were changed in the SAH+irisin+vehicle group as previously described when compared to the vehicle group. However, the application of genipin reversed the protective change (**Figures 8C,G–I**). Meanwhile, SOD2, which is an important component of antioxidant enzymes in biological systems, was decreased after the administration of genipin in the SAH+irisin+Genipin group when compared to the SAH+irisin+vehicle group (**Figures 8C,F**). Furthermore, we observed that, in the SAH+irisin+genipin group, the mitochondrial biogenesis markers, including TFAM and PGC-1α, were partially decreased after the administration of genipin, when compared to the SAH+irisin+vehicle group (**Figures 8C–E**).

DISCUSSION

Several novel findings were made in the present study: (1) endogenous irisin in the brain increased at 12 h while it decreased at 24 h after SAH; (2) intracerebroventricular administration of recombinant irisin significantly attenuated neurobehavioral deficits of the experimental mice at 24 h after SAH; (3) neuronal apoptosis and excessive oxidative stress, which were key pathologic processes in the process of EBI, could be alleviated by irisin administration; (4) the potential mechanism of the neuroprotective effects of irisin might be related to the maintenance of mitochondrial homeostasis; and (5) the inhibitor of UCP-2 partially offset the beneficial effects of exogenous irisin. Thus, irisin may regulate neuronal apoptosis and excessive oxidative stress, at least partially, through the UCP-2 pathway (**Figure 9**).

In the present study, we found that the protein level of irisin in the ipsilateral hemisphere increased at 12 h while it decreased at 24 h after injury. Interestingly, currently available evidence could not explain how this brain injury affects the expression of FNDC5 and the secretion of irisin. We found several possibilities. Firstly, in most instances, the hormones would be redistributed by the self-regulating system of the body to respond to emergencies. Thus, the irisin level increased in the compensatory period. However, at 24 h after SAH, which was reported to be the key time-point of the EBI phase, the oxidative stress and the subsequent cascade response may disturb the self-regulation and reduce the irisin levels. Secondly, the normal movement of the post-SAH mice would be reduced, thus the reduced muscle metabolism would be another reason for the downregulation of the exercise-liked irisin. Finally, the acute stroke event would affect the neuron-bone-muscle axon, which might also attenuate irisin levels after SAH.

Previous researches have gradually demonstrated the neuroprotective roles of irisin (Li et al., 2017; Asadi et al., 2018; Tu et al., 2018; Lourenco et al., 2019; Wu H. et al., 2019). In the experimental models of neurodegenerative disorders, irisin showed remarkable abilities in memory enhancing and synaptic remodeling (Kim and Song, 2018; Lourenco et al., 2019). Meanwhile, in brain injury models, the beneficial roles of

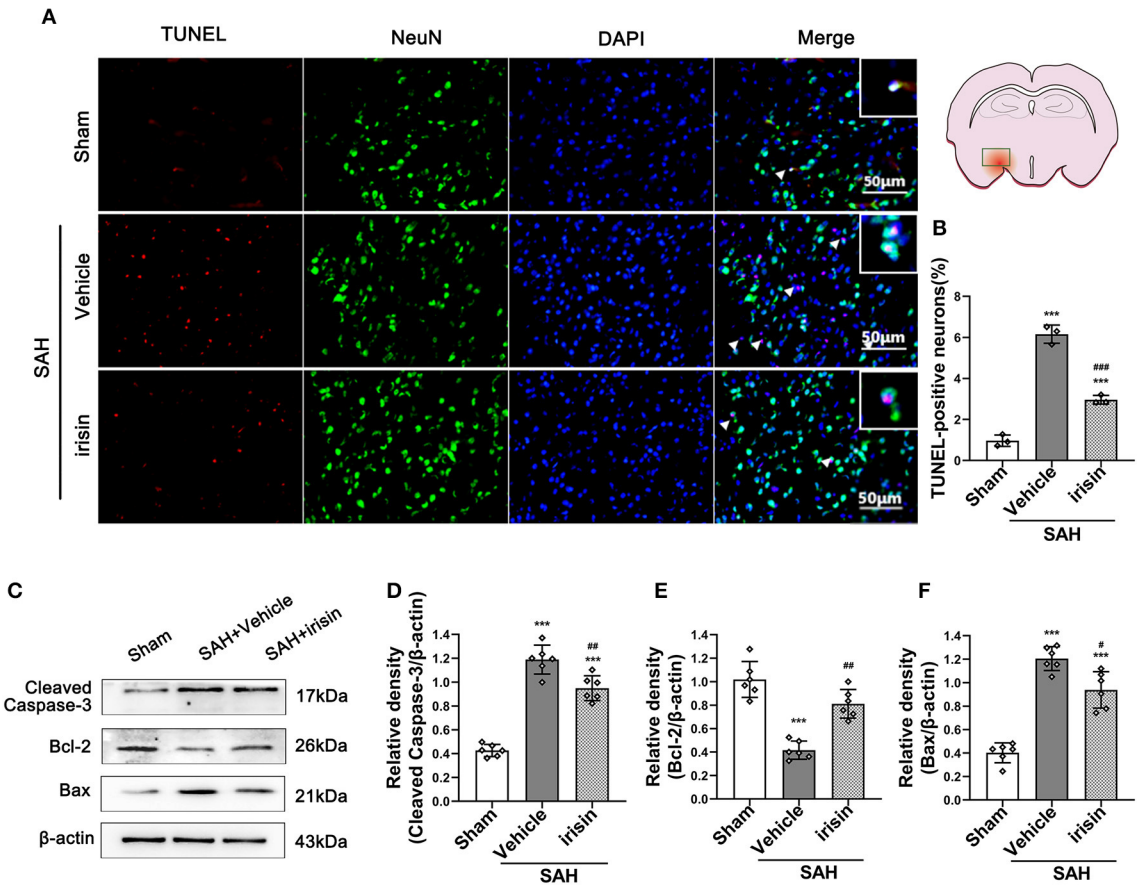

FIGURE 4 | Anti-apoptosis effects of exogenous irisin treatment on neurons 24 h after SAH. **(A,B)** TUNEL-positive neurons were significantly decreased after exogenous irisin administration. Scale bar = 50 μm, $n = 3$ for each group. **(C–F)** Representative western blotting images and relative density analysis of Bax, Bcl-2, and cleaved caspase-3 at 24 h after SAH. Exogenous irisin treatment significantly improved the expressions of Bcl-2 **(E)** and result in a decreased level of apoptotic marker cleaved caspase-3 **(D)** and Bax **(F)**, $n = 6$ for each group. Data were presented as mean ± SD. The one-way ANOVA was used followed by the Tukey's HSD *post-hoc* test and the Holm–Bonferroni correction method. $^{***}P < 0.001$ vs. Sham group; $^{\#}P < 0.05$, $^{\#\#}P < 0.01$, $^{\#\#\#}P < 0.001$ vs. SAH+Vehicle group. Vehicle group, sterile 0.9% of NaCl; TUNEL, TdT-UTP nick end labeling.

irisin are thought to be exerted against the deterioration of these cascade lesions in EBI, especially about the apoptosis and the oxidative stress (Li et al., 2017; Guo et al., 2019). For example, Guo et al. (2019) suggested that irisin peptide could attenuate brain damage both morphologically and functionally, as well as protect the blood–brain barrier (BBB) from disruption after focal cerebral ischemia/reperfusion. In line with this, Li et al. (2017) demonstrated that, by activating the Akt and ERK1/2 signaling pathways, irisin can reduce ischemia-induced neuronal injury. After brain ischemic stroke, exogenous irisin treatment inhibited the activation of Iba-1^{+} and MPO-1^{+} cells, which are the markers of microglia and neutrophils. Meanwhile, the expression of pro-inflammatory cytokines mRNA as IL-6 and TNF-α were reduced. More importantly, the levels of the oxidative stress parameters, involving nitrotyrosine (NO2-Tyr), superoxide anion, 4-hydroxynonenal (4-HNE), were also decreased after irisin administration. This evidence indicated the potential anti-inflammatory and antioxidant properties of irisin. In clinical research, irisin was also reported as a prognostic indicator in patients after ischemic stroke (Tu et al., 2018; Wu H. et al., 2019).

Neuronal apoptosis, which directly leads to neuronal death and function loss, was thought to be one of the main reasons for neurological deficits (Pang et al., 2018). Accumulative evidence displayed that irisin can play an anti-apoptotic role in multiple disease models (Natalicchio et al., 2017; Askari et al., 2018; Pang et al., 2018; Storlino et al., 2020). Even in the brain stroke models, researchers have validated the property of irisin. As Asadi et al. (2018) reported, irisin peptide could protect brain tissues against ischemic damage by reducing neural apoptosis. Meanwhile, irisin administration reduced brain edema without disturbing BBB permeability. In the present study, TUNEL-positive cells were decreased after irisin administration. Also, the pro-apoptotic marker Bax and caspase-3 activation were significantly reduced, while the anti-apoptotic marker Bcl-2 was increased in the irisin-treated group after SAH. These results revealed irisin represented an anti-apoptotic effect after SAH.

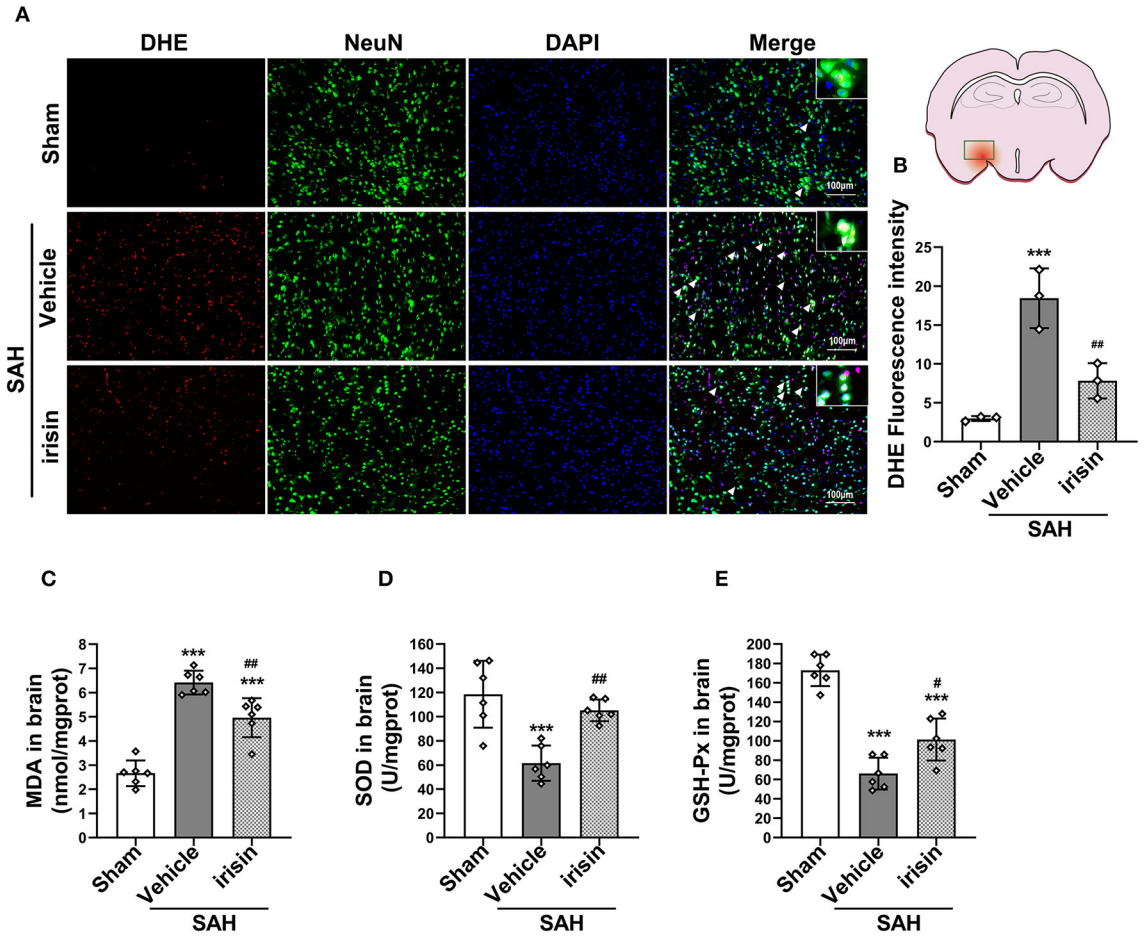

FIGURE 5 | Effect of exogenous irisin treatment on SAH-induced oxidative stress 24 h after SAH. **(A,B)** A lower red fluorescence intensity (DHE) was observed in the irisin-intervened group, Scale bar = 100 μm, $n = 3$ for each group. **(C)** Levels of oxidative markers were analyzed, MDA levels were significantly decreased after irisin treatment. **(D,E)** SOD and GSH-PX levels were increased with the irisin intervention, $n = 6$ for each group. Data were presented as mean ± SD. The one-way ANOVA was used followed by the Tukey's HSD *post-hoc* test and the Holm–Bonferroni correction method. $^{***}P < 0.001$ vs. Sham group; $^{\#}P < 0.05$, $^{\#\#}P < 0.01$ vs. SAH + Vehicle group. Vehicle, sterile 0.9% of NaCl; DHE, dihydroethidium; SOD, Superoxide Dismutase; GSH-PX, Glutathione Peroxidase Activity.

Notably, excessive oxidative stress could also trigger neuronal apoptosis, which is one of the common characteristics of EBI (Mo et al., 2019; Pang et al., 2019). As our previous study expounded, strategies to block oxidative stress-related pathways could improve the outcomes after SAH (Pang et al., 2018). The ROS, which would be excessively produced after acute brain injury, was recognized as the crucial factor in the oxidative stress reaction (Fan et al., 2017). When the endogenous anti-oxidant system could not effectively scavenge ROS, oxidative stress was aggravated, followed by cell death (Le Belle et al., 2011). Consistent with our findings, irisin has been shown to have a latent anti-oxidative property (Li et al., 2017; Askari et al., 2018; Bi et al., 2019). Our data showed that irisin administration could reduce oxidative stress as measured by the expression of anti-ROS markers, SOD and GSH-PX, and the pro-ROS marker, MDA, as well as DHE staining. It is not clear, however, how irisin mediates these interlaced pathological processes after SAH.

Cerebral metabolism is highly active, and the maintenance of these metabolic activities depends on the energy provided by mitochondria. After brain damage, the energy engine, mitochondria, could not meet the urgently needed energy demand (Sheng and Cai, 2012). Then, the imbalance of mitochondrial dynamics would be the initial process of numerous deleterious cascades, including inflammatory infiltration, cell apoptosis, excessive ROS generation, and oxidative stress damage (Sims and Muyderman, 2010). These pathological processes commonly develop in the EBI process as previously mentioned in Mo et al. (2019). However, to maintain homeostasis, mitochondria are continually undergoing division and fusion (Fan et al., 2017). More importantly, mitochondrial biogenesis is also happening, which is one of the main ways to supplement the nascent mitochondria (Pfanner et al., 2019).

As previously reported, mitochondrial morphology is vital for sustaining mitochondrial dynamics after cerebral injury (Wei

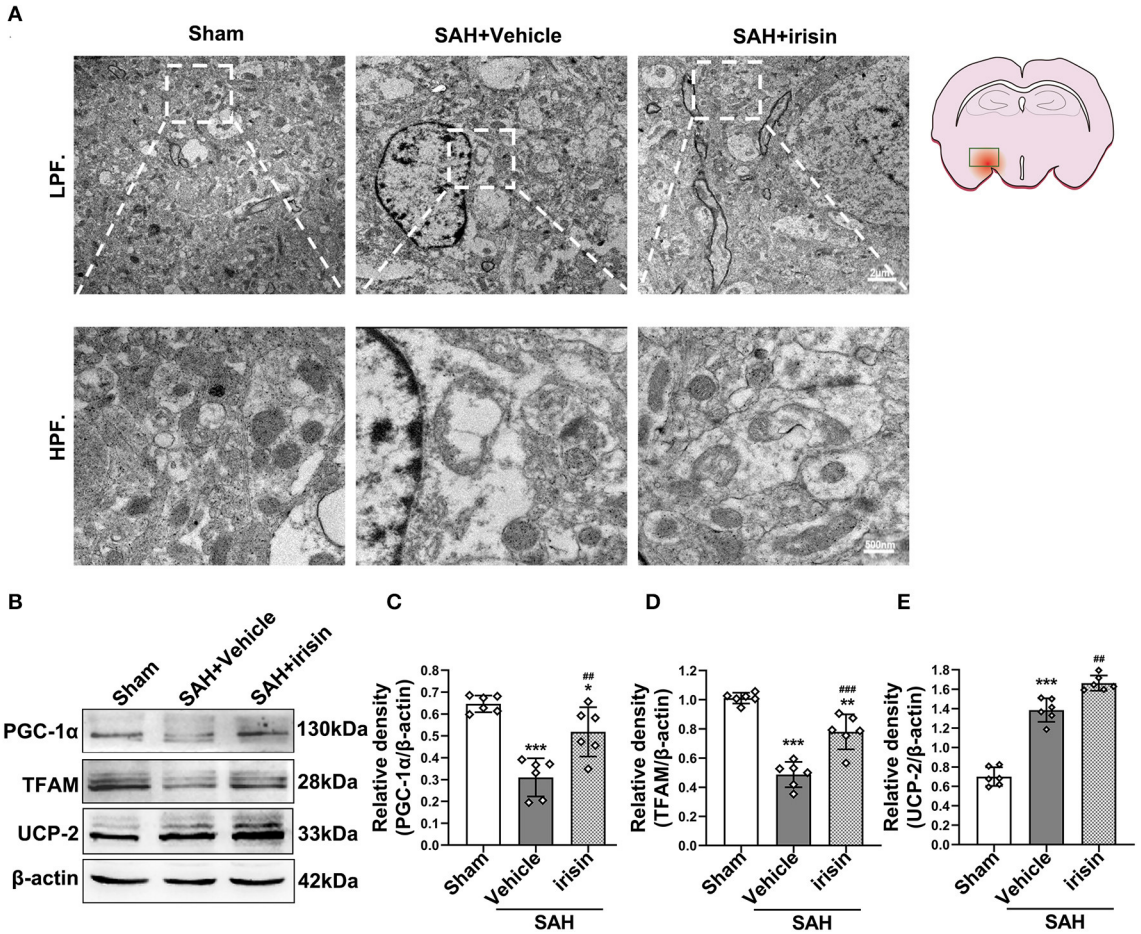

FIGURE 6 | Effect of exogenous irisin treatment on mitochondrial morphology and mitochondrial biogenesis in mice brain 24 h after SAH. **(A)** Less mitochondrial swelling and vacuolization were observed under the TEM after irisin treatment, Scale bar = 2 μm, 500 nm, $n = 3$ for each group. **(B–E)** Representative western blotting images and relative density analysis of TFAM, PGC-1α, and UCP-2 24 h after SAH. Exogenous irisin treatment significantly improved the expressions of TFAM and PGC-1α. The UCP-2 expression increased after SAH and a higher level was observed after irisin treatment, $n = 6$ for each group. All data were presented as mean ± SD. The one-way ANOVA was used followed by the Tukey's HSD *post-hoc* test and the Holm–Bonferroni correction method. $^{*}P < 0.05$, $^{**}P < 0.01$, $^{***}P < 0.001$ vs. Sham group; $^{\#\#}P < 0.01$, $^{\#\#\#}P < 0.001$ vs. SAH + Vehicle group. Vehicle group, sterile 0.9% of NaCl; UCP-2, Uncoupling Protein-2; SAH, subarachnoid hemorrhage.

et al., 2019; Lai et al., 2020). In our current study, the results observed from TEM indicated that nascent mitochondria were increased, with less vacuole and less swelling mitochondria after irisin treatment. The mitochondrial transcription factor A (TFAM), was also evaluated to be increased by the irisin treatment after SAH. In parallel, the increased expression of PGC-1α was observed in the irisin treatment group. Previous studies revealed that in the regulation of the mitochondrial biological activities, especially for mitochondrial biogenesis, PGC-1α played a crucial role (Fernandez-Marcos and Auwerx, 2011). Recent literature also confirmed that the upregulation of neuronal PGC-1 α, the nodal regulator of mitochondrial biogenesis, would help to ameliorate cognitive impairment induced by chronic cerebral hypoperfusion (Han et al., 2020). Thus, these results indicated that irisin may be performing the roles of maintaining mitochondria morphology, as well as promoting mitochondrial biogenesis to complement the normal mitochondria after SAH. Since the normal mitochondrial functions were maintained, subsequent cascades, including apoptosis and oxidative stress, would be alleviated.

Numerous molecular regulatory processes might be related to mitochondrial biogenesis (Pfanner et al., 2019). It is noteworthy that UCP-2, an endogenous inducible protein located in the inner membrane of mitochondria, is thought to be one of the protagonists in the UCP family for regulating mitochondrial metabolism and ROS generation (Mattiasson et al., 2003; Mattiasson and Sullivan, 2006; Mailloux and Harper, 2011). By promoting mitochondrial biogenesis, UCP-2 can directly regulate synaptic plasticity and neurotransmission, which are important in supporting neuron function and survival (Pfanner et al., 2019). Notably, the UCP-2 protein level increased after the SAH in our experiment, which is in line with a previous study

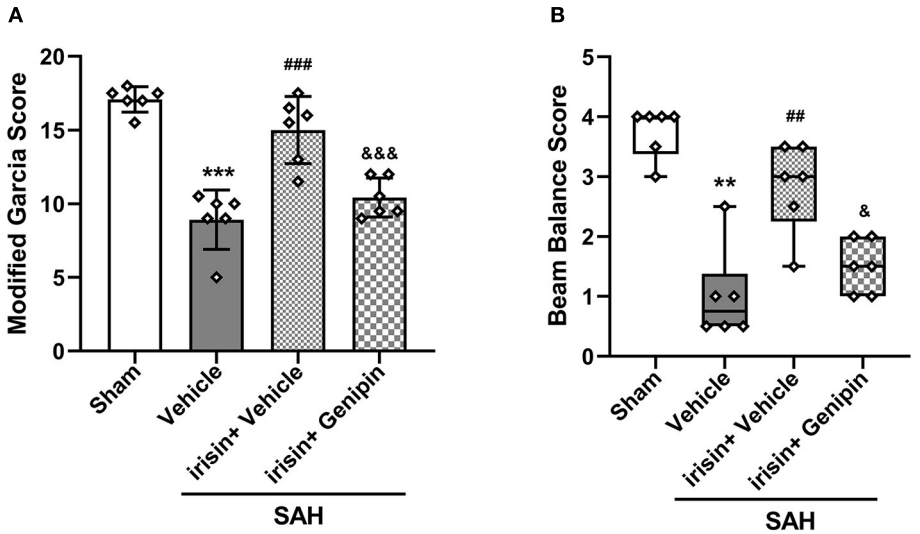

FIGURE 7 | Inhibition of UCP-2 pathway blunted the beneficial effect of irisin treatment on short-term neurologic function after SAH. **(A,B)** Genipin significantly blunted the protective effect of irisin treatment on neurological deficits at 24 h after SAH, $n = 6$ for each group. The modified Garcia test scores were represented as mean ± SD; the one-way ANOVA was used followed by the Tukey's HSD *post-hoc* test and the Holm–Bonferroni correction method. The beam balance test scores were represented as median 25th−75th percentiles, and the Mann–Whitney *U*-test and the Kruskal–Wallis test followed by the Steel–Dwass method of multiple comparisons were used to analyze the difference between groups. $^{**}P < 0.01$, $^{***}P < 0.001$ vs. Sham group; $^{\#\#}P < 0.01$, $^{\#\#\#}P < 0.001$ vs. SAH + Vehicle group; $^{\&}P < 0.05$, $^{\&\&\&}P < 0.001$ vs. SAH + irisin + Vehicle group. Vehicle group, sterile 0.9% of NaCl; SAH, subarachnoid hemorrhage.

(Mo et al., 2019). Early brain damage could lead to excessive ROS production, subsequently, activating UCP-2 to induce proton leak (Mailloux and Harper, 2011; Mo et al., 2019). After brain injury, the UCP-2 promotion could be a self-protective regulatory mechanism, for it could provide negative feedback for ROS production (Mailloux and Harper, 2011). Strikingly, after the irisin treatment, the level of UCP-2 protein was further increased, which was in parallel with the increase of the mitochondrial biogenesis marker proteins. Consistent with our conjecture, the inhibition of UCP-2 by genipin decreased the PGC-1α and TFAM levels, indicating that the mitochondrial biogenesis process would be impacted partially. In agreement with these observations, we further found that the inhibition of UCP-2 significantly reversed the anti-apoptosis and anti-oxidative stress effects of irisin. These results revealed an important functional loop between mitochondrial biogenesis and irisin, which might be, at least in part, regulated by UCP-2 protein.

It is noteworthy that exercise is closely related to the level of increase of the endogenous irisin. Meanwhile, irisin is determined as one of the endogenous molecules to exert neuroprotective effects (Li et al., 2017; Lourenco et al., 2019). For those suffering from acute or chronic nervous system disorders, physical exercise is well-accepted as an effective approach for reducing the risk of illness and improving the outcomes of patients (Dobkin, 2008; Tan et al., 2014). On the other hand, the rupture of intracranial aneurysm is one of the main incentives of SAH; thus, the patients who bear intracranial aneurysm would be advised not to do strenuous exercise; otherwise, it could cause a ruptured aneurysm. Our research might help to establish alternative approaches for those patients to share the exercise benefits, while more clinical data are needed to support the notion.

There are still several limitations to our study. Firstly, in the system of skeletal and muscle, the receptor (s) of irisin has been gradually excavated (Kim et al., 2018; Farmer, 2019). However, the irisin related receptor (s) and targets in CNS are still needed to be identified in future studies. Second, this study focused on irisin-mediated mitochondrial biogenesis and UCP-2 related targets. We could not exclude that the neuroprotective effects of irisin were the results of other forms of mitochondria protections. Third, although the intracerebroventricular administration of irisin assured the protein could perform its roles in CNS, a cross-talk of the influence between the irisin serum concentration and cerebrospinal fluid (CSF) should be illustrated more clearly. The relevance of actual irisin plasma levels with or without exercise would be researched in future studies. Last, considering the numerable variables of the female rodents and the influence of estrogen, we only used male mice for this study. The results would be more convincing if the experiment could be carried out in both female and male mice.

CONCLUSION

The current study suggests that irisin exerts anti-apoptosis and anti-oxidative stress roles in the process of the EBI phase after experimental SAH, potentially by maintaining mitochondrial homeostasis. Focusing on metabolic-related cytokine and targeting mitochondria-centered pathological cascades, a novel therapeutic strategy to address the challenges in EBI is emerging.

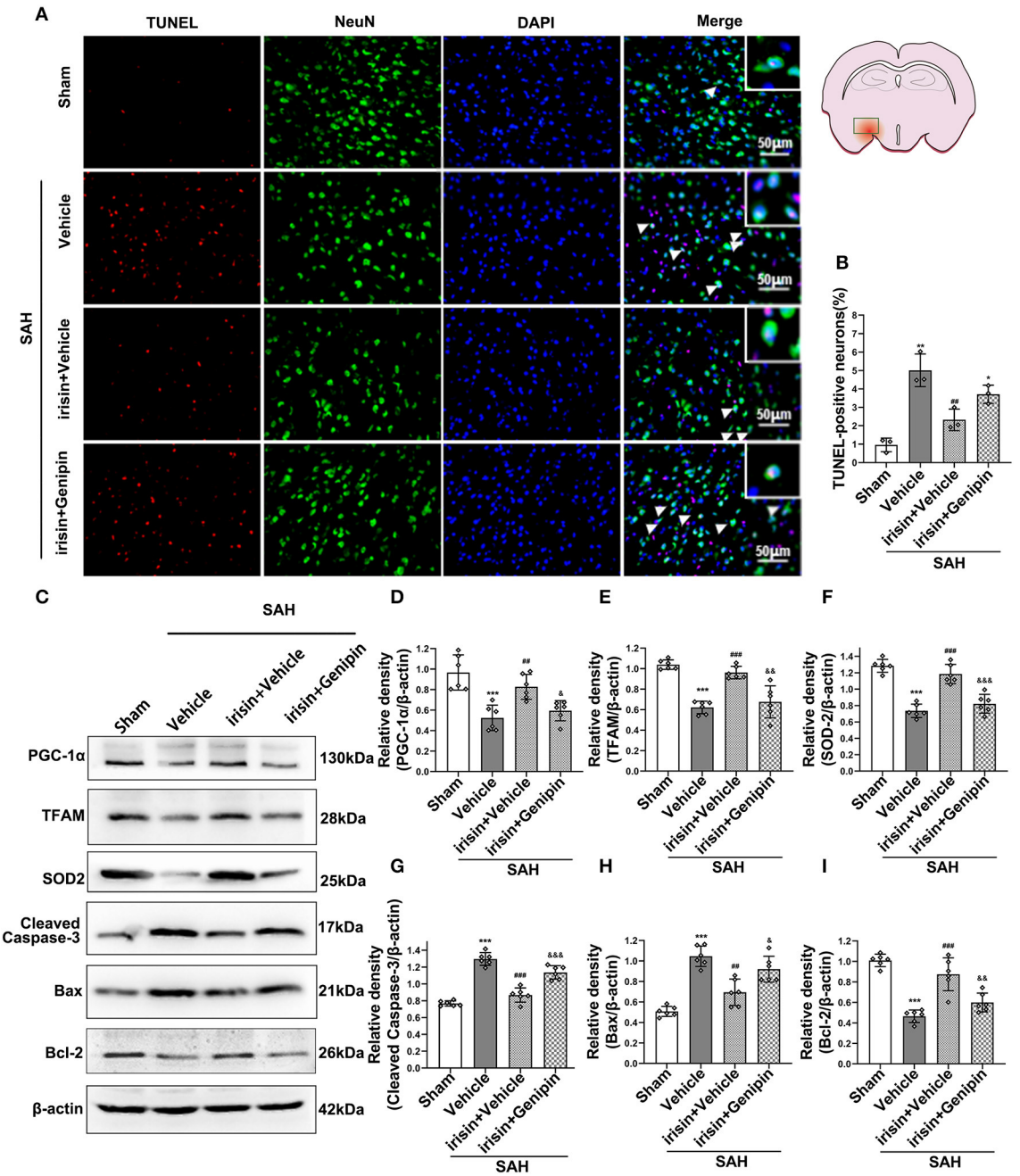

FIGURE 8 | Inhibition of UCP-2 pathway reversed the beneficial effects of irisin on apoptosis, mitochondrial function, and oxidative stress after SAH. **(A,B)** TUNEL-positive neurons were significantly increased after genipin administration in the irisin treatment group. Scale bar = 50 μm, $n = 3$ for each group (The area of observation was circled in red). **(C–I)** Representative western blotting images and relative density analysis of proteins related to mitochondrial biogenesis (TFAM, PGC-1α), oxidative stress (SOD2), and apoptotic markers (Cleaved caspase-3, Bax, Bcl-2) at 24 h after SAH. As an exogenous UCP-2 inhibitor, genipin significantly blunted the expressions of PGC-1α, TFAM, SOD2, and Bcl-2 **(D,E,F,I)** and resulted in an increased level of cleaved caspase-3 and Bax **(G,H),** $n = 6$ for each group. All data were presented as mean ± SD. The one-way ANOVA was used followed by the Tukey's HSD *post-hoc* test and the Holm–Bonferroni correction method. $^{*}P < 0.05$, $^{**}P < 0.01$, $^{***}P < 0.001$ vs. Sham group; $^{\#\#}P < 0.01$, $^{\#\#\#}P < 0.001$ vs. SAH + Vehicle group. $^{\&}P < 0.05$, $^{\&\&}P < 0.01$, $^{\&\&\&}P < 0.001$ vs. SAH + irisin + Vehicle group. Vehicle group, sterile 0.9% of NaCl; TUNEL, TdT-UTP nick end labeling; SOD, Superoxide Dismutase; UCP-2, Uncoupling Protein-2.

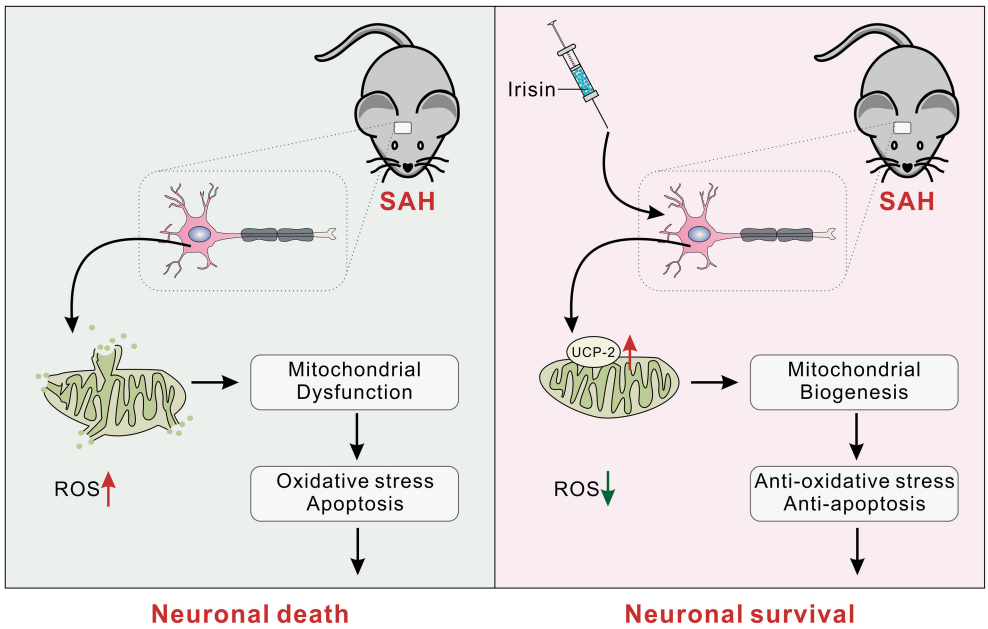

FIGURE 9 | The schematic of irisin on mitochondrial biogenesis following SAH. SAH, subarachnoid hemorrhage.

DATA AVAILABILITY STATEMENT

The original contributions presented in the study are included in the article/**Supplementary Material**, further inquiries can be directed to the corresponding author/s.

ETHICS STATEMENT

The animal study was reviewed and approved by Animal Committee of the Ethics Committee of Southwest Medical University.

AUTHOR CONTRIBUTIONS

TT designed and performed the experiment, collected and analyzed the data, and prepared the manuscript. SY and JPa were involved in the experiment design. XZ, LZ, and YZ were involved in behavioral testing and biochemical analysis. YX and KG were involved in preparing the animal models and participated in interpreting the results. LC participated in the manuscript revision. JPe and YJ contributed to the study concept and design, secured funding for the project, and prepared and critically revised the manuscript. All authors contributed to the article and approved the submitted version.

FUNDING

This work was supported by grants from the Young Elite Scientist Sponsorship Program by the China Association for Science and Technology, the National Natural Science Foundation of China (81771278, 81801176, and 81971132), and the Sichuan Science and Technology Program (2019JDTD0004 and 2019JDRC0062).

SUPPLEMENTARY MATERIAL

The Supplementary Material for this article can be found online at: https://www.frontiersin.org/articles/10.3389/fnagi.2021.640215/full#supplementary-material

REFERENCES

Asadi, Y., Gorjipour, F., Behrouzifar, S., and Vakili, A. (2018). Irisin peptide protects brain against ischemic injury through reducing apoptosis and enhancing BDNF in a rodent model of stroke. *Neurochem. Res.* 43, 1549–1560. doi: 10.1007/s11064-018-2569-9

Askari, H., Rajani, S. F., Poorebrahim, M., Haghi-Aminjan, H., Raeis-Abdollahi, E., and Abdollahi, M. (2018). A glance at the therapeutic potential of irisin against diseases involving inflammation, oxidative stress, and apoptosis: an introductory review. *Pharmacol. Res.* 129, 44–55. doi: 10.1016/j.phrs.2018.01.012

Bi, J., Zhang, J., Ren, Y., Du, Z., Li, Q., Wang, Y., et al. (2019). Irisin alleviates liver ischemia-reperfusion injury by inhibiting excessive mitochondrial fission, promoting mitochondrial biogenesis and decreasing oxidative stress. *Redox Biol.* 20, 296–306. doi: 10.1016/j.redox.2018.10.019

Bolanos, J. P., Moro, M. A., Lizasoain, I., and Almeida, A. (2009). Mitochondria and reactive oxygen and nitrogen species in neurological disorders and stroke: therapeutic implications. *Adv. Drug Deliv. Rev.* 61, 1299–1315. doi: 10.1016/j.addr.2009.05.009

Bostrom, P., Wu, J., Jedrychowski, M. P., Korde, A., Ye, L., Lo, J. C., et al. (2012). A PGC1-alpha-dependent myokine that drives brown-fat-like development of white fat and thermogenesis. *Nature* 481, 463–468. doi: 10.1038/nature10777

Cahill, J., Calvert, J. W., and Zhang, J. H. (2006). Mechanisms of early brain injury after subarachnoid hemorrhage. *J. Cereb. Blood Flow Metab.* 26, 1341–1353. doi: 10.1038/sj.jcbfm.9600283

Cahill, J., and Zhang, J. H. (2009). Subarachnoid hemorrhage: is it time for a new direction? *Stroke* 40, S86–87. doi: 10.1161/STROKEAHA.108.533315

Dobkin, B. H. (2008). Training and exercise to drive poststroke recovery. *Nat. Clin. Pract. Neurol.* 4, 76–85. doi: 10.1038/ncpneuro0709

Dun, S. L., Lyu, R. M., Chen, Y. H., Chang, J. K., Luo, J. J., and Dun, N. J. (2013). Irisin-immunoreactivity in neural and non-neural cells of the rodent. *Neuroscience* 240, 155–162. doi: 10.1016/j.neuroscience.2013.02.050

Fan, L. F., He, P. Y., Peng, Y. C., Du, Q. H., Ma, Y. J., Jin, J. X., et al. (2017). Mdivi-1 ameliorates early brain injury after subarachnoid hemorrhage via the suppression of inflammation-related blood-brain barrier disruption and endoplasmic reticulum stress-based apoptosis. *Free Radic. Biol. Med.* 112, 336–349. doi: 10.1016/j.freeradbiomed.2017.08.003

Farmer, S. R. (2019). Boning up on irisin. *N. Engl. J. Med.* 380, 1480–1482. doi: 10.1056/NEJMcibr1900041

Fernandez-Marcos, P. J., and Auwerx, J. (2011). Regulation of PGC-1alpha, a nodal regulator of mitochondrial biogenesis. *Am. J. Clin. Nutr.* 93, 884S—890S. doi: 10.3945/ajcn.110.001917

Gao, X., Wang, Y. C., Liu, Y., Yue, Q., Liu, Z., Ke, M., et al. (2017). Nanoagonist-mediated endothelial tight junction opening: a strategy for safely increasing brain drug delivery in mice. *J. Cereb. Blood Flow Metab.* 37, 1410–1424. doi: 10.1177/0271678X16656198

Guo, P., Jin, Z., Wu, H., Li, X., Ke, J., Zhang, Z., et al. (2019). Effects of irisin on the dysfunction of blood-brain barrier in rats after focal cerebral ischemia/reperfusion. *Brain Behav.* 9:e01425. doi: 10.1002/brb3.1425

Hagberg, H., Mallard, C., Rousset, C. I., and Thornton, C. (2014). Mitochondria: hub of injury responses in the developing brain. *Lancet Neurol.* 13, 217–232. doi: 10.1016/S1474-4422(13)70261-8

Han, B., Jiang, W., Liu, H., Wang, J., Zheng, K., Cui, P., et al. (2020). Upregulation of neuronal PGC-1alpha ameliorates cognitive impairment induced by chronic cerebral hypoperfusion. *Theranostics* 10, 2832–2848. doi: 10.7150/thno.37119

Hayakawa, K., Esposito, E., Wang, X., Terasaki, Y., Liu, Y., Xing, C., et al. (2016). Transfer of mitochondria from astrocytes to neurons after stroke. *Nature* 535, 551–555. doi: 10.1038/nature18928

Hocking, S., Samocha-Bonet, D., Milner, K. L., Greenfield, J. R., and Chisholm, D. J. (2013). Adiposity and insulin resistance in humans: the role of the different tissue and cellular lipid depots. *Endocr. Rev.* 34, 463–500. doi: 10.1210/er.2012-1041

Kim, H., Wrann, C. D., Jedrychowski, M., Vidoni, S., Kitase, Y., Nagano, K., et al. (2018). Irisin mediates effects on bone and fat via alphaV integrin receptors. *Cell* 175, 1756–1768 e1717. doi: 10.1016/j.cell.2018.10.025

Kim, O. Y., and Song, J. (2018). The role of irisin in Alzheimer's disease. *J. Clin. Med.* 7:407. doi: 10.3390/jcm7110407

Lai, Y., Lin, P., Chen, M., Zhang, Y., Chen, J., Zheng, M., et al. (2020). Restoration of L-OPA1 alleviates acute ischemic stroke injury in rats via inhibiting neuronal apoptosis and preserving mitochondrial function. *Redox Biol.* 34:101503. doi: 10.1016/j.redox.2020.101503

Lawton, M. T., and Vates, G. E. (2017). Subarachnoid hemorrhage. *N. Engl. J. Med.* 377, 257–266. doi: 10.1056/NEJMcp1605827

Le Belle, J. E., Orozco, N. M., Paucar, A. A., Saxe, J. P., Mottahedeh, J., Pyle, A. D., et al. (2011). Proliferative neural stem cells have high endogenous ROS levels that regulate self-renewal and neurogenesis in a PI3K/Akt-dependant manner. *Cell Stem Cell* 8, 59–71. doi: 10.1016/j.stem.2010.11.028

Li, D. J., Li, Y. H., Yuan, H. B., Qu, L. F., and Wang, P. (2017). The novel exercise-induced hormone irisin protects against neuronal injury via activation of the Akt and ERK1/2 signaling pathways and contributes to the neuroprotection of physical exercise in cerebral ischemia. *Metab. Clin. Exp.* 68, 31–42. doi: 10.1016/j.metabol.2016.12.003

Lourenco, M. V., Frozza, R. L., de Freitas, G. B., Zhang, H., Kincheski, G. C., Ribeiro, F. C., et al. (2019). Exercise-linked FNDC5/irisin rescues synaptic plasticity and memory defects in Alzheimer's models. *Nat. Med.* 25, 165–175. doi: 10.1038/s41591-018-0275-4

Mailloux, R. J., and Harper, M. E. (2011). Uncoupling proteins and the control of mitochondrial reactive oxygen species production. *Free Radic. Biol. Med.* 51, 1106–1115. doi: 10.1016/j.freeradbiomed.2011.06.022

Mattiasson, G., Shamloo, M., Gido, G., Mathi, K., Tomasevic, G., Yi, S., et al. (2003). Uncoupling protein-2 prevents neuronal death and diminishes brain dysfunction after stroke and brain trauma. *Nat. Med.* 9, 1062–1068. doi: 10.1038/nm903

Mattiasson, G., and Sullivan, P. G. (2006). The emerging functions of UCP2 in health, disease, and therapeutics. *Antioxid. Redox Signal.* 8, 1–38. doi: 10.1089/ars.2006.8.1

Mo, J., Enkhjargal, B., Travis, Z. D., Zhou, K., Wu, P., Zhang, G., et al. (2019). AVE 0991 attenuates oxidative stress and neuronal apoptosis via Mas/PKA/CREB/UCP-2 pathway after subarachnoid hemorrhage in rats. *Redox Biol.* 20, 75–86. doi: 10.1016/j.redox.2018.09.022

Natalicchio, A., Marrano, N., Biondi, G., Spagnuolo, R., Labarbuta, R., Porreca, I., et al. (2017). The myokine irisin is released in response to saturated fatty acids and promotes pancreatic beta-cell survival and insulin secretion. *Diabetes* 66, 2849–2856. doi: 10.2337/db17-0002

Pang, J., Peng, J., Matei, N., Yang, P., Kuai, L., Wu, Y., et al. (2018). Apolipoprotein E exerts a whole-brain protective property by promoting M1? Microglia quiescence after experimental subarachnoid hemorrhage in mice. *Transl. Stroke Res.* 9, 654–668. doi: 10.1007/s12975-018-0665-4

Pang, J., Peng, J., Yang, P., Kuai, L., Chen, L., Zhang, J. H., et al. (2019). White matter injury in early brain injury after subarachnoid hemorrhage. *Cell Transplant* 28, 26–35. doi: 10.1177/0963689718812054

Peng, J., Pang, J., Huang, L., Enkhjargal, B., Zhang, T., Mo, J., et al. (2019a). LRP1 activation attenuates white matter injury by modulating microglial polarization through Shc1/PI3K/Akt pathway after subarachnoid hemorrhage in rats. *Redox Biol.* 21:101121. doi: 10.1016/j.redox.2019.101121

Peng, J., Wu, Y., Pang, J., Sun, X., Chen, L., Chen, Y., et al. (2019b). Single clip: an improvement of the filament-perforation mouse subarachnoid haemorrhage model. *Brain Inj.* 33, 701–711. doi: 10.1080/02699052.2018.1531310

Pfanner, N., Warscheid, B., and Wiedemann, N. (2019). Mitochondrial proteins: from biogenesis to functional networks. *Nat. Rev. Mol. Cell Biol.* 20, 267–284. doi: 10.1038/s41580-018-0092-0

Piya, M. K., Harte, A. L., Sivakumar, K., Tripathi, G., Voyias, P. D., James, S., et al. (2014). The identification of irisin in human cerebrospinal fluid: influence of adiposity, metabolic markers, and gestational diabetes. *Am. J. Physiol. Endocrinol. Metab.* 306, E512–E518. doi: 10.1152/ajpendo.00308.2013

Ruan, Q., Zhang, L., Ruan, J., Zhang, X., Chen, J., Ma, C., et al. (2018). Detection and quantitation of irisin in human cerebrospinal fluid by tandem mass spectrometry. *Peptides* 103, 60–64. doi: 10.1016/j.peptides.2018.03.013

Sheng, Z. H., and Cai, Q. (2012). Mitochondrial transport in neurons: impact on synaptic homeostasis and neurodegeneration. *Nat. Rev. Neurosci.* 13, 77–93. doi: 10.1038/nrn3156

Sims, N. R., and Muyderman, H. (2010). Mitochondria, oxidative metabolism and cell death in stroke. *Biochim. Biophys. Acta* 1802, 80–91. doi: 10.1016/j.bbadis.2009.09.003

Storlino, G., Colaianni, G., Sanesi, L., Lippo, L., Brunetti, G., Errede, M., et al. (2020). Irisin prevents disuse-induced osteocyte apoptosis. *J. Bone Miner. Res.* 35, 766–775. doi: 10.1002/jbmr.3944

Tan, C. O., Meehan, W. P. III., Iverson, G. L., and Taylor, J. A. (2014). Cerebrovascular regulation, exercise, and mild traumatic brain injury. *Neurology* 83, 1665–1672. doi: 10.1212/WNL.0000000000000944

Tu, T., Peng, J., and Jiang, Y. (2020). FNDC5/Irisin: a new protagonist in acute brain injury. *Stem Cells Dev.* 29, 533–543. doi: 10.1089/scd.2019.0232

Tu, W. J., Qiu, H. C., Cao, J. L., Liu, Q., Zeng, X. W., and Zhao, J.Z. (2018). Decreased concentration of irisin is associated with poor functional outcome in ischemic stroke. *Neurotherapeutics* 15, 1158–1167. doi: 10.1007/s13311-018-0651-2

Wei, N., Pu, Y., Yang, Z., Pan, Y., and Liu, L. (2019). Therapeutic effects of melatonin on cerebral ischemia reperfusion injury: role of Yap-OPA1 signaling pathway and mitochondrial fusion. *Biomed. Pharmacother.* 110, 203–212. doi: 10.1016/j.biopha.2018.11.060

Wu, H., Guo, P., Jin, Z., Li, X., Yang, X., Tang, C., et al. (2019). Serum levels of irisin predict short-term outcomes in ischemic stroke. *Cytokine* 122:154303. doi: 10.1016/j.cyto.2018.02.017

Wu, Y., Pang, J., Peng, J., Cao, F., Guo, Z., Jiang, L., et al. (2019). Apolipoprotein E deficiency aggravates neuronal injury by enhancing neuroinflammation via the JNK/c-jun pathway in the early phase of experimental subarachnoid hemorrhage in mice. *Oxid. Med. Cell. Longev.* 2019:3832648. doi: 10.1155/2019/3832648

Xie, Y., Peng, J., Pang, J., Guo, K., Zhang, L., Yin, S., et al. (2020). Biglycan regulates neuroinflammation by promoting M1 microglial activation in early brain injury after experimental subarachnoid hemorrhage. *J. Neurochem.* 152, 368–380. doi: 10.1111/jnc.14926

Conflict of Interest: The authors declare that the research was conducted in the absence of any commercial or financial relationships that could be construed as a potential conflict of interest.

frontiers in Aging Neuroscience

ORIGINAL RESEARCH
published: 25 February 2021
doi: 10.3389/fnagi.2021.626334

Reduced Superficial Capillary Density in Cerebral Infarction Is Inversely Correlated With the NIHSS Score

William Robert Kwapong†, Yuying Yan†, Zilong Hao and Bo Wu**

Department of Neurology, West China Hospital, Sichuan University, Chengdu, China

Purpose: The retina and the brain share similar neuronal and microvascular features, therein we aimed to assess the structural and microvascular changes in the macula and choriocapillaris (CC) in patients with cerebral infarction when compared with healthy controls using optical coherence tomography angiography (OCTA).

Methods: OCTA was used to image and measure the capillary density in the radial peripapillary capillaries (RPC), superficial capillary plexus (SCP), deep capillary plexus (DCP), choriocapillaris (CC), and mean area of the foveal avascular zone (FAZ) in all participants. Twenty-two cerebral infarction patients based on their magnetic resonance imaging (MRI) and 25 healthy controls were included in our study.

Results: Density of the RPC ($P < 0.001$), SCP ($P = 0.001$), DCP ($P < 0.001$) and CC ($P < 0.001$) were significantly reduced in cerebral infarction patients when compared with healthy controls, respectively. Retinal thickness measurements ($P < 0.05$) were significantly reduced in cerebral infarction patients when compared with healthy controls. The mean FAZ area was significantly larger ($P = 0.012$) in cerebral infarction patients when compared with healthy controls. National Institute of Health Stroke Scale (NIHSS) inversely correlated with SCP density in cerebral infarction patients (Rho = −0.409, $P = 0.001$). Receiver operating characteristics curve analysis showed that the blood flow of the choriocapillaris had the highest index [area under the receiver operating characteristic (AUROC) = 0.964] to discriminate cerebral infarction patients from the healthy controls.

Conclusions: Our study suggests that cerebral microcirculation dysfunction which occurs in cerebral infarction is mirrored in the macula and choroidal microcirculation. OCTA has the potential to non-invasively characterize the macula and choroidal changes in cerebral infarction *in vivo*.

Keywords: cerebral infarction, macula capillaries, choriocapillaris, optical coherence tomography angiography, foveal avascular zone

OPEN ACCESS

Edited by:
Wang Lin,
Zhejiang University, China

Reviewed by:
West Greenlee M. Heather,
Iowa State University, United States
Henri Leinonen,
University of California, Irvine, United States

****Correspondence:***
Zilong Hao,
zhilong1983@126.com
Bo Wu,
dr.bowu@hotmail.com

†These authors have contributed equally to this work and share first authorship

Received: *06 November 2020*
Accepted: *02 February 2021*
Published: *25 February 2021*

Citation:
Kwapong WR, Yan Y, Hao Z and Wu B (2021) Reduced Superficial Capillary Density in Cerebral Infarction Is Inversely Correlated With the NIHSS Score. Front. Aging Neurosci. 13:626334. doi: 10.3389/fnagi.2021.626334

INTRODUCTION

Stroke has been reported to be one of the common causes of death worldwide and is the leading cause of death in China (Zhou et al., 2019). Zhou et al. (2019) reported that with the rapid socioeconomic transition in China, the prevalence of stroke and its risk factors is bound to increase. The pathological changes of stroke involve a decrease in blood flow which leads to insufficient

oxygen and cell death in the brain and spinal cord. Unfortunately, the classical clinical manifestation of ischemic stroke, which comprises abrupt unresponsiveness in the face, arm, or leg, particularly on one side of the body, is only apparent after immense blood flow loss in the brain and cell death. Although the neurological discrepancies are typical examples of stroke sequelae, these discrepancies go together with stroke-induced visual dysfunction in over 60% of stroke cases (Rowe, 2017).

Cerebral infarction, a common incidental discovery on magnetic resonance imaging (MRI), has been reported to be linked to ischemic stroke and help foretell its development (Vermeer et al., 2007); it has also been suggested that cerebral infarction is associated with subtle neurological deficits (Vermeer et al., 2007). Nonetheless, the understanding of the pathophysiology of cerebral infarction remains inadequate. Although cerebral microcirculation dysfunction (mainly cerebral ischemia) has been suggested to play a crucial role in the disease pathogenesis of cerebral infarction, gaining more comprehension is challenging due to the scarcity of non-invasive tools that evaluate the cerebral microcirculation quantitatively and consistently.

The retina, an extension of the central nervous system, has been reported to share many neuronal and microvascular features with the brain because of their similar anatomy, physiology, and embryology (Erskine and Herrera, 2014); besides, accumulating reports (Ong et al., 2013, 2015) have suggested that retinal thickness and microvasculature reflect the microstructural and microcirculation of the brain. Recent reports have shown that the retina is a reliable route to access cerebral microcirculation because of their similarities (London et al., 2013). Previous reports (Cooper et al., 2006; Ikram et al., 2006; de Jong et al., 2008; Cheung et al., 2010) using retinal imaging tools such as the fundus camera have suggested that retinal vascular damage such as retinal hemorrhage and microaneurysms are associated with predictors of stroke, cerebral white matter lesions, and other cerebrovascular diseases. Moreover, retinal ischemia, ischemia which affects the retinal cell loss and damage of the optic nerve, has been suggested to co-exist with cerebral infarction and may be responsible for many of the visual impairments that occur in this disease (Osborne et al., 2004; Cooper et al., 2006). Nonetheless, these retinopathy manifestations have been reported to be somewhat late pointers of retinal damage and reflect the late phase of retinal microvascular and structural damage.

Optical coherence tomography angiography (OCTA) is an imaging tool that can non-invasively image the retinal and choroidal microcirculation *in vivo*; OCTA helps clinicians to visualize the retinal and choroidal capillary anastomoses at a high resolution. Advances in the imaging and quantification software of the OCTA have now enabled a more objective quantitative assessment of the capillary network in the retina and choroid, which reflect earlier and subtler changes in the retinal and choroidal microcirculation before the apparent retinal signs emerge.

In this study, we assessed whether OCTA technology has the potential to characterize the retinal structure and retinal and choroidal microvascular changes in patients with cerebral infarction.

MATERIALS AND METHODS

Data Avaliability Statement

The data that support the findings of this study are available on request from the corresponding author. The data are not publicly available due to privacy or ethical restrictions.

Study Population

Patients presenting to the Neurology Department of West China Hospital, China, were recruited from May 2020 to October 2020. Patients were included if they were Chinese, had cerebral infarction confirmed with magnetic resonance imaging (MRI), could sit adequately, and tolerate retinal imaging using the OCTA. Infarction lesions were confirmed on MR diffusion-weighted imaging consistent with clinical symptoms, as shown in (**Figure 1**). MR and OCTA imaging were done within 7 days after admission to our hospital. National Institute of Health Stroke Scale (NIHSS) scores were documented. Inclusion criteria of our cerebral infarction patients were as follows: (1) age 20–70 years; and (2) had cerebral infarction which was identified within 1 week of onset. Eligible cerebral infarction cases were matched to controls of the same age group, sex, and race with no self-reported history of stroke or any neurological deficits. Written informed consent was obtained from each participant and approval of our project was obtained from the Ethics Committee of West China Hospital of Sichuan University.

The exclusion criteria of our participants were as follows: (1) diagnosed with diabetic retinopathy or other retinal diseases; (2) Glaucoma; (3) presence of metal fragments in the eyes, brain, or spinal cord; (4) significant media opacities that preclude imaging of the macula; (5) participants with uncertain diagnoses; and (6) participants with a pacemaker or other internal devices; Ultimately, 25 patients were recruited for the ischemic stroke group, and 25 age- and sex-matched controls were enrolled.

After collecting the demographics and clinical information of the participants, ophthalmological examinations such as visual acuity, fundus examination, intraocular pressure examination, and spectral-domain optical coherence tomography (SD-OCT) imaging were completed.

Visual acuity under illumination was completed for each eye using Snellen charts and later converted to the logarithm of the minimum angle of resolution (LogMAR).

Spectral-Domain Optical Coherence Tomography Imaging

Macula Structure

The peripapillary retinal nerve fiber layer (pRNFL) thickness was obtained using the optic nerve head map protocol; the scanning range covered a circle of 3.45 mm in diameter centered on the optic disc. Ganglion cell complex (GCC) thickness was obtained using the GCC scanning protocol which was acquired through scans centered 1 mm temporal to the fovea

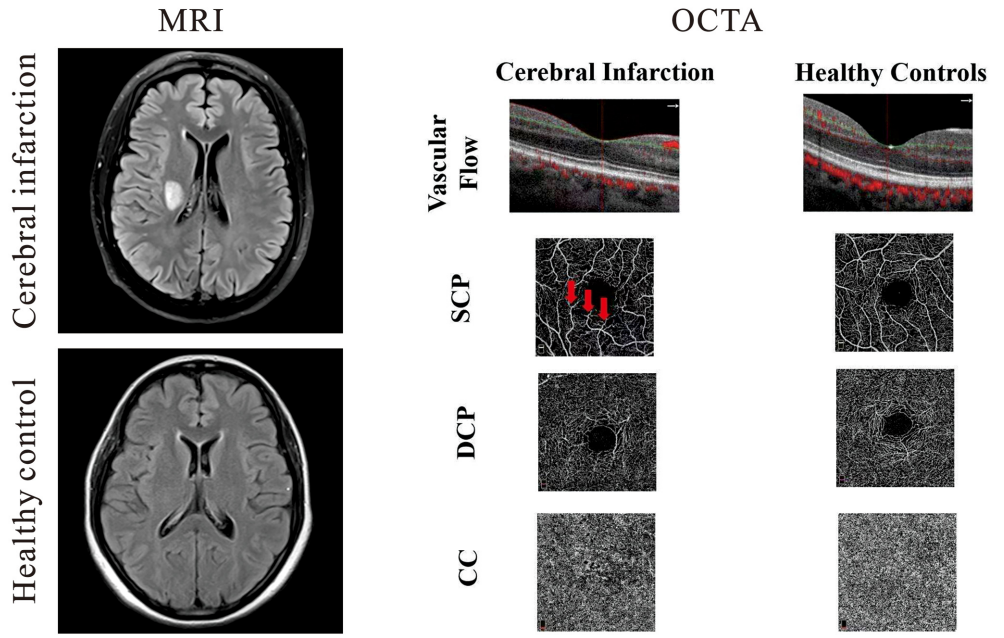

FIGURE 1 | Representative magnetic resonance imaging (MRI) and optical coherence tomography angiography (OCTA) images of cerebral infarction and healthy controls. On the left panel, the upper image shows a T2-weighted MRI of a patient with cerebral infarction beside the right lateral ventricle while the lower right image shows a T2–weighted image of healthy control. Cerebral infarction patients showed reduced vascular flow when compared with healthy controls; macula capillaries were more interrupted in cerebral infarction images when compared with healthy controls. Red arrows represent areas of capillary dropout (middle panel).

and covered a square grid (7 mm × 7 mm) on the central macula. Imaging of the structure of the macula was done with the Avanti RTVue-XR (Optovue, Fremont, California, LA, USA, 2017 version).

Capillaries of the Macula and Choroid

Using the split-spectrum amplitude decorrelation algorithm, OCT angiography (OCTA) images were obtained with Avanti RTVue-XR. The built-in algorithm (version 2017.1.0.151) was equipped with a three-dimensional Projection Artifact Removal (3D PAR) to help reduce all projection artifacts in the deeper layers while keeping their outline and improving the foveal avascular zone (FAZ) area (Liu et al., 2018).

The radial peripapillary capillaries (RPC) network was obtained in scans within a 0.7 mm wide elliptical annular region extending outward from the optic disc boundary, and the vasculature within the internal limiting membrane and the retinal nerve fiber layer (RNFL) were analyzed using the built-in software.

The parafoveal capillary network was obtained through 3 × 3 mm^2 scans within the annular zone of 0.6 mm–2.5 mm diameter around the foveal center. The superficial capillary plexus (SCP) was 3 μm below the internal limiting membrane to the outer boundary of the inner plexiform layer. The deep capillary plexus (DCP) was described as 15 μm below the INL to 70 μm. The choriocapillaris (CC) was defined as the microvessels within the Bruch's membrane and the upper boundary of the stroma of the choroid.

The capillary density of the SCP, DCP, and CC was defined as the percentage area occupied by the microvasculature in the analyzed region (3 × 3 mm^2) and was generated in the whole scan area in all sections of the applied grid according to the Early Treatment Diabetic Retinopathy Study (ETDRS) as previously reported (Yang et al., 2019).

Images with signal quality less than 6 on a scale of 10 were excluded from our data analyses (Lim et al., 2018). Images with motion artifacts seen on the en face images such as irregular patterns of vessels or blurred segmentation of the microvascular plexuses were rejected. Images of good technical quality were included in our data analyses.

Statistical Analyses

Demographics and clinical information of our participants were described with frequencies (%) and standard deviations as appropriate. Chi-square or independent sample *t*-tests were used to compare the clinical and demographic information between the two groups when appropriate. A generalized estimating equation (GEE) was used to compare the structure, macula microvasculature, and CC between cerebral infarction patients and healthy controls; after, these parameters were then assessed again using GEE while adjusting for inter-eye dependencies, signal quality, and risk factors (gender, hypertension, diabetes, and age). Intraocular pressure of each eye was included as a covariate when analyzing the macula structural thickness between the two groups. The area under the receiver operating characteristic (AUROC) was used to determine the diagnostic

TABLE 1 | Demographics and clinical data.

	Cerebral infarction	Healthy controls	*P*-value
Number	22	25	
Gender (F:M)	2:20	3:22	0.891
Age (years)	54.35 (11.42)	54.41 (9.97)	0.985
BMI	24.23 (2.54)	23.95 (2.16)	0.793
Hypertension (number)	9	3	<0.05
Diabetes (number)	5	1	<0.05
Hyperlipidemia	5	0	<0.05
Smokers (number)	14	9	0.083
Alcohol (Smokers)	8	6	0.311
Location of infarction			
Subcortical *n* (%)	15 (68.2)		
Cortical and subcortical *n* (%)	1 (4.5)		
Brain stem	6 (27.3)		
NIHSS score	2.53 (2.32)	0	
Ophthalmology exam			
IOP (mmHg)	15.28 (2.48)	14.96 (2.32)	0.812
AL (mm)	23.16 (1.19)	23.45 (0.78)	0.958
Visual acuity, Snellen chart	0.74 (0.31)	1.10 (0.17)	<0.001
Visual acuity, LogMAR	0.21 (0.23)	−0.05 (0.07)	<0.001

Data were expressed as mean (standard deviations) or percentages. Chi-square or independent sample t-tests were used in comparing characteristics between groups. Text in blue font indicates location of infarct.

accuracy of the analyzed parameters discriminating between cerebral infarction patients and healthy controls. An AUROC of 1.0 indicated perfect discrimination while 0.5 indicated accidental discrimination. *P*-values less than 0.05 were considered statistically significant. SPSS version 22 was used to perform the statistical analyses.

RESULTS

Twenty-five patients with cerebral infarction were enrolled in this study. Owing to the poor quality of OCTA images of both eyes (movement artifacts, segmentation errors, and signal quality less than 6), three cerebral infarction patients were excluded from our data analyses. Thus, 22 cerebral infarction patients and 25 healthy controls were included in our data analyses. Of our 22 cerebral infarction patients, 15 had subcortical infarction, one had cortical and subcortical infarction, and six had brain stem infarction as shown in (**Table 1**). There were no significant differences in age, gender, axial length, and IOP between the two groups. Significant differences ($P < 0.05$) were shown in the risk factors such as hypertension and diabetes between the two groups (**Table 1**). Cerebral infarction patients showed significantly reduced visual acuity when compared with healthy controls ($P < 0.001$).

Cross-sectional OCTA images of the macula with visible flow signal through the center of the fovea and in the circumferential portion of the macula were significantly different between the two groups; cerebral infarction patients showed significantly reduced vascular flow when compared with the healthy controls (**Figure 1**). On the en face angiograms, cerebral infarction patients showed narrower and interrupted capillaries when compared with healthy controls (**Figure 1**, middle column). Signal quality was significantly different ($P = 0.03$) between patients with cerebral infarction (8.33 ± 1.17) and healthy controls (9.03 ± 0.72).

Macula Thickness Between Ischemic Stroke and Healthy Controls

pRNFL thickness ($P = 0.008$), RNFL thickness ($P = 0.02$, **Table 2**) and GCC thickness ($P = 0.018$, **Table 2**) were significantly reduced in cerebral infarction patients when compared with healthy controls, respectively.

The mean FAZ area was significantly larger in cerebral infarction patients when compared with healthy controls ($P < 0.001$, **Table 2**).

The Capillary Density Between Ischemic Stroke and Healthy Controls

RPC density ($P < 0.001$, **Table 2**), SCP density ($P = 0.001$, **Table 2**) and DCP density ($P < 0.001$, **Table 2**) were significantly reduced in cerebral infarction patients when compared with healthy controls, respectively. The density in the choriocapillaris was significantly reduced in cerebral infarction patients when compared with healthy controls ($P < 0.001$, **Table 2**).

Mean area of the FAZ in cerebral infarction patients inversely correlated with the DCP density (Rho = −0.288, $P = 0.001$) and blood flow in the choriocapillaris (Rho = −0.264, $P = 0.002$), respectively.

NIHSS also inversely correlated with the SCP density in patients with cerebral infarction (Rho = −0.409, $P = 0.001$).

AUROC analysis was used to reflect the diagnostic accuracy for each OCTA parameter to provide a distinction between cerebral infarction patients and healthy controls. The highest AUROC result was the choriocapillaris blood flow (0.964, 95% CI = 0.889–0.994; **Figure 2**, **Table 3**).

DISCUSSION

In our observational cross-sectional study, we assessed the retinal, structural, and microvascular changes in patients with cerebral infarction. Our current study compared the sub-retinal thicknesses and microvascular densities in the two macula capillary plexuses (superficial and deep), capillaries around the optic nerve, and choriocapillaris. When compared with healthy controls, patients with cerebral infarction showed significantly thinner sub-retina thickness (pRNFL, RNFL, and GCC) and significantly reduced RPC, SCP, DCP, and CC densities. Our report adds to the notion that gradual modifications occur in the retinal structure and microvasculature and choriocapillaris in patients with cerebral infarction. Taken together with accumulating reports, our current study shows that changes in retinal structure and microvasculature and choriocapillaris using the OCTA may potentially be used in monitoring the retinal changes in cerebral infarction.

Our findings on the sub-retinal layer thinning (pRNFL, RNFL, GCC) in cerebral infarction patients when compared with healthy controls are congruent with previous reports on cerebral vascular diseases (Kim et al., 2011; Moss, 2015). The pRNFL, RNFL, and GCC contains axons, cell bodies, and dendrites, thus a significant thinning of these layers reflects a significant neuronal

TABLE 2 | Comparison of the macula and choriocapillaris between cerebral infarction and healthy controls.

	Cerebral infarction	Healthy controls	*P*-value	*P-value*
RPC (%)	49.02 (3.0)	53.01 (2.54)	<0.001	*<0.001*
pRNFL (μm)	112.41 (11.89)	120.71 (8.68)	0.003	*0.008*
RNFL (μm)	104.02 (8.63)	108.94 (7.65)	0.025	*0.020*
GCC (μm)	98.43 (6.73)	101.74 (5.05)	0.014	*0.018*
SCP (%)	45.93 (3.69)	48.22 (1.43)	0.002	*0.001*
DCP (%)	48.50 (3.48)	52.54 (2.27)	<0.001	*<0.001*
FAZ (mm^2)	0.30 (0.10)	0.22 (0.63)	<0.001	*<0.001*
Choriocapillaris (%)	61.61 (4.58)	68.75 (1.11)	<0.001	*<0.001*

Data were adjusted for intereye dependencies, hypertension, diabetes, age, gender, and signal quality. P-value: adjusted for signal quality. P-value (italics): adjusted for signal quality and risk factor. Text in blue font indicates the significance of OCT changes with (last column, P value indented) and without (first P value column, P value not indented) adjusting for risk factors.

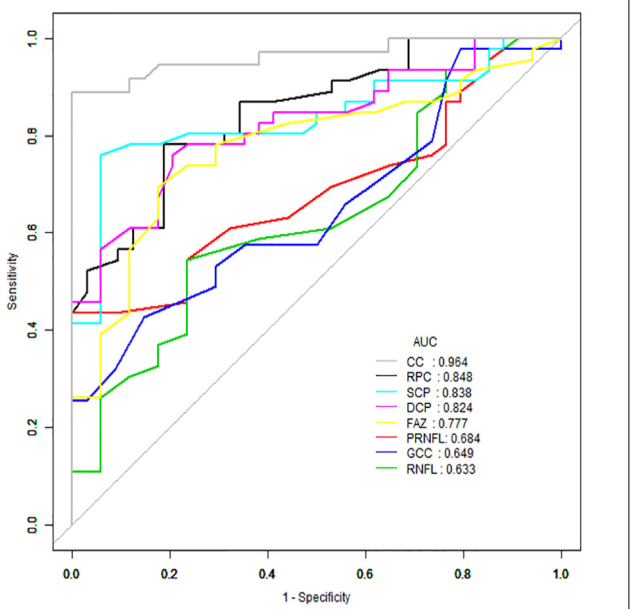

FIGURE 2 | Receiver operating characteristic (ROC) curve analysis of the macula parameters and choriocapillaris (CC). The highest area under the curve (AUC) was the choriocapillaris blood flow (0.964, 95% CI = 0.889–0.994).

TABLE 3 | ROC curve analysis of the macula and choriocapillaris of cerebral infarction and healthy controls.

	AUC	Sensitivity	Specificity
RPC (%)	0.848	78.26	81.25
pRNFL (μm)	0.684	43.48	100
RNFL (μm)	0.633	54.35	76.47
GCC (μm)	0.649	42.55	85.29
SCP (%)	0.838	76.09	94.12
DCP (%)	0.824	76.09	79.41
FAZ (mm^2)	0.777	69.57	82.35
Choriocapillaris (%)	0.964	88.89	100

and axonal loss which is congruent with previous cerebral reports (Brundel et al., 2012; Smith et al., 2012).

The growing number of reports (Mitchell et al., 2005; Baker et al., 2008; Wang et al., 2011; Kawasaki et al., 2012) providing evidence of significantly altered retinal microvascular structures in cerebral infarction indicates the importance of assessing the retinal microvasculature *in vivo*. This may shed light on the role of the microcirculatory networks and the development of the disease. Moreover, currently available and widely accepted imaging modalities such as magnetic resonance angiography are expensive, lack specificity, and have their contraindications. Therein, the use of retinal imaging may help in understanding the pathologic mechanism underlying the disease cascade and can be complementary to these neuroimaging tools. The OCTA is an imaging tool that helps in the acquisition of high-resolution *in vivo* cross-sectional images and assessable measurements of the optic disc, macula, and choriocapillaris, which have been reported to be associated with the cerebral structures (microvasculature and microstructure). It has been suggested to be particularly useful in many neurodegenerative diseases and a useful tool in examining the course of development (Wylęgała, 2018; Pujari et al., 2020). The usefulness and potential of OCTA to determine capillary-level detail make it an important imaging modality that can provide in-depth information regarding impaired perfusion. It allows clinicians to assess the severity of ischemia (Pujari et al., 2020) with much more precision which may be beneficial in understanding the pathophysiology of cerebral infarction.

Our data observed a significant dropout of macula microvasculature (SCP and DCP) in cerebral infarction patients when compared with healthy controls. Previous cerebral imaging reports have suggested that vascular dysfunction leads to cerebral hypoperfusion during the development of ischemic cerebrovascular lesions (Kunz and Iadecola, 2009; Hu et al., 2017). Moreover, it has been suggested that before cerebral infarction, most patients may have had combinations of large-vessel stenosis, small vessel disease, and a propensity to form either cardiac emboli or arterial thrombi with atherosclerotic lesions. This may then result in neural cell loss/death and a significant reduction in cerebral microcirculation dropout. With the association between cerebral microcirculation and retina microcirculation, the retinal microcirculation may be reflective of the pathophysiological cascade in cerebral infarction. Ideally, we found that the capillary damage in the deep plexus was more severe than in the superficial plexus. The deep capillary plexus which is located in the deepest part of the inner retina is reported to consist solely of capillaries, unlike the superficial plexus which consists of capillaries, arterioles, and venules. The capillaries in the DCP are thinner and have a smaller cross-sectional area

making them sensitive to any disease that affects the retina. However, our study is observational and did not explore the contributory mechanisms.

Our report also showed that patients with cerebral infarction have a significantly reduced RPC density when compared with healthy controls. Our report is in agreement with a previous study that showed reduced vascular density around the optic nerve using fundus photography (Sprodhuber et al., 2018). Although vessels imaged and measured from fundus photography are considerably larger in diameter than those obtained from the OCTA (Forrester et al., 1996), our report echoes the aforementioned report.

A novel finding in our study was the significant density dropout in the choriocapillaris of cerebral infarction patients when compared with healthy controls. It has been suggested that the occurrence of cerebral infarction is associated with aging and atherosclerosis of the vessels (Lernfelt et al., 2002; Liu et al., 2017), which create an ischemic environment, therein affecting the structure and microvasculature of the choroid. Significant dropout in the choriocapillaris remained after adjusting for age and other risk factors suggesting that changes in the choriocapillaris due to the disease mechanism. Future studies will be needed to validate our hypothesis.

The FAZ is located in the inner retina (mostly in the deep capillary plexus region) and it is made up of photoreceptor cells and bound by interconnected capillary anastomoses (Tick et al., 2011; Bates et al., 2018). Our current study showed that the FAZ area was larger in cerebral infarction patients when compared with healthy participants and observed significant inverse associations between the FAZ area and DCP and CC, respectively. The FAZ enlargement in patients with cerebral infarction may be due to retinal degeneration as seen in our current report and previous reports. Another possible explanation for the FAZ enlargement may be the significant dropout in the microvascular as shown in our current report as well.

An inverse correlation between the NIHSS score and density in the SCP was another new finding in our report. NIHSS, an important indicator to assess the severity of a stroke, has been reported to reflect the severity of neurological impairment (Lyden, 2017). An inverse correlation between NIHSS score and the density in the SCP of patients with cerebral infarction indicates that the higher the NIHSS score, the lower the density in the SCP and *vice versa*. Although this is the first report to highlight the correlation between these two parameters, future studies are needed to validate our speculation.

The significant difference between healthy controls and cerebral infarction provides a potentially clinically useful screening indicator for detecting the presence of cerebral infarction. Despite a promising area under the curve (AUC) in the ROC analysis with a lower 95% CI of greater than 0.5, studies using a longitudinal approach may be needed to validate our findings. Nonetheless, our results suggest that measurement of the blood flow in the choriocapillaris using OCTA can be used to identify cerebral infarction patients and may constitute an early indicator to help screen for patients with cerebral infarction. Identifying the significant reduction of the choriocapillaris in cerebral infarction patients before the occurrence of the apparent retinopathy signs seen on fundus photography may help clinicians to apply earlier implementation of treatment and may be useful to predict the progression of the disease as well.

A major limitation in our current study is the small sample size and inclusion of only Chinese participants. Second, individuals were excluded with a known vascular disease from our study; therein, we could not determine whether these results were translatable to individuals with retinal and choriocapillaris changes due to other causes. Another limitation is the statistical difference in the clinical information such as the number of hypertensives and diabetics included in our data. The OCTA technique requires participants to focus and cooperate, which makes some of the images obtained unsuitable for analysis.

CONCLUSIONS

Notwithstanding our limitations, we showed that patients with cerebral infarction can be imaged and detected by the OCTA which is a quick, non-invasive, inexpensive tool based on the significant reduction of blood flow in the choriocapillaris. Our report showed that patients with cerebral infarction have significantly reduced macular microvascular and choriocapillaris densities when compared with healthy controls. We also showed that reduced SCP density is inversely correlated with NIHSS score in cerebral infarction patients. Our findings suggest that these microvascular changes in the retina and choriocapillaris may reflect the cerebral microcirculation in cerebral infarction and demonstrate the potential of OCTA for early screening of cerebral infarction patients.

DATA AVAILABILITY STATEMENT

The raw data supporting the conclusions of this article will be made available by the authors, without undue reservation.

ETHICS STATEMENT

The studies involving human participants were reviewed and approved by West China Hospital Ethics Committee. The patients/participants provided their written informed consent to participate in this study.

AUTHOR CONTRIBUTIONS

All authors listed have made a substantial, direct and intellectual contribution to the work, and approved it for publication.

FUNDING

This work was supported by National Key Development Plan for Precision Medicine Research (2017YFC0910004), National Natural Science Foundation of China (81671146 and 81870937), and the 1.3.5 project for disciplines of excellence, West China Hospital, Sichuan University (ZYG D18009).

REFERENCES

Baker, M. L., Hand, P. J., Wang, J. J., and Wong, T. Y. (2008). Retinal signs and stroke: revisiting the link between the eye and brain. *Stroke* 39, 1371–1379. doi: 10.1161/STROKEAHA.107.496091

Bates, N. M., Tian, J., Smiddy, W. E., Lee, W. H., Somfai, G. M., Feuer, W. J., et al. (2018). Relationship between the morphology of the foveal avascular zone, retinal structure and macular circulation in patients with diabetes mellitus. *Sci. Rep.* 8:5355. doi: 10.1038/s41598-018-23604-y

Brundel, M., de Bresser, J., van Dillen, J., Kappelle, L. J., and Biessels, G. J. (2012). Cerebral microinfarcts: a systematic review of neuropathological studies. *J. Cereb. Blood Flow. Metab.* 32, 425–436. doi: 10.1038/jcbfm.2011.200

Cheung, N., Mosley, T., Islam, A., Islam, A., Kawasaki, R., Sharrett, R. A., et al. (2010) Retinal microvascular abnormalities and subclinical magnetic resonance imaging brain infarct: a prospective study. *Brain* 133, 1987–1993. doi: 10.1093/brain/awq127

Cooper, L. S., Wong, T. Y., Klein, R., Sharrett, A. R., Bryan, R. N., Hubbard, L. D., et al. (2006). Retinal microvascular abnormalities and MRI-defined subclinical cerebral infarction: the atherosclerosis risk in communities study. *Stroke* 37, 82–86. doi: 10.1161/01.STR.0000195134.04355.e5

de Jong, F. J., Vernooij, M. W., Ikram, M. K., Ikram, M. A., Hofman, A., Krestin, G. P., et al. (2008). Arteriolar oxygen saturation, cerebral blood flow and retinal vessel diameters. The rotterdam study. *Ophthalmology* 115, 887–892. doi: 10.1016/j.ophtha.2007.06.036

Erskine, L., and Herrera, E. (2014). Connecting the retina to the brain. *ASN Neuro.* 6:1759091414562107. doi: 10.1177/1759091414562107

Forrester, J., Dick, A., McMenamin, P., and Wr, L. (1996). *The Eye: Basic Science in Practice*, 2nd Edition Edinburgh: Saunders.

Hu, X., De Silva, T. M., Chen, J., and Faraci, F. M. (2017). Cerebral vascular disease and neurovascular injury in ischemic stroke. *Circ. Res.* 120, 449–471. doi: 10.1161/CIRCRESAHA.116.308427

Ikram, M. K., De Jong, F. J., Van Dijk, E. J., Prins, N. D., Hofman, A., Breteler, M. M. B., et al. (2006). Retinal vessel diameters and cerebral small vessel disease: the rotterdam scan study. *Brain* 129, 182–188. doi: 10.1093/brain/awh688

Kawasaki, R., Xie, J., and Cheung, N. (2012 Retinal microvascular signs and risk of stroke: the Multi-Ethnic study of atherosclerosis (MESA). *Stroke* 43, 3245–3251. doi: 10.1161/STROKEAHA.112.673335

Kim, M., Park, K. H., Kwon, J. W., Jeoung, J. W., Kim, T. W., and Kim, D. M. (2011). Retinal nerve fiber layer defect and cerebral small vessel disease. *Invest. Ophthalmol. Vis. Sci.* 52, 6882–6886. doi: 10.1167/iovs.11-7276

Kunz, A., and Iadecola, C. (2009). Cerebral vascular dysregulation in the ischemic brain. *Handb. Clin. Neurol.* 92, 283–305. doi: 10.1016/S0072-9752(08)01914-3

Lernfelt, B., Forsberg, M., Blomstrand, C., Mellström, D., and Volkmann, R. (2002). Cerebral atherosclerosis as predictor of stroke and mortality in representative elderly population. *Stroke* 33, 224–229. doi: 10.1161/hs0102.102009

Lim, H. B., Kim, Y. W., Kim, J. M., Jo, Y. J., and Kim, J. Y. (2018). The importance of signal strength in quantitative assessment of retinal vessel density using optical coherence tomography angiography. *Sci. Rep.* 8:12897. doi: 10.1038/s41598-018-31321-9

Liu, L., Gao, J., Bao, W., Hu, C., Xu, Y., Zhao, B., et al. (2018). Analysis of foveal microvascular abnormalities in diabetic retinopathy using optical coherence tomography angiography with projection artifact removal. *J. Ophthalmol.* 2018, 1–9. doi: 10.1155/2018/3926745

Liu, J., Zhu, Y., Wu, Y., Liu, Y., Teng, Z., Hao, Y., et al. (2017). Association of carotid atherosclerosis and recurrent cerebral infarction in the Chinese population: a meta-analysis. *Neuropsychiatr. Dis. Treat.* 13, 527–533. doi: 10.2147/NDT.S124386

London, A., Benhar, I., and Schwartz, M. (2013). The retina as a window to the brain-from eye research to CNS disorders. *Nat. Rev. Neurol.* 9, 44–53. doi: 10.1038/nrneurol.2012.227

Lyden, P. (2017). Using the National Institutes of health stroke scale. *Stroke* 48, 513–519. doi: 10.1161/STROKEAHA.116.015434

Mitchell, P., Wang, J. J., Wong, T. Y., Smith, W., Klein, R., and Leeder, S. R. (2005). Retinal microvascular signs and risk of stroke and stroke mortality. *Neurology* 65, 1005–1009. doi: 10.1212/01.wnl.0000179177.15900.ca

Moss, H. E. (2015). Retinal vascular changes are a marker for cerebral vascular diseases. *Curr. Neurol. Neurosci. Rep.* 15:40. doi: 10.1007/s11910-015-0561-1

Ong, Y. T., De Silva, D. A., Cheung, C. Y., Chang, H.-M., Chen, C. P., Wong, M. C., et al. (2013). Microvascular structure and network in the retina of patients with ischemic stroke. *Stroke* 44, 2121–2127. doi: 10.1161/STROKEAHA.113.001741

Ong, Y. T., Hilal, S., Cheung, C. Y., Venketasubramanian, N., Niessen, W. J., Vrooman, H., et al. (2015). Retinal neurodegeneration on optical coherence tomography and cerebral atrophy. *Neurosci. Lett.* 584, 12–16. doi: 10.1016/j.neulet.2014.10.010

Osborne, N. N., Casson, R. J., Wood, J. P., Chidlow, G., Graham, M., and Melena, J. (2004). Retinal ischemia: mechanisms of damage and potential therapeutic strategies. *Prog. Retin. Eye. Res.* 23, 91–147. doi: 10.1016/j.preteyeres.2003.12.001

Pujari, A., Bhaskaran, K., Sharma, P., Singh, P., Phuljhele, S., Saxena, R., et al. (2020). OCTA in neuro-ophthalmology: current clinical role and future perspectives. *Surv. Ophthalmol.* doi: 10.1016/j.survophthal.2020.10.009. [Online ahead of print].

Rowe, F. J. (2017). Stroke survivors' views and experiences on impact of visual impairment. *Brain Behav.* 7:e00778. doi: 10.1002/brb3.778

Smith, E. E., Schneider, J. A., Wardlaw, J. M., and Greenberg, S. M. (2012). Cerebral microinfarcts: the invisible lesions. *Lancet Neurol.* 11, 272–282. doi: 10.1016/S1474-4422(11)70307-6

Sprodhuber, A., Wolz, J., Budai, A., Laumeier, I., Audebert, H. J., and Michelson, G. (2018). The role of retinal vascular density as a screening tool for ageing and stroke. *Ophthalmic. Res.* 60, 1–8. doi: 10.1159/000488491

Tick, S., Rossant, F., Ghorbel, I., Gaudric, A., Sahel, A. J., Ghorbel, I., et al. (2011). Foveal shape and structure in a normal population. *Invest. Ophthalmol. Vis. Sci.* 52, 5105–5110. doi: 10.1167/iovs.10-7005

Vermeer, S. E., Longstreth, W. T.Jr., and Koudstaal, P. J. (2007). Silent brain infarcts: a systematic review. *Lancet Neurol.* 6, 611–619. doi: 10.1016/S1474-4422(07)70170-9

Wang, J. J., Baker, M. L., Hand, P. J., Hankey, G. J., Lindley, R. I., Rochtchina, E., et al. (2011). Transient ischemic attack and acute ischemic stroke: associations with retinal microvascular signs. *Stroke* 42, 404–408. doi: 10.1161/STROKEAHA.110.598599

Wylęgała, A. (2018). Principles of OCTA and applications in clinical neurology. *Curr. Neurol. Neurosci.* 18:96. doi: 10.1007/s11910-018-0911-x

Yang, J., Wang, E., Zhao, X., Xia, S., Yuan, M., Chen, H., et al. (2019). Optical coherence tomography angiography analysis of the choriocapillary layer in treatment-naive diabetic eyes. *Graefes. Arch. Clin. Exp. Ophthalmol.* 257, 1393–1399. doi: 10.1007/s00417-019-4326-x

Zhou, M., Wang, H., Zeng, X., Yin, P., Zhu, J., Zhu, W., et al. (2019). Mortality, morbidity, and risk factors in China and its provinces, 1990-2017: a systematic analysis for the global burden of disease Study 2017. *Lancet* 394, 1145–1158. doi: 10.1016/S0140-6736(19)30427-1

Conflict of Interest: The authors declare that the research was conducted in the absence of any commercial or financial relationships that could be construed as a potential conflict of interest.

frontiers in Aging Neuroscience

ORIGINAL RESEARCH
published: 14 April 2021
doi: 10.3389/fnagi.2021.637363

Nomogram to Predict Cognitive Dysfunction After a Minor Ischemic Stroke in Hospitalized-Population

Li Gong[1†], Haichao Wang[1†], Xiaofeng Zhu[2†], Qiong Dong[1], Qiuyue Yu[1], Bingjie Mao[1,3], Longyan Meng[1], Yanxin Zhao[1] and Xueyuan Liu[1*]*

[1] Department of Neurology, Shanghai Tenth People's Hospital, Tongji University, Shanghai, China, [2] Department of Nursing, Huashan Hospial North, Fudan University, Shanghai, China, [3] Nanjing Medical University, Nanjing, China

An easily scoring system to predict the risk of cognitive impairment after minor ischemic stroke has not been available. We aimed to develop and externally validate a nomogram for predicting the probability of post-stroke cognitive impairment (PSCI) among hospitalized population with minor stroke. Moreover, the association of Trimethylamine N-oxide (TMAO) with PSCI is also investigated. We prospectively conducted a developed cohort on collected data in stroke center from June 2017 to February 2018, as well as an external validation cohort between June 2018 and February 2019. The main outcome is cognitive impairment defined as <22 Montreal Cognition Assessment (MoCA) score points 6 – 12 months following a minor stroke onset. Based on multivariate logistic models, the nomogram model was generated. Plasma TMAO levels were assessed at admission using liquid chromatography tandem mass spectrometry. A total of 228 participants completed the follow-up data for generating the nomogram. After multivariate logistic regression, seven variables remained independent predictors of PSCI to compose the nomogram included age, female, Fazekas score, educational level, number of intracranial atherosclerotic stenosis (ICAS), HbA1c, and cortical infarction. The area under the receiver-operating characteristic (AUC-ROC) curve of model was 0.829, C index was good (0.810), and the AUC-ROC of the model applied in validation cohort was 0.812. Plasma TMAO levels were higher in patients with cognitive impairment than in them without cognitive dysfunction (median 4.56 vs. 3.22 μmol/L; $p \leq 0.001$). In conclusion, this scoring system is the first nomogram developed and validated in a stroke center cohort for individualized prediction of cognitive impairment after minor stroke. Higher plasma TMAO level at admission suggests a potential marker of PSCI.

Keywords: trimethylamine-N-oxide, nomogram, minor stroke, post-stroke cognitive impairment, cognitive dysfunction

OPEN ACCESS

Edited by:
Feng Yan,
Zhejiang University, China

Reviewed by:
Jinhua Gu,
Nantong Maternity and Child Health Hospital, China
Lianhua Zhao,
Tianjin TEDA Hospital, China

***Correspondence:**
Xueyuan Liu
Liuxy@tongji.edu.cn
Yanxin Zhao
zhao_yanxin@126.com

[†]These authors have contributed equally to this work

Received: *03 December 2020*
Accepted: *04 March 2021*
Published: *14 April 2021*

Citation:
Gong L, Wang H, Zhu X, Dong Q, Yu Q, Mao B, Meng L, Zhao Y and Liu X (2021) Nomogram to Predict Cognitive Dysfunction After a Minor Ischemic Stroke in Hospitalized-Population. Front. Aging Neurosci. 13:637363. doi: 10.3389/fnagi.2021.637363

INTRODUCTION

Post-stroke cognitive impairment (PSCI) causes a great burden to stroke survivors. Even minor stroke survivors are at increased risk of developing cognitive impairment (Gong et al., 2020), affecting executive function, speech ability. However, due to the absence of disabling conditions, they are more likely to be neglected for their cognitive dysfunction. Cognitive impairment at acute stage of non-disabling ischemic stroke has been related to advanced age, educational level, severity of intracranial atherosclerotic stenosis (ICAS), infarct location, and evidence of white

matter hyperintensity (WMH). Our previous finding has suggested intestinal microbiota may play an important role in the cognitive performance post-stroke (Liu et al., 2020). Trimethylamine N-oxide (TMAO) is a metabolite generated primarily from dietary choline, phosphatidylcholine, and L-carnitine through the action of gut microbiota, and is a potential novel risk factor for stroke severity (Wu et al., 2020), but its relation to cognitive dysfunction after minor stroke has been less well-established.

Cognitive performance may vary from the acute to chronic stages of stroke, but few studies have used externally validated models to predict PSCI (Kandiah et al., 2016; Chander et al., 2017), and there is a need for risk scoring system to predict PSCI for individual minor stroke survivor. Nomogram is an useful tool for clinicians to make a visualized and quick risk assessment, and has been widely used for clinical decision-making in a particular patient. However, this model has only recently been applied to predict stroke outcomes (Busch et al., 2018), and is needed for validating in PSCI. The main objective of this study was to develop and externally validate a nomogram model to predict the potential risk of cognitive dysfunction beyond 6-month minor stroke.

METHODS

Study Design, Participants, Patient Consents

This was a longitudinal, prediction model development and validation study, which included data in stroke center from June 2017 to February 2018. Participants were enrolled if they met the following criteria: (1) age 18 or older, (2) diagnosed with acute ischemic stroke based on diffusion-weighted magnetic resonance imaging (MRI) within 2 weeks, (3) National Institutes of Health Stroke Scale (NIHSS) score under 5, (4) no history of psychiatric disorders or diagnosis of cognitive impairment before the onset of the current stroke, and (5) complete data for all variables of interest. Validation cohort included subjects, admitted between June 2018 and February 2019, from the same stroke center. The same inclusion/exclusion criteria were applied to the external validation cohort. The study was approved by the Ethics Committee of Shanghai Tenth People's Hospital (Shanghai, China) and was conducted in accordance with the Declaration of Helsinki principles. All of the participants and their caregivers provided written informed consent.

Outcome and Cognitive Assessment

The outcome measure was cognitive impairment defined as <22 Montreal Cognition Assessment (MoCA) score points 6–12 months following a minor stroke onset. Cognitive status was evaluated by an experienced neurologist via structured clinical interview and the MoCA, a sensitive and widely used measure of PSCI as our previous work described. The scores of the MoCA scale range from 0 to 30, with higher scores indicating a better cognitive function. Our goal was to develop a model that clinician could use to predict any cognition decline after minor stroke.

Predictors and Sample Collection

The demographic and clinical data were collected at the admission as our previously published study (Gong et al., 2020). Several neuroimaging variables were also evaluated: intracranial stenosis as a narrowing exceeding 50% of the luminal diameter by MRA, severity white matter hyperintensity (WMH) by Fazekas scores, and the distribution of lesions (cortical, subcortical, deep area, and sub-tentorium).

Fasting serum samples were routinely performed on the second day after admission to the hospital for routine biochemical tests and TMAO levels from validation cohort. Whole-blood samples were centrifuged into plasma, separated into vials, and stored in a −80°C refrigerator until analysis. All chemicals and solvents were analytical or HPLC grade. Water, methanol, acetonitrile, formic acid was purchased from Thermo Fisher Scientific (Thermo Fisher Scientific, Waltham, MA, USA). Chloroform was from Sinopharm Chemical Reagent Co., Ltd. (Shanghai, China). Firstly, 100 μL of sample was added to a 1.5 mL Eppendorf tube, 300 μL of ice-cold mixture of methanol and acetonitrile (2/1, v/v) (containing 0.01 mol/L BHT) was added, and the mixtures were vortexed for 30 s, ultrasonicated at ambient temperature for 10 min, stored at −20°C for 30 min. The extract was centrifuged at 13000 rpm, 4°C for 15 min. 200 μL of supernatant in a glass vial was dried in a freeze concentration centrifugal dryer 200 μL mixture of methanol and water (2/98, v/v) were added to each sample, then samples vortexed for 30 s and ultrasonicated at ambient temperature for 2 min. 200 μL chloroform were added to each sample, stored at 4°C for 10 min. Samples were centrifuged at 13000 rpm, 4°C for 5 min. The supernatants (100μL) from each tube were collected using crystal syringes, filtered through 0.22 μm microfilters and transferred to LC vials. The vials were stored at −80°C until LC-MS analysis. An AB ExionLC (AB SCIEX, Framingham, MA) coupled with an AB SCIEX API 6500 Qtrap+ System (AB SCIEX, Framingham, MA) was used to analyze the metabolic profiling in ESI positive and negative ion modes and AB SCIEX OS workstation (version 1.7.1). A Waters UPLC HSS T3 column (1.8 μm, 2.1 × 100 mm) were employed in positive and negative ion modes. The binary gradient elution system consisted of (A) water (containing 0.1 % formic acid, v/v) and (B) acetonitrile and separation was achieved using the following gradient: 0 min, 0% B; 1 min, 0% B; 3.5 min, 100% B; 4.5 min, 100% B; 4.51 min, 0% B; 6 min, 0% B. All the samples were kept at 4°C during the analysis. The injection volume was 5 μL. Using an electrospray ion source (ESI), the analyte was analyzed in a multi-reaction detection (MRM) mode under positive and negative ion modes scanning, which greatly improved sensitivity. At the same time, the mass spectrometry parameters such as DP and CE were optimized, and the target compound ion pair can be quickly screened and determined under the optimal conditions. The optimized mass spectrum analysis conditions were as follows: positive mode: collision gas 35; ion spray voltage: 5500 V; ion spray temperature: 600°C; ion source gas1: 60; gas2: 50;The QCs were injected at regular intervals (every 6∼8 samples) throughout the analytical run to provide a set of data from which repeatability can be assessed.

Follow-Up

A total of 269 patients enrolled in the present study were scheduled for out-patient follow-up 6–12 months. The same neuropsychological tests were performed by an experienced neuropsychologist who was blinded to the medical records of the participants. Finally, 228 subjects (85%) took part in the follow-up visit. The remaining 41 subjects were lost in the follow-up list due to the following reasons: two death, 18 away from Shanghai, and 21 refusal. As for the validation cohort, a total of 66 participants completed the follow-up visit, with four subjects lost, two way from Shanghai and three refusal (**Supplementary Figure 1**).

Statistical Analysis

The data are presented as mean ± standard deviation for continuous quantitative variables, and as frequencies and rate (%) for categorical variables. Initially, the Kolmogorov- Smirnov test was applied to detect normal distributions among the

TABLE 1 | Characteristics and univariate comparison of PSCI (MoCA < 22) and non-PSCI (MoCA ≥ 22) groups in development cohort.

Variables	*n* = 228	MoCA < 22 (*n* = 122)	MoCA ≥ 22 (*n* = 106)	*p*-value
Age (mean ± SD, years)	62.16 ± 10.63	64.32 ± 9.82	60.55 ± 11.03	0.018*
Sex (male, %)	162 (71.1)	80 (65.6)	82 (77.4)	0.027*
Education (mean ± SD, years)	7.04 ± 4.94	10.38 ± 3.42	7.04 ± 4.94	0.033*
NIHSS score (mean ± SD)	1.91 ± 1.18	2.08 ± 1.18	1.72 ± 1.15	0.021*
mRS score of 0-2, n(%)	161 (70.6)	80 (65.6)	81 (76.4)	0.073
Intravenous thrombolysis, *n* (%)	49 (18.2)	21 (19.6)	28 (17.3)	0.626
History of disease and medication, *n* (%)				
TIA or prior stroke	58 (25.4)	28 (23.0)	30 (28.3)	0.355
Hypertension	149 (65.4)	89 (73.)	60 (56.6)	0.010*
Diabetes	73 (32.0)	43 (35.2)	30 (28.3)	0.262
Hyperglycaemia	25 (11.0)	18 (14.8)	7 (4.4)	0.049*
Atrial fibrillation	11 (4.8)	7 (35.7)	4 (3.8)	0.490
Use of antihypertensives	141 (61.8)	86 (70.5)	55 (51.9)	0.004*
Use of antithrombotics	21 (9.2)	12 (9.8)	9 (8.5)	0.726
Use of lipid-lowering drugs	24 (10.5)	17 (13.9)	7 (4.4)	0.072
Use of anti-diabetics	66 (28.9)	40 (32.8)	26 (24.5)	0.170
Current or previous smoking	135 (59.2)	70 (57.3)	65 (61.3)	0.672
Current or previous drinking	77 (33.8)	41 (33.6)	36 (40.0)	0.550
Laboratory tests				
TC, mmol/L	4.36 ± 1.08	4.34 ± 1.16	4.39 ± 0.97	0.672
TG, mmol/L	1.92 ± 1.37	1.90 ± 0.97	1.93 ± 1.28	0.242
LDL, mmol/L	2.24 ± 0.92	2.21 ± 0.97	2.28 ± 0.86	0.537
HDL, mmol/L	1.12 ± 0.71	1.01 ± 0.25	1.15 ± 1.00	0.390
FPG, mmol/L	6.35 ± 2.40	6.45 ± 2.44	6.23 ± 2.38	0.708
HbA1c, mg/dL	6.81 ± 1.70	7.88 ± 1.86	6.74 ± 1.48	0.037
Hcy, umol/L	11.15 ± 8.64	11.17 ± 10.36	11.19 ± 7.84	0.065
Uric acid, umol/L	326.08 ± 98.01	324.66 ± 102.90	327.71 ± 92.51	0.815
Neuroimaging characteristics				
Fazekas score (mean ± SD)	2.20 ± 1.69	2.23 ± 1.39	1.23 ± 2.38	0.028*
ICAS ≥ 50%, *n* (%)	100 (43.9)	60 (49.2)	40 (37.7)	0.011*
ICAS number	1.32 ± 0.84	2.23 ± 1.39	1.23 ± 2.38	0.003*
OCSP (ACI, %)	146 (64.0)	35 (53.0)	111 (48.7)	0.221
Distribution of infarcts				0.017*
Cortical	42 (18.4)	31 (25.4)	11 (10.4)	0.003*
Sub-cortical	64 (28.1)	34 (27.9)	30 (28.3)	0.942
Deep area	68 (29.8)	29 (23.8)	39 (36.8)	0.032
Subtentorial	54 (23.7)	28 (23.0)	26 (24.0)	0.780

*PSCI, post-stroke cognitive impairment; TIA, transient ischemic stroke; NIHSS, National institute of Health Stroke Scale; mRS, modified ranking scale; ICAS, intracranial atherosclerosis stenosis; TC, total cholesterol; TG, total triglyceride; LDL, low density lipoprotein; HDL, high density lipoprotein; FPG, fasting plasma glucose; HbA1c, glycated hemoglobin; Hcy, homocystine; OCSP, Oxfordshire Community Stroke Project; ACI, anterior cerebral infarction. *p < 0.05.*

quantitative variables. Subsequently, we used either Student's *t*-test to compare the normally distributed quantitative variables, and Chi-square test for the normally distributed qualitative variables. Mann-Whitney U test was applied to compare variables with a non-normal distribution. Multivariate logistic regression analysis was performed to evaluate the strength of the aforementioned association according to the odds ratio (OR) and corresponding 95% confidence interval (CI), using the forward Wald method, with the F probability of entry set at 0.05 and that of removal set at 0.10. Variables with $p < 0.05$ in multivariate analysis were incorporated into R language to establish the nomogram of the prediction model. To discriminate patients with and without PSCI, area under the receiver-operating characteristic curve (AUC-ROC) was accessed to calculate the predictive accuracy of the nomogram model. Then Bootstrap method (1,000 times of resampling) was used for internal verification to calculate the corrected C index, which is equivalent to AUC-ROC, ranging from 0.5 to 1.0, with higher score indicating better predictive accuracy. The model built from the development cohort was then applied to the validation cohort and performance was also assessed by AUC-ROC. Calibration of the risk prediction model was assessed in the development cohort by the plot comparing the observed probability of PSCI according to the total score of the nomogram against the predicted probability based on the nomogram and by using the Hosmer-Lemeshow test that assesses whether or not the observed event rates matched the expected rates in patients with minor stroke. Finally, the relationship between TMAO levels and PSCI in patients with minor stroke from validation cohort was evaluated by Mann-Whitney U test. A 2-tailed *P*-values < 0.05 were considered statistically significant. R software, version 3.6.2 (2019 The R Foundation for Statistical Computing Platform) and SPSS 20(SPSS, Inc., USA), Prism 7 (2018 GraphPad Software, La Jolla, CA) were used for all data analysis.

RESULTS

Characteristics of the Subjects in Development Cohort

Among 228 individual subjects who completed a follow-up visit (median follow-up time: 272 days), 122 subjects (53.5%) were identified as having PSCI. The average age of the patients was 62.61 ± 10.63 years old, including 162 males (71.1%), 149 patients with hypertension (65.4%), 73 patients with diabetes (32%), and 21 patients with hyperlipidemia (11%). The average length of education was 7.04 ± 4.94 years, and NIHSS score was 1.91 ± 1.18. Age, gender, education, hypertension, NIHSS score, Fazekas score, number of ICAS, cortical infarcts, HbA1c were found to be significantly different between PSCI (MoCA<22) and non-PSCI (MoCA≥22) groups (**Table 1**) in univariate analysis ($p < 0.05$) and were included in the initial regression model.

Development of an Individualized Prediction Model

In binary logistic regression model, hypertension and NIHSS score were eliminated for their little significance. As shown in **Table 2**, seven potential predictors yielded by the binomial logistic regression model (LR method) were considered for model development: age (OR1.032, 95%CI 1.002–1.063), female (OR1.032, 95%CI 1.002–1.063), Fazekas score (OR 1.181, 95%CI 1.018–1.369), educational level (OR 0.937, 95%CI 0.883–0.993), number of ICAS (OR 1.070, 95%CI 1.070–1.733), HbA1c (OR 1.228, 95%CI 1.023–1.475), and cortical infarction (OR5.556, 95%CI 1.427–21.635). Furthermore, A prediction model was established using the nomogram on the basis of these seven factors. A summary of the point value of each factor used to calculate the total score presented in **Figure 1**. The area under the ROC curve of the development model was 0.829, with sensitivity 67.9%, specificity 82.8% (**Figure 2**).

Apparent Performance of the PSCI-Risk Nomogram and External Validation

The calibration curve of the nomogram for the predicted probability of PSCI in patients with minor stroke demonstrated good agreement in this cohort (**Figure 3**). The results of the 1000 bootstrap samples estimated the AUC to be 0.810, which suggested the model's good discrimination. As shown in **Figure 4**, the area under the ROC curve of the validation cohort was 0.812, which presents 88.2% of sensitivity, 63.3% of specificity.

TABLE 2 | Descriptive statistics and adjusted association between each predictor and PSCI in development cohort.

					95% CI of OR	
	β	*S.E*	*p*-value	OR	Lower	Upper
Age	0.031	0.015	0.035*	1.032	1.002	1.063
Age(female)	−0.710	0.281	0.011*	2.035	1.173	3.530
Fazekas score	0.166	0.075	0.028*	1.181	1.018	1.369
Cortical infarcts	1.715	0.694	0.013*	5.556	1.427	21.635
Education	−0.066	0.030	0.029*	0.937	0.883	0.993
ICAS number	0.309	0.123	0.012*	1.362	1.070	1.733
HbA1c	0.205	0.093	0.028*	1.228	1.023	1.475

*PSCI, post-stroke cognitive impairment; ICAS, intracranial atherosclerosis stenosis; HbA1c, glycated hemoglobin. *p < 0.05.*

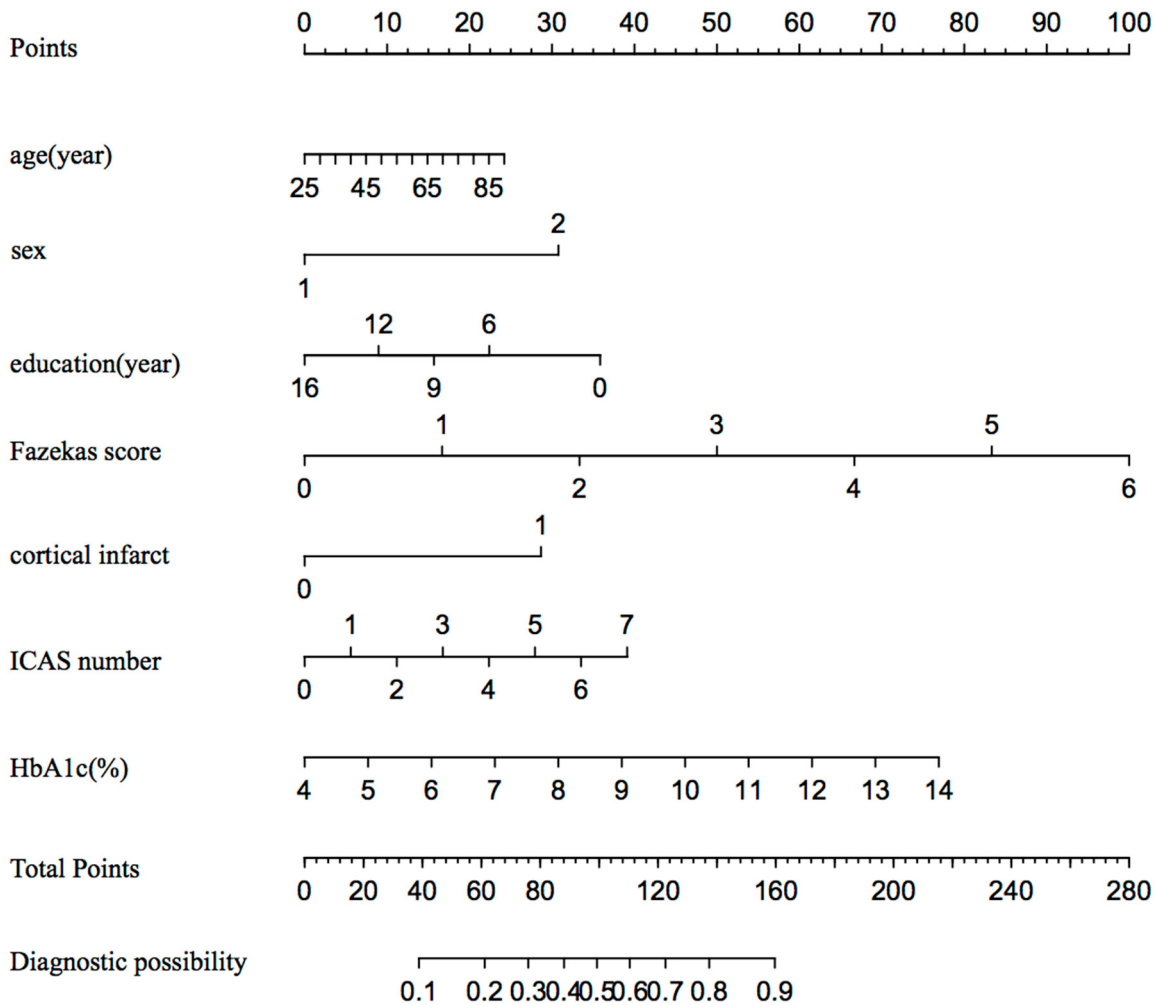

FIGURE 1 | The nomogram for predicting the probability of PSCI among minor stroke. ICAS indicates intracranial atherosclerosis stenosis; and HbA1c, glycated hemoglobin.

Relationship Between TMAO and Post-stroke Cognitive Impairment

In validation cohort, blood samples of all 66 patients were collected, plasma TMAO levels were higher in patients with cognitive impairment than in patients without cognitive dysfunction after 6 months of a stroke onset (median 4.56 vs. 3.22 μ mol/L; $p \leq 0.001$). However, there were no significant difference in L-carnitine and choline levels (**Figure 5**).

DISCUSSION

This study presented and externally validated the nomogram based upon the age stage, sex, years of education, WMH score, severity of intracranial atherosclerotic stenosis, infarct location, and HbA1c level to predict the probability of cognitive dysfunction following minor stroke. The model provides clinicians with practical tool for quick and individualized prediction of cognitive performance after minor stroke using readily available clinical information.

To date, the most widely accepted time point of PSCI evaluation has been under debate, which ranges from 3 to 6 month (Levine et al., 2015; Chander et al., 2017). The reason for choosing 6–12 months after stroke as the observation point is mainly based on two reasons. First, repeated evaluation of cognitive status by MoCA scale within relatively short time, such as 3 months, may be affected by the learning effect, which commonly results in false negative outcome. Second, our previous finding shows incidence of PSCI at acute phase has reached a high level (>50%) (Gong et al., 2020). Therefore, we chose the 6 to 12 months as time point to evaluate PSCI for consideration that the cognitive condition of survivors may be in a relatively stable status during this time.

Consistent with existing findings, demographic variables (age, sex, years of education) played important roles in predicting PSCI (Ojala-Oksala et al., 2012; Gong et al., 2020). In addition, imaging

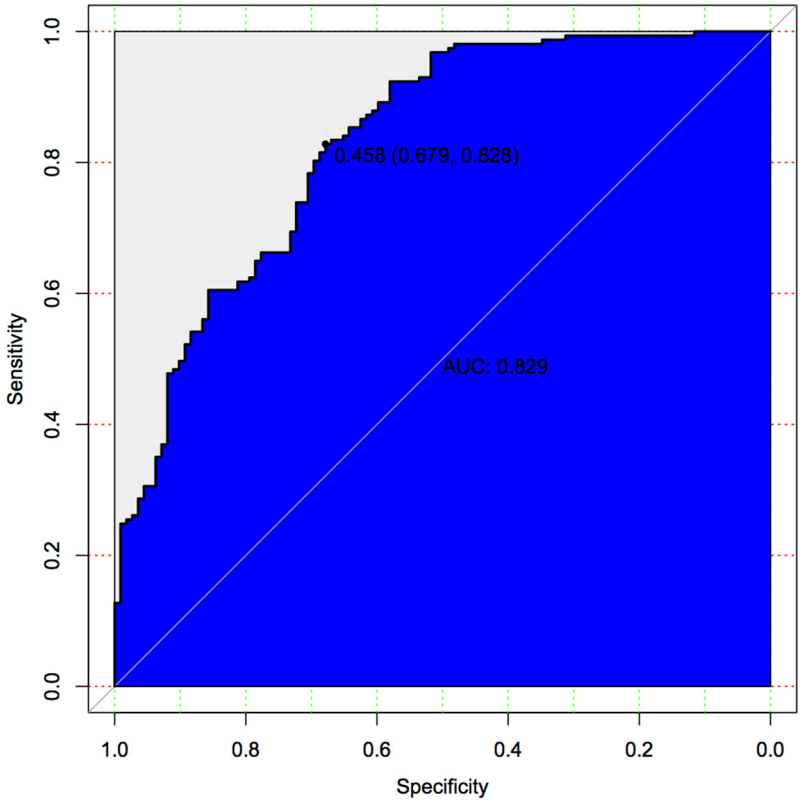

FIGURE 2 | Predictive model based on logistic analysis for early diagnosis of PSCI in development cohort.

variables are corroborated by the existing literature identified as being important risk factors for PSCI. The strongest predictor of PSCI in our model is WMH as previously reported. The relationship between WMH and cognitive decline was similar to the CHANGE score (Kandiah et al., 2016; Chander et al., 2017), as well as similar to the association between cerebral small vascular disease burden and cognitive performance (Yang et al., 2015; Jiang et al., 2019). In contrast, this relationship between chronic brain lesion and cognitive dysfunction is not supported by the outcome of the study that enrolled patients with a minor stoke/TIA (Mandzia et al., 2016). This difference might be explained by the fact that 46 percent of 92 patients were diffusion-weighted imaging positive, and assessment of their specific domains of executive function, psychomotor processing speed, but not assessed by MoCA. It has been widely accepted that oxidative stress and neuroinflammation have pathological roles in cognitive dysfunction. Due to the decreased antioxidative nature, brain white matter is more vulnerable to the oxidative stress following a stroke onset, contributing to loss of white matter integrity and cognitive impairment (Besga et al., 2017; Boots et al., 2020). In addition, the present data revealed higher risk of cognitive dysfunction was not only associated with WMH score and cortical infarcts (Saczynski et al., 2009), but also with the number of ICAS. This positive association between ICAS and cognitive impairment not only supports, but also extends our previous cross-sectional finding. ICAS may suggest systemic microcirculation dysfunction, higher resistance in small vessels, and impaired vascular reactivity, finally resulting in decreased cerebral perfusion (Zhu et al., 2014; Gong et al., 2020). In fact, few studies have explored the association of HbA1c level with cognitive dysfunction after minor stroke, while a recent population-based cohort study has emphasized the contributions of diabetes (HbA1c $\geq$ 6.5%), but not prediabetic stage (HbA1c $\geq$ 5.7%), in post-stroke dementia (Shang et al., 2020). Although inclusion of other variables and more detailed characteristics (e.g., sample of cerebrospinal fluid, fMRI data, and PET-CT) may increase the discriminative ability of our model, we intentionally limited the set of predictors to demographic and imaging/blood variables readily available in most stroke centers. This could make the present model more practical, and thereby permit it more universal in the course of stroke management, which is the most valuable part of this model.

An important result in the present study was the establishment of a nomogram model to predict PSCI, which has not been reported previously among survivors with minor stroke. Moreover, this model showed excellent discrimination and calibration when applied to the external validation cohort. The calibration belt indicated that predicting power generated this model is as good as to represent actual risk. Although a few previous studies have examined the relationship between risk

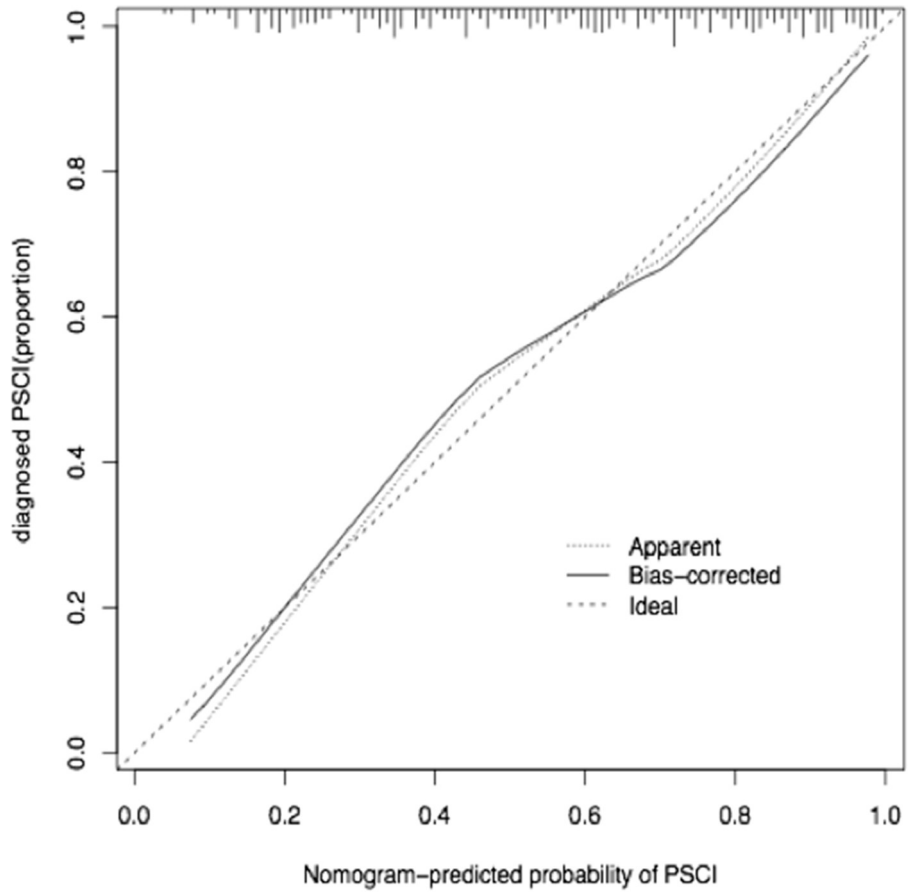

FIGURE 3 | Calibration curve for nomogram-predicted probability of PSCI in minor-stroke patients.

score and PSCI, there is growing evidence that nomograms have a better performance compared with risk scores (Cappellari et al., 2018, 2019). In contrast to risk group, a nomogram model provides a visualized and individualized estimate of the predicting probability of a specific outcome for an individual patient, as well as an important tool of medical decision making based on the individual's disease characteristics. Thus, this model showing good predicting ability suggests that it is suitable for clinicians to have readily evaluation of the probability of cognitive decline before discharge.

Although our primary goal was to develop a nomogram model to predict PSCI, we also investigated the relationship between TMAO levels and cognitive decline. Our results demonstrated an association between higher plasma TMAO levels at admission and increased risk of PSCI. The present findings are partly in line with a recently 1-year longitudinal study that included 256 patients with acute ischemic stroke and reported an association of increased plasma TMAO levels with PSCI (Zhu et al., 2020). However, it should be noted that no measures of dietary intake or biochemical precursors of TMAO are available in numerous prior studies (Yin et al., 2015; Olek et al., 2019; Wu et al., 2020), which can directly affect TMAO levels. For that, in the present study, we measured these important precursors such as L-carnitine and choline, and phosphatidylcholine, but did not find an association of PSCI with them. Thus, it further suggests that serum concentration TMAO may be a metabolic marker of intestinal microbiota independently related with cognitive dysfunction beyond a minor stroke. Although previous studies have reported that TMAO may involve different processes of stroke pathogenesis including cholesterol metabolism, platelet reactivity, and glucose tolerance, we consider diversity of gut microbiota is more likely to explain the mechanism of our results partly because of our prior published finding (Liu et al., 2020). Furthermore, a recently novel research indicated that the alteration of gut microbiota composition contributes to pro-inflammatory microglia activation, leading to dementia-associated neuroinflammation (Wang et al., 2019), which may be another evidence explaining the present result. However, the relationship should be interpreted cautiously for the small sample size, and needs to be confirmedzin the future with a larger sample size.

The major strengths of our study include the longitudinal hospital-based design with a relatively low ratio of loss-up, as well as the good predicting ability validated by an external cohort.

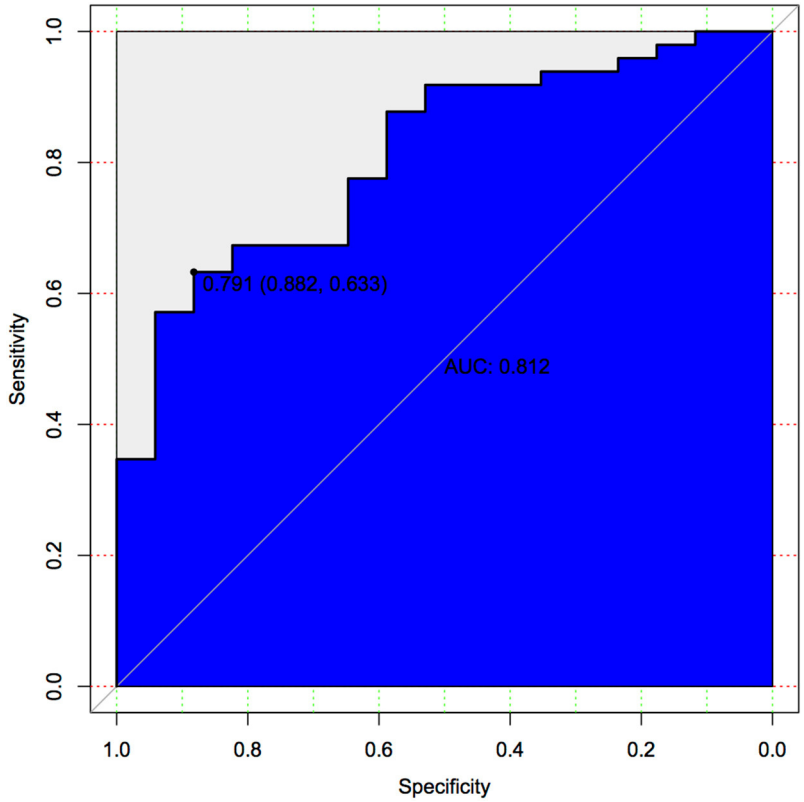

FIGURE 4 | Predictive model based on logistic analysis for early diagnosis of PSCI in validation cohort.

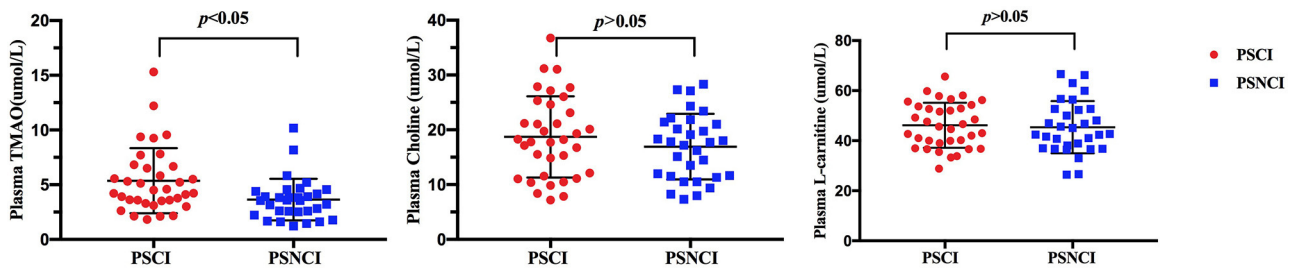

FIGURE 5 | Comparison of serum TMAO, choline, and L-carnitine levels between minor-stroke patients with and without PSCI. PSCI indicates post-stroke cognitive impairment; and PSNCI, post-stroke non-cognitive impairment.

In addition, we use the same 3T MRI scanner for its sufficient sensitivity to detect either small vessel disease such as WMC, small infarcts, or ICAS. These lesions have great influence on cognitive impairment. However, this study has some limitations to consider. Firstly, the relationship between PSCI and plasma levels of TMAO may be dynamic and influenced by multiple variables such as diet, gut microbiota, but we cannot exclude the influence of these potential confounders due to the small number of external validation cohort. The serum TMAO level in this study was detected at the day after admission to stroke center in the validation cohort and it must be better to conduct dynamic comparison of the results after 6 months, which is warranted in our further research. Secondly, even though we have tried to exclude the prior cognitive impairment in any kinds, the concept of PSCI overlaps with AD, even some other neurodegeneration diseases like FTD. In that way, it should be noted it is difficult to exactly differentiate whether vascular cognitive impairment or early AD causes PSCI in this cross-sectional study, for that they commonly share similar risk factors, such as existing vascular damage and diabetes. Indeed, inclusion of more variables such as Apolipoprotein E (ApoE) or PET-CT may increase the predicting power. However, it should be noted

that this could limit the practice and availability of the present model because those more detailed variables are not routinely tested in most stroke centers. What we are most concerned about in this study is to provide clinicians with a universal and quick tool, promoting early identification and timely intervention in the course of stroke management.

Conclusion

This study provides an easy-to-use nomogram model to predict cognitive outcome beyond an minor stroke onset. This externally well-validated nomogram provides clinician a new tool more useful than traditional risk scores in patient counseling, because it can be readily and quickly applicable in presenting a visualized risk for each individual stroke survivor with an APP in mobile phone. In addition, we find the association of plasma TMAO level with PSCI, suggesting this metabolic marker linking intestinal microbiota to cognitive dysfunction. Future studies are warranted to investigate this potential target in cognitive impairment after minor stroke.

DATA AVAILABILITY STATEMENT

The original contributions generated for the study are included in the article/**Supplementary Material**, further inquiries can be directed to the corresponding authors.

ETHICS STATEMENT

The studies involving human participants were reviewed and approved by the Ethics Committee of Shanghai Tenth People's Hospital (Shanghai, China) and was conducted in accordance with the Declaration of Helsinki principles. The patients/participants provided their written informed consent to participate in this study.

AUTHOR CONTRIBUTIONS

LG performed most of the experiments, interpreted data, and wrote the first draft of the paper. HW, XZ, and QD performed a part of experiments, analyzed the data, and collect blood samples. QD, QY, BM, and LM all took part to conceive the study and a part of sample collection. YZ critically edited the manuscript and supervised the study. XL mainly provided funding and designed the study. All authors contributed to the article and approved the submitted version.

FUNDING

This work was supported by grants from the National Natural Science Foundation of China (Nos. 81901183 and 81771131), the Shanghai Municipal Key Clinical Specialty (No. shslczdzk06102), and the Science and Technology Commission of Shanghai Municipality (Nos. 17411950100 and 19140900105).

ACKNOWLEDGMENTS

We are grateful to Dr. WL Cai and Dr. RL Zhang (from Department of Radioloy, Shanghai Tenth People's Hospital, Tongji University) for their radiological diagnosis.

SUPPLEMENTARY MATERIAL

The Supplementary Material for this article can be found online at: https://www.frontiersin.org/articles/10.3389/fnagi.2021.637363/full#supplementary-material

REFERENCES

Besga, A., Chyzhyk, D., Gonzalez-Ortega, I., Echeveste, J., Graña-Lecuona, M., Graña, M., et al. (2017). White matter tract integrity in Alzheimer's disease vs. late onset bipolar disorder and its correlation with systemic inflammation and oxidative stress biomarkers. *Front. Aging Neurosci.* 9:179. doi: 10.3389/fnagi.2017.00179

Boots, E. A., Castellanos, K. J., Zhan, L., Barnes, L. L., Tussing-Humphreys, L., Deoni, S. C. L., et al. (2020). Inflammation, cognition, and white matter in older adults: an examination by race. *Front. Aging Neurosci.* 12:553998. doi: 10.3389/fnagi.2020.553998

Busch, R. M., Hogue, O., Kattan, M. W., Hamberger, M., Drane, D. L., Hermann, B., et al. (2018). Nomograms to predict naming decline after temporal lobe surgery in adults with epilepsy. *Neurology* 91, 2144–2152. doi: 10.1212/WNL.0000000000006629

Cappellari, M., Mangiafico, S., Saia, V., Pracucci, G., Nappini, S., Nencini, P., et al. (2019). IER-SICH nomogram to predict symptomatic intracerebral hemorrhage after thrombectomy for stroke. *Stroke* 50, 909–916. doi: 10.1161/STROKEAHA.118.023316

Cappellari, M., Turcato, G., Forlivesi, S., Zivelonghi, C., Bovi, P., Bonetti, B., et al. (2018). STARTING-SICH nomogram to predict symptomatic intracerebral hemorrhage after intravenous yhrombolysis for Stroke. *Stroke* 49, 397–404. doi: 10.1161/STROKEAHA.117.018427

Chander, R. J., Lam, B. Y. K., Lin, X., Ng, A. Y. T., Wong, A. P. L., Mok, V. C., et al. (2017). Development and validation of a risk score (CHANGE) for cognitive impairment after ischemic stroke. *Sci. Rep.* 7:12441. doi: 10.1038/s41598-017-12755-z

Gong, L., Wang, H., Dong, Q., Zhu, X., Zheng, X., Gu, Y., et al. (2020). Intracranial atherosclerotic stenosis is related to post-stroke cognitive impairment: a cross-sectional study of minor stroke. *Curr. Alzheimer Res.* 17, 177–184. doi: 10.2174/1567205017666200303141920

Jiang, Y., Wong, A., Yuan, Z., Xu, K., Zhang, K., Zhu, Z., et al. (2019). Total cerebral small vessel disease burden Is related to worse performance on the mini-mental state examination and incident dementia: a prospective 5-year follow-up. *J. Alzheimers Dis.* 69, 253–262. doi: 10.3233/JAD-181135

Kandiah, N., Chander, R. J., Lin, X., Ng, A., Poh, Y. Y., Cheong, C. Y., et al. (2016). Cognitive impairment after mild Stroke: development and validation of the SIGNAL2 Risk Score. *J. Alzheimers Dis.* 49, 1169–1177. doi: 10.3233/JAD-150736

Levine, D. A., Galecki, A. T., Langa, K. M., Unverzagt, F. W., Kabeto, M. U., Giordani, B., et al. (2015). Trajectory of cognitive decline after incident stroke. *JAMA* 314, 41–51. doi: 10.1001/jama.2015.6968

Liu, Y., Kong, C., Gong, L., Zhang, X., Zhu, Y., Wang, H., et al. (2020). The association of post-stroke cognitive impairment and gut microbiota and its vorresponding metabolites. *J. Alzheimers Dis.* 73, 1455–1466. doi: 10.3233/JAD-191066

Mandzia, J. L., Smith, E. E., Horton, M., Hanly, P., Barber, P. A., Godzwon, C., et al. (2016). Imaging and baseline predictors of cognitive performance in minor ischemic stroke and patients with transient ischemic attack at 90 days. *Stroke* 47, 726–731. doi: 10.1161/STROKEAHA.115.011507

Ojala-Oksala, J., Jokinen, H., Kopsi, V., Lehtonen, K., Luukkonen, L., Paukkunen, A., et al. (2012). Educational history is an independent predictor of cognitive deficits and long-term survival in postacute patients with mild to moderate ischemic stroke. *Stroke* 43, 2931–2935. doi: 10.1161/STROKEAHA.112.667618

Olek, R. A., Samulak, J. J., Sawicka, A. K., Hartmane, D., Grinberga, S., Pugovics, O., et al. (2019). Increased Trimethylamine N-Oxide is not associated with oxidative stress markers in healthy aged women. *Oxid. Med. Cell. Longev.* 2019:6247169. doi: 10.1155/2019/6247169

Saczynski, J. S., Sigurdsson, S., Jonsdottir, M. K., Eiriksdottir, G., Jonsson, P. V., Garcia, M. E., et al. (2009). Cerebral infarcts and cognitive performance: importance of location and number of infarcts. *Stroke* 40, 677–682. doi: 10.1161/STROKEAHA.108.530212

Shang, Y., Fratiglioni, L., Marseglia, A., Plym, A., Welmer, A. K., Wang, H. X., et al. (2020). Association of diabetes with stroke and post-stroke dementia: a population-based cohort study. *Alzheimers Dement.* 16, 1003–1012. doi: 10.1002/alz.12101

Wang, X., Sun, G., Feng, T., Zhang, J., Huang, X., Wang, T., et al. (2019). Sodium oligomannate therapeutically remodels gut microbiota and suppresses gut bacterial amino acids-shaped neuroinflammation to inhibit Alzheimer's disease progression. *Cell Res.* 29, 787–803. doi: 10.1038/s41422-019-0216-x

Wu, C., Xue, F., Lian, Y., Zhang, J., Wu, D., Xie, N., et al. (2020). Relationship between elevated plasma trimethylamine N-oxide levels and increased stroke injury. *Neurology* 94, 667–677. doi: 10.1212/WNL.0000000000008862

Yang, J., Wong, A., Wang, Z., Liu, W., Au, L., Xiong, Y., et al. (2015). Risk factors for incident dementia after stroke and transient ischemic attack. *Alzheimers Dement.* 11, 16–23. doi: 10.1016/j.jalz.2014.01.003

Yin, J., Liao, S. X., He, Y., Wang, S., Xia, G. H., Liu, F. T., et al. (2015). Dysbiosis of gut microbiota with reduced Trimethylamine-N-Oxide level in patients with large-artery atherosclerotic stroke or transient ischemic attack. *J. Am. Heart Assoc.* 4:e002699. doi: 10.1161/JAHA.115.002699

Zhu, C., Li, G., Lv, Z., Li, J., Wang, X., Kang, J., et al. (2020). Association of plasma trimethylamine-N-oxide levels with post-stroke cognitive impairment: a 1-year longitudinal study. *Neurol. Sci.* 41, 57–63. doi: 10.1007/s10072-019-04040-w

Zhu, J., Wang, Y. J., Li, J., Deng, J., and Zhou, H. D. (2014). Intracranial artery stenosis and progression from mild cognitive impairment to Alzheimer disease. *Neurology* 82, 842–849. doi: 10.1212/WNL.0000000000000185

Conflict of Interest: The authors declare that the research was conducted in the absence of any commercial or financial relationships that could be construed as a potential conflict of interest.

frontiers in Aging Neuroscience

REVIEW
published: 08 June 2021
doi: 10.3389/fnagi.2021.687246

Mitophagy in Cerebral Ischemia and Ischemia/Reperfusion Injury

Luoan Shen[1†], Qinyi Gan[1†], Youcheng Yang[1], Cesar Reis[2], Zheng Zhang[1], Shanshan Xu[3], Tongyu Zhang[4] and Chengmei Sun[1,3]**

[1] Zhejiang University-University of Edinburgh Institute, School of Medicine, Zhejiang University, Haining, China, [2] VA Loma Linda Healthcare System, Loma Linda University, Loma Linda, CA, United States, [3] Institute for Advanced Study, Shenzhen University, Shenzhen, China, [4] Department of Neurosurgery, Xuanwu Hospital, Capital Medical University, Beijing, China

Ischemic stroke is a severe cerebrovascular disease with high mortality and morbidity. In recent years, reperfusion treatments based on thrombolytic and thrombectomy are major managements for ischemic stroke patients, and the recanalization time window has been extended to over 24 h. However, with the extension of the time window, the risk of ischemia/reperfusion (I/R) injury following reperfusion therapy becomes a big challenge for patient outcomes. I/R injury leads to neuronal death due to the imbalance in metabolic supply and demand, which is usually related to mitochondrial dysfunction. Mitophagy is a type of selective autophagy referring to the process of specific autophagic elimination of damaged or dysfunctional mitochondria to prevent the generation of excessive reactive oxygen species (ROS) and the subsequent cell death. Recent advances have implicated the protective role of mitophagy in cerebral ischemia is mainly associated with its neuroprotective effects in I/R injury. This review discusses the involvement of mitochondria dynamics and mitophagy in the pathophysiology of ischemic stroke and I/R injury in particular, focusing on the therapeutic potential of mitophagy regulation and the possibility of using mitophagy-related interventions as an adjunctive approach for neuroprotective time window extension after ischemic stroke.

Keywords: mitophagy, mitochondrial dysfunction, ischemic stroke, ischemia/reperfusion injury (I/R injury), recanalization therapy, therapeutic window

OPEN ACCESS

Edited by:
Hailiang Tang,
Fudan University, China

Reviewed by:
Huiqing Wang,
Shandong University, China
Jun Ren,
University of Washington, United States

***Correspondence:**
Tongyu Zhang
dr_tongyuzhang@163.com
Chengmei Sun
chengmeisun1756@gmail.com

† These authors have contributed equally to this work

Received: *29 March 2021*
Accepted: *10 May 2021*
Published: *08 June 2021*

Citation:
Shen L, Gan Q, Yang Y, Reis C, Zhang Z, Xu S, Zhang T and Sun C (2021) Mitophagy in Cerebral Ischemia and Ischemia/Reperfusion Injury. Front. Aging Neurosci. 13:687246. doi: 10.3389/fnagi.2021.687246

INTRODUCTION

Stroke is a sudden onset of cerebral blood circulation disorders caused by cerebral infarction or hemorrhage (Shi et al., 2021). Depending on the area of the brain affected, patients may present with different symptoms, among which the most common ones are the acute onset of weakness in one-side of the body and a reduced speaking ability (Nor et al., 2005). Stroke is the fifth leading cause of death according to American Heart Association (AHA). Around 795,000 people suffer from either new or recurrent stroke each year (Virani Salim et al., 2020). There are two major types of stroke: ischemic stroke and hemorrhagic stroke. In ischemic stroke, blood flow is blocked by thrombosis formed around the ruptured atherosclerotic plaques in the artery, while hemorrhagic stroke usually results from bleeding induced by blood vessel rupture.

Ischemic stroke accounts for about 87% of all stroke cases. Thus it is under great attention in research and clinical practice. Blocked blood flow leads to the lack of oxygen and nutrients, triggering an ischemic cascade in the brain. The production of adenosine triphosphate (ATP) would be disrupted, which is often a lethal situation to vulnerable brain cells that are highly

energy-dependent. In detail, failure in ATP generation can result in the weakened activity of ATP-dependent ion channels, including sodium channels, thus causing intracellular hyperosmolarity (Deb et al., 2010). Also, increased anaerobic respiration during ischemia produces byproduct lactic acid, leading to metabolic acidosis. Severe alternations in the ion balance can cause cytotoxic edema, disrupt the glutamate receptor activity, which eventually damages DNA and structural proteins or even leads to cell deaths (Nishizawa, 2001; Deb et al., 2010). Irreversible neuropathological changes in neurons usually occur within 20–30 min after ischemia (Ordy et al., 1993).

Reperfusion treatments which aim at restoring blood flow and oxygen to the ischemic area before neuronal damage, are the primary management for ischemic stroke patients in the clinic. Intravenous tissue plasminogen activator (IV tPA) is the only FDA-approved thrombolytic agent for treating acute stroke. Previous evidence suggests it only shows significant clinical improvement when given within 3 h after ischemia (Kwiatkowski et al., 1999). Another randomized trial study performed in 2017 indicated that intravenous therapies within 6 h still benefit over safety concerns (Berkhemer et al., 2014). Mechanical thrombectomy, a surgical procedure to remove thrombosis from arteries, is another commonly used reperfusion therapy. Thrombectomy is efficient in reducing post-stroke disability, though its efficacy and safety can only be ensured within 8 h after the stroke onset (Jovin et al., 2015). In recent years, two high-quality clinical trials focusing on delayed recanalization indicate that reperfusion treatment given at 24 h or even later after the stroke onset still show some improved prognosis in selected patients, thus extending the therapeutic window to 24 h in specific patient populations (Ragoschke-Schumm and Walter, 2018). However, all current treatments have the major limitation of increasing the risk of intracranial hemorrhage (ICH) when given outside the therapeutic window, which can further damage the brain tissue. This subsequent injury following reperfusion therapy is termed as ischemia/reperfusion (I/R) injury, a process that involves reoxygenation-induced reactive oxygen species (ROS) production, calcium overload, and tissue damage. Therefore, extending the reperfusion time window after ischemic stroke while providing neuroprotection is extremely important for disease management.

Autophagy is a natural process that degrades unnecessary or damaged organelles and proteins to maintain cellular homeostasis. Autophagy can be activated after ischemic stroke when brain cells are exposed to the risk of oxygen and nutrients deficiency. To be more specific, oxygen-glucose deprivation stimulates the increase in AMP/ATP ratio, which is an activator for the AMPK pathway (Oakhill et al., 2011; Jiang et al., 2018). Upregulation of the AMPK pathway can thus initiate autophagy via direct activation of the ULK complex through phosphorylating of Ser 317 and Ser 777, or indirect activation of ULK through inhibiting the activity of mTOR, as mTOR suppresses Ulk1 activation by phosphorylating Ulk1 Ser 757 and disrupting the interaction between Ulk1 and AMPK (Egan et al., 2011; Kim J. et al., 2011). Previous researches shows controversial results regarding the role of autophagy after ischemic stroke. Some studies show that autophagy provides neuroprotection and improves clinical outcomes by significantly reducing ischemic damage of neurons, glia, and endothelial cells (Papadakis et al., 2013; Jiang et al., 2015; Dai et al., 2017). Meanwhile, other findings suggest that excess autophagy might be harmful to brain cells (Li et al., 2017; Mo et al., 2020). To sum up, despite the controversial evidence, it is generally agreed that moderate autophagy is protective, while excessive autophagy may contribute to cell deaths during ischemia (Mo et al., 2020). Ischemic preconditioning (IPC), a strategy that uses short periods of vascular occlusion and reperfusion to prevent fetal ischemic events and recanalization, can activate the neuroprotective program in the brain via triggering adaptive autophagy targeting damaged organelles and alleviating oxidative stress in the acute ischemic stroke (Yang et al., 2020; Ajoolabady et al., 2021). In addition, cerebral ischemia postconditioning, which reduces maladaptive autophagy by applying short periods of reperfusion interrupted by ischemia at the beginning of recanalization, has been induced to suppress reperfusion injury, indicating its protective role in treating ischemic stroke (Vinten-Johansen, 2017; Ajoolabady et al., 2021).

Mitophagy, a type of selective autophagy, can remove dysfunctional mitochondria. Mitochondria play a central role in cellular energy production, calcium homeostasis maintenance and ROS regulation. Mitochondrial dysfunction can increase oxidative stress and cellular damage (Liu, 1999; Indo et al., 2007). Mitophagy mainly work as a mitochondrial quality control through the clearance of damaged mitochondria. In mammals, dysfunctional mitochondria can be cleared either via PINK1-Parkin dependent ubiquitination pathway or via the activation of mitophagy receptors, thus reducing ROS generation from mitochondria (Lemasters, 2005) and protecting cells against unfavorable niche (Huang et al., 2011). Under the condition of ischemic stroke, malfunctioned mitochondria increase the release of pro-apoptotic factors including cytochrome c, to induce cell deaths in the affected area (Jürgensmeier et al., 1998; Lemasters, 2005). It is worth note that mitophagy may have different effects during the first ischemic phase and later the reperfusion phase. Studies have indicated that mitophagy exerts its protective role mainly during the reperfusion phase (Kumar et al., 2016).

In recent years, the role of mitophagy in acute stroke has been extensively studied. Most studies indicate a neuroprotection role of mitophagy in alleviating reperfusion injury through multiple mechanisms. This review summarizes the role of mitophagy in ischemic stroke and I/R injury, proposing mitophagy-related interventions as an adjunctive approach for ischemic stroke management. Updates regarding delayed recanalization and the potential involvement of mitophagy in it were also discussed.

MITOCHONDRIA AND MITOPHAGY

Mitochondria are an important organelles that is mainly responsible for energy production. However, damaged mitochondria release harmful ROS and other oxidants, such as H_2O_2 and peroxynitrite, into the cytoplasm and cause damage to the proteins, nuclear acid, and membranes (Zhou et al., 2011). Worse over, cytochrome c, a mitochondrial intermembrane space

protein, will be released under severe mitochondrial damage, which triggers caspase cascade and finally apoptosis (Ott et al., 2002). Therefore, rapid degradation of damaged mitochondria is necessary for cell survival. Mitophagy is a process during which damaged or aging mitochondria are selectively wrapped by phagophores and undergo lysosomal degradation to maintain cell homeostasis and prevent cell apoptosis. Mitophagy starts with the formation of the phagophore, a membrane structure isolated from the endoplasmic reticulum. Phagophore then recognizes damaged mitochondria through LC3 adaptors or LC3 receptors and engulfs damaged mitochondria for autosomal degradation. Currently, the mitophagy pathways consist of two major types: ubiquitin-mediated pathway and receptor-mediated pathway (**Figure 1**).

Ubiquitin-Mediated Pathway

The PTEN-induced putative kinase protein 1 (PINK1) and Parkin-mediated ubiquitination pathway are some of the most well-characterized mitophagy mechanisms. In healthy mitochondria, PINK1, a serine/threonine kinase, is imported from the cytoplasm continuously, and undergoes cleavage by the mitochondrial proteases mitochondrial-processing peptidase (MPP) and presenilin associated rhomboid like (PARL) (Greene et al., 2012). Upon ischemic stroke, the mitochondria membrane is depolarized, which prevents the import of PINK1 and results in the accumulation of PINK1 on the mitochondrial membrane. As a result, the kinase activity of full-length PINK1 induces phosphorylation of E3 ligase Parkin, which activates the enzymatic function of Parkin and leads to ubiquitination of several mitochondrial proteins (Kazlauskaite et al., 2015). Meanwhile, PINK1 phosphorylates ubiquitin and results in binding of phosphorylated ubiquitin and Parkin, where the ligase activity is further improved (Koyano et al., 2014; Kazlauskaite et al., 2015).

Once Parkin is activated, it conjugates ubiquitin moieties onto the OMM proteins and thereby mitophagy is induced. Some ubiquitinated mitochondrial proteins, such as MFN1, are degraded, which is essential for the mitochondrial fission and mitophagy (Tanaka et al., 2010). Other ubiquitinated proteins recruit autophagy adaptor proteins such as optineurin (OPTN) and nuclear dot protein 52 (NDP52), which anchors the marked mitochondria to autophagosome by its LC3-interacting region (LIR) motifs, thereby mitophagy is initiated (Lazarou et al., 2015). Moreover, PINK1 can recruit OPTN and NDP52 independently of parkin, which subsequently recruits several autophagy initiation factors, such as unc-51-like autophagy activating kinase 1 (ULK1), for mediating phagophore synthesis and elongation (Wong and Holzbaur, 2014; Lazarou et al., 2015).

Several other E3 ligases have also been discovered to initiate mitophagy. Some mechanisms are related to PINK1/Parkin mediated mitophagy and some are independent of Parkin. For example, overexpression of mitochondrial ubiquitin ligase 1 (MUL1) mediates the degradation of mitofusin by ubiquitination, which rescues the PINK1/parkin mutant phenotype (Yun et al., 2014). In mature neurons, MUL1 is also important for the contact of ER and mitochondria and the absence of it impairs the Ca^{2+} homeostasis in mitochondria and reduces the intake of Ca^{2+} from ER. This leads to activation of calcineurin, which activate Drp1 and therefore induce

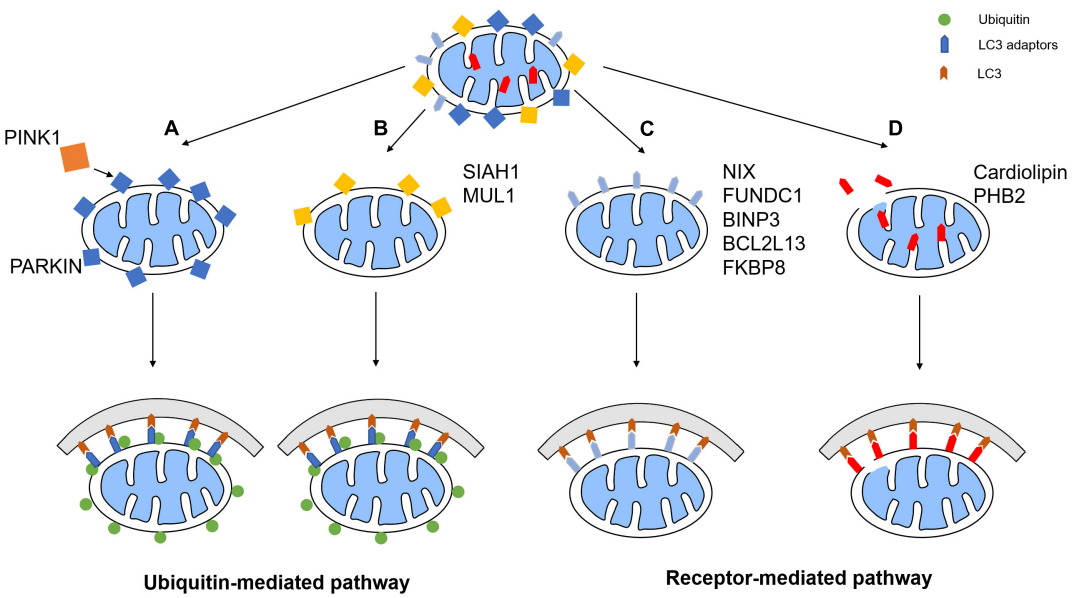

FIGURE 1 | Mitophagy pathways. The mitophagy pathways can be generally divided into two types: ubiquitin-mediated pathway and receptor-mediated pathway. **(A)** PINK1 phosphorylates the E3 ubiquitin ligase Parkin, which promotes the ubiquitination of OMM proteins. Some of these proteins recruit LC3 adaptors, which induces mitophagy. **(B)** Other E3 ligases such as SIAH1 and MUL1 also has similar pathways. **(C)** Some mitophagy receptors such as NIX, FUNDC1, BNIP3, BCL2L13, and FKBP8, are upregulated or activated under certain conditions, therefore recruiting phagophore to initiate mitophagy. **(D)** IMM receptors including cardiolipin and PHB2 recruits phagophore by interacting with LC3 to promote mitophagy.

mitochondria fission. Fragmented mitochondria lose their membrane potential, and PINK1/Parkin mediated mitophagy is induced (Puri et al., 2019). Another E3 ligase, seven *in absentia* homolog (SIAH)-1, is recruited by synphilin-1 when full-length PINK1 is present. SIAH-1 promotes mitophagy through ubiquitination of mitochondrial proteins independently of Parkin (Szargel et al., 2016).

In addition to the benefits of PINK1-Parkin mediated ubiquitination, deubiquitinases are essential for correct mitophagy. The deubiquitination of Parkin is carried out directly by ubiquitin-specific peptidase 8 (USP8) (Durcan et al., 2014), while USP15 deubiquitinates the substrates of Parkin to inhibit mitophagy (Cornelissen et al., 2014). Several other deubiquitinases, such as USP30, USP35, and USP33 (Bingol et al., 2014; Wang Y. et al., 2015; Niu et al., 2020), counteract ubiquitin-mediated mitophagy by removing ubiquitin chains from the mitochondrial membrane. Therefore, a fine-tuned balance between ubiquitination and deubiquitination is established for the regulation of mitophagy.

Receptor-Mediated Pathway

An alternative pathway of mitophagy is through mitophagy receptor signaling. Multiple mitophagy receptors are currently identified in mammalian cells (Ren et al., 2018), which contains a least one LIR for the direct binding of autophagy mediator LC3 and the subsequent phagosome engulfment.

A critical receptor in the turnover of mitochondria in erythrocytes is an OMM protein named BCL2 interacting protein 3 like (BINP3-L, also known as NIX) (Sandoval et al., 2008). It is transcriptionally upregulated during erythrocytes maturation to clear mitochondria. In conditions of hypoxia, the BINP3-L is induced along with its homolog, BNIP3, promoting mitophagy through OPA1 disassembly and DRP1 recruitment, which is transcriptionally regulated by forkhead box O3 (FOXO3) and hypoxia-inducible factor (HIF), thereby inducing mitochondrial fission and inhibiting mitochondrial fusion (Sowter et al., 2001; Mammucari et al., 2007). Moreover, its binding affinity to LC3 is further improved by the phosphorylation of the LIR under stress conditions (Rogov et al., 2017).

Another essential mitophagy receptor is the FUN14 domain containing 1 (FUNDC1), which mediates mitophagy under hypoxic conditions (Liu et al., 2012). FUNDC1 activity is regulated by its phosphorylation state. In non-stress conditions, it is suppressed by phosphorylation of Src at Tyr18 and casein kinase II (CK2) at Ser13 (Chen et al., 2014). Under hypoxia, PGAM5 phosphatase dephosphorylate FUNDC1, which activates the LIR motif on FUNDC1 and induce mitophagy. Moreover, FUNDC1 recruits Drp1 and disrupts its physical association with OPA1 under stress (important for mitochondria dynamic), thereby inducing mitochondrial fission and inhibiting mitochondrial fusion (Chen et al., 2016).

Additionally, there are multiple other mitophagy receptors. On the outer mitochondrial membrane, BCL 2 Like 13 (BCL2L13) and FKBP prolyl isomerase 8 (FKBP8) have been shown to mediate mitophagy by binding LC3 via the LIR motif independently of Parkin (Murakawa et al., 2015; Bhujabal et al., 2017). Some receptors also locate in the IMM, such as prohibitin 2 (PHB2) and cardiolipin. Once the OMM is depolarized or damaged, PHB2 will interact with LC3 to directly promote mitophagy (Wei et al., 2017). However, the depletion of PHB2 upon OMM rupture destabilizes PINK1 through the activation of PARL and therefore leads to cleavage of full-length PGAM5 (Yan et al., 2020). This abolishes PGAM5-involved PINK1 stabilization and thereby inhibits PINK1/Parkin-dependent mitophagy. Recently, cardiolipin, a phospholipid, has also been identified as a mitophagy receptor, whose primary synthesis is conducted in the IMM. When encountering OMM rupture, cardiolipin is released to the OMM and interacts with LC3, triggering a signaling cascade that results in engulfment of the mitochondria (Chu et al., 2013).

Mitochondria Dynamics and Its Relationship With Mitophagy

To adapt to the external environment, mitochondria fuses both the inner and outer membranes or undergo fission and separate into several mitochondria. These two essential processes in mitochondria dynamics are termed fusion and fission. When confronting cellular stress, fusion is promoted to ensure energy production by repairing partially damaged mitochondria (Youle and van der Bliek, 2012).On the other hand, fission is necessary for mitophagy since it enables the separation of depolarized mitochondria, allowing the preservation of "the healthy part" in mitochondria and reduces unnecessary loss during mitophagy. Depending on the quality of mitochondria, either fusion or fission will be activated along with the inhibition of the other (Twig et al., 2008).

In mammalian cells, MFN1, MFN2, and OPA1, which are GTPases, mediate the fusion of the mitochondria (Wu et al., 2019). These proteins are often modified post-transcriptionally to control their potency. For MFN1, extracellular regulated kinase (ERK) can phosphorylate it at Thr562 to suppress fusion. MFN1 can also be ubiquitinated by MARCH5 for degradation (Park et al., 2014). Mitogen-activated protein kinase 8 (MAPK8, also known as JNK) phosphorylates MFN2 at Ser27 under stress for subsequent ubiquitination by E3 ligases Parkin (Gegg et al., 2010), HUWE1 (Leboucher et al., 2012), and mitochondrial ubiquitin ligase membrane-associated RING-CH (MARCH5) (Sugiura et al., 2013). MFN1 and MFN2 can be deubiquitinated by USP30, where inhibition of it will lead to non-degradative ubiquitination of MFN1/2 (Yue et al., 2014). For OPA1, it is regulated by changes in the protease activity of YME1L and OMA1, which is responsive to intramitochondrial signals (Griparic et al., 2007; Head et al., 2009).

The mitochondrial fission is regulated mainly by a cytosol protein, DRP1, whose recruitment is mediated by mitochondrial fission factors such as MFF. DRP1 can be phosphorylated by protein kinase A at Ser637 and Ser656, which inhibits its activity. Dephosphorylation of DRP1 is mediated by the calcium-dependent protein phosphatase calcineurin or by protein phosphatase 2A (PP2A) for enhanced fragmentation under stress (Chang and Blackstone, 2007; Cribbs and Strack, 2007). Moreover, energy-sensing adenosine monophosphate (AMP)-activated protein kinase (AMPK) phosphorylates MFF under

energy stress, which recruits Drp1 and accelerate mitochondrial fission (Toyama et al., 2016).

Mitophagy is closely interrelated with mitochondrial dynamics as multiple mitophagy proteins are found to promote fission and facilitate mitophagy. For instance, phosphorylated Parkin can ubiquitinate MFN1 and MFN2 for degradation, which decreases mitochondrial fusion and enhance fragmentation, leading to the initiation of mitophagy (Tanaka et al., 2010). During mitophagy, MFN2 is also phosphorylated by PINK1 to recruit Parkin for further mitophagy (Chen and Dorn, 2013).

PATHOPHYSIOLOGY OF ISCHEMIC-REPERFUSION INJURY (FIGURE 2)

Clinical Classification of Ischemic Stroke

Ischemic stroke, also known as cerebral ischemia, is the significant type of all stroke cases. This disease occurs when blood clots or plaques block or narrow the brain arteries. Depending on the pathological condition, ischemic stroke can be divided into several subtypes: Intracranial arterial stenosis, acute arterial occlusion, and chronic arterial occlusion. Intracranial arterial stenosis refers to the narrowing of arteries caused by the formation of fatty deposits called atherosclerotic plaques and the concurrent thickening of vessel walls. In Intracranial arteries, including middle cerebral arteries, basilar artery, carotid arteries, and intracranial vertebral arteries, narrowed blood vessels can significantly reduce blood flow, leading to an ischemic event (Chimowitz et al., 2005; Banerjee and Chimowitz, 2017). A systematic analysis focusing on the role of intracranial atherosclerosis in ischemic stroke indicates that atherosclerosis-inducing stenosis graded higher than 30% can be a cause of fatal brain infarction (Mazighi et al., 2008). The atherosclerotic plaque is thrombogenic. Once its cap is ruptured, an unstable clot can be formed to narrow or completely occlude the arteries. The blood clot that blocks the affected site can form locally or originate elsewhere, such as in the heart, and embolize through the circulatory system. Rupture of plaques and clot embolisms is usually linked with acute arterial occlusion, manifesting stroke symptoms within hours (Malhotra et al., 2017). The occlusion can also be chronic (lasting more than 4 weeks) if the brain alters the cerebral hemodynamics and compensates the blood flow by building a collateral circulation in response to the reduced arterial blood supply (Sundaram et al., 2017). In that case, with sufficient collateral compensation, the disease can be asymptomatic and benign (Powers et al., 2000); Chronic occlusion without enough compensation from collateral circulation might still result in chronic cerebral hypoperfusion, leading to ischemic infarction. In some cases, patients with chronic occlusion may spontaneously recanalize over a long time (more than 3 months) (Delgado et al., 2015).

Management of Ischemic Stroke

Thrombolytic agents and recanalization procedures are developed as reperfusion strategies to recover the blood flow in affected arteries. Usually, different therapeutic approaches are given to these three subtypes of stroke in the clinic setting. Due to technical limits, severe stenosis and acute occlusion of arteries are difficult to distinguish accurately (Clevert et al., 2006). Still, the correct diagnosis can be beneficial for optimal treatment and a better prognosis. Intravenous thrombolysis is the only approved therapy for AIS patients and can be given within 3 h of symptom onset. However, clinical outcomes of thrombolytic medical treatment alone for patients with severe stenosis and occlusion have shown worse than expected prognosis and less efficacy (Mokin et al., 2012). Clinical trials focusing on lysis of clots suggest that intravenous thrombolytic therapy alone has a low recanalization rate of only 30–40% among patients (Chen et al., 2012). Another analysis of clinical outcomes of intravenous thrombolysis for internal carotid artery occlusion suggests the rate of favorable outcomes be 25% (Mokin et al., 2012). Revascularization treatments, including stenting or endarterectomy, have thus been advised for patients with moderate or severe stenosis. Compared with intravenous thrombolysis, thrombectomy recipients have a significantly reduced incidence of ipsilateral stroke, meaning a better prognosis. Arterial therapies also achieve a better outcome in patients with acute occlusion (Mokin et al., 2012). However, in the clinic setting, endarterectomy is not considered as an option by many in treating complete ICA occlusion since this operation is still technically challenging to perform in preventing postoperative thrombus generation and maintaining a good prognosis (Kao et al., 2007; Chen et al., 2012; Faggioli et al., 2013). Until now, the search for effective treatments for chronic occlusion continues. Medical treatment like anti-platelet aggression drugs or intravenous tissue plasminogen activator can be given to patients to decrease the risk of stroke. Surgical approaches like endarterectomy and stenting can also be used in treating chronic occlusion, though they still show some seeming drawbacks. Like in acute occlusion, endarterectomy might fail in cases with complex clot organization, and the successful rate of recanalization only achieves 40% in patients with chronic occlusion (Thompson et al., 1986; Xu et al., 2018). Hypoperfusion still occurs in patients who have failed to restore blood flow in recanalization therapies, which is presumed to result in the recurrence of ischemic events (Grubb et al., 1998). Also, in the process of stenting, the clot may detach when the stent is released, blocking the intracranial artery and may therefore causing post-operative complications (Xu et al., 2018).

Ischemia-Reperfusion Injury

In patients receiving recanalization therapies, sudden restoration of blood flow can sometimes be harmful, leading to the so-called 'reperfusion injury.' I/R injury refers to the tissue reoxygenation injury caused by the sudden return of blood supply to formerly ischemic or anoxic tissues. During the ischemia phase, the blood supply below standard functional requirements will cause deficiencies in oxygen and nutrients, leading to metabolic disturbances (Irie et al., 2014) and inflammatory response (Jin et al., 2013) in affected areas. Restoration of blood flow thus has been considered as a fundamental treatment to preserve tissue function. Loads of research and clinical trials on

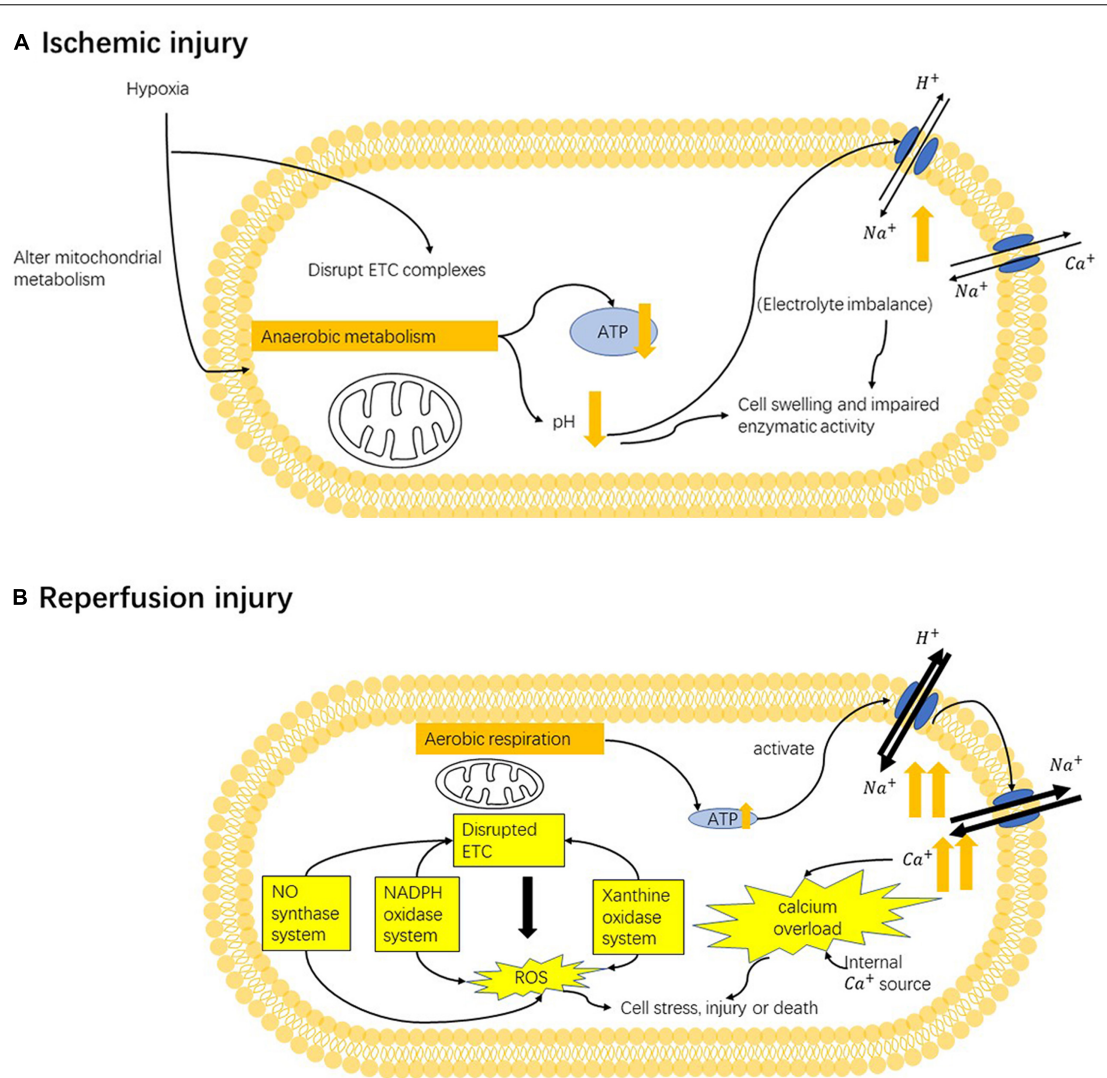

FIGURE 2 | Mechanism of ischemia-reperfusion injury. **(A)** In the ischemic state, hypoxia (oxygen deficiency) converts mitochondrial metabolism from aerobic to anaerobic, resulting in lower ATP generation. Anaerobic respiration also induces metabolic acidosis and leads to the activation ion-exchange channels. Altered electrolyte imbalance can cause cell swelling and impair enzymatic activity. Moreover, under hypoxia, the mitochondrial electron-transport chains (ETCs) are also disrupted. **(B)** In the reperfusion state, mitochondrial damage and cellular alternations caused by previous hypoxia can stimulate the production of reactive oxygen species (ROS) from multiple sources: the NADPH oxidase system, nitric oxide synthase system, xanthine oxidase system and mainly mitochondrial electron-transport chains. Such enhanced oxidative stress can target mitochondria ETC and cause further damage ETC, causing more ROS production. Oxidative stress can cause secondary cellular damage. Restoration of oxygen can induce the overactivation of pumps that are inhibited by ischemia-induced ATP deficiency, which rapidly triggers the influx of sodium ions and later calcium ions. Altering calcium homeostasis causes cellular damage, stimulates ROS production and induces cell death by triggering the opening of mPTP and activating apoptotic pathway.

reperfusion treatments have shown that reperfusion therapies, including intravenous thrombolytic agents and endovascular interventions like mechanical thrombectomy, are relatively safe and can help with the recovery of acute ischemic stroke (AIS) patients when given inside a narrow time window (Kwiatkowski et al., 1999; Lees et al., 2010; Berkhemer et al., 2014; Jovin et al., 2015). However, reperfusion might also cause secondary injury in the previously ischemic tissues since the resupply of nutrients and oxygen can trigger considerable ROS production and accumulation and meanwhile alters calcium homeostasis, resulting in excessive oxidative stress and local inflammation. Such cellular changes cause cell damage and may activate the cell death pathway in the former ischemic tissues.

Process and Mechanisms of I/R Injury (Figure 2)

Excessive Oxidative Stress Plays a Critical Part in I/R Injury

Oxidative stress is a disturbance in the balance between free radicals and antioxidant ability, and it often occurs when the production of ROS surpasses antioxidant defense. In the ischemic

stage, obstructed blood flow with less oxygen and nutrient supply induces a shift in mitochondrial metabolism from aerobic to anaerobic, thus producing a lower concentration of ATP and antioxidative agents in cells. Later return of blood flow to the ischemic tissue can cause the reactivation of mitochondrial aerobic respiration and thus increase the production of ROS. Because of the decreased level of antioxidative agents, oxidation exceeds antioxidation during the reperfusion period, thus causing increased oxidative stress. Enzyme systems, including xanthine oxidase system, the NADPH oxidase system, nitric oxide (NO) synthase system, and mitochondria electron transport chain, are involved mainly in the occurrence of oxidative stress.

In normal cells, purine metabolism initiates from converting ATP to inosine with the participation of deaminases and nucleotidases, followed by its further transformation into hypoxanthine. Oxidation of hypoxanthine to xanthine and xanthine to uric acid later occurs, and xanthine dehydrogenase (XDH) and xanthine oxidase (XOD) separately function in these two oxidation processes. XDH utilizes NAD^+ as an electron acceptor to produce NADH, and ischemia state can induce its shift to XOD that uses O_2 as an acceptor (Kinuta et al., 1989). Restoration of blood flow and oxygen can stimulate the oxidation process in purine metabolism. Since the level of XOD is previously promoted, the formation of uric acid in the reperfusion phase is accompanied by the production of highly reactive superoxide anion ($O2^-$). Superoxide can be later shifted to hydrogen peroxide (H_2O_2) and the hydroxyl radical (OH•), which further stimulates oxidative stress and causes damage.

NADPH oxidases are the primary source of ROS. They oxidize NADPH to $NADP^+$ and deliver electrons to O_2, thus generating superoxide or H_2O_2. Nox/Duox family of NADPH oxidases has been reported to involve in ROS production during I/R injury by their facilitated activity (Wang et al., 2006; Simone et al., 2014). Nox2 has been a focus in I/R injury that occurs in stroke. Nox subunit-deficient mice and mice with apocynin (a Nox-2 inhibitor) pretreatment show remarkably decreased infarct volume and improved the clinical outcome of stroke (Chen et al., 2009; Jackman et al., 2009), suggesting that Nox-induced ROS plays a considerable role in I/R injury.

Besides immediately producing ROS, NADPH oxidases are also regulating ROS production by stimulating NO synthase system. NO, also known as endothelium-derived relaxing factor, is made from L-arginine by nitric oxide synthase (NOS) of three sources: Neuron NOS (nNOS), inducible NOS (iNOS), and endothelial NOS (eNOS). The role of NO is variable: It generally works as an anti-oxidant agent, but its interaction with the superoxide anion can lead to the formation of the peroxynitrite ($ONOO^-$) (Marla et al., 1997). ROS created by NADPH oxidases can oxidize tetrahydrobiopterin (BH_4), an essential cofactor that mediates eNOS activity. BH_4 oxidation later induces the uncoupling of eNOS, resulting in decreased NO production and increased $ONOO^-$ production from eNOS (Landmesser et al., 2003).

Mitochondria are the major site of oxidative stress generation, action, and injury. ROS can be generated from ETC. In ischemia, cellular stress can induce post-translational modifications of oxidative phosphorylation proteins in ETC, making them more sensitive to reoxygenation (Prabu et al., 2006). Disrupted ETC complexes can result in higher mitochondrial membrane potentials, positively associated with more ROS generation (Prabu et al., 2006). Enhanced oxidative stress can target mitochondria and further damage ETC, causing more ROS generation (Indo et al., 2007) subsequently. ROS from exogenous origins and mitochondrial ROS generation can lead to mitochondria DNA damage (Indo et al., 2007). In addition, too much oxidative stress can cellular damage or death (**Figure 2**).

Calcium Overload: Another Disturbance in Ischemia-Reperfusion Injury

In addition to oxidative stress caused by different sources, calcium overload, abnormally increased intracellular Ca^{2+} level is another major pathology that plays an important role in reperfusion injury. Anaerobic respiration in ischemia decreases intracellular pH; thus, the Na^+/H^+ exchanger (NHE) allows for the influx of Na^+ to maintain the pH. NHE is generally inactivate during ischemia, but its activity can be increased during reperfusion, leading to a large Na^+ influx (Allen and Xiao, 2003). A lower level of ATP in ischemia also weakens the activity of energy-dependent Na^+ pump, resulting in a higher level of intracellular Na^+. A study in 1987 suggested that the precedent sodium imbalance be a cause of calcium overload using an energy-repleted Na^+ loading model (Grinwald and Brosnahan, 1987). Failing to return to normal Na^+ balance upon oxygen restoration can promote the function of Na^+/Ca^{2+} exchanger (NCX) that is sensitive to intracellular Na^+ level, thus leading to higher Ca^{2+} influx. Calcium overload is also induced by elevated Ca^{2+} release and limited Ca^{2+} uptake from an internal source, including endoplasmic reticulum (ER) or Golgi apparatus (Chami et al., 2008). Promoted uptake of Ca^{2+} by mitochondria later occurs following cytosolic calcium overload (Brookes et al., 2004). Cytosolic and mitochondrial calcium overload can cause cellular damage in various ways, including disrupting mitochondrial function (Wang M. et al., 2015), promoting ROS production (Zhu et al., 2018), and inducing cell death (Boehning et al., 2004; Zhu et al., 2018) (**Figure 2**).

Mitochondria-Dependent Cell Death in I/R Injury

Cellular alternations, including increased oxidative stress and calcium overload, can lead to apoptosis with the involvement of mitochondria. This process is initiated by changes in mitochondrial membrane permeability controlled by mitochondrial permeability transition pore (mPTP). The activity of mPTP is likely to be mediated by mitochondrial matrix Ca^{2+} level, and the mitochondrial calcium overload resulting from cytosolic calcium overload can facilitate the opening of mPTP (Qian et al., 1999). ROS production during I/R injury, especially hydroxyl radicals and hydrogen peroxide, have also been found indispensable in mPTP opening (Assaly et al., 2012). Permeabilized membrane allows for the activation and insertion of pro-apoptotic Bcl-2 family members BAX and BAK into mitochondria membrane (Wei et al., 2000; Kirkland et al., 2002). This helps with transferring mitochondrial proteins including cytochrome c from mitochondria to the cytosol, followed by the interaction between cytochrome c and two cofactors, apoptotic

protease activating factor 1 (APAF-1) and pro-caspase-9, to form the apoptosome, which eventually activates caspase–9-caspase-3 signaling cell death pathway with proteolytic events and DNA fragmentation (Broughton et al., 2009). This pathway is referred to as caspase-dependent apoptotic pathway.

Another cell death pathway, caspase-independent apoptosis, can be activated when cellular energy is running out (Daugas et al., 2000). Poly (ADP-ribose) polymerase-1 (PARP-1) is a nuclear enzyme that locates in the upstream of the pathway (Yu et al., 2002). ROS-induced DNA damage can trigger PARP-1 overactivation, in which NAD+ is used, thus depleting energy storage. Yu et al. (2002) also found that PARP-1 activation can lead to the release of its downstream target apoptosis-inducing factor (AIF, a mitochondrial flavoprotein) from mitochondrial intermembrane to nucleus, causing chromatin condensation and large-scale DNA fragmentation. Studies have indicated that AIF does not have a direct DNA fragmentation effect (Susin et al., 1999; Wang et al., 2002). Thus, it probably needs a downstream effector during this process. Studies have suggested that endonuclease G might interact with AIF and cause DNA fragmentation (Wang et al., 2002; Lee et al., 2005), though their interaction is still unclear. PARP-1-induced cell death is a unique cell death pathway. It generally exhibits characteristics of apoptosis, and it is also considered necrotic by some researchers since classic apoptosis is energy-dependent (Ha and Snyder, 1999).

The Brain Is Susceptible to I/R Injury

I/R injury can occur in many organs and tissues, including the brain, heart, skeletal muscles, and kidney. Some common features are shared by I/R injury in these areas, including the elevated production of ROS, calcium overload, inflammation, and the opening of mPTP. Yet, organ-specific characteristics can affect the severity of I/R injury in different organs. Brain, the organ where irreversible damage occurs within 20 min after ischemia and a narrow time window (generally 3–4.5 h) can be given for reperfusion therapy, is considered very susceptible to I/R injury (Ordy et al., 1993). ROS in the brain is mostly generated from mitochondria rather than other enzymatic ROS sources as a metabolically active area. The brain accounts for more than 20% of total body oxygen consumption but with a relatively low antioxidative agent level compared with other organs, making it vulnerable to oxidative stress (Markesbery and Lovell, 2007; Damle et al., 2009; Kalogeris et al., 2012).

Moreover, accumulated labile iron in the brain can react with H_2O_2 to produce highly reactive •OH. This reaction stimulates the oxidation and peroxidation of massively accumulated polyunsaturated fatty acid in the brain, causing even more oxidative stress (Ferretti et al., 2008). Because of the brain's susceptibility to I/R injury, finding targets to prevent reperfusion injury to the brain is significant in treating stroke.

Extending the Therapeutic Time Window in Ischemic Stroke: Delayed Recanalization

Successful recanalization of the occluded vessel as early as possible has been widely accepted as the vital principle of AIS treatment. Unfortunately, for many years, most AIS patients were prevented from receiving effective recanalization therapy because of a narrow therapeutic window. In recent years, a series of clinical trials have indicated that delayed recanalization may still have benefits in ischemic brains during an expanded therapeutic window, up to more than 24 h, several days, and even more than 1 month after symptom onset [Reviewed by Kang et al. (2020)].

Clinically, advances in imaging techniques have allowed better characterization of brain tissue and vessel status in AIS. Markers of brain ischemia are instructed by perfusion-weighted imaging/diffusion-weighted imaging (PWI/DWI) mismatch and DWI/fluid-attenuated inversion recovery (DWI/FLAIR) mismatch on magnetic resonance imaging (MRI). MRI scanning with PWI or computed tomography (CT) perfusion (CTP) scanning shows different hypoperfusion levels. Given these developments, together with advances in intravascular interventional devices, expanding the recanalization time window in certain patients is possible.

Increasing randomized studies have demonstrated that delayed recanalization has beneficial effects on 90-day outcomes. Two high-quality, randomized controlled clinical trials (DAWN and DEFUSE 3) of endovascular mechanical thrombectomy reported that selective delayed recanalization based on imaging mismatch improved patients' 90-day outcomes, even when performed at 16–24 h after symptom onset (Ragoschke-Schumm and Walter, 2018).

In summary, despite the risk of I/R injury, which might increase with the delayed time point for recanalization, delayed recanalization is still beneficial for a certain subtype of patients.

MITOPHAGY IN I/R INJURY

Mitophagy Is Activated Upon Ischemic Stroke

Enhanced mitochondrial fragmentation and fission were observed during both the ischemic phase and I/R injury. During OGD in rat cardiomyocyte cell line (H9C2 cells), massive mitochondria fragmentation was observed (Kim H. et al., 2011). Reoxygenation of mice cardiomyocyte cell line (HL1 cells) and neonatal primary cardiomyocytes show mitochondria fission (Ong et al., 2010; Disatnik et al., 2013). *In vivo* experiments using mice, 24-h left anterior descending permanent ligation model show consistent results (Kim H. et al., 2011). The brain tissue has a very similar situation as cardiomyocytes. Following OGD/reoxygenation, enhanced mitochondria fragmentation was observed in mice N2a neuroblastoma and primary rat neurons (Sanderson et al., 2015; Tang et al., 2016), accompanied by Opa1 processing and cytochrome C release. *In vivo* experiments in CA1 hippocampal neurons of rats have consistent results (Kumar et al., 2016).

Later, researchers found that mitophagy pathways are activated during ischemic/reperfusion through multiple signals. During the ischemic phase, ATP production rapidly decreases, which activates AMPK pathways to initiate autophagy via direct activation of the ULK complex through phosphorylating of Ser 317 and Ser 777, or indirect activation of ULK through inhibiting

the activity of mTOR, as mTOR suppresses Ulk1 activation by phosphorylating Ulk1 Ser 757 and disrupting the interaction between Ulk1 and AMPK (Kim J. et al., 2011; Zaha and Young, 2012). The activated ULK1 complex will then activate the class III PI3K complex (beclin 1, VPS34, and VPS15) that initiates the nucleation of phagophore (Kim J. et al., 2011). ULK1 has also been found to activate the FUNDC1 receptor, which may collaterally activate mitophagy (Kundu et al., 2008) (**Figure 3**).

During the reperfusion phase, the mechanistic target of rapamycin (mTOR) pathways is inhibited by ROS signals, thereby promoting the autophagosome's initiation and nucleation (Alexander et al., 2010). ROS has been found to activate mitophagy via BNIP3, while high levels of BNIP3 can induce apoptosis (Scherz-Shouval et al., 2007). PINK1/Parkin-mediated mitophagy is also activated in brain damage induced by cerebral ischemia and reperfusion. Lan et al. (2018) found significant increases in PINK1 accumulation in the outer membrane of mitochondria. They increased Parkin/p62 mitochondrial translocation after reperfusion, along with upregulation of autophagy markers LC3B, Beclin1, LAMP-1, with a peak at 24 h (**Figure 3**).

Mitophagy Exerts Its Protective Role Mainly During the Reperfusion Phase

Various studies have already demonstrated the protective role of enhanced mitophagy in attenuating brain injury after tMCAO in rats (Li et al., 2014; Di et al., 2015). However, whether mitophagy exerts its protective role during the ischemic phase of the reperfusion phase is unclear. Ischemia and reperfusion have different pathophysiology related to mitochondria. Thus, a series of studies have focused on distinguishing the ischemic and reperfusion phase. Intriguingly, mitophagy was identified to have a particular role during the reperfusion phase but may not the ischemic phase.

Inhibition of Drp1 was neuroprotective in response to OGD *in vitro* and transient focal ischemia *in vivo* (Grohm et al., 2012) and cardioprotective in cultured HL-1 cardiomyocytes subjected to OGD and reoxygenation (Dong et al., 2016). However, cardioprotection was only seen when inhibition of Drp1 was initiated as a pretreatment. When inhibiting Drp1 during reoxygenation, cell death was paradoxically exacerbated, indicating mitophagy is essential in protecting cells from reperfusion injury. In another study, researchers found that mitochondrial DNA level (which can be used as a marker for mitochondrial mass) does not decrease but significantly increase during the first few hours in the ischemic phase of stroke (Yin et al., 2008), which could indicate that mitochondrial biogenesis, but not mitophagy, is part of the post-stroke repair mechanisms during the ischemic phase. Kumar et al. (2016) also identified distinct phases of mitochondria during OGD and reoxygenation. During OGD occurs first round of fission, reoxygenation initially induces fusion but followed by massive fragmentation. These results have identified the distinct nature of the ischemic phase and reperfusion phase, in which mitophagy seems to have a unique protective role only in the reperfusion phase. However, given these results, which monitor mitophagy accurately to different phases, a fuller picture of mitophagy dynamic in the

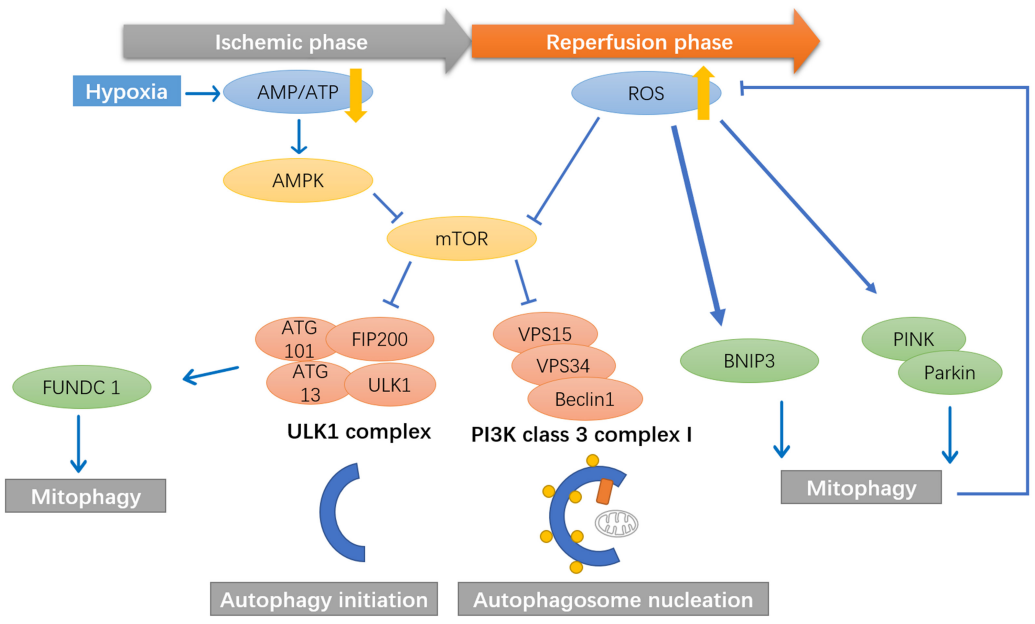

FIGURE 3 | Mitophagy pathways are activated during ischemic/reperfusion through multiple signals. During the ischemic phase, ATP production rapidly decrease, which activates AMPK pathways to initiate autophagy. AMPK activates the phosphorylation of ULK1, which will then activate the class III PI3K complex (beclin 1, VPS34, and VPS15) that initiate the nucleation of phagophore. ULK1 has also been found to activate the FUNDC1 receptor, which may collaterally activate mitophagy. During the reperfusion phase, the mTOR pathways is inhibited by ROS signals, thereby promote the initiation and nucleation of the autophagosome. ROS has been found to activate BNIP3 and PINK1/Parkin mediated mitophagy in cerebral ischemia and reperfusion.

ischemic/reperfusion process is emerging, but still with some obscurity. Thus, a more comprehensive and accurate evaluation of different time points is required to fully explain the role of mitophagy in both ischemic and reperfusion injuries.

The Interplay Between Mitophagy and IR Injury

Mitochondria-Dependent Cell Death in I/R Injury

During both the ischemic phase and IR injury, mitochondrial-dependent cell apoptosis is one of the critical events defining cell fate. The BCL-2 family proteins, which is a significant regulator of outer mitochondrial membrane permeability and play an essential role in the intrinsic apoptotic pathway (Chao and Korsmeyer, 1998), provide the mitochondria for the function of "sensing" apoptotic stress. The BCL-2 family has been classified into two groups: anti-apoptotic proteins (including Bcl-2, Bcl-xL, and Bcl-w) and pro-apoptotic proteins (including Bax, Bak, etc.) (Oltvai et al., 1993). Under stress conditions such as ischemic insults and IR injury, the anti-apoptotic protein Bcl-2 is phosphorylated and releases Beclin1 to activate autophagy and mitophagy. Bcl-2 prevents the release of pro-apoptotic proteins by maintaining the integrity of the mitochondrial membrane. This process inhibits cell apoptosis (Praharaj et al., 2019). However, pro-apoptotic BCL-3 subgroup proteins are also found to be upregulated after ischemic stroke, which induces the release of cytochrome c from mitochondria intermembrane into the cytosol. Cytochrome c interacts with the protein cofactor Apaf-1 and procaspase-9 form apoptosome (Gibson and Davids, 2015). Thus, ischemia and IR injury may elicit complex apoptotic effects involving mitochondria. The activities of anti- and pro-apoptotic proteins are correlated with the ROS concentration.

Mitophagy and Ca^{2+} Overload

Calcium overload is an essential pathology in I/R injury as it promotes the opening of mPTP, which activates apoptotic factors such as the Bcl-2 family and leads to cell apoptosis eventually. Recent evidence suggests a link between mitophagy and Ca^{2+} regulation. Many mitophagic proteins are also involved in mitochondrial calcium regulation. For instance, in PINK1/Parkin mediated mitophagy, many Ca^{2+} sensing proteins are ubiquitinated, which disturb the function as a Ca^{2+} buffering system, such as MFNs (de Brito and Scorrano, 2008; Gegg et al., 2010; Filadi et al., 2015), DRP1 (Cereghetti et al., 2008; Wang et al., 2011), VDAC1 (Gincel et al., 2001; Geisler et al., 2010) and BCL2 (Rong et al., 2008; Chen et al., 2010). Moreover, PINK1 phosphorylates mitochondrial rho GTPase 1 (RHOT1), which is an essential regulator of the Ca^{2+} sensitive characteristics in ER phospholipid exchange (Kornmann et al., 2011) and mitochondrial dynamics (Saotome et al., 2008). Parkin mediates the ubiquitination and degradation of MICU-1, which also affects the stability of MICU2 (Matteucci et al., 2018). Additionally, depending on the calcium level in the ER, Ca^{2+} can be either pro- or anti-autophagic (Cárdenas et al., 2010).

Mitophagy and Oxidative Stress

Oxidative stress is one of the most critical pathological brain damage processes in acute ischemic stroke (Chamorro et al., 2016). ROS and reactive nitrogen species (RNS) are crucial mediators in cerebral ischemia-reperfusion injury. ROS/RNS at a low level is beneficial for facilitating adaptation to stress as a redox signaling, whereas ROS/RNS at a high level is deleterious (Scialò et al., 2016). ROS and RNS have mainly been generated from the electron transport chain (ETC) complexes I and complex III in mitochondria, and excessive ROS/RNS primarily induces mitochondria injury. Under normal condition, less than 10% of oxygen receive electrons to generate superoxide in ETC. However, upon IR injury, the ischemic brains produce a large amount of NO and superoxide anion (O_2^-) simultaneously. The rapid reaction of NO and O_2^- leads to the formation of $ONOO^-$, a representative/critical cytotoxic factor for both oxidative and nitrosative stress (Marla et al., 1997). $ONOO^-$ is a highly active cytotoxic molecule to aggravate neuronal damage, disrupt the blood–brain-barrier (BBB) integrity, and mediate hemorrhagic transformation via triggering numerous cellular signaling cascades, which represents a vital pathogenic mechanism in ischemic stroke (Marla et al., 1997). Mitophagy has regulatory effects on oxidative stress since damaged mitochondria will lead to the release of more ROS. ROS can directly induce mitophagy (Wang et al., 2012), which has been shown beneficial in various disease conditions as mitophagy attenuates oxidative stress. However, multiple studies have demonstrated that $ONOO^-$ induces excessive mitophagy activation by tyrosine nitration of Drp1 and mediates mitochondrial recruitment of Drp1, thus aggravating cerebral I/R injury (Feng et al., 2017). This raises the question of whether mitophagy is beneficial or detrimental in response to I/R injury and will be discussed later. Indeed, $ONOO^-$-mediated mitophagy is suspected to be excessive and could be a crucial therapeutic target for IR injury.

Mitophagy and Inflammation

Anti-inflammation is another function of mitophagy. Upon mitochondria dysfunction, leaked mitochondrial ROS can activate inflammasomes, contributing to inflammation (Murakami et al., 2012). Mitophagy has shown a positive effect in kidney disease, ischemic stroke, and I/R injury. For instance, upon encountering I/R injury, kidney tubules rich in mitochondria will enhance autophagy (including mitophagy) to protect cells from ROS-triggered inflammatory response (Kimura et al., 2011; Zhou et al., 2011). In ischemic stroke, overexpression of the ATF4 gene can enhance mitophagy and inhibit NLRP3 inflammasome-mediated inflammatory response (He et al., 2019). Inducing Parkin-dependent mitophagy can improve inflammatory response and prevent cell death in myocardial I/R injury (Yao et al., 2019).

Therapeutic Potential of Mitophagy Regulation in I/R Injury

Recent years boosts the research of mitophagy in cerebral ischemia and reperfusion, most of them demonstrating the protective role of mitophagy. However, excessive mitophagy, which is probably induced by certain oxidative stress conditions, has also been shown to be deleterious in cerebral ischemia and reperfusion processes. In pre-clinical studies, several

therapeutic agents have been proposed to ameliorate cerebral I/R injury, either through enhancing or inhibiting certain types of mitophagy. These mitophagy-related interventions could be proposed as adjunctive approaches for ischemic stroke management.

Studies investigating the role of mitophagy in I/R injury after 2018 are summarized as follows and in **Table 1**. Earlier studies have been reviewed by Anzell et al. (2018) and Guan et al. (2018). The role of autophagy and potential strategies in ischemic stroke is also comprehensively summarized in a recent review (Ajoolabady et al., 2021).

Protective Role of Enhanced Mitophagy in IR Injury

Zhang and Yu (2018) found that after reperfusion, NR4A1 was significantly elevated in the brain tissue, inhibiting the activation of protective mitophagy through the MAPK–ERK–CREB signaling pathway. Genetic ablation of NR4A1 reduced the cerebral infarction area and neuronal apoptosis. As demonstrated by functional study, NR4A1 modulated cerebral IR injury by inducing mitochondrial damage. Higher NR4A1 promoted mitochondrial potential reduction, aggravated cellular oxidative stress, and initiated caspase-9-dependent apoptosis. Mechanistically, NR4A1 induced mitochondrial damage by disrupting Mfn2-related mitophagy. Knockdown of NR4A1 reversed mitophagic activity, sending a prosurvival signal for mitochondria in the setting of cerebral IR injury (Zhang and Yu, 2018).

Electroacupuncture (EA) has been shown effective in treating ischemic stroke. Recently, Wang et al. (2019) demonstrated that EA ameliorates nitro/oxidative stress-induced mitochondrial functional damage and reduces the accumulation of damaged mitochondria via Pink1/Parkin-mediated mitophagy clearance to protect cells against neuronal injury in cerebral I/R. Later, Mao et al. (2020) also found EA pretreatment has a protective effect on cerebral I/R injury through promoting mitophagy, based on the results that the number of autophagosomes, FUNDC1, p62, and the ratio of LC3-II/I were significantly increased. Still, mitochondrial membrane potential and autophagy-related protein p-mTORC1 significantly decreased in the I/R group (Mao et al., 2020).

He et al. (2019) showed that ATF4 overexpression induced by AAV was protective against cerebral I/R injury by upregulating Parkin expression, enhance mitophagy activity and inhibit NLRP3 inflammasome-mediated inflammatory response.

A series of natural compounds have been found to possess the ability to promote mitophagy and attenuate I/R injuries. Curcumin is a complex extracted from the traditional edible herb which can protect neurons in rats after brain I/R injury (Wang and Xu, 2020). Curcumin reduced the levels of ROS while increased state 3 respiration to prevent the impairment of mitochondrial function from cerebral I/R. Furthermore, curcumin enhanced the co-localization of LC3B and mitochondrial marker VDAC1, the ratio of LC3-II to LC3-I, suggesting the protective role of curcumin exerts through enhancing mitophagy. Wu et al. (2020) found that garciesculenxanthone B (GeB), a new xanthone compound from *Garcinia esculenta*, can promote the PINK1-Parkin-mediated mitophagy pathway and protects the brain from I/R injury. Treatment with GeB dose-dependently promoted the degradation of mitochondrial proteins Tom20, Tim23, and MFN1 in YFP-Parkin HeLa cells and SH-SY5Y cells. GeB stabilized PINK1 and triggered Parkin translocation to the impaired mitochondria to induce mitophagy, and these effects were abolished by knockdown of PINK1. *In vivo* experiments demonstrated that GeB partially rescued ischemia-reperfusion-induced brain injury in mice. Another two natural compounds named Gerontoxanthone I (GeX1) and Macluraxanthone (McX), were also screened out to possess the ability to enhance mitophagy (Xiang et al., 2020). GeX1 and McX directly stabilized PINK1 on the outer membrane of the mitochondria and then recruited Parkin to mitochondria, suggesting that GeX1 and McX mediate mitophagy through the PINK1-Parkin pathway. GeX1 and McX treatment decreased cell apoptosis and the ROS level in an IR injury model in H9c2 cells. Additionally, a tablet derives from Chinese classical prescriptions of Angong Niuhuang Pills with modified compositions has also been shown to attenuate cerebral I/R injury by improving mitophagy and mitochondrial quality control (Zhang et al., 2020a). The tablets elevated the ratio of Bcl-2/Bax, inhibited apoptosis, decreased the infarction volume, and improved the MCAO rats' behavioral performance.

Although the precise molecular regulatory network of these natural compounds has not been fully addressed, considering the

TABLE 1 | Summary of Part 3.4 Therapeutic potential of mitophagy in I/R injury.

Therapy	Mitophagy	Other pathways involved	Reference
Electroacupuncture	Activate PINK/Parkin-mediated mitophagy	PI3K/Akt signaling pathway	Wang et al., 2019; Mao et al., 2020
ATF4 overexpression	Activate PINK/Parkin-mediated mitophagy	Inhibit NLRP3 inflammasome-mediated inflammatory response	He et al., 2019
Curcumin	Activate	/	Wang and Xu, 2020
GeB	Activate PINK/Parkin-mediated mitophagy	/	Wu et al., 2020
GeX1 and McX	Activate PINK/Parkin-mediated mitophagy	/	Xiang et al., 2020
ANNAO	Activate	/	Zhang et al., 2020a
A sphingosine kinase 2-mimicking TAT-peptide	Activating BNIP3-mediated mitophagy	/	Chen et al., 2020
Enhance retrograde transport of mitochondria	Assisted activation	/	Zheng et al., 2019a,b
Naringin	Inhibit	Inhibit $ONOO^-$ mediated mitophagy	Feng et al., 2018
Rehmapicroside	Inhibit	Inhibit $ONOO^-$ mediated mitophagy	Zhang et al., 2020b

advantages of natural compounds such as low toxicity and safe pharmacokinetic profiles including high utility rate and effective elimination, drugs derived from natural compounds are of high translational value.

Chen et al. (2020) demonstrated that a sphingosine kinase 2-mimicking TAT-peptide protects neurons against ischemia-reperfusion injury by activating BNIP3-mediated mitophagy. sphingosine kinase 2 (SPK2) interacts with Bcl-2 via its BH3 domain, activating autophagy or mitophagy by inducing the dissociation of Beclin-1/Bcl-2 or Bcl-2/BNIP3 complexes and protects neurons against ischemic injury.

Different from cardiac muscle, the long axon is a highly distinct morphology of neurons, where located more than half of total mitochondria content in neurons (Nafstad and Blackstad, 1966). However, under stress conditions, autophagy and mitophagy events are concentrated in the soma (Maday and Holzbaur, 2014), but not in exon, evidenced by concentrated autophagosomes and lysosomes in the soma (Farías et al., 2017). Thus, it is unclear how mitochondria in distal axons are cleared in ischemic neurons (Ashrafi et al., 2014). Zheng et al. (2019a,b) have identified unique mitochondria movement in neurons, from axon to soma for degradation. Upon oxygen and glucose deprivation-reperfusion, axonal mitochondria showed loss of anterograde motility but increased retrograde motion upon reperfusion, meaning axonal mitochondria are transported to the neuronal soma for degradation. Anchoring of axonal mitochondria by syntaphilin blocked neuronal mitophagy and aggravated injury. Conversely, induced binding of mitochondria to dynein reinforced retrograde transport and enhanced mitophagy prevent mitochondrial dysfunction and attenuate neuronal damage. Therefore, regulating mitochondria motility in neurons would be another direction for enhancing mitophagy and attenuating I/R neuronal injury.

$ONOO^-$ Induces Deleterious Mitophagy

Feng et al. (2018) found that naringin, a natural antioxidant, could inhibit $ONOO^-$ mediated mitophagy activation and attenuate cerebral I/R injury. Naringin possessed strong $ONOO^-$ scavenging capability and inhibited the production of superoxide and nitric oxide in IR injury conditions. Naringin inhibited the expression of NADPH oxidase subunits and iNOS in rat brains subjected to 2 h ischemia plus 22 h reperfusion. Naringin can cross the blood-brain barrier, decreases neurological deficit score, reduces infarct size, and attenuates apoptosis in the ischemia-reperfused rat brains. Furthermore, naringin decreased the ratio of LC3-II to LC3-I in mitochondria. It inhibited the translocation of Parkin to the mitochondria, suggesting naringin prevents the brain from I/R injury via attenuating $ONOO^-$-mediated excessive mitophagy.

Rehmapicroside, a natural compound from a medicinal plant, can inhibit $ONOO^-$-mediated mitophagy activation (Zhang et al., 2020b). *In vitro*, rehmapicroside reacted with $ONOO^-$ directly to scavenge $ONOO^-$, decreased $O2^-$ and $ONOO^-$, up-regulated Bcl-2 but down-regulated Bax, Caspase-3 and cleaved Caspase-3, and down-regulated PINK1, Parkin, p62 and the ratio of LC3-II to LC3-I in the OGD/RO-treated PC12 cells. *In vivo*, rehmapicroside suppressed 3-nitrotyrosine formation, Drp1 nitration as well as NADPH oxidases and iNOS expression in the ischemia-reperfused rat brains; it also prevented the translocations of PINK1, Parkin, and Drp1 into the mitochondria for mitophagy activation; finally, rehmapicroside ameliorated infarct sizes and improved neurological deficit scores in the rats with transient MCAO cerebral ischemia.

Deng et al. (2020) demonstrate that lncRNA SNHG14 promotes OGD/R-induced neuron injury by inducing excessive mitophagy via miR-182-5p/BINP3 axis in HT22 mouse hippocampal neuronal cells. SNHG14 and BNIP3 were highly expressed, and miR-182-5p was down-regulated in the OGD/R-induced HT22 cells. OGD/R-induced HT22 cells exhibited an increase in apoptosis. SNHG14 overexpression promoted apoptosis and the expression of cleaved-caspase-3 and cleaved-caspase-9 in the OGD/R-induced HT22 cells. Moreover, SNHG14 up-regulation enhanced the expression of BNIP3, Beclin-1, and LC3II/LC3I in the OGD/R-induced HT22 cells. Furthermore, SNHG14 regulated BNIP3 expression by sponging miR-182-5p. MiR-182-5p overexpression or BNIP3 knockdown repressed apoptosis in OGD/R-induced HT22 cells, which was abolished by SNHG14 up-regulation.

Taken together, inhibiting the $ONOO^-$-mediated excessive mitophagy activation exerts neuroprotective effects, with several potential drug candidates being discovered to attenuate cerebral IR injury. Although most studies have demonstrated the possible protective effects of mitophagy upon IR injury, mitophagy is a double-edged sword and requires more studies to test its clinical potential.

DISCUSSION AND FUTURE PERSPECTIVES

In the treatment of ischemic stroke, reperfusion with thrombolysis and thrombectomy are key to restoring blood flow and improving patient outcomes. However, restoration of blood flow in patients with AIS may result in secondary reperfusion injury. Resupply of oxygen can cause the overactivation of enzymes and pumps that are previously inhibited by ischemia-induced ATP deficiency, thus resulting in the boost of reactive oxygen species (ROS) production and altering calcium homeostasis in both cytoplasm and mitochondria. Such alternations can induce mitochondrial DNA damage and promote the opening of mPTP, which triggers apoptosis-related factors and result in cell death.

Mitophagy is an essential cellular process that maintains mitochondrial quality. While IR injury primarily induces mitochondrial dysfunction and leads to dysregulation of oxidative stress, calcium homeostasis, and cell apoptosis, regulation of mitochondria dynamics (fission and fusion) and activation of a moderate level mitophagy can contribute to the adjustment of cellular mitochondria quality. Identifying and targeting mitophagy-related pathways molecules may benefit certain subsets of patients with ischemic stroke. And some mitophagy regulators discussed above have already shown great potential in clinical application. For example, for acute ischemic stroke patients, taking some herbal agents prior to reaching

the hospital, and more importantly, during the long recovery stage, may provide vital neuroprotection effects and lead to a better prognosis. To address the clinical potential of mitophagy, further elucidation of mitophagy and its crosstalk mechanism under stroke conditions is required; further discovery of therapeutic targets and drug development for manipulating the mitophagy pathways are needed.

AUTHOR CONTRIBUTIONS

CS and TZ: conceptualization and supervision. LS, QG, YY, and CS: literature search and writing. LS, QG, and YY: figure sketching. CR, SX, ZZ, and TZ: editing and formatting. TZ: funding acquisition. All authors have read and agreed to the published version of the manuscript.

FUNDING

This research was supported by Beijing Postdoctoral Science Foundation to TZ (No. 2020-ZZ-020); China Postdoctoral Science Foundation to TZ (Nos. 2019TQ0216 and 2019M660716), and by the donated funding from Ningbo Guangyuan Zhi Xin Biotechnology Co., Ltd. (HX201910082).

REFERENCES

Ajoolabady, A., Wang, S., Kroemer, G., Penninger, J. M., Uversky, V. N., Pratico, D., et al. (2021). Targeting autophagy in ischemic stroke: from molecular mechanisms to clinical therapeutics. *Pharmacol. Therap.* 225:107848. doi: 10.1016/j.pharmthera.2021.107848

Alexander, A., Cai, S.-L., Kim, J., Nanez, A., Sahin, M., MacLean, K. H., et al. (2010). ATM signals to TSC2 in the cytoplasm to regulate mTORC1 in response to ROS. *Proc. Natl. Acad. Sci. U.S.A.* 107, 4153–4158. doi: 10.1073/pnas.0913860107

Allen, D. G., and Xiao, X.-H. (2003). Role of the cardiac Na+/H+ exchanger during ischemia and reperfusion. *Cardiovasc. Res.* 57, 934–941. doi: 10.1016/S0008-6363(02)00836-2

Anzell, A. R., Maizy, R., Przyklenk, K., and Sanderson, T. H. (2018). Mitochondrial quality control and disease: insights into ischemia-reperfusion injury. *Mol. Neurobiol.* 55, 2547–2564. doi: 10.1007/s12035-017-0503-9

Ashrafi, G., Schlehe, J. S., LaVoie, M. J., and Schwarz, T. L. (2014). Mitophagy of damaged mitochondria occurs locally in distal neuronal axons and requires PINK1 and Parkin. *J. Cell Biol.* 206, 655–670. doi: 10.1083/jcb.201401070

Assaly, R., de Tassigny, A. D. A., Paradis, S., Jacquin, S., Berdeaux, A., and Morin, D. (2012). Oxidative stress, mitochondrial permeability transition pore opening and cell death during hypoxia–reoxygenation in adult cardiomyocytes. *Eur. J. Pharmacol.* 675, 6–14. doi: 10.1016/j.ejphar.2011.11.036

Banerjee, C., and Chimowitz, M. I. (2017). Stroke caused by atherosclerosis of the major intracranial arteries. *Circ. Res.* 120, 502–513. doi: 10.1161/CIRCRESAHA.116.308441

Berkhemer, O. A., Fransen, P. S. S., Beumer, D., van den Berg, L. A., Lingsma, H. F., Yoo, A. J., et al. (2014). A randomized trial of intraarterial treatment for acute ischemic stroke. *New Engl. J. Med.* 372, 11–20. doi: 10.1056/NEJMoa1411587

Bhujabal, Z., Birgisdottir, ÅB., Sjøttem, E., Brenne, H. B., Øvervatn, A., Habisov, S., et al. (2017). FKBP8 recruits LC3A to mediate Parkin-independent mitophagy. *EMBO Rep.* 18, 947–961. doi: 10.15252/embr.201643147

Bingol, B., Tea, J. S., Phu, L., Reichelt, M., Bakalarski, C. E., Song, Q., et al. (2014). The mitochondrial deubiquitinase USP30 opposes parkin-mediated mitophagy. *Nature* 510, 370–375. doi: 10.1038/nature13418

Boehning, D., Patterson, R. L., and Snyder, S. H. (2004). Apoptosis and calcium: new roles for cytochrome c and inositol 1,4,5-trisphosphate. *Cell Cycle* 3, 252–254.

Brookes, P. S., Yoon, Y., Robotham, J. L., Anders, M. W., and Sheu, S. S. (2004). Calcium, ATP, and ROS: a mitochondrial love-hate triangle. *Am. J. Physiol. Cell Physiol.* 287, C817–C833. doi: 10.1152/ajpcell.00139.2004

Broughton, B. R., Reutens, D. C., and Sobey, C. G. (2009). Apoptotic mechanisms after cerebral ischemia. *Stroke* 40:e0331-39. doi: 10.1161/strokeaha.108.531632

Cárdenas, C., Miller, R. A., Smith, I., Bui, T., Molgó, J., Müller, M., et al. (2010). Essential regulation of cell bioenergetics by constitutive InsP3 receptor Ca2+ transfer to mitochondria. *Cell* 142, 270–283. doi: 10.1016/j.cell.2010.06.007

Cereghetti, G. M., Stangherlin, A., de Brito, O. M., Chang, C. R., Blackstone, C., Bernardi, P., et al. (2008). Dephosphorylation by calcineurin regulates translocation of Drp1 to mitochondria. *Proc. Natl. Acad. Sci. U.S.A.* 105:15803. doi: 10.1073/pnas.0808249105

Chami, M., Oulès, B., Szabadkai, G., Tacine, R., Rizzuto, R., and Paterlini-Bréchot, P. (2008). Role of SERCA1 truncated isoform in the proapoptotic calcium transfer from ER to Mitochondria during ER stress. *Mol. Cell* 32, 641–651. doi: 10.1016/j.molcel.2008.11.014

Chamorro, Á, Dirnagl, U., Urra, X., and Planas, A. M. (2016). Neuroprotection in acute stroke: targeting excitotoxicity, oxidative and nitrosative stress, and inflammation. *Lancet Neurol.* 15, 869–881. doi: 10.1016/S1474-4422(16)00114-9

Chang, C. R., and Blackstone, C. (2007). Cyclic AMP-dependent protein kinase phosphorylation of Drp1 regulates its GTPase activity and mitochondrial morphology. *J. Biol. Chem.* 282, 21583–21587. doi: 10.1074/jbc.C700083200

Chao, D. T., and Korsmeyer, S. J. (1998). BCL-2 family: regulators of cell death. *Annu. Rev. Immunol.* 16, 395–419.

Chen, D., Gao, F., Li, B., Wang, H., Xu, Y., Zhu, C., et al. (2010). Parkin mono-ubiquitinates Bcl-2 and regulates autophagy. *J. Biol. Chem.* 285, 38214–38223. doi: 10.1074/jbc.M110.101469

Chen, G., Han, Z., Feng, D., Chen, Y., Chen, L., Wu, H., et al. (2014). A regulatory signaling loop comprising the PGAM5 phosphatase and CK2 controls receptor-mediated mitophagy. *Mol. Cell* 54, 362–377. doi: 10.1016/j.molcel.2014.02.034

Chen, H., Song, Y. S., and Chan, P. H. (2009). Inhibition of NADPH Oxidase is neuroprotective after Ischemia—reperfusion. *J. Cereb. Blood Flow Metab.* 29, 1262–1272. doi: 10.1038/jcbfm.2009.47

Chen, J.-L., Wang, X.-X., Chen, L., Tang, J., Xia, Y.-F., Qian, K., et al. (2020). A sphingosine kinase 2-mimicking TAT-peptide protects neurons against ischemia-reperfusion injury by activating BNIP3-mediated mitophagy. *Neuropharmacology* 181:108326. doi: 10.1016/j.neuropharm.2020.108326

Chen, K.-H., Chao, C.-C., Tang, S.-C., and Jeng, J.-S. (2012). Distinguishing critical Stenosis from occlusion of the internal carotid artery by carotid duplex in a patient with acute ischemic stroke. *J. Med. Ultrasound* 20, 58–60. doi: 10.1016/j.jmu.2012.01.003

Chen, M., Chen, Z., Wang, Y., Tan, Z., Zhu, C., Li, Y., et al. (2016). Mitophagy receptor FUNDC1 regulates mitochondrial dynamics and mitophagy. *Autophagy* 12, 689–702. doi: 10.1080/15548627.2016.1151580

Chen, Y., and Dorn, G. W. (2013). PINK1-phosphorylated mitofusin 2 is a Parkin receptor for culling damaged mitochondria. *Science* 340, 471–475. doi: 10.1126/science.1231031

Chimowitz, M. I., Lynn, M. J., Howlett-Smith, H., Stern, B. J., Hertzberg, V. S., Frankel, M. R., et al. (2005). Comparison of Warfarin and Aspirin for symptomatic intracranial arterial stenosis. *N. Engl. J. Med.* 352, 1305–1316. doi: 10.1056/NEJMoa043033

Chu, C. T., Ji, J., Dagda, R. K., Jiang, J. F., Tyurina, Y. Y., Kapralov, A. A., et al. (2013). Cardiolipin externalization to the outer mitochondrial membrane acts as an elimination signal for mitophagy in neuronal cells. *Nat. Cell Biol.* 15, 1197–1205. doi: 10.1038/ncb2837

Clevert, D. A., Johnson, T., Michaely, H., Jung, E. M., Flach, P. M., Strautz, T. I., et al. (2006). High-grade stenoses of the internal carotid artery: comparison of high-resolution contrast enhanced 3D MRA, duplex sonography and power doppler imaging. *Eur. J. Radiol.* 60, 379–386. doi: 10.1016/j.ejrad.2006.07.012

Cornelissen, T., Haddad, D., Wauters, F., Van Humbeeck, C., Mandemakers, W., Koentjoro, B., et al. (2014). The deubiquitinase USP15 antagonizes Parkin-mediated mitochondrial ubiquitination and mitophagy. *Hum. Mol. Genet.* 23, 5227–5242. doi: 10.1093/hmg/ddu244

Cribbs, J. T., and Strack, S. (2007). Reversible phosphorylation of Drp1 by cyclic AMP-dependent protein kinase and calcineurin regulates mitochondrial fission and cell death. *EMBO Rep.* 8, 939–944. doi: 10.1038/sj.embor.7401062

Dai, S. H., Chen, T., Li, X., Yue, K. Y., Luo, P., Yang, L. K., et al. (2017). Sirt3 confers protection against neuronal ischemia by inducing autophagy: involvement of the AMPK-mTOR pathway. *Free Radic. Biol. Med.* 108, 345–353. doi: 10.1016/j.freeradbiomed.2017.04.005

Damle, S. S., Moore, E. E., Babu, A. N., Meng, X., Fullerton, D. A., and Banerjee, A. (2009). Hemoglobin-based oxygen carrier induces Heme Oxygenase-1 in the heart and lung but not brain. *J. Am. College Surg.* 208, 592–598. doi: 10.1016/j.jamcollsurg.2009.01.015

Daugas, E., Susin, S. A., Zamzami, N., Ferri, K. F., Irinopoulou, T., Larochette, N., et al. (2000). Mitochondrio-nuclear translocation of AIF in apoptosis and necrosis. *FASEB J.* 14, 729–739.

de Brito, O. M., and Scorrano, L. (2008). Mitofusin 2 tethers endoplasmic reticulum to mitochondria. *Nature* 456, 605–610. doi: 10.1038/nature07534

Deb, P., Sharma, S., and Hassan, K. M. (2010). Pathophysiologic mechanisms of acute ischemic stroke: an overview with emphasis on therapeutic significance beyond thrombolysis. *Pathophysiology* 17, 197–218. doi: 10.1016/j.pathophys.2009.12.001

Delgado, M. G., Vega, P. P., Lahoz, C. H., and Calleja, S. (2015). Late spontaneous recanalization of symptomatic atheromatous internal carotid artery occlusion. *Vascular* 23, 211–216. doi: 10.1177/1708538114535392

Deng, Z., Ou, H., Ren, F., Guan, Y., Huan, Y., Cai, H., et al. (2020). LncRNA SNHG14 promotes OGD/R-induced neuron injury by inducing excessive mitophagy via miR-182-5p/BINP3 axis in HT22 mouse hippocampal neuronal cells. *Biol. Res.* 53:38. doi: 10.1186/s40659-020-00304-4

Di, Y., He, Y.-L., Zhao, T., Huang, X., Wu, K.-W., Liu, S.-H., et al. (2015). Methylene blue reduces acute cerebral ischemic injury via the induction of mitophagy. *Mol. Med.* 21, 420–429. doi: 10.2119/molmed.2015.00038

Disatnik, M.-H., Ferreira, J. C. B., Campos, J. C., Gomes, K. S., Dourado, P. M. M., Qi, X., et al. (2013). Acute inhibition of excessive mitochondrial fission after myocardial infarction prevents long-term cardiac dysfunction. *J. Am. Heart Assoc.* 2:e000461. doi: 10.1161/JAHA.113.000461

Dong, Y., Undyala, V. V. R., and Przyklenk, K. (2016). Inhibition of mitochondrial fission as a molecular target for cardioprotection: critical importance of the timing of treatment. *Basic Res. Cardiol.* 111:59. doi: 10.1007/s00395-016-0578-x

Durcan, T. M., Tang, M. Y., Pérusse, J. R., Dashti, E. A., Aguileta, M. A., McLelland, G. L., et al. (2014). USP8 regulates mitophagy by removing K6-linked ubiquitin conjugates from parkin. *EMBO J.* 33, 2473–2491. doi: 10.15252/embj.201489729

Egan, D. F., Shackelford, D. B., Mihaylova, M. M., Gelino, S., Kohnz, R. A., Mair, W., et al. (2011). Phosphorylation of ULK1 (hATG1) by AMP-activated protein kinase connects energy sensing to mitophagy. *Science* 331, 456–461. doi: 10.1126/science.1196371

Faggioli, G., Pini, R., Mauro, R., Freyrie, A., Gargiulo, M., and Stella, A. (2013). Contralateral carotid occlusion in endovascular and surgical carotid revascularization: a single centre experience with literature review and meta-analysis. *Eur. J. Vasc. Endovasc. Surg.* 46, 10–20. doi: 10.1016/j.ejvs.2013.03.021

Farías, G. G., Guardia, C. M., De Pace, R., Britt, D. J., and Bonifacino, J. S. (2017). BORC/kinesin-1 ensemble drives polarized transport of lysosomes into the axon. *Proc. Natl. Acad. Sci. U.S.A.* 114, E2955–E2964. doi: 10.1073/pnas.1616363114

Feng, J., Chen, X., Lu, S., Li, W., Yang, D., Su, W., et al. (2018). Naringin attenuates cerebral ischemia-reperfusion injury through inhibiting peroxynitrite-mediated mitophagy activation. *Mol. Neurobiol.* 55, 9029–9042. doi: 10.1007/s12035-018-1027-7

Feng, J., Chen, X., and Shen, J. (2017). Reactive nitrogen species as therapeutic targets for autophagy: implication for ischemic stroke. *Expert Opin. Therap. Targets* 21, 305–317. doi: 10.1080/14728222.2017.1281250

Ferretti, G., Bacchetti, T., Masciangelo, S., Nanetti, L., Mazzanti, L., Silvestrini, M., et al. (2008). Lipid peroxidation in stroke patients. *Clin. Chem. Lab. Med.* 46, 113–117. doi: 10.1515/CCLM.2008.011

Filadi, R., Greotti, E., Turacchio, G., Luini, A., Pozzan, T., and Pizzo, P. (2015). Mitofusin 2 ablation increases endoplasmic reticulum–mitochondria coupling. *Proc. Natl. Acad. Sci. U.S.A.* 112:E2174. doi: 10.1073/pnas.1504880112

Gegg, M. E., Cooper, J. M., Chau, K.-Y., Rojo, M., Schapira, A. H. V., and Taanman, J.-W. (2010). Mitofusin 1 and mitofusin 2 are ubiquitinated in a PINK1/parkin-dependent manner upon induction of mitophagy. *Hum. Mol. Genet.* 19, 4861–4870. doi: 10.1093/hmg/ddq419

Geisler, S., Holmström, K. M., Skujat, D., Fiesel, F. C., Rothfuss, O. C., Kahle, P. J., et al. (2010). PINK1/Parkin-mediated mitophagy is dependent on VDAC1 and p62/SQSTM1. *Nat. Cell Biol.* 12, 119–131. doi: 10.1038/ncb2012

Gibson, C. J., and Davids, M. S. (2015). BCL-2 antagonism to target the intrinsic mitochondrial pathway of apoptosis. *Clin. Cancer Res.* 21, 5021–5029. doi: 10.1158/1078-0432.CCR-15-0364

Gincel, D., Zaid, H., and Shoshan-Barmatz, V. (2001). Calcium binding and translocation by the voltage-dependent anion channel: a possible regulatory mechanism in mitochondrial function. *Biochem. J.* 358(Pt 1), 147–155.

Greene, A. W., Grenier, K., Aguileta, M. A., Muise, S., Farazifard, R., Haque, M. E., et al. (2012). Mitochondrial processing peptidase regulates PINK1 processing, import and Parkin recruitment. *EMBO Rep.* 13, 378–385. doi: 10.1038/embor.2012.14

Grinwald, P. M., and Brosnahan, C. (1987). Sodium imbalance as a cause of calcium overload in post-hypoxic reoxygenation injury. *J. Mol. Cell. Cardiol.* 19, 487–495. doi: 10.1016/S0022-2828(87)80400-5

Griparic, L., Kanazawa, T., and van der Bliek, A. M. (2007). Regulation of the mitochondrial dynamin-like protein Opa1 by proteolytic cleavage. *J. Cell Biol.* 178, 757–764. doi: 10.1083/jcb.200704112

Grohm, J., Kim, S. W., Mamrak, U., Tobaben, S., Cassidy-Stone, A., Nunnari, J., et al. (2012). Inhibition of Drp1 provides neuroprotection in vitro and in vivo. *Cell Death Differ.* 19, 1446–1458. doi: 10.1038/cdd.2012.18

Grubb, J. R. L., Derdeyn, C. P., Fritsch, S. M., Carpenter, D. A., Yundt, K. D., Videen, T. O., et al. (1998). Importance of hemodynamic factors in the prognosis of symptomatic carotid occlusion. *JAMA* 280, 1055–1060. doi: 10.1001/jama.280.12.1055

Guan, R., Zou, W., Dai, X., Yu, X., Liu, H., Chen, Q., et al. (2018). Mitophagy, a potential therapeutic target for stroke. *J. Biomed. Sci.* 25:87. doi: 10.1186/s12929-018-0487-4

Ha, H. C., and Snyder, S. H. (1999). Poly(ADP-ribose) polymerase is a mediator of necrotic cell death by ATP depletion. *Proc. Natl. Acad. Sci. U.S.A.* 96, 13978–13982. doi: 10.1073/pnas.96.24.13978

He, Q., Li, Z., Meng, C., Wu, J., Zhao, Y., and Zhao, J. (2019). Parkin-dependent mitophagy is required for the inhibition of ATF4 on NLRP3 inflammasome activation in cerebral ischemia-reperfusion injury in rats. *Cells* 8:897. doi: 10.3390/cells8080897

Head, B., Griparic, L., Amiri, M., Gandre-Babbe, S., and van der Bliek, A. M. (2009). Inducible proteolytic inactivation of OPA1 mediated by the OMA1 protease in mammalian cells. *J. Cell Biol.* 187, 959–966. doi: 10.1083/jcb.200906083

Huang, C., Andres, A. M., Ratliff, E. P., Hernandez, G., Lee, P., and Gottlieb, R. A. (2011). Preconditioning involves selective mitophagy mediated by Parkin and p62/SQSTM1. *PLoS One* 6:e20975. doi: 10.1371/journal.pone.0020975

Indo, H. P., Davidson, M., Yen, H. C., Suenaga, S., Tomita, K., Nishii, T., et al. (2007). Evidence of ROS generation by mitochondria in cells with impaired electron transport chain and mitochondrial DNA damage. *Mitochondrion* 7, 106–118. doi: 10.1016/j.mito.2006.11.026

Irie, M., Fujimura, Y., Yamato, M., Miura, D., and Wariishi, H. (2014). Integrated MALDI-MS imaging and LC-MS techniques for visualizing spatiotemporal metabolomic dynamics in a rat stroke model. *Metabolom. J. Metabol. Soc.* 10, 473–483. doi: 10.1007/s11306-013-0588-8

Jackman, K. A., Miller, A. A., De Silva, T. M., Crack, P. J., Drummond, G. R., and Sobey, C. G. (2009). Reduction of cerebral infarct volume by apocynin requires pretreatment and is absent in Nox2-deficient mice. *Br. J. Pharmacol.* 156, 680–688. doi: 10.1111/j.1476-5381.2008.00073.x

Jiang, S., Li, T., Ji, T., Yi, W., Yang, Z., Wang, S., et al. (2018). AMPK: potential therapeutic target for ischemic stroke. *Theranostics* 8, 4535–4551. doi: 10.7150/thno.25674

Jiang, T., Yu, J. T., Zhu, X. C., Zhang, Q. Q., Tan, M. S., Cao, L., et al. (2015). Ischemic preconditioning provides neuroprotection by induction of AMP-activated protein kinase-dependent autophagy in a rat model of ischemic stroke. *Mol. Neurobiol.* 51, 220–229. doi: 10.1007/s12035-014-8725-6

Jin, R., Liu, L., Zhang, S., Nanda, A., and Li, G. (2013). Role of inflammation and its mediators in acute ischemic stroke. *J. Cardiovasc. Transl. Res.* 6, 834–851. doi: 10.1007/s12265-013-9508-6

Jovin, T. G., Chamorro, A., Cobo, E., de Miquel, M. A., Molina, C. A., Rovira, A., et al. (2015). Thrombectomy within 8 hours after symptom onset in ischemic stroke. *N. Engl. J. Med.* 372, 2296–2306. doi: 10.1056/NEJMoa1503780

Jürgensmeier, J. M., Xie, Z., Deveraux, Q., Ellerby, L., Bredesen, D., and Reed, J. C. (1998). Bax directly induces release of cytochrome c from isolated mitochondria. *Proc. Natl. Acad. Sci. U.S.A.* 95, 4997–5002. doi: 10.1073/pnas.95.9.4997

Kalogeris, T., Baines, C. P., Krenz, M., and Korthuis, R. J. (2012). "Chapter Six - cell biology of ischemia/reperfusion injury," in *International Review of Cell and Molecular Biology*, ed. K. W. Jeon (Cambridge, MA: Academic Press), 229–317.

Kang, R., Gamdzyk, M., Tang, H., Luo, Y., Lenahan, C., and Zhang, J. H. (2020). Delayed recanalization-How late is Not Too Late? *Transl. Stroke Res.* 12, 382–393. doi: 10.1007/s12975-020-00877-y

Kao, H. L., Lin, M. S., Wang, C. S., Lin, Y. H., Lin, L. C., Chao, C. L., et al. (2007). Feasibility of endovascular recanalization for symptomatic cervical internal carotid artery occlusion. *J. Am. Coll. Cardiol.* 49, 765–771. doi: 10.1016/j.jacc.2006.11.029

Kazlauskaite, A., Martínez-Torres, R. J., Wilkie, S., Kumar, A., Peltier, J., Gonzalez, A., et al. (2015). Binding to serine 65-phosphorylated ubiquitin primes Parkin for optimal PINK1-dependent phosphorylation and activation. *EMBO Rep.* 16, 939–954. doi: 10.15252/embr.201540352

Kim, H., Scimia, M. C., Wilkinson, D., Trelles, R. D., Wood, M. R., Bowtell, D., et al. (2011). Fine-tuning of Drp1/Fis1 availability by AKAP121/Siah2 regulates mitochondrial adaptation to hypoxia. *Mol. Cell* 44, 532–544. doi: 10.1016/j.molcel.2011.08.045

Kim, J., Kundu, M., Viollet, B., and Guan, K.-L. (2011). AMPK and mTOR regulate autophagy through direct phosphorylation of Ulk1. *Nat. Cell Biol.* 13, 132–141. doi: 10.1038/ncb2152

Kimura, T., Takabatake, Y., Takahashi, A., Kaimori, J.-Y., Matsui, I., Namba, T., et al. (2011). Autophagy protects the proximal tubule from degeneration and acute ischemic injury. *J. Am. Soc. Nephrol.* 22, 902–913. doi: 10.1681/ASN.2010070705

Kinuta, Y., Kimura, M., Itokawa, Y., Ishikawa, M., and Kikuchi, H. (1989). Changes in xanthine oxidase in ischemic rat brain. *J. Neurosurg.* 71, 417–420. doi: 10.3171/jns.1989.71.3.0417

Kirkland, R. A., Windelborn, J. A., Kasprzak, J. M., and Franklin, J. L. (2002). A Bax-induced pro-oxidant state is critical for cytochrome c release during programmed neuronal death. *J. Neurosci.* 22, 6480–6490. doi: 10.1523/jneurosci.22-15-06480.2002

Kornmann, B., Osman, C., and Walter, P. (2011). The conserved GTPase Gem1 regulates endoplasmic reticulum-mitochondria connections. *Proc. Natl. Acad. Sci. U.S.A.* 108, 14151–14156. doi: 10.1073/pnas.1111314108

Koyano, F., Okatsu, K., Kosako, H., Tamura, Y., Go, E., Kimura, M., et al. (2014). Ubiquitin is phosphorylated by PINK1 to activate parkin. *Nature* 510, 162–166. doi: 10.1038/nature13392

Kumar, R., Bukowski, M. J., Wider, J. M., Reynolds, C. A., Calo, L., Lepore, B., et al. (2016). Mitochondrial dynamics following global cerebral ischemia. *Mol. Cell. Neurosci.* 76, 68–75. doi: 10.1016/j.mcn.2016.08.010

Kundu, M., Lindsten, T., Yang, C.-Y., Wu, J., Zhao, F., Zhang, J., et al. (2008). Ulk1 plays a critical role in the autophagic clearance of mitochondria and ribosomes during reticulocyte maturation. *Blood* 112, 1493–1502. doi: 10.1182/blood-2008-02-137398

Kwiatkowski, T. G., Libman, R. B., Frankel, M., Tilley, B. C., Morgenstern, L. B., Lu, M., et al. (1999). Effects of tissue plasminogen activator for acute ischemic stroke at one year. *N. Engl. J. Med.* 340, 1781–1787. doi: 10.1056/NEJM199906103402302

Lan, R., Wu, J.-T., Wu, T., Ma, Y.-Z., Wang, B.-Q., Zheng, H.-Z., et al. (2018). Mitophagy is activated in brain damage induced by cerebral ischemia and reperfusion via the PINK1/Parkin/p62 signalling pathway. *Brain Res. Bull.* 142, 63–77. doi: 10.1016/j.brainresbull.2018.06.018

Landmesser, U., Dikalov, S., Price, S. R., McCann, L., Fukai, T., Holland, S. M., et al. (2003). Oxidation of tetrahydrobiopterin leads to uncoupling of endothelial cell nitric oxide synthase in hypertension. *J. Clin. Invest.* 111, 1201–1209. doi: 10.1172/jci14172

Lazarou, M., Sliter, D. A., Kane, L. A., Sarraf, S. A., Wang, C., Burman, J. L., et al. (2015). The ubiquitin kinase PINK1 recruits autophagy receptors to induce mitophagy. *Nature* 524, 309–314. doi: 10.1038/nature14893

Leboucher, G. P., Tsai, Y. C., Yang, M., Shaw, K. C., Zhou, M., Veenstra, T. D., et al. (2012). Stress-induced phosphorylation and proteasomal degradation of mitofusin 2 facilitates mitochondrial fragmentation and apoptosis. *Mol. Cell* 47, 547–557. doi: 10.1016/j.molcel.2012.05.041

Lee, B. I., Lee, D. J., Cho, K. J., and Kim, G. W. (2005). Early nuclear translocation of endonuclease G and subsequent DNA fragmentation after transient focal cerebral ischemia in mice. *Neurosci. Lett.* 386, 23–27. doi: 10.1016/j.neulet.2005.05.058

Lees, K. R., Bluhmki, E., von Kummer, R., Brott, T. G., Toni, D., Grotta, J. C., et al. (2010). Time to treatment with intravenous alteplase and outcome in stroke: an updated pooled analysis of ECASS, ATLANTIS, NINDS, and EPITHET trials. *Lancet* 375, 1695–1703. doi: 10.1016/S0140-6736(10)60491-6

Lemasters, J. J. (2005). Selective mitochondrial autophagy, or mitophagy, as a targeted defense against oxidative stress, mitochondrial dysfunction, and aging. *Rejuvenat. Res.* 8, 3–5. doi: 10.1089/rej.2005.8.3

Li, L., Chen, J., Sun, S., Zhao, J., Dong, X., and Wang, J. (2017). Effects of estradiol on Autophagy and Nrf-2/ARE signals after cerebral ischemia. *Cell Physiol. Biochem.* 41, 2027–2036. doi: 10.1159/000475433

Li, Q., Zhang, T., Wang, J., Zhang, Z., Zhai, Y., Yang, G.-Y., et al. (2014). Rapamycin attenuates mitochondrial dysfunction via activation of mitophagy in experimental ischemic stroke. *Biochem. Biophys. Res. Commun.* 444, 182–188. doi: 10.1016/j.bbrc.2014.01.032

Liu, L., Feng, D., Chen, G., Chen, M., Zheng, Q., Song, P., et al. (2012). Mitochondrial outer-membrane protein FUNDC1 mediates hypoxia-induced mitophagy in mammalian cells. *Nat. Cell Biol.* 14, 177–185. doi: 10.1038/ncb2422

Liu, S. S. (1999). Cooperation of a "reactive oxygen cycle" with the Q cycle and the proton cycle in the respiratory chain–superoxide generating and cycling mechanisms in mitochondria. *J. Bioenerg. Biomembr.* 31, 367–376. doi: 10.1023/a:1018650103259

Maday, S., and Holzbaur, E. L. F. (2014). Autophagosome biogenesis in primary neurons follows an ordered and spatially regulated pathway. *Dev. Cell* 30, 71–85. doi: 10.1016/j.devcel.2014.06.001

Malhotra, K., Goyal, N., and Tsivgoulis, G. (2017). Internal carotid artery occlusion: pathophysiology, diagnosis, and management. *Curr. Atheroscler. Rep.* 19:41. doi: 10.1007/s11883-017-0677-7

Mammucari, C., Milan, G., Romanello, V., Masiero, E., Rudolf, R., Del Piccolo, P., et al. (2007). FoxO3 controls autophagy in skeletal muscle in vivo. *Cell Metab.* 6, 458–471. doi: 10.1016/j.cmet.2007.11.001

Mao, C., Hu, C., Zhou, Y., Zou, R., Li, S., Cui, Y., et al. (2020). Electroacupuncture pretreatment against cerebral ischemia/reperfusion injury through mitophagy. *Evid. Based Complement. Altern. Med.* 2020:7486041. doi: 10.1155/2020/7486041

Markesbery, W. R., and Lovell, M. A. (2007). Damage to lipids, proteins, DNA, and RNA in mild cognitive impairment. *Archiv. Neurol.* 64, 954–956. doi: 10.1001/archneur.64.7.954

Marla, S. S., Lee, J., and Groves, J. T. (1997). Peroxynitrite rapidly permeates phospholipid membranes. *Proc. Natl. Acad. Sci. U.S.A.* 94, 14243–14248.

Matteucci, A., Patron, M., Vecellio Reane, D., Gastaldello, S., Amoroso, S., Rizzuto, R., et al. (2018). Parkin-dependent regulation of the MCU complex component MICU1. *Sci. Rep.* 8:14199. doi: 10.1038/s41598-018-32551-7

Mazighi, M., Labreuche, J., Gongora-Rivera, F., Duyckaerts, C., Hauw, J. J., and Amarenco, P. (2008). Autopsy prevalence of intracranial atherosclerosis in patients with fatal stroke. *Stroke* 39, 1142–1147. doi: 10.1161/strokeaha.107.496513

Mo, Y., Sun, Y.-Y., and Liu, K.-Y. (2020). Autophagy and inflammation in ischemic stroke. *Neural Regenerat. Res.* 15, 1388–1396. doi: 10.4103/1673-5374.274331

Mokin, M., Kass-Hout, T., Kass-Hout, O., Dumont, T. M., Kan, P., Snyder, K. V., et al. (2012). Intravenous thrombolysis and endovascular therapy for acute ischemic stroke with internal carotid artery occlusion: a systematic review of clinical outcomes. *Stroke* 43, 2362–2368. doi: 10.1161/strokeaha.112.655621

Murakami, T., Ockinger, J., Yu, J., Byles, V., McColl, A., Hofer, A. M., et al. (2012). Critical role for calcium mobilization in activation of the NLRP3 inflammasome. *Proc. Natl. Acad. Sci. U.S.A.* 109, 11282–11287. doi: 10.1073/pnas.1117765109

Murakawa, T., Yamaguchi, O., Hashimoto, A., Hikoso, S., Takeda, T., Oka, T., et al. (2015). Bcl-2-like protein 13 is a mammalian Atg32 homologue that

mediates mitophagy and mitochondrial fragmentation. *Nat. Commun.* 6:7527. doi: 10.1038/ncomms8527

Nafstad, P. H. J., and Blackstad, T. W. (1966). Distribution of mitochondria in pyramidal cells and boutons in hippocampal cortex. *Zeitschrift Zellforschung Mikroskopische Anatomie* 73, 234–245. doi: 10.1007/BF00334866

Nishizawa, Y. (2001). Glutamate release and neuronal damage in ischemia. *Life Sci.* 69, 369–381. doi: 10.1016/S0024-3205(01)01142-0

Niu, K., Fang, H., Chen, Z., Zhu, Y., Tan, Q., Wei, D., et al. (2020). USP33 deubiquitinates PRKN/parkin and antagonizes its role in mitophagy. *Autophagy* 16, 724–734. doi: 10.1080/15548627.2019.1656957

Nor, A. M., Davis, J., Sen, B., Shipsey, D., Louw, S. J., Dyker, A. G., et al. (2005). The Recognition of Stroke in the Emergency Room (ROSIER) scale: development and validation of a stroke recognition instrument. *Lancet Neurol.* 4, 727–734. doi: 10.1016/S1474-4422(05)70201-5

Oakhill, J. S., Steel, R., Chen, Z. P., Scott, J. W., Ling, N., Tam, S., et al. (2011). AMPK is a direct adenylate charge-regulated protein kinase. *Science* 332, 1433–1435. doi: 10.1126/science.1200094

Oltvai, Z. N., Milliman, C. L., and Korsmeyer, S. J. (1993). Bcl-2 heterodimerizes in vivo with a conserved homolog, Bax, that accelerates programmed cell death. *Cell* 74, 609–619.

Ong, S.-B., Subrayan, S., Lim, S. Y., Yellon, D. M., Davidson, S. M., and Hausenloy, D. J. (2010). Inhibiting mitochondrial fission protects the heart against ischemia/reperfusion injury. *Circulation* 121, 2012–2022. doi: 10.1161/CIRCULATIONAHA.109.906610

Ordy, J. M., Wengenack, T. M., Bialobok, P., Coleman, P. D., Rodier, P., Baggs, R. B., et al. (1993). Selective vulnerability and early progression of Hippocampal CA1 pyramidal cell degeneration and GFAP-positive astrocyte reactivity in the rat four-vessel occlusion model of transient global ischemia. *Exper. Neurol.* 119, 128–139. doi: 10.1006/exnr.1993.1014

Ott, M., Robertson, J. D., Gogvadze, V., Zhivotovsky, B., and Orrenius, S. (2002). Cytochrome c release from mitochondria proceeds by a two-step process. *Proc. Natl. Acad. Sci. U.S.A.* 99, 1259–1263. doi: 10.1073/pnas.241655498

Papadakis, M., Hadley, G., Xilouri, M., Hoyte, L. C., Nagel, S., McMenamin, M. M., et al. (2013). Tsc1 (hamartin) confers neuroprotection against ischemia by inducing autophagy. *Nat. Med.* 19, 351–357. doi: 10.1038/nm.3097

Park, Y. Y., Nguyen, O. T. K., Kang, H., and Cho, H. (2014). MARCH5-mediated quality control on acetylated Mfn1 facilitates mitochondrial homeostasis and cell survival. *Cell Death Dis.* 5:e1172. doi: 10.1038/cddis.2014.142

Powers, W. J., Derdeyn, C. P., Fritsch, S. M., Carpenter, D. A., Yundt, K. D., Videen, T. O., et al. (2000). Benign prognosis of never-symptomatic carotid occlusion. *Neurology* 54, 878–882. doi: 10.1212/wnl.54.4.878

Prabu, S. K., Anandatheerthavarada, H. K., Raza, H., Srinivasan, S., Spear, J. F., and Avadhani, N. G. (2006). Protein kinase A-mediated phosphorylation modulates cytochrome c oxidase function and augments hypoxia and myocardial ischemia-related injury. *J. Biol. Chem.* 281, 2061–2070. doi: 10.1074/jbc.M507741200

Praharaj, P. P., Naik, P. P., Panigrahi, D. P., Bhol, C. S., Mahapatra, K. K., Patra, S., et al. (2019). Intricate role of mitochondrial lipid in mitophagy and mitochondrial apoptosis: its implication in cancer therapeutics. *Cell. Mol. Life Sci.* 76, 1641–1652. doi: 10.1007/s00018-018-2990-x

Puri, R., Cheng, X.-T., Lin, M.-Y., Huang, N., and Sheng, Z.-H. (2019). Mul1 restrains Parkin-mediated mitophagy in mature neurons by maintaining ER-mitochondrial contacts. *Nat. Commun.* 10:3645. doi: 10.1038/s41467-019-11636-5

Qian, T., Herman, B., and Lemasters, J. J. (1999). The mitochondrial permeability transition mediates both necrotic and apoptotic death of hepatocytes exposed to Br-A23187. *Toxicol. Appl. Pharmacol.* 154, 117–125. doi: 10.1006/taap.1998.8580

Ragoschke-Schumm, A., and Walter, S. (2018). DAWN and DEFUSE-3 trials: is time still important? *Der Radiol.* 58(Suppl. 1), 20–23. doi: 10.1007/s00117-018-0406-4

Ren, J., Sowers, J. R., and Zhang, Y. (2018). Metabolic stress, autophagy, and cardiovascular aging: from pathophysiology to therapeutics. *Trends Endocrinol. Metab.* 29, 699–711. doi: 10.1016/j.tem.2018.08.001

Rogov, V. V., Suzuki, H., Marinkoviæ, M., Lang, V., Kato, R., Kawasaki, M., et al. (2017). Phosphorylation of the mitochondrial autophagy receptor Nix enhances its interaction with LC3 proteins. *Sci. Rep.* 7:1131. doi: 10.1038/s41598-017-01258-6

Rong, Y.-P., Aromolaran, A. S., Bultynck, G., Zhong, F., Li, X., McColl, K., et al. (2008). Targeting Bcl-2-IP3 receptor interaction to reverse Bcl-2's inhibition of apoptotic calcium signals. *Mol. Cell* 31, 255–265. doi: 10.1016/j.molcel.2008.06.014

Sanderson, T. H., Raghunayakula, S., and Kumar, R. (2015). Neuronal hypoxia disrupts mitochondrial fusion. *Neuroscience* 301, 71–78. doi: 10.1016/j.neuroscience.2015.05.078

Sandoval, H., Thiagarajan, P., Dasgupta, S. K., Schumacher, A., Prchal, J. T., Chen, M., et al. (2008). Essential role for Nix in autophagic maturation of erythroid cells. *Nature* 454, 232–235. doi: 10.1038/nature07006

Saotome, M., Safiulina, D., Szabadkai, G., Das, S., Fransson, A., Aspenstrom, P., et al. (2008). Bidirectional Ca2+-dependent control of mitochondrial dynamics by the Miro GTPase. *Proc. Natl. Acad. Sci. U.S.A.* 105, 20728–20733. doi: 10.1073/pnas.0808953105

Scherz-Shouval, R., Shvets, E., Fass, E., Shorer, H., Gil, L., and Elazar, Z. (2007). Reactive oxygen species are essential for autophagy and specifically regulate the activity of Atg4. *EMBO J.* 26, 1749–1760.

Scialò, F., Sriram, A., Fernández-Ayala, D., Gubina, N., Lõhmus, M., Nelson, G., et al. (2016). Mitochondrial ROS produced via reverse electron transport extend animal lifespan. *Cell Metab.* 23, 725–734. doi: 10.1016/j.cmet.2016.03.009

Shi, Q., Cheng, Q., and Chen, C. (2021). The role of autophagy in the pathogenesis of ischemic stroke. *Curr. Neuropharmacol.* 19, 629–640. doi: 10.2174/1570159x18666200729101913

Simone, S., Rascio, F., Castellano, G., Divella, C., Chieti, A., Ditonno, P., et al. (2014). Complement-dependent NADPH oxidase enzyme activation in renal ischemia/reperfusion injury. *Free Radic. Biol. Med.* 74, 263–273. doi: 10.1016/j.freeradbiomed.2014.07.003

Sowter, H. M., Ratcliffe, P. J., Watson, P., Greenberg, A. H., and Harris, A. L. (2001). HIF-1-dependent regulation of hypoxic induction of the cell death factors BNIP3 and NIX in human tumors. *Cancer Res.* 61, 6669–6673.

Sugiura, A., Nagashima, S., Tokuyama, T., Amo, T., Matsuki, Y., Ishido, S., et al. (2013). MITOL regulates endoplasmic reticulum-mitochondria contacts via Mitofusin2. *Mol. Cell* 51, 20–34. doi: 10.1016/j.molcel.2013.04.023

Sundaram, S., Kannoth, S., Thomas, B., Sarma, P. S., and Sylaja, P. N. (2017). Collateral assessment by CT angiography as a predictor of outcome in symptomatic cervical internal carotid artery occlusion. *Am. J. Neuroradiol.* 38, 52–57. doi: 10.3174/ajnr.A4957

Susin, S. A., Lorenzo, H. K., Zamzami, N., Marzo, I., Snow, B. E., Brothers, G. M., et al. (1999). Molecular characterization of mitochondrial apoptosis-inducing factor. *Nature* 397, 441–446. doi: 10.1038/17135

Szargel, R., Shani, V., Abd Elghani, F., Mekies, L. N., Liani, E., Rott, R., et al. (2016). The PINK1, synphilin-1 and SIAH-1 complex constitutes a novel mitophagy pathway. *Hum. Mol. Genet.* 25, 3476–3490. doi: 10.1093/hmg/ddw189

Tanaka, A., Cleland, M. M., Xu, S., Narendra, D. P., Suen, D. F., Karbowski, M., et al. (2010). Proteasome and p97 mediate mitophagy and degradation of mitofusins induced by Parkin. *J. Cell Biol.* 191, 1367–1380. doi: 10.1083/jcb.201007013

Tang, J., Hu, Z., Tan, J., Yang, S., and Zeng, L. (2016). Parkin protects against oxygen-glucose deprivation/reperfusion insult by promoting Drp1 degradation. *Oxid. Med. Cell. Long.* 2016:8474303. doi: 10.1155/2016/8474303

Thompson, J. E., Austin, D. J., and Patman, R. D. (1986). Carotid endarterectomy for cerebrovascular insufficiency: long-term results in 592 patients followed up to thirteen years. *Surg. Clin. North Am.* 66, 233–253. doi: 10.1016/s0039-6109(16)43878-8

Toyama, E. Q., Herzig, S., Courchet, J., Lewis, T. L. Jr., Losón, O. C., Hellberg, K., et al. (2016). AMP-activated protein kinase mediates mitochondrial fission in response to energy stress. *Science* 351, 275–281. doi: 10.1126/science.aab4138

Twig, G., Elorza, A., Molina, A. J. A., Mohamed, H., Wikstrom, J. D., Walzer, G., et al. (2008). Fission and selective fusion govern mitochondrial segregation and elimination by autophagy. *EMBO J.* 27, 433–446. doi: 10.1038/sj.emboj.7601963

Vinten-Johansen, J. (2007). Postconditioning: a mechanical maneuver that triggers biological and molecular cardioprotective responses to reperfusion. *Heart Fail. Rev.* 12, 235–244. doi: 10.1007/s10741-007-9024-3

Virani Salim, S., Alonso, A., Benjamin Emelia, J., Bittencourt Marcio, S., Callaway Clifton, W., Carson April, P., et al. (2020). Heart disease and stroke statistics—2020 update: a report from the American heart association. *Circulation* 141:e0139-96. doi: 10.1161/CIR.0000000000000757

Wang, H., Chen, S., Zhang, Y., Xu, H., and Sun, H. (2019). Electroacupuncture ameliorates neuronal injury by Pink1/Parkin-mediated mitophagy clearance in

cerebral ischemia-reperfusion. *Nitric Oxide Biol. Chem.* 91, 23–34. doi: 10.1016/j.niox.2019.07.004

Wang, H., Song, P., Du, L., Tian, W., Yue, W., Liu, M., et al. (2011). Parkin ubiquitinates Drp1 for proteasome-dependent degradation: implication of dysregulated mitochondrial dynamics in Parkinson disease. *J. Biol. Chem.* 286, 11649–11658. doi: 10.1074/jbc.M110.144238

Wang, M., Sun, G.-B., Zhang, J.-Y., Luo, Y., Yu, Y.-L., Xu, X.-D., et al. (2015). Elatoside C protects the heart from ischaemia/reperfusion injury through the modulation of oxidative stress and intracellular Ca^{2+} homeostasis. *Intern. J. Cardiol.* 185, 167–176. doi: 10.1016/j.ijcard.2015.03.140

Wang, Y., Serricchio, M., Jauregui, M., Shanbhag, R., Stoltz, T., Di Paolo, C. T., et al. (2015). Deubiquitinating enzymes regulate PARK2-mediated mitophagy. *Autophagy* 11, 595–606. doi: 10.1080/15548627.2015.1034408

Wang, Q., Tompkins, K. D., Simonyi, A., Korthuis, R. J., Sun, A. Y., and Sun, G. Y. (2006). Apocynin protects against global cerebral ischemia–reperfusion-induced oxidative stress and injury in the gerbil hippocampus. *Brain Res.* 1090, 182–189. doi: 10.1016/j.brainres.2006.03.060

Wang, W., and Xu, J. (2020). Curcumin attenuates cerebral ischemia-reperfusion injury through regulating mitophagy and preserving mitochondrial function. *Curr. Neurovasc. Res.* 17, 113–122. doi: 10.2174/1567202617666200225122620

Wang, X., Yang, C., Chai, J., Shi, Y., and Xue, D. (2002). Mechanisms of AIF-Mediated Apoptotic DNA Degradation in *Caenorhabditis elegans*. *Science* 298, 1587–1592. doi: 10.1126/science.1076194

Wang, Y., Nartiss, Y., Steipe, B., McQuibban, G. A., and Kim, P. K. (2012). ROS-induced mitochondrial depolarization initiates PARK2/PARKIN-dependent mitochondrial degradation by autophagy. *Autophagy* 8, 1462–1476. doi: 10.4161/auto.21211

Wei, M. C., Lindsten, T., Mootha, V. K., Weiler, S., Gross, A., Ashiya, M., et al. (2000). tBID, a membrane-targeted death ligand, oligomerizes BAK to release cytochrome c. *Genes Dev.* 14, 2060–2071.

Wei, Y., Chiang, W. C., Sumpter, R. Jr., Mishra, P., and Levine, B. (2017). Prohibitin 2 is an inner mitochondrial membrane mitophagy receptor. *Cell* 168, 224–238.e210. doi: 10.1016/j.cell.2016.11.042

Wong, Y. C., and Holzbaur, E. L. (2014). Optineurin is an autophagy receptor for damaged mitochondria in parkin-mediated mitophagy that is disrupted by an ALS-linked mutation. *Proc. Natl. Acad. Sci. U.S.A.* 111, E4439–E4448. doi: 10.1073/pnas.1405752111

Wu, M., Lu, G., Lao, Y.-Z., Zhang, H., Zheng, D., Zheng, Z.-Q., et al. (2020). Garciesculenxanthone B induces PINK1-Parkin-mediated mitophagy and prevents ischemia-reperfusion brain injury in mice. *Acta Pharmacol. Sin.* 42, 199–208. doi: 10.1038/s41401-020-0480-9

Wu, N. N., Zhang, Y., and Ren, J. (2019). Mitophagy, mitochondrial dynamics, and homeostasis in cardiovascular aging. *Oxid. Med. Cell. Long.* 2019:9825061. doi: 10.1155/2019/9825061

Xiang, Q., Wu, M., Zhang, L., Fu, W., Yang, J., Zhang, B., et al. (2020). Gerontoxanthone I and macluraxanthone induce mitophagy and attenuate ischemia/reperfusion injury. *Front. Pharmacol.* 11:452. doi: 10.3389/fphar.2020.00452

Xu, B., Li, C., Guo, Y., Xu, K., Yang, Y., and Yu, J. (2018). Current understanding of chronic total occlusion of the internal carotid artery. *Biomed. Rep.* 8, 117–125. doi: 10.3892/br.2017.1033

Yan, C., Gong, L., Chen, L., Xu, M., Abou-Hamdan, H., Tang, M., et al. (2020). PHB2 (prohibitin 2) promotes PINK1-PRKN/Parkin-dependent mitophagy by the PARL-PGAM5-PINK1 axis. *Autophagy* 16, 419–434. doi: 10.1080/15548627.2019.1628520

Yang, T., Sun, Y., Li, Q., Li, S., Shi, Y., Leak, R. K., et al. (2020). Ischemic preconditioning provides long-lasting neuroprotection against ischemic stroke: The role of Nrf2. *Exp. Neurol.* 325:113142. doi: 10.1016/j.expneurol.2019.113142

Yao, L., Chen, H., Wu, Q., and Xie, K. (2019). Hydrogen-rich saline alleviates inflammation and apoptosis in myocardial I/R injury via PINK-mediated autophagy. *Int. J. Mol. Med.* 44, 1048–1062. doi: 10.3892/ijmm.2019.4264

Yin, W., Signore, A. P., Iwai, M., Cao, G., Gao, Y., and Chen, J. (2008). Rapidly increased neuronal mitochondrial biogenesis after hypoxic-ischemic brain injury. *Stroke* 39, 3057–3063. doi: 10.1161/STROKEAHA.108.520114

Youle, R. J., and van der Bliek, A. M. (2012). Mitochondrial fission, fusion, and stress. *Science* 337, 1062–1065. doi: 10.1126/science.1219855

Yu, S.-W., Wang, H., Poitras, M. F., Coombs, C., Bowers, W. J., Federoff, H. J., et al. (2002). Mediation of poly(ADP-Ribose) Polymerase-1-dependent cell death by apoptosis-inducing factor. *Science* 297:259. doi: 10.1126/science.1072221

Yue, W., Chen, Z., Liu, H., Yan, C., Chen, M., Feng, D., et al. (2014). A small natural molecule promotes mitochondrial fusion through inhibition of the deubiquitinase USP30. *Cell Res.* 24, 482–496. doi: 10.1038/cr.2014.20

Yun, J., Puri, R., Yang, H., Lizzio, M. A., Wu, C., Sheng, Z. H., et al. (2014). MUL1 acts in parallel to the PINK1/parkin pathway in regulating mitofusin and compensates for loss of PINK1/parkin. *eLife* 3:e01958. doi: 10.7554/eLife.01958

Zaha, V. G., and Young, L. H. (2012). AMP-activated protein kinase regulation and biological actions in the heart. *Circ. Res.* 111, 800–814. doi: 10.1161/CIRCRESAHA.111.255505

Zhang, Y., Cao, M., Wu, Y., Wang, J., Zheng, J., Liu, N., et al. (2020a). Improvement in mitochondrial function underlies the effects of ANNAO tablets on attenuating cerebral ischemia-reperfusion injuries. *J. Ethnopharmacol.* 246:112212. doi: 10.1016/j.jep.2019.112212

Zhang, Y., He, Y., Wu, M., Chen, H., Zhang, L., Yang, D., et al. (2020b). Rehmapicroside ameliorates cerebral ischemia-reperfusion injury via attenuating peroxynitrite-mediated mitophagy activation. *Free Radic. Biol. Med.* 160, 526–539. doi: 10.1016/j.freeradbiomed.2020.06.034

Zhang, Z., and Yu, J. (2018). NR4A1 promotes cerebral ischemia reperfusion injury by repressing Mfn2-mediated mitophagy and inactivating the MAPK-ERK-CREB signaling pathway. *Neurochem. Res.* 43, 1963–1977. doi: 10.1007/s11064-018-2618-4

Zheng, Y., Wu, X., Chen, Z., and Zhang, X. (2019a). Come and eat: mitochondrial transport guides mitophagy in ischemic neuronal axons. *Autophagy* 15, 1483–1484. doi: 10.1080/15548627.2019.1618099

Zheng, Y., Zhang, X., Wu, X., Jiang, L., Ahsan, A., Ma, S., et al. (2019b). Somatic autophagy of axonal mitochondria in ischemic neurons. *J. Cell Biol.* 218, 1891–1907. doi: 10.1083/jcb.201804101

Zhou, R., Yazdi, A. S., Menu, P., and Tschopp, J. (2011). A role for mitochondria in NLRP3 inflammasome activation. *Nature* 469, 221–225. doi: 10.1038/nature09663

Zhu, P., Hu, S., Jin, Q., Li, D., Tian, F., Toan, S., et al. (2018). Ripk3 promotes ER stress-induced necroptosis in cardiac IR injury: a mechanism involving calcium overload/XO/ROS/mPTP pathway. *Redox Biol.* 16, 157–168. doi: 10.1016/j.redox.2018.02.019

Conflict of Interest: The authors declare that this study received funding from Ningbo Guangyuan Zhi Xin Biotechnology Co., Ltd. The funder was not involved in the study design, collection, analysis, interpretation of data, the writing of this article or the decision to submit it for publication.

frontiers in Aging Neuroscience

REVIEW
published: 15 July 2021
doi: 10.3389/fnagi.2021.698601

Research Progress on the Mechanism of Mitochondrial Autophagy in Cerebral Stroke

Li Lei[1†], *Shuaifeng Yang*[1†], *Xiaoyang Lu*[2†], *Yongfa Zhang*[1*] *and Tao Li*[1*]

[1]*Department of Neurosurgery, The First People's Hospital of Yunnan Province (Kunhua Hospital/The Affiliated Hospital of Kunming University of Science and Technology), Kunming, China,* [2]*Translational Neurosurgery and Neurobiology, University Hospital Aachen, RWTH Aachen, Aachen, Germany*

Mitochondrial autophagy is an early defense and protection process that selectively clears dysfunctional or excessive mitochondria through a distinctive mechanism to maintain intracellular homeostasis. Mitochondrial dysfunction during cerebral stroke involves metabolic disbalance, oxidative stress, apoptosis, endoplasmic reticulum stress, and abnormal mitochondrial autophagy. This article reviews the research progress on the mechanism of mitochondrial autophagy in ischemic stroke to provide a theoretical basis for further research on mitochondrial autophagy and the treatment of ischemic stroke.

Keywords: mitochondrial autophagy, PINK1/Parkin, FUNDC1, NIX/BNIP3, cerebral stroke

OPEN ACCESS

Edited by:
Lin Wang,
Zhejiang University, China

Reviewed by:
Cameron Lenahan,
Burrell College of Osteopathic Medicine, United States
Yuchun Zuo,
Central South University, China

***Correspondence:**
Yongfa Zhang
13888168098@163.com
Tao Li
taoli_kh@163.com

[†]These authors have contributed equally to this work

Received: *21 April 2021*
Accepted: *02 June 2021*
Published: *15 July 2021*

Citation:
Lei L, Yang S, Lu X, Zhang Y and Li T (2021) Research Progress on the Mechanism of Mitochondrial Autophagy in Cerebral Stroke. Front. Aging Neurosci. 13:698601. doi: 10.3389/fnagi.2021.698601

INTRODUCTION

Stroke is a sudden disease with disturbance of cerebral blood circulation, which has surpassed ischemic heart disease, lung cancer, chronic obstructive pulmonary disease, and liver cancer to become the disease with the highest age-standardized mortality rate in China. According to the latest disease burden report in 2015, stroke has become not only the first cause of disease burden, but also the second leading cause of death and disability in the world (GBD 2015 DALYs and HALE Collaborators, 2016; GBD 2015 Mortality and Causes of Death Collaborators, 2016), and an important cause of premature death. Stroke is primarily divided into two categories: ischemic stroke (accounting for 60% of all strokes) and hemorrhagic stroke (Krishnamurthi et al., 2013). At present, studies have found a substantial link between mitochondrial dysfunction and the occurrence and development of ischemic stroke. Moreover, the abnormal autophagy is profoundly involved in mitochondrial dysfunction.

AUTOPHAGY

Autophagy is a process defined by the degradation of abnormal proteins and damaged organelles by bilayer membranes such as exfoliated endoplasmic reticulum or Golgi complex under physiological or pathological circumstances and mediated by autophagy-related proteins. The bilayer structures fuse with lysosomes to form autophagy lysosomes, which degrades the contents of biological macromolecules and organelles, so as to maintain cell homeostasis by meeting the needs of cellular metabolism and organelle renewal (Parzych and Klionsky, 2014; Tagaya and Arasaki, 2017). Autophagy is essential for neuronal survival in the central nervous system. According to the mechanism and the mode of action, autophagy can be divided into three types: macroautophagy, microautophagy, and chaperone-mediated autophagy (CMA). Among them, macroautophagy is the most thoroughly studied. Mitochondrial autophagy, also called mitophagy, is a kind of macrophage autophagy, which selectively degrades damaged mitochondria through autophagy

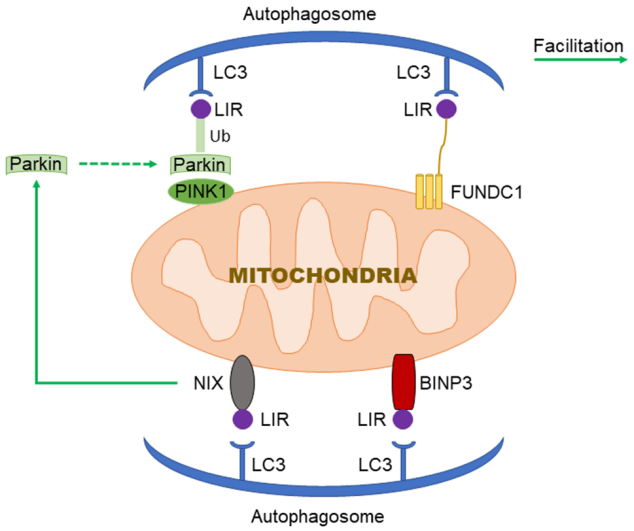

FIGURE 1 | Three signaling pathways regulating mitochondrial autophagy. In PTEN Induced Putative Kinase 1 (PINK1)/Parkin pathway, PINK1 functions as the initiator which recognizes the disturbed outer membrane potential and activates Parkin and ubiquitin phosphorylation, and then the complex is combined by LC3 to autophagosome; FUN14 Domain-Containing 1 (FUNDC1) is a three transmembrane protein having the LC3 interaction region (LIR) motif on the N-terminal which can be recognized by LC3; both BNIP3 and NIX have LIR motif, additionally, NIX can facilitate the localization of Parkin to the damaged mitochondria.

mechanism to sustain the stability of the intracellular environment. Mitochondrial autophagy plays an important role in regulating cellular homeostasis, proliferation, differentiation, genetics, aging, and cell death, as well as in controlling the quantity and quality of mitochondria (Glick et al., 2010).

THE REGULATORY MECHANISM OF MITOCHONDRIAL AUTOPHAGY

PTEN Induced Putative Kinase 1 (PINK1)/Parkin Signaling in Mitochondrial Autophagy

PTEN Induced Putative Kinase 1 (PINK1)/Parkin-mediated autophagy is the most common type of mitochondrial autophagy in mammalian cells (He et al., 2019). PINK1 is a nuclear-encoded mitochondrial serine (Ser)/threonine kinase (Eiyama and Okamoto, 2015; Quinn et al., 2020), which is divided into N-terminal mitochondrial targeting signal (MTS), α-helical transmembrane domain (TM), serine/threonine kinase domain, and C-terminal mitochondrial outer membrane retention signal peptide sequence (Deas et al., 2011), it can mediate the ubiquitination of substrates, and can regulate protein degradation and signal transduction. Parkin is an E3 ubiquitin ligase encoded by the Park2 gene. Genetic studies have shown that PINK1 plays a role in the upstream of Parkin, and PINK1 and Parkin are in the same pathway to preserve mitochondrial functions (Poole et al., 2008; Whitworth and Pallanck, 2009; Tanaka, 2020). In healthy cells, PINK1 is transported to the mitochondrial inner membrane, where it is cut and degraded rapidly by the ubiquitin-protease system, when the intracellular mitochondrial membrane is damaged, and consequently, the transmembrane potential is disturbed, the transport of PINK1 into the mitochondria will be blocked and PINK1 will accumulate in the outer membrane of the mitochondria, which then mediates the activation of Parkin and ubiquitin phosphorylation (Poole et al., 2008; Jin and Youle, 2013; Durcan and Fon, 2015; Okatsu et al., 2015a; Yamano et al., 2016). PINK1 can simultaneously phosphorylate Ser65 in the N-terminal ubiquitin-like domain of Parkin and produce Ser65 phosphorylated Parkin (Kondapalli et al., 2012; Iguchi et al., 2013; Okatsu et al., 2015b; Yang et al., 2020), phosphorylated Ser65 activates its ubiquitin ligase activity, which is able to connect the polyubiquitin chain to the mitochondrial outer membrane protein (Kazlauskaite et al., 2014), the complex is recognized by LC3, binds to the autophagosome, and then fuses with the lysosome to form the autophagy lysosome that finally degrades the damaged mitochondria. Studies from the Boule laboratory have confirmed that PINK1/Parkin-regulated mitochondrial autophagy plays a key role in the clearance of damaged mitochondria (Lazarou et al., 2015). Mitochondria maintain metabolic balance through continuous fusion and division. Additionally, the fusion/division and the mitochondrial autophagy influence each other; malfunctioning mitochondria are effectively removed by mitochondrial autophagy, and only the mitochondria with normal membrane potential can enter the normal fusion-division cycle (Twig et al., 2008), PINK1 and Parkin are of importance in the process of mitochondrial fusion and division. Related studies have shown that PINK1 and Parkin can promote mitochondrial division and regulate mitochondrial movement by mediating Miro phosphorylation to isolate damaged mitochondria (Poole et al., 2008), maintaining energy balance, and avoiding oxidative stress (Zhuang et al., 2016; **Figure 1**).

Mitochondrial Autophagy Regulated by FUN14 Domain-Containing 1 (FUNDC1)

FUN14 Domain-Containing 1 (FUNDC1) is a new type of mitochondrial membrane protein that mediates mitochondrial autophagy in mammalian cells, it mainly acts in controlling mitochondrial autophagy by regulating the phosphorylation level of FUNDC1 on the mitochondrial membrane. FUNDC1 is a protein located in the outer membrane of mitochondria, which contains three transmembrane domains, as well as the N-terminal domain exposed to the cytoplasm and the C-terminal domain inserted into the mitochondrial inner membrane. It has been found that FUNDC1 contains a typical LC3 interaction region (LIR) sequence consisting of amino acid residues at the N-terminal on the cytoplasmic side (Liu et al., 2014; Cai et al., 2021). Under physiological conditions, FUNDC1 inhibits mitochondrial autophagy due to the phosphorylation of Tyr18 in the LIR motif of sarcoma (Src) gene kinase, leading to the inability of FUNDC1 to recruit LC3 and to combine with it, which reduces the interaction between FUNDC1 and LC3 (Liu et al., 2012; Chen et al., 2016; Kuang et al., 2016). Studies have shown that mitochondrial autophagy receptor protein,

FUNDC1, is involved in mitochondrial autophagy under the condition of hypoxia in mammalian cells (Wang et al., 2018), when Src kinase and CK2 (formerly known as casein kinase 2) are inactivated during hypoxia or mitochondrial uncoupling, Ser17 on FUNDC1 is dephosphorylated by unc-51-like kinase 1 (ULK1) and Ser13 is dephosphorylated by phosphoglycerol mutase family 5 (PGAM5; Liu et al., 2014; Chen et al., 2016, 2017; Kuang et al., 2016), enhancing FUNDC-LC3 interaction and mitochondrial autophagy (Imai et al., 2010; Liu et al., 2014; Lv et al., 2017). Thus, it can be seen that FUNDC1 phosphorylation or dephosphorylation functions as a specific mitochondrial autophagy receptor in the process of mitochondrial autophagy induced by hypoxia. In addition, FUNDC1 can regulate mitochondrial division-fusion and mitochondrial autophagy by interacting with mitochondrial mitotic protein, dynamin-related protein 1 (Drp1), and optic nerve dystrophin 1 or with Drp1 and calcitonin (Ding and Yin, 2012; Iguchi et al., 2013; Wu et al., 2016a).

BNIP3/NIX Pathway in Mitochondrial Autophagy

BNIP3 (B Lymphoma-2 gene/adenovirus E1B interacting protein 3) and NIX (BNIP3L) are pro-apoptotic mitochondrial proteins located in the outer membrane of mitochondria (Kubli et al., 2007; Liu et al., 2019; Xu et al., 2019), they have 56% homology in amino acid sequence. Under certain conditions, the LIR sequence interacts with the recruited autophagy related protein, LC3, to form an autophagosome to clear the damaged mitochondria (Springer and Macleod, 2016; Šprung et al., 2018; Roperto et al., 2019). It has been reported that BNIP3/NIX mediates mitochondrial autophagy through upstream hypoxia-inducible 1 factor (HIF-1) regulation (Chourasia and Macleod, 2015); the competitive binding of BNIP3 and NIX to the anti-apoptotic protein, Bcl-2, will make Bcl-2-Beclin-1 complex dissociate and release Beclin-1, subsequently activating mitochondrial autophagy and reducing the apoptosis (Zhang et al., 2008). BNIP3 and NIX can promote the enhancement of mitochondrial autophagy by inhibiting the mammalian rapamycin target protein (mTOR) to activate protein Rheb. The upregulation of BNIP3 and NIX expression can be mediated by forkhead box O3 (FOXO3). Some studies have found that BNIP3 and NIX can not only induce cell death, but also increase their expression level under hypoxia, reducing reactive oxygen species (ROS) production and promoting cell survival, and can participate in the regulation of mitochondrial autophagy (de Vries and Przedborski, 2013). BNIP3 can increase the localization of mitochondrial kinesin-associated protein 1, thus promoting the phagocytosis of damaged mitochondria (Liu, 2015). Additionally, BNIP3 promotes the release of cytochrome C. Other studies have found that mitochondrial oxidative phosphorylation uncoupling agent carbonyl cyanide m-chlorophenyl hydrazone (CCCP) treatment on Hela cells can improve the interaction between NIX and LC3, indicating that NIX may also be involved in depolarization-induced mitochondrial autophagy (Novak et al., 2010). NIX mainly regulates mitochondrial autophagy at baseline under physiological conditions and mediates mitochondrial clearance during erythrocyte development by increasing the production of ROS (Novak and Dikic, 2011; Shi et al., 2014). Moreover, NIX can promote the localization of Parkin to the damaged mitochondria, increase the ubiquitination of mitochondrial membrane proteins by Parkin, and eventually induce mitochondrial autophagy through the interaction between p62 and LC3 (Geisler et al., 2010).

MITOCHONDRIAL AUTOPHAGY AND STROKE

Neurological impairment caused by mitochondrial dysfunction is significantly associated with stroke, the main mechanisms include increased adenosine triphosphate (ATP), increased ROS level, and oxidative stress overload. Under mild ischemia or tolerable hypoxic stress, mitochondrial autophagy can benefit cell homeostasis and promote cell survival. On the contrary, vulnerable brain cells in the ischemic core area of persistent ischemia or reperfusion begin to die, which will lead to excessive long–term autophagy hyperactivity, causing cell damage or death (Zhang X. et al., 2013). Therefore, in the course of a stroke, it may be a possible solution of protecting neurons and preventing cell death to regulate the quantity and quality of mitochondria through the process of mitochondrial autophagy (Wong and Cuervo, 2010; **Figure 2**).

ROS and Stroke

Mitochondria are vital organelles that produce energy, regulate cell signals and apoptosis, and are also the major source of ROS (Murphy, 2009). When cerebral ischemia occurs, the decrease of blood flow leads to oxygen and glucose deficiency and changes in mitochondrial structure. Excitatory amino acid toxicity, hypoxia, calcium overload, and other factors cause mitochondrial oxidative phosphorylation disorder (Li et al., 2015; Khandelwal et al., 2016), thus the excessive ROS produced by damaged nerve cells cannot be eliminated by related enzymes. In turn, it results in the destruction of the redox balance of lipids and proteins and extensive cell damage, which further aggravates the mitochondrial damage. Increased level of ROS-enhanced oxidative stress response and excessive generation of ROS can activate hypoxia-inducible factor 1 (HIF-1) and FOXO3, these transcription factors then induce the transcription of BNIP3 and NIX, and LC3 and BNIP3, respectively (Li et al., 2015). HIF-1 is the main factor in the survival response of cells to hypoxia, which can induce the transcription of BNIP3 and NIX genes. Their protein products compete with Beclin-1 to bind Bcl-2 to release Beclin-1 and allow it to induce autophagy (Mahalingaiah and Singh, 2014). It has been found that the increase of intracellular ROS may trigger the FOXO3 signaling pathway, which activates the transcription of ubiquitin-proteasome pathway and autophagy-related genes (such as the genes encoding LC3 and BNIP3), thus inducing autophagy (Aucello et al., 2009). After 3 days of ischemia/reperfusion, superoxide dismutase (SOD) and glutathione peroxidase (GSH-Px) in brain tissue decreased significantly. With the intervention using Salvianolic acid, oxygen-free radicals were effectively scavenged in rats, and ischemia-reperfusion injury was significantly suppressed

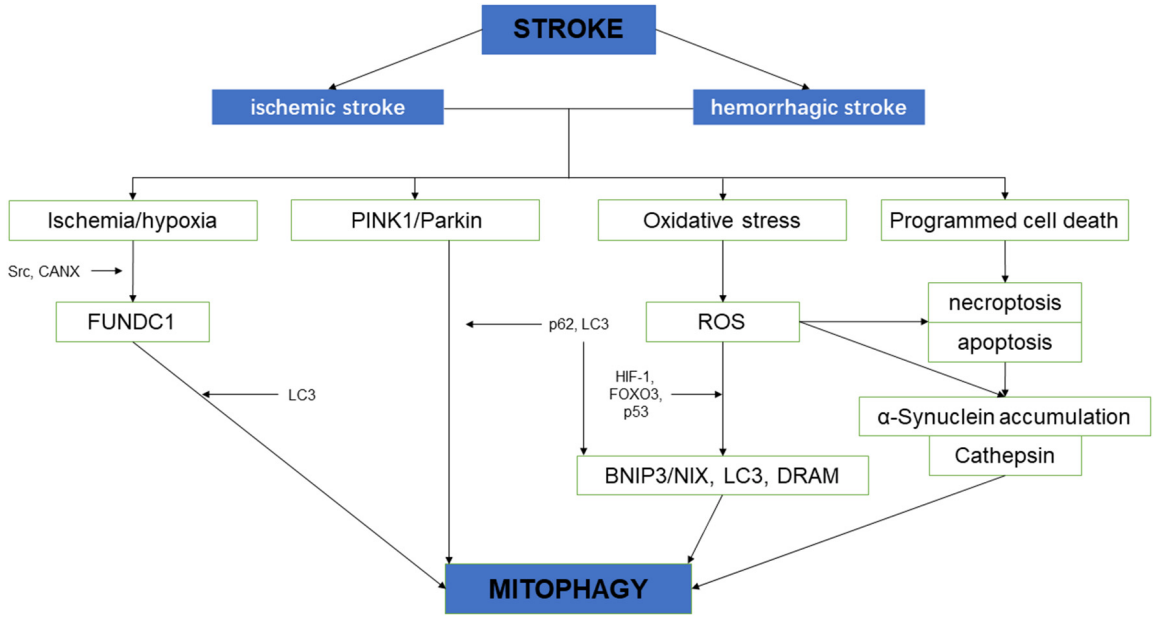

FIGURE 2 | The schematic diagram depicting the relationship between cerebral stroke and mitochondrial autophagy.

(Xu et al., 2017). Hypoxic preconditioning can activate the HIF-1/Beclin-1 signaling pathway to facilitate autophagy and protect against ischemic and hypoxic injury (Semenza, 2011; Lu et al., 2018). When cells were exposed to hypoxia, the transcriptional level of BNIP3/NIX was directly regulated by HIF-1α and activated (Tracy et al., 2007). Bellot confirmed in a variety of cell types that hypoxia promoted the inhibition of proline hydroxylase (PHD) activity through ROS produced by mitochondria (Bellot et al., 2009), suppressed the degradation of HIF-1α, and up-regulated the expression of autophagy genes such as Beclin-1 and Atg5 to promote mitochondrial autophagy (Jin and Youle, 2012). ROS not only induces mitochondrial autophagy through the HIF-1 signaling pathway (Dias et al., 2013), but also facilitates mitochondrial autophagy by activating the PINK1/Parkin pathway. In addition, ROS can induce autophagy by inhibiting the activity of protein kinase B (Akt) and mTOR in the PI3K/Akt/mTOR signaling pathway (Mellor et al., 2011; van der Vos et al., 2012; Zhang J. et al., 2013; Fiorini et al., 2015; Hambright et al., 2015; Duan et al., 2016).

The PINK1/Parkin Signaling Pathway and Ischemic Stroke

The PINK1-Parkin pathway is one of the typical signaling pathways in mitochondrial autophagy. Under physiological conditions, PINK1 and Parkin form a strict mitochondrial regulation mechanism and keep a mutual balance, preventing injury of autophagy caused by excessive mitochondrial autophagy. During mitochondrial dysfunction caused by ischemic stroke (Lazarou et al., 2012; Wauer et al., 2015), the PINK1/Parkin pathway mediates the polyubiquitin of the functional or structural proteins in the damaged mitochondria (Riley et al., 2013; Trempe et al., 2013; Kumar et al., 2015; Okatsu et al., 2015b; Yamano et al., 2015). PINK1 can quickly sense the membrane potential abnormality of the damaged mitochondria, recruit Parkin to gather to the damaged ones, and induce mitochondrial autophagy (Lee et al., 2010). In recent years, there has been an increase in the research on this mechanism in stroke, which illustrates to some extent that the PINK1-Parkin pathway is involved in the process of brain injury in stroke. Safarpour's studies on ischemic stroke using neurons found that knockout of PINK1 or Parkin gene could result in excitatory amino acid toxicity to the neurons, and it was confirmed that either PINK1 or Parkin gene deletion could aggravate neuronal damage in ischemic stroke. Wu et al. (2018) established the ischemic stroke cell model using rat hippocampal neurons *in vitro*. The results showed that PINK1/Parkin-mediated mitochondrial autophagy could play a neuroprotective role in rat hippocampal neurons. It was also revealed that H2 and rapamycin could increase cell survival, increase the expression of LC3-II, PINK1 and Parkin, reduce the loss of mitochondrial membrane potential, and inhibit the level of ROS and the rate of apoptosis. After autophagy inhibitor 3-methyladeine (3-MA) treatment, mitochondrial autophagy was inhibited, and the cell survival was significantly downscaled, accompanied by a significant increase in the level of ROS and the rate of apoptosis. It was found that in the pathophysiological process of ischemic stroke, PINK1/Parkin signaling pathway exerted a protective effect by mediating mitochondrial autophagy; it was also reported that the expression of LC3B and Beclin-1 was gradually up-regulated and reached the peak 24 h after cerebral ischemia-reperfusion, and the mitochondrial translocation of Parkin and the expression of PINK1 in mitochondrial outer membrane increased significantly at 24 h of reperfusion. When treated with a PINK1 inhibitor, the expression of LC3B and

Beclin-1 is decreased, the mitochondrial translocation of Parkin is lessened, and the volume of cerebral infarction is increased significantly. In addition, laboratory studies have proven that in the course of ischemic brain injury, silencing the Parkin gene can interfere with mitochondrial autophagy induced by OGD (oxygen-glucose deprivation) reperfusion model, and further aggravate neuronal injury.

Mitochondrial Autophagy and Cerebral Stroke Regulated by NIX/BNIP3

Under normal conditions, the expression of BNIP3/NIX is low in most organs, but under hypoxic-ischemic conditions, its transcriptional level is directly regulated by HIF-1α and activated (Tracy et al., 2007; Semenza, 2011; Guo, 2017; Yuan et al., 2017). Neuronal excitatory injury can induce mitochondrial autophagy during cerebral ischemia (Borsello et al., 2003; Shacka et al., 2007), which might occur *via* up-regulation of the expression of p53 and damage regulatory autophagy modulator DRAM(an autophagy regulator), and in turn, modulating autophagy by influencing Beclin-1 and LC3 (Rami et al., 2008; Wang et al., 2009; Poluzzi et al., 2014; Maejima et al., 2016). Mitochondrial autophagy can play a neuroprotective role by inhibiting apoptosis in the model of transient ischemia and hypoxia, in which the expression of Beclin-1 protein and the ratio of LC3-II/I is increased, while the expression of p62, TOM20, and HSP60 is decreased, and the progression of cerebral infarction is mild (Huang et al., 2016). In the model of long-term ischemia or permanent middle cerebral artery occlusion (MCAO), the detection of mitochondrial autophagy-related proteins, including Beclin-1, LC3, p62, TOM20, and HSP60 also shows that mitochondrial autophagy is inhibited and that the volume of cerebral infarction increases significantly. However, overactivated autophagy induces neuronal apoptosis and brain tissue injury (Li et al., 2015). Autophagy inhibitor 3-MA exerts the neuroprotective effect by inhibiting the up-regulation of LC3-II and cathepsin B induced by ischemia, preventing the programmed cell death of hippocampal CA1 neurons, and thus reducing the infarct volume and brain edema (Kubota et al., 2010). It is confirmed that the inhibition of Beclin-1 can reduce the cell death caused by MCAO (Xing et al., 2012). Recent research shows that necrostatin-1 treatment suppresses autophagic-associated proteins (LC3-II, Beclin-1) and maintains p62 at a normal level at 24 and 72 h after intracerebral hemorrhage (ICH) in a mouse model; the study also proves that the specific inhibitor, necrostatin-1, inhibits apoptosis and autophagy to exert the neuroprotective effects after ICH (Sekerdag et al., 2018). Zhang et al. (2011) reported that atorvastatin (ATV) weakens the neuroprotective effect of endoplasmic reticulum stress-related apoptosis through the reduction of autophagy in MCAO rats (Yuan et al., 2017), suggesting that compounds that inhibit autophagy may reduce the neuroprotective effect of angiotensin after cerebral ischemia (Adhami et al., 2006). Rapamycin, an inhibitor of mTOR, can activate autophagy after permanent ischemia and ischemia-reperfusion, increase the phosphorylation of Akt and cAMP response element binding protein (CREB), reduce infarction volume, improve stroke prognosis, and participate in protection against cerebral ischemic injury (Sheng et al., 2010). Carloni et al. (2010) used Rapamycin in the neonatal hypoxic-ischemic brain damage model and found that the expression of Beclin-1 was significantly up-regulated and the death of hippocampal and cortical neurons decreased significantly. The study speculated that drugs that appropriately up-regulate autophagy may have a certain neuroprotective effect in patients with large area cerebral infarction or transient ischemic attack (TIA; Carloni et al., 2008). Zheng et al. (2009) applied the ribonucleic acid (RNA) interference technique to the rat model of cerebral ischemia to down-regulate the expression of Beclin-1 in the ischemic brain and inhibit mitochondrial autophagy and noted that it can alleviate cerebral ischemic injury, inhibit neuronal apoptosis in cortex and striatum, and improve the symptoms of neurological impairment. Recent studies have shown that the re-expression of BNIP3L in mouse cortex and striatum transfected with recombinant adeno-associated virus can reverse the loss of BNIP3L after ischemia and promote mitochondrial autophagy. Additionally, this study found that only high expression of wild-type BNIP3L could reverse mitochondrial autophagy and reduce ischemic cerebral infarction volume after cerebral ischemia, whereas high expression monomer mutant BNIP3L could not have such effect. These results suggest that BNIP3L dimer formation is necessary to induce the mitochondrial autophagy to exert a neuroprotective effect, and the decrease of BNIP3L dimer is a key factor for the loss of mitochondrial autophagy in ischemic brain tissue. In ischemia and reperfusion, when the Parkin gene is knockout *in vivo* and *in vitro*, BNIP3L is still able to promote mitochondrial autophagy, and the mitochondrial autophagy-related proteins such as Parkin, FUNDC1, Bcl2-L-13, Prohibitin2, and BNIP3L/NIX can be detected. It was suggested that only the protein level of BNIP3L/NIX decreased with the prolonged duration of ischemia time. Recently, a series of studies have reported that tumor suppressor gene p53 and DRAM have an important relationship with the occurrence of autophagy during cerebral ischemia. Nerve excitatory injury can up-regulate the expression of p53 and DRAM, and then induce autophagy by regulating Beclin-1 and LC3 (Wang et al., 2009; Zhang et al., 2009; Sano et al., 2020).

The Ischemic Stroke Regulated by FUNDC1

FUNDC1 is a membrane protein located in mitochondria. FUNDC1 binds to LC3 through its LIR domain, causing an autophagic bilayer membrane to envelop mitochondria, inducing mitochondrial autophagy. The resulting mitochondrial autophagy inhibits apoptosis and protects neurons. FUNDC1 is a bridge between tissue-type plasminogen activator (tPA)-regulated apoptosis and mitosis in ischemia-reperfusion injury (IR) damage (Cai et al., 2021; Li et al., 2021). The tPA plays an important role in the treatment of acute cerebral ischemic injury, it has the thrombolytic effect in blood vessels and is also an important neuroprotective agent in the ultra-early ischemic stroke (Jeanneret and Yepes, 2017; Zhou et al., 2018; Yepes, 2019). FUNDC1 is associated with mitosis and is widely involved in the course of IR. The tPA exerts neuroprotective effects by increasing the phosphorylation of AMPK and the expression

of FUNDC1, thereby inhibiting apoptosis and improving mitochondrial function. Knocking out the tPA gene significantly aggravated brain injury and increased neuronal apoptosis and mitochondrial damage (Echeverry et al., 2010; Wu et al., 2012; An et al., 2014). Mitochondrial oxidative stress induced by blood re-flow after ischemia can lead to mitochondrial dysfunction and promote the release of cytochrome and Bcl family members (Cai et al., 2021). Recent studies have uncovered that FUNDC1 aggregates on the mitochondrial membrane by mediating the interaction between FUNDC1 and CANX protein on ER under anoxic conditions. Under hypoxic stress, the process of mitochondrial autophagy is activated. The separation of FUNDC1 from CANX, and the recruitment of DNM1L/Drp1 then lead to mitochondrial division (Wu et al., 2016b).

SUMMARY AND OUTLOOK

Mitochondria are the key target of cerebral stroke research. As a fundamental organelle, mitochondria play a pivotal role in the fate of neurons suffering an ischemic or hemorrhagic attack, causing neuronal death through a variety of biochemical and molecular processes. In recent years, there are numerous studies with respect to the correlation of cerebral stroke and mitochondrial autophagy, and also some preclinical studies aimed at interfering with autophagy to treat central nervous system diseases (Papadakis et al., 2013; Salminen et al., 2013). However, there is still a shortage of research on mitochondrial autophagy and hemorrhagic stroke, and it is an undeniable fact that the current results show some contradictions. Although the exact role of mitochondrial autophagy in stroke is controversial, it may also become a new hot spot in basic research and potential clinical application. It has been confirmed that drugs such as metformin, resveratrol, ginkgetin, and ezetimibe can activate autophagy to exert an anti-ischemic effect. For example, resveratrol protects the brain from NLRP3 injury by inhibiting the activation of NLRP3 inflammatory bodies through Sirt1-dependent autophagy; ginkgetin can alleviate cerebral ischemia/reperfusion induced autophagy and apoptosis by inhibiting the NF-κB/p53 signaling pathway (He et al., 2017; Yu et al., 2018; Pan et al., 2019). However, due to a lack of studies on drug side effects in experimental animals and the results of clinical trials, the conclusion that if autophagy modulating drugs mediate cytoprotection or cytotoxicity in cerebral stroke remains unavailable. We believe that the in-depth study of the molecular biological mechanism of mitochondrial autophagy will provide new perspectives, treatment strategies, and potential therapeutic targets for stroke and other diseases.

AUTHOR CONTRIBUTIONS

LL, SY, and XL presented the idea and wrote the manuscript. YZ and TL revised the article and are corresponding authors. All authors contributed to the article and approved the submitted version.

FUNDING

This work was supported by National Natural Science Foundation of China (Grant No. 82001278), The Fund for Young Doctors with the First People's Hospital of Yunnan Province (Grant No. KHBS-2020-014), Yunnan Fundamental Research Projects, and Joint Projects of Yunnan Provincial Science and Technology Department, and Kunming Medical University for Applied Basic Research.

REFERENCES

Adhami, F., Liao, G., Morozov, Y. M., Schloemer, A., Schmithorst, V. J., Lorenz, J. N., et al. (2006). Cerebral ischemia-hypoxia induces intravascular coagulation and autophagy. *Am. J. Pathol.* 169, 566–583. doi: 10.2353/ajpath.2006.051066

An, J., Haile, W. B., Wu, F., Torre, E., and Yepes, M. (2014). Tissue-type plasminogen activator mediates neuroglial coupling in the central nervous system. *Neuroscience* 257, 41–48. doi: 10.1016/j.neuroscience.2013.10.060

Aucello, M., Dobrowolny, G., and Musarò, A. (2009). Localized accumulation of oxidative stress causes muscle atrophy through activation of an autophagic pathway. *Autophagy* 5, 527–529. doi: 10.4161/auto.5.4.7962

Bellot, G., Garcia-Medina, R., Gounon, P., Chiche, J., Roux, D., Pouysségur, J., et al. (2009). Hypoxia-induced autophagy is mediated through hypoxia-inducible factor induction of BNIP3 and BNIP3L *via* their BH3 domains. *Mol. Cell. Biol.* 29, 2570–2581. doi: 10.1128/MCB.00166-09

Borsello, T., Croquelois, K., Hornung, J. P., and Clarke, P. G. (2003). N-methyl-d-aspartate-triggered neuronal death in organotypic hippocampal cultures is endocytic, autophagic and mediated by the c-Jun N-terminal kinase pathway. *Eur. J. Neurosci.* 18, 473–485. doi: 10.1046/j.1460-9568.2003.02757.x

Cai, Y., Yang, E., Yao, X., Zhang, X., Wang, Q., Wang, Y., et al. (2021). FUNDC1-dependent mitophagy induced by tPA protects neurons against cerebral ischemia-reperfusion injury. *Redox Biol.* 38:101792. doi: 10.1016/j.redox.2020.101792

Carloni, S., Buonocore, G., and Balduini, W. (2008). Protective role of autophagy in neonatal hypoxia-ischemia induced brain injury. *Neurobiol. Dis.* 32, 329–339. doi: 10.1016/j.nbd.2008.07.022

Carloni, S., Girelli, S., Scopa, C., Buonocore, G., Longini, M., and Balduini, W. (2010). Activation of autophagy and Akt/CREB signaling play an equivalent role in the neuroprotective effect of rapamycin in neonatal hypoxia-ischemia. *Autophagy* 6, 366–377. doi: 10.4161/auto.6.3.11261

Chen, M., Chen, Z., Wang, Y., Tan, Z., Zhu, C., Li, Y., et al. (2016). Mitophagy receptor FUNDC1 regulates mitochondrial dynamics and mitophagy. *Autophagy* 12, 689–702. doi: 10.1080/15548627.2016.1151580

Chen, Z., Liu, L., Cheng, Q., Li, Y., Wu, H., Zhang, W., et al. (2017). Mitochondrial E3 ligase MARCH5 regulates FUNDC1 to fine-tune hypoxic mitophagy. *EMBO Rep.* 18, 495–509. doi: 10.15252/embr.201643309

Chourasia, A. H., and Macleod, K. F. (2015). Tumor suppressor functions of BNIP3 and mitophagy. *Autophagy* 11, 1937–1938. doi: 10.1080/15548627.2015.1085136

Deas, E., Plun-Favreau, H., Gandhi, S., Desmond, H., Kjaer, S., Loh, S. H., et al. (2011). PINK1 cleavage at position A103 by the mitochondrial protease PARL. *Hum. Mol. Genet.* 20, 867–879. doi: 10.1093/hmg/ddq526

de Vries, R. L., and Przedborski, S. (2013). Mitophagy and Parkinson's disease: be eaten to stay healthy. *Mol. Cell. Neurosci.* 55, 37–43. doi: 10.1016/j.mcn.2012.07.008

Dias, V., Junn, E., and Mouradian, M. M. (2013). The role of oxidative stress in Parkinson's disease. *J. Parkinsons Dis.* 3, 461–491. doi: 10.3233/JPD-130230

Ding, W. X., and Yin, X. M. (2012). Mitophagy: mechanisms, pathophysiological roles and analysis. *Biol. Chem.* 393, 547–564. doi: 10.1515/hsz-2012-0119

Duan, P., Hu, C., Quan, C., Yu, T., Zhou, W., Yuan, M., et al. (2016). 4-Nonylphenol induces apoptosis, autophagy and necrosis in Sertoli cells:

involvement of ROS-mediated AMPK/AKT-mTOR and JNK pathways. *Toxicology* 341–343, 28–40. doi: 10.1007/s00701-016-2824-2

Durcan, T. M., and Fon, E. A. (2015). The three 'P's of mitophagy: PARKIN, PINK1 and post-translational modifications. *Genes Dev.* 29, 989–999. doi: 10.1101/gad.262758.115

Echeverry, R., Wu, J., Haile, W. B., Guzman, J., and Yepes, M. (2010). Tissue-type plasminogen activator is a neuroprotectant in the mouse hippocampus. *J. Clin. Invest.* 120, 2194–2205. doi: 10.1172/JCI41722

Eiyama, A., and Okamoto, K. (2015). PINK1/Parkin-mediated mitophagy in mammalian cells. *Curr. Opin. Cell Biol.* 33, 95–101. doi: 10.1016/j.ceb.2015.01.002

Fiorini, C., Cordani, M., Gotte, G., Picone, D., and Donadelli, M. (2015). Onconase induces autophagy sensitizing pancreatic cancer cells to gemcitabine and activates Akt/mTOR pathway in a ROS-dependent manner. *Biochim. Biophys. Acta* 1853, 549–560. doi: 10.1016/j.bbamcr.2014.12.016

GBD 2015 DALYs and HALE Collaborators (2016). Global, regional and national disability-adjusted life-years (DALYs) for 315 diseases and injuries and healthy life expectancy (HALE), 1990–2015: a systematic analysis for the Global Burden of Disease Study 2015. *Lancet* 388, 1603–1658. doi: 10.1016/S0140-6736(16)31460-X

GBD 2015 Mortality and Causes of Death Collaborators (2016). Global, regional and national life expectancy, all-cause mortality and cause-specific mortality for 249 causes of death, 1980–2015: a systematic analysis for the Global Burden of Disease Study 2015. *Lancet* 388, 1459–1544. doi: 10.1016/S0140-6736(16)31012-1

Geisler, S., Holmström, K. M., Skujat, D., Fiesel, F. C., Rothfuss, O. C., Kahle, P. J., et al. (2010). PINK1/Parkin-mediated mitophagy is dependent on VDAC1 and p62/SQSTM1. *Nat. Cell Biol.* 12, 119–131. doi: 10.1038/ncb2012

Glick, D., Barth, S., and Macleod, K. F. (2010). Autophagy: cellular and molecular mechanisms. *J. Pathol.* 221, 3–12. doi: 10.1002/path.2697

Guo, Y. (2017). Role of HIF-1a in regulating autophagic cell survival during cerebral ischemia reperfusion in rats. *Oncotarget* 8, 98482–98494. doi: 10.18632/oncotarget.21445

Hambright, H. G., Meng, P., Kumar, A. P., and Ghosh, R. (2015). Inhibition of PI3K/AKT/mTOR axis disrupts oxidative stress-mediated survival of melanoma cells. *Oncotarget* 6, 7195–7208. doi: 10.18632/oncotarget.3131

He, Q., Li, Z., Wang, Y., Hou, Y., Li, L., and Zhao, J. (2017). Resveratrol alleviates cerebral ischemia/reperfusion injury in rats by inhibiting NLRP3 inflammasome activation through Sirt1-dependent autophagy induction. *Int. Immunopharmacol.* 50, 208–215. doi: 10.1016/j.intimp.2017.06.029

He, L., Zhou, Q., Huang, Z., Xu, J., Zhou, H., Lv, D., et al. (2019). PINK1/Parkin-mediated mitophagy promotes apelin-13-induced vascular smooth muscle cell proliferation by AMPKα and exacerbates atherosclerotic lesions. *J. Cell. Physiol.* 234, 8668–8682. doi: 10.1002/jcp.27527

Huang, Y., Chen, H. J., Zhu, J. H., Zhao, F. Y., Qu, Y., and Mu, D. Z. (2016). [Effects of PINK1 gene on cell apoptosis and cell autophagy in neonatal mice with hypoxic-ischemic brain damage]. *Zhongguo Dang Dai Er Ke Za Zhi* 18, 263–269. doi: 10.7499/j.issn.1008-8830.2016.03.015

Iguchi, M., Kujuro, Y., Okatsu, K., Koyano, F., Kosako, H., Kimura, M., et al. (2013). Parkin-catalyzed ubiquitin-ester transfer is triggered by PINK1-dependent phosphorylation. *J. Biol. Chem.* 288, 22019–22032. doi: 10.1074/jbc.M113.467530

Imai, Y., Kanao, T., Sawada, T., Kobayashi, Y., Moriwaki, Y., Ishida, Y., et al. (2010). The loss of PGAM5 suppresses the mitochondrial degeneration caused by inactivation of PINK1 in Drosophila. *PLoS Genet.* 6:e1001229. doi: 10.1371/journal.pgen.1001229

Jeanneret, V., and Yepes, M. (2017). Tissue-type plasminogen activator is a homeostatic regulator of synaptic function in the central nervous system. *Neural Regen. Res.* 12, 362–365. doi: 10.4103/1673-5374.202924

Jin, S. M., and Youle, R. J. (2012). PINK1- and Parkin-mediated mitophagy at a glance. *J. Cell Sci.* 125, 795–799. doi: 10.1242/jcs.093849

Jin, S. M., and Youle, R. J. (2013). The accumulation of misfolded proteins in the mitochondrial matrix is sensed by PINK1 to induce PARK2/Parkin-mediated mitophagy of polarized mitochondria. *Autophagy* 9, 1750–1757. doi: 10.4161/auto.26122

Kazlauskaite, A., Kondapalli, C., Gourlay, R., Campbell, D. G., Ritorto, M. S., Hofmann, K., et al. (2014). Parkin is activated by PINK1-dependent phosphorylation of ubiquitin at Ser65. *Biochem. J.* 460, 127–139. doi: 10.1042/BJ20140334

Khandelwal, P., Yavagal, D. R., and Sacco, R. L. (2016). Acute ischemic stroke intervention. *J. Am. Coll. Cardiol.* 67, 2631–2644. doi: 10.1016/j.jacc.2016.03.555

Kondapalli, C., Kazlauskaite, A., Zhang, N., Woodroof, H. I., Campbell, D. G., Gourlay, R., et al. (2012). PINK1 is activated by mitochondrial membrane potential depolarization and stimulates Parkin E3 ligase activity by phosphorylating Serine 65. *Open Biol.* 2:120080. doi: 10.1098/rsob.120080

Krishnamurthi, R. V., Feigin, V. L., Forouzanfar, M. H., Mensah, G. A., Connor, M., Bennett, D. A., et al. (2013). Global and regional burden of first-ever ischaemic and haemorrhagic stroke during 1990–2010: findings from the Global Burden of Disease Study 2010. *Lancet Glob. Health* 1, e259–e281. doi: 10.1016/S2214-109X(13)70089-5

Kuang, Y., Ma, K., Zhou, C., Ding, P., Zhu, Y., Chen, Q., et al. (2016). Structural basis for the phosphorylation of FUNDC1 LIR as a molecular switch of mitophagy. *Autophagy* 12, 2363–2373. doi: 10.1080/15548627.2016.1238552

Kubli, D. A., Ycaza, J. E., and Gustafsson, A. B. (2007). Bnip3 mediates mitochondrial dysfunction and cell death through Bax and Bak. *Biochem. J.* 405, 407–415. doi: 10.1042/BJ20070319

Kubota, C., Torii, S., Hou, N., Saito, N., Yoshimoto, Y., Imai, H., et al. (2010). Constitutive reactive oxygen species generation from autophagosome/lysosome in neuronal oxidative toxicity. *J. Biol. Chem.* 285, 667–674. doi: 10.1074/jbc.M109.053058

Kumar, A., Aguirre, J. D., Condos, T. E., Martinez-Torres, R. J., Chaugule, V. K., Toth, R., et al. (2015). Disruption of the autoinhibited state primes the E3 ligase parkin for activation and catalysis. *EMBO J.* 34, 2506–2521. doi: 10.15252/embj.201592337

Lazarou, M., Jin, S. M., Kane, L. A., and Youle, R. J. (2012). Role of PINK1 binding to the TOM complex and alternate intracellular membranes in recruitment and activation of the E3 ligase Parkin. *Dev. Cell* 22, 320–333. doi: 10.1016/j.devcel.2011.12.014

Lazarou, M., Sliter, D. A., Kane, L. A., Sarraf, S. A., Wang, C., Burman, J. L., et al. (2015). The ubiquitin kinase PINK1 recruits autophagy receptors to induce mitophagy. *Nature* 524, 309–314. doi: 10.1038/nature14893

Lee, J. Y., Nagano, Y., Taylor, J. P., Lim, K. L., and Yao, T. P. (2010). Disease-causing mutations in parkin impair mitochondrial ubiquitination, aggregation and HDAC6-dependent mitophagy. *J. Cell Biol.* 189, 671–679. doi: 10.1083/jcb.201001039

Li, L., Tan, J., Miao, Y., Lei, P., and Zhang, Q. (2015). ROS and autophagy: interactions and molecular regulatory mechanisms. *Cell. Mol. Neurobiol.* 35, 615–621. doi: 10.1007/s10571-015-0166-x

Li, S., Zhou, Y., Gu, X., Zhang, X., and Jia, Z. (2021). NLRX1/FUNDC1/NIPSNAP1–2 axis regulates mitophagy and alleviates intestinal ischaemia/reperfusion injury. *Cell Prolif.* 54:e12986. doi: 10.1111/cpr.12986

Liu, L., Feng, D., Chen, G., Chen, M., Zheng, Q., Song, P., et al. (2012). Mitochondrial outer-membrane protein FUNDC1 mediates hypoxia-induced mitophagy in mammalian cells. *Nat. Cell Biol.* 14, 177–185. doi: 10.1038/ncb2422

Liu, K. E. and Frazier, W. A. (2015). Phosphorylation of the BNIP3 C-terminus inhibits mitochondrial damage and cell death without blocking autophagy. *PLoS One* 10:e0129667. doi: 10.1371/journal.pone.0129667

Liu, H., Huang, H., Li, R., Bi, W., Feng, L., E, L., et al. (2019). Mitophagy protects SH-SY5Y neuroblastoma cells against the TNFα-induced inflammatory injury: involvement of microRNA-145 and Bnip3. *Biomed. Pharmacother.* 109, 957–968. doi: 10.1016/j.biopha.2018.10.123

Liu, L., Sakakibara, K., Chen, Q., and Okamoto, K. (2014). Receptor-mediated mitophagy in yeast and mammalian systems. *Cell Res.* 24, 787–795. doi: 10.1038/cr.2014.75

Lu, N., Li, X., Tan, R., An, J., Cai, Z., Hu, X., et al. (2018). HIF-1α/beclin1-mediated autophagy is involved in neuroprotection induced by hypoxic preconditioning. *J. Mol. Neurosci.* 66, 238–250. doi: 10.1007/s12031-018-1162-7

Lv, M., Wang, C., Li, F., Peng, J., Wen, B., Gong, Q., et al. (2017). Structural insights into the recognition of phosphorylated FUNDC1 by LC3B in mitophagy. *Protein Cell* 8, 25–38. doi: 10.1007/s13238-016-0328-8

Maejima, Y., Isobe, M., and Sadoshima, J. (2016). Regulation of autophagy by Beclin 1 in the heart. *J. Mol. Cell. Cardiol.* 95, 19–25. doi: 10.1016/j.yjmcc.2015.10.032

Mahalingaiah, P. K., and Singh, K. P. (2014). Chronic oxidative stress increases growth and tumorigenic potential of MCF-7 breast cancer cells. *PLoS One* 9:e87371. doi: 10.1371/journal.pone.0087371

Mellor, K. M., Bell, J. R., Young, M. J., Ritchie, R. H., and Delbridge, L. M. (2011). Myocardial autophagy activation and suppressed survival signaling is associated with insulin resistance in fructose-fed mice. *J. Mol. Cell. Cardiol.* 50, 1035–1043. doi: 10.1016/j.yjmcc.2011.03.002

Murphy, M. P. (2009). How mitochondria produce reactive oxygen species. *Biochem. J.* 417, 1–13. doi: 10.1042/BJ20081386

Novak, I., and Dikic, I. (2011). Autophagy receptors in developmental clearance of mitochondria. *Autophagy* 7, 301–303. doi: 10.4161/auto.7.3.14509

Novak, I., Kirkin, V., McEwan, D. G., Zhang, J., Wild, P., Rozenknop, A., et al. (2010). Nix is a selective autophagy receptor for mitochondrial clearance. *EMBO Rep.* 11, 45–51. doi: 10.1038/embor.2009.256

Okatsu, K., Kimura, M., Oka, T., Tanaka, K., and Matsuda, N. (2015a). Unconventional PINK1 localization to the outer membrane of depolarized mitochondria drives Parkin recruitment. *J. Cell Sci.* 128, 964–978. doi: 10.1242/jcs.161000

Okatsu, K., Koyano, F., Kimura, M., Kosako, H., Saeki, Y., Tanaka, K., et al. (2015b). Phosphorylated ubiquitin chain is the genuine Parkin receptor. *J. Cell Biol.* 209, 111–128. doi: 10.1083/jcb.201410050

Pan, J., Li, X., Guo, F., Yang, Z., Zhang, L., and Yang, C. (2019). Ginkgetin attenuates cerebral ischemia-reperfusion induced autophagy and cell death *via* modulation of the NF-κB/p53 signaling pathway. *Biosci. Rep.* 39:BSR20191452. doi: 10.1042/BSR20191452

Papadakis, M., Hadley, G., Xilouri, M., Hoyte, L. C., Nagel, S., McMenamin, M. M., et al. (2013). Tsc1 (hamartin) confers neuroprotection against ischemia by inducing autophagy. *Nat. Med.* 19, 351–357. doi: 10.1038/nm.3097

Parzych, K. R., and Klionsky, D. J. (2014). An overview of autophagy: morphology, mechanism and regulation. *Antioxid. Redox Signal.* 20, 460–473. doi: 10.1089/ars.2013.5371

Poluzzi, C., Casulli, J., Goyal, A., Mercer, T. J., Neill, T., and Iozzo, R. V. (2014). Endorepellin evokes autophagy in endothelial cells. *J. Biol. Chem.* 289, 16114–16128. doi: 10.1074/jbc.M114.556530

Poole, A. C., Thomas, R. E., Andrews, L. A., McBride, H. M., Whitworth, A. J., and Pallanck, L. J. (2008). The PINK1/Parkin pathway regulates mitochondrial morphology. *Proc. Natl. Acad. Sci. U S A* 105, 1638–1643. doi: 10.1073/pnas.0709336105

Quinn, P. M. J., Moreira, P. I., Ambrósio, A. F., and Alves, C. H. (2020). PINK1/PARKIN signalling in neurodegeneration and neuroinflammation. *Acta Neuropathol. Commun.* 8:189. doi: 10.1186/s40478-020-01062-w

Rami, A., Langhagen, A., and Steiger, S. (2008). Focal cerebral ischemia induces upregulation of Beclin 1 and autophagy-like cell death. *Neurobiol. Dis.* 29, 132–141. doi: 10.1016/j.nbd.2007.08.005

Riley, B. E., Lougheed, J. C., Callaway, K., Velasquez, M., Brecht, E., Nguyen, L., et al. (2013). Structure and function of Parkin E3 ubiquitin ligase reveals aspects of RING and HECT ligases. *Nat. Commun.* 4:1982. doi: 10.1038/ncomms2982

Roperto, S., De Falco, F., Perillo, A., Catoi, C., and Roperto, F. (2019). Mitophagy mediated by BNIP3 and BNIP3L/NIX in urothelial cells of the urinary bladder of cattle harbouring bovine papillomavirus infection. *Vet. Microbiol.* 236:108396. doi: 10.1016/j.vetmic.2019.108396

Salminen, A., Kaarniranta, K., Kauppinen, A., Ojala, J., Haapasalo, A., Soininen, H., et al. (2013). Impaired autophagy and APP processing in Alzheimer's disease: the potential role of Beclin 1 interactome. *Prog. Neurobiol.* 106–107, 33–54. doi: 10.1016/j.pneurobio.2013.06.002

Sano, H., Futamura, M., Gaowa, S., Kamino, H., Nakamura, Y., Yamaguchi, K., et al. (2020). p53/Mieap-regulated mitochondrial quality control plays an important role as a tumor suppressor in gastric and esophageal cancers. *Biochem. Biophys. Res. Commun.* 529, 582–589. doi: 10.1016/j.bbrc.2020.05.168

Sekerdag, E., Solaroglu, I., and Gursoy-Ozdemir, Y. (2018). Cell death mechanisms in stroke and novel molecular and cellular treatment options. *Curr. Neuropharmacol.* 16, 1396–1415. doi: 10.2174/1570159X16666180302115544

Semenza, G. L. (2011). Hypoxia-inducible factor 1: regulator of mitochondrial metabolism and mediator of ischemic preconditioning. *Biochim. Biophys. Acta* 1813, 1263–1268. doi: 10.1016/j.bbamcr.2010.08.006

Shacka, J. J., Lu, J., Xie, Z. L., Uchiyama, Y., Roth, K. A., and Zhang, J. (2007). Kainic acid induces early and transient autophagic stress in mouse hippocampus. *Neurosci. Lett.* 414, 57–60. doi: 10.1016/j.neulet.2006.12.025

Sheng, R., Zhang, L. S., Han, R., Liu, X. Q., Gao, B., and Qin, Z. H. (2010). Autophagy activation is associated with neuroprotection in a rat model of focal cerebral ischemic preconditioning. *Autophagy* 6, 482–494. doi: 10.4161/auto.6.4.11737

Shi, R. Y., Zhu, S. H., Li, V., Gibson, S. B., Xu, X. S., and Kong, J. M. (2014). BNIP3 interacting with LC3 triggers excessive mitophagy in delayed neuronal death in stroke. *CNS Neurosci. Ther.* 20, 1045–1055. doi: 10.1111/cns.12325

Springer, M. Z., and Macleod, K. F. (2016). In brief: mitophagy: mechanisms and role in human disease. *J. Pathol.* 240, 253–255. doi: 10.1002/path.4774

Šprung, M., Dikic, I., and Novak, I. (2018). Flow cytometer monitoring of bnip3- and bnip3L/nix-dependent mitophagy. *Methods Mol. Biol.* 1759, 105–110. doi: 10.1007/7651_2017_14

Tagaya, M., and Arasaki, K. (2017). Regulation of mitochondrial dynamics and autophagy by the mitochondria-associated membrane. *Adv. Exp. Med. Biol.* 997, 33–47. doi: 10.1007/978-981-10-4567-7_3

Tanaka, K. (2020). The PINK1-parkin axis: an overview. *Neurosci. Res.* 159, 9–15. doi: 10.1016/j.neures.2020.01.006

Tracy, K., Dibling, B. C., Spike, B. T., Knabb, J. R., Schumacker, P., and Macleod, K. F. (2007). BNIP3 is an RB/E2F target gene required for hypoxia-induced autophagy. *Mol. Cell. Biol.* 27, 6229–6242. doi: 10.1128/MCB.02246-06

Trempe, J. F., Sauvé, V., Grenier, K., Seirafi, M., Tang, M. Y., Ménade, M., et al. (2013). Structure of parkin reveals mechanisms for ubiquitin ligase activation. *Science* 340, 1451–1455. doi: 10.1126/science.1237908

Twig, G., Elorza, A., Molina, A. J., Mohamed, H., Wikstrom, J. D., Walzer, G., et al. (2008). Fission and selective fusion govern mitochondrial segregation and elimination by autophagy. *EMBO J.* 27, 433–446. doi: 10.1038/sj.emboj.7601963

van der Vos, K. E., Eliasson, P., Proikas-Cezanne, T., Vervoort, S. J., van Boxtel, R., Putker, M., et al. (2012). Modulation of glutamine metabolism by the PI(3)K-PKB-FOXO network regulates autophagy. *Nat. Cell Biol.* 14, 829–837. doi: 10.1038/ncb2536

Wang, Y., Dong, X. X., Cao, Y., Liang, Z. Q., Han, R., Wu, J. C., et al. (2009). p53 induction contributes to excitotoxic neuronal death in rat striatum through apoptotic and autophagic mechanisms. *Eur. J. Neurosci.* 30, 2258–2270. doi: 10.1111/j.1460-9568.2009.07025.x

Wang, L., Wang, P., Dong, H., Wang, S., Chu, H., Yan, W., et al. (2018). Ulk1/FUNDC1 prevents nerve cells from hypoxia-induced apoptosis by promoting cell autophagy. *Neurochem. Res.* 43, 1539–1548. doi: 10.1007/s11064-018-2568-x

Wauer, T., Simicek, M., Schubert, A., and Komander, D. (2015). Mechanism of phospho-ubiquitin-induced PARKIN activation. *Nature* 524, 370–374. doi: 10.1038/nature14879

Whitworth, A. J., and Pallanck, L. J. (2009). The PINK1/Parkin pathway: a mitochondrial quality control system? *J. Bioenerg. Biomembr.* 41, 499–503. doi: 10.1007/s10863-009-9253-3

Wong, E., and Cuervo, A. M. (2010). Autophagy gone awry in neurodegenerative diseases. *Nat. Neurosci.* 13, 805–811. doi: 10.1038/nn.2575

Wu, W., Li, W., Chen, H., Jiang, L., Zhu, R., and Feng, D. (2016a). FUNDC1 is a novel mitochondrial-associated-membrane (MAM) protein required for hypoxia-induced mitochondrial fission and mitophagy. *Autophagy* 12, 1675–1676. doi: 10.1080/15548627.2016.1193656

Wu, W., Lin, C., Wu, K., Jiang, L., Wang, X., Li, W., et al. (2016b). FUNDC1 regulates mitochondrial dynamics at the ER-mitochondrial contact site under hypoxic conditions. *EMBO J.* 35, 1368–1384. doi: 10.15252/embj.201593102

Wu, X., Li, X., Liu, Y., Yuan, N., Li, C., Kang, Z., et al. (2018). Hydrogen exerts neuroprotective effects on OGD/R damaged neurons in rat hippocampal by protecting mitochondrial function *via* regulating mitophagy mediated by PINK1/Parkin signaling pathway. *Brain Res.* 1698, 89–98. doi: 10.1016/j.brainres.2018.06.028

Wu, F., Wu, J., Nicholson, A. D., Echeverry, R., Haile, W. B., Catano, M., et al. (2012). Tissue-type plasminogen activator regulates the neuronal uptake of glucose in the ischemic brain. *J. Neurosci.* 32, 9848–9858. doi: 10.1523/JNEUROSCI.1241-12.2012

Xing, S., Zhang, Y., Li, J., Zhang, J., Li, Y., Dang, C., et al. (2012). Beclin 1 knockdown inhibits autophagic activation and prevents the secondary neurodegenerative damage in the ipsilateral thalamus following focal cerebral infarction. *Autophagy* 8, 63–76. doi: 10.4161/auto.8.1.18217

Xu, D., Chen, P., Wang, B., Wang, Y., Miao, N., Yin, F., et al. (2019). NIX-mediated mitophagy protects against proteinuria-induced tubular cell apoptosis and renal injury. *Am. J. Physiol. Renal Physiol.* 316, F382–F395. doi: 10.1152/ajprenal.00360.2018

Xu, S., Zhong, A., Ma, H., Li, D., Hu, Y., Xu, Y., et al. (2017). Neuroprotective effect of salvianolic acid B against cerebral ischemic injury in rats *via* the CD40/NF-κB pathway associated with suppression of platelets activation and neuroinflammation. *Brain Res.* 1661, 37–48. doi: 10.1016/j.brainres.2017.02.011

Yamano, K., Matsuda, N., and Tanaka, K. (2016). The ubiquitin signal and autophagy: an orchestrated dance leading to mitochondrial degradation. *EMBO Rep.* 17, 300–316. doi: 10.15252/embr.201541486

Yamano, K., Queliconi, B. B., Koyano, F., Saeki, Y., Hirokawa, T., Tanaka, K., et al. (2015). Site-specific interaction mapping of phosphorylated ubiquitin to uncover parkin activation. *J. Biol. Chem.* 290, 25199–25211. doi: 10.1074/jbc.M115.671446

Yang, X., Pan, W., Xu, G., and Chen, L. (2020). Mitophagy: a crucial modulator in the pathogenesis of chronic diseases. *Clin. Chim. Acta* 502, 245–254. doi: 10.1016/j.cca.2019.11.008

Yepes, M. (2019). The plasminogen activation system promotes neurorepair in the ischemic brain. *Curr. Drug Targets* 20, 953–959. doi: 10.2174/1389450120666181211144550

Yu, J., Li, X., Matei, N., McBride, D., Tang, J., Yan, M., et al. (2018). Ezetimibe, a NPC1L1 inhibitor, attenuates neuronal apoptosis through AMPK dependent autophagy activation after MCAO in rats. *Exp. Neurol.* 307, 12–23. doi: 10.1016/j.expneurol.2018.05.022

Yuan, Y., Zheng, Y., Zhang, X., Chen, Y., Wu, X., Wu, J., et al. (2017). BNIP3L/NIX-mediated mitophagy protects against ischemic brain injury independent of PARK2. *Autophagy* 13, 1754–1766. doi: 10.1080/15548627.2017.1357792

Zhang, H., Bosch-Marce, M., Shimoda, L. A., Tan, Y. S., Baek, J. H., Wesley, J. B., et al. (2008). Mitochondrial autophagy is an HIF-1-dependent adaptive metabolic response to hypoxia. *J. Biol. Chem.* 283, 10892–10903. doi: 10.1074/jbc.M800102200

Zhang, X., Deguchi, S., Deguchi, K., Ohta, Y., Yamashita, T., Shang, J., et al. (2011). Amlodipine and atorvastatin exert protective and additive effects *via* antiapoptotic and antiautophagic mechanisms after transient middle cerebral artery occlusion in Zucker metabolic syndrome rats. *J. Neurosci. Res.* 89, 1228–1234. doi: 10.1002/jnr.22633

Zhang, J., Kim, J., Alexander, A., Cai, S., Tripathi, D. N., Dere, R., et al. (2013). A tuberous sclerosis complex signalling node at the peroxisome regulates mTORC1 and autophagy in response to ROS. *Nat. Cell Biol.* 15, 1186–1196. doi: 10.1038/ncb2822

Zhang, X. D., Wang, Y., Wang, Y., Zhang, X., Han, R., Wu, J. C., et al. (2009). p53 mediates mitochondria dysfunction-triggered autophagy activation and cell death in rat striatum. *Autophagy* 5, 339–350. doi: 10.4161/auto.5.3.8174

Zhang, X., Yan, H., Yuan, Y., Gao, J., Shen, Z., Cheng, Y., et al. (2013). Cerebral ischemia-reperfusion-induced autophagy protects against neuronal injury by mitochondrial clearance. *Autophagy* 9, 1321–1333. doi: 10.4161/auto.25132

Zheng, Y. Q., Liu, J. X., Li, X. Z., Xu, L., and Xu, Y. G. (2009). RNA interference-mediated downregulation of Beclin1 attenuates cerebral ischemic injury in rats. *Acta Pharmacol. Sin.* 30, 919–927. doi: 10.1038/aps.2009.79

Zhou, H., Zhu, P., Wang, J., Zhu, H., Ren, J., and Chen, Y. (2018). Pathogenesis of cardiac ischemia reperfusion injury is associated with CK2α-disturbed mitochondrial homeostasis *via* suppression of FUNDC1-related mitophagy. *Cell Death Differ.* 25, 1080–1093. doi: 10.1038/s41418-018-0086-7

Zhuang, N., Li, L., Chen, S., and Wang, T. (2016). PINK1-dependent phosphorylation of PINK1 and Parkin is essential for mitochondrial quality control. *Cell Death Dis.* 7:e2501. doi: 10.1038/cddis.2016.396

Conflict of Interest: The authors declare that the research was conducted in the absence of any commercial or financial relationships that could be construed as a potential conflict of interest.

frontiers in Aging Neuroscience

REVIEW
published: 07 September 2021
doi: 10.3389/fnagi.2021.721428

Mitochondrial Dynamics: A Potential Therapeutic Target for Ischemic Stroke

*Xiangyue Zhou[1], Hanmin Chen[1], Ling Wang[2], Cameron Lenahan[3], Lifei Lian[4], Yibo Ou[1] and Yue He[1]**

[1] Department of Neurosurgery, Tongji Hospital, Tongji Medical College, Huazhong University of Science and Technology, Wuhan, China, [2] Department of Operating Room, Tongji Hospital, Tongji Medical College, Huazhong University of Science and Technology, Wuhan, China, [3] Department of Biomedical Sciences, Burrell College of Osteopathic Medicine, Las Cruces, NM, United States, [4] Department of Neurology, Tongji Hospital, Tongji Medical College, Huazhong University of Science and Technology, Wuhan, China

Stroke is one of the leading causes of death and disability worldwide. Brain injury after ischemic stroke involves multiple pathophysiological mechanisms, such as oxidative stress, mitochondrial dysfunction, excitotoxicity, calcium overload, neuroinflammation, neuronal apoptosis, and blood-brain barrier (BBB) disruption. All of these factors are associated with dysfunctional energy metabolism after stroke. Mitochondria are organelles that provide adenosine triphosphate (ATP) to the cell through oxidative phosphorylation. Mitochondrial dynamics means that the mitochondria are constantly changing and that they maintain the normal physiological functions of the cell through continuous division and fusion. Mitochondrial dynamics are closely associated with various pathophysiological mechanisms of post-stroke brain injury. In this review, we will discuss the role of the molecular mechanisms of mitochondrial dynamics in energy metabolism after ischemic stroke, as well as new strategies to restore energy homeostasis and neural function. Through this, we hope to uncover new therapeutic targets for the treatment of ischemic stroke.

Keywords: energy metabolism, ischemic stroke, molecular mechanisms, mitochondrial dynamics, therapeutic target

OPEN ACCESS

Edited by:
Lin Wang,
Zhejiang University, China

Reviewed by:
Hailiang Tang,
Fudan University, China
Anwen Shao,
Zhejiang University, China

****Correspondence:***
Yue He
drhywind@163.com

Received: *07 June 2021*
Accepted: *16 August 2021*
Published: *07 September 2021*

Citation:
Zhou X, Chen H, Wang L, Lenahan C, Lian L, Ou Y and He Y (2021) Mitochondrial Dynamics: A Potential Therapeutic Target for Ischemic Stroke. Front. Aging Neurosci. 13:721428. doi: 10.3389/fnagi.2021.721428

INTRODUCTION

Stroke is an acute cerebrovascular disease resulting in cerebral blood circulation disorders due to the sudden rupture or occlusion of blood vessels in the brain. Stroke is associated with high morbidity, mortality, and rates of disability (GBD 2016 Stroke Collaborators, 2019), and can be classified as either ischemic or hemorrhagic. Currently, stroke has become the second leading cause of death globally (Lindsay et al., 2019), and is the primary cause of death in China (Wang Y. et al., 2020). It has been a difficult endeavor to save more lives and improve neurological recovery after stroke. As such, this challenge emphasizes the growing need for therapeutic agents that can mitigate brain injury and promote neurological recovery after stroke.

Energy metabolism is an important basis for cellular function, as it is the process by which cells utilize nutrient substances, such as sugars and fats, and produce adenosine triphosphate (ATP). Additionally, ATP is broadly used in cellular activities, and is necessary for ensuring a normal cell

lifespan. Mitochondria, which are commonly considered the powerhouse of the cell, are a major site of oxidative metabolism in eukaryotes, and are where sugars, fats, and amino acids are ultimately oxidized to release energy (Cardoso et al., 2010). The state of cellular energy metabolism is closely associated with mitochondrial dynamics, which refers to the dynamic process of mitochondrial fusion and division. Mitochondria maintain a steady state in the mitochondrial network through continuous fusion-division, thus maintaining the normal physiological function of cells (Dorn and Kitsis, 2015). Mitochondrial dynamics are involved in the formation and regulation of mitochondrial permeability transition pores (MPTPs), reactive oxygen species (ROS), and neuronal apoptosis (Roy et al., 2015). Mitochondrial dynamics can affect energy metabolism and post-stroke neuronal function by regulating the number, morphology, and function of mitochondria.

To identify potential interventional targets and novel diagnostic methods, it is crucial to understand the molecular mechanisms, especially those of mitochondrial dynamics after ischemic stroke. Herein, we will discuss the role of mitochondrial dynamics, as well as the energy metabolism involved in ischemic stroke. Moreover, an improved understanding of how mitochondrial dynamics affect energy metabolism will provide opportunities for the development of new therapeutic strategies targeting mitochondrial fusion and division after ischemic stroke.

MITOCHONDRIAL DYNAMICS AND ENERGY METABOLISM IN THE BRAIN

Cell energy metabolism refers to the metabolic pathway of ATP synthesis associated with nicotinamide adenine dinucleotide (NADH) turnover (Rigoulet et al., 2020). This pathway mainly includes the decompositional metabolism of sugar (aerobic oxidation, glycolysis, and phosphate sugar pathway), the tricarboxylic acid (TCA) cycle, fatty acid oxidation and synthesis, amino acid metabolism, and vitamin metabolism. Mitochondria are "energy factories" in eukaryotic cells, and are key sites of oxidative phosphorylation. Mitochondria are organelles that are present in most cells and are coated by two layers of membrane. Mitochondria can be divided into four functional regions: the outer mitochondrial membrane (OMM), intermembrane space (IMS), inner mitochondrial membrane (IMM), and mitochondrial matrix (listed in order from outside to inside). The proton concentration gradient originating from the electron transport chain in the IMM drives ATP generation (Scheffler, 2001). Moreover, mitochondria are highly mobile. Mitochondrial dynamics include fusion, division, selective degradation, and transport processes. Dynamic changes in mitochondria are important for immunity, apoptosis, and the cell cycle. These dynamic transformations are mainly mediated by large GTPases that belong to the dynamin family (Tilokani et al., 2018). In addition to generating energy, mitochondria can also drive cell dysfunction or death either passively (through ROS toxicity) or actively (through programed necrosis and apoptosis). Mitochondrial division and fusion play central roles in these processes (Dorn and Kitsis, 2015).

Mitochondrial Dynamics

Mitochondrial fusion refers to the merging of two mitochondria into a single mitochondrion (**Figure 1**). Because mitochondria have two layers of membrane, the process of mitochondrial fusion consists of outer membrane fusion and inner membrane fusion (**Table 1**). The tether is a physical connection between the two mitochondrial outer membranes, and is a prerequisite for actual membrane fusion (Koshiba et al., 2004). Mitofusin1 (Mfn1) and Mfn2 mediate fusion of the OMM, and optic atrophy protein 1 (Opa1) mediates fusion of the IMM (Chiurazzi et al., 2020). The overexpression of Mfn2 could increase mitochondrial fusion (Qin et al., 2020). However, the absence of Mfn1, Mfn2 (Hoppins, 2014), or Opa1 can lead to mitochondrial fragmentation (Song et al., 2007). Mitochondrial fusion can also facilitate the exchange of matrix contents among mitochondria through brief contact without resulting in a morphological merge. This is described as kiss-and-run fusion events (Chan, 2020). Mitochondrial fusion, and the material exchanged between mitochondria, optimize mitochondrial function and avoid damage accumulation due to mutations in mitochondrial DNA aging (Westermann, 2010; Chen et al., 2011; Cohen and Tareste, 2018).

Mitochondrial fission is the division of a mitochondrion into two smaller mitochondria (**Figure 1**), and dynamin-related GTPase1 (Drp1) plays a crucial role in this process (**Table 1**). Drp1 is recruited through four single-way transmembrane Drp1 receptors anchored on the OMM: mitochondrial fission factors (Mffs), mitochondrial kinetic proteins 49 and 51(MiD49 and MiD51), and Fis1 (Pagliuso et al., 2018). Mitochondrial fission usually occurs at the endoplasmic reticulum (ER)-mitochondrial contact site (Lewis et al., 2016). Additionally, the contraction of mitochondria is Drp1-independent, and ER tubules are more important in defining the position of mitochondrial fission sites (Friedman et al., 2011). However, mitochondrial fusion and fission are colocalized in ER membrane contact sites (MCSs; Guo et al., 2018). Therefore, mitochondrial fission and fusion could be regulated by controlling certain enzyme-like nodes on the ER MCS (Abrisch et al., 2020). Mitochondrial fission can irreparably fragment mitochondria, remove organelles to maintain mitochondria quality, and protect the normal function of the mitochondrial network (Nunnari, 2007).

Mitochondrial dynamics can regulate mitochondrial morphology, promote mitochondrial substance exchange, maintain mitochondrial DNA and inheritance, and eliminate damaged mitochondria. Normal regulation of mitochondrial dynamics is important in maintaining regular cell activity. Dysregulation of Mitochondrial dynamics plays an important role in driving cell death. Mitochondrial dynamics also play a role in necroptosis. The mitochondrial phosphatase, PGAM5, dephosphorylates Drp1Ser-637, leading to increased ROS and mitochondrial division, as well as promotion of necroptosis (Wang et al., 2012; Yu et al., 2020). When the energy supply is decreased, the increased levels of ADP and AMP can promote mitochondrial division and induce autophagy by activating MiD51 and Mff, respectively (Ducommun et al., 2015; Toyama et al., 2016). In addition, the reduction in Opa1 leads to an increase in autophagy (White et al., 2009). Mitochondrial fission is a necessary step in apoptosis (Xie et al., 2018). Apoptosis

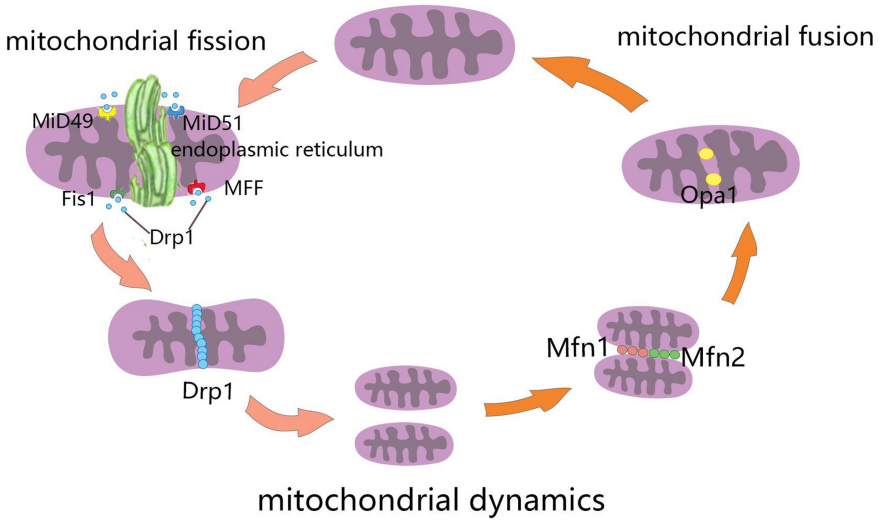

FIGURE 1 | Schematic diagram of mitochondrial dynamics. Mitochondrial fission is the division of mitochondria into two smaller mitochondria, and the dynamin-related GTPase Drp1 plays a crucial role in this process. Drp1 was recruited through four single-way transmembrane Drp1 receptors anchored on the outer mitochondrial membrane (OMM): mitochondrial fission factors (Mff), mitochondrial kinetic proteins 49 and 51(MiD49 and MiD51), and Fis1. Mitochondrial fusion refers to the merging of two mitochondria into one. Mitofusin1 (Mfn1) and mitofusin2 (Mfn2) mediate mitochondrial outer membrane fusion, and optic atrophy protein 1 (Opa1) mediates the fusion of mitochondrial inner membrane.

is a unique and important mode of programed cell death (Elmore, 2007) that maintains the number of cells in tissues, and it functions as a defense mechanism in the immune response (Norbury and Hickson, 2001). Drp1 can promote Bax translocation to the mitochondria (Montessuit et al., 2010), change the permeability of the mitochondrial membrane, release cytochrome C (Cyt-c), cause a cascade reaction, and lead to apoptosis. Mitochondrial fusion can protect cells from apoptosis (Bueler, 2010). Opa1 maintains the stability of mitochondrial cristae (Varanita et al., 2015) and Mfn2 interferes with Bax translocation by promoting mitochondrial fusion (Neuspiel et al., 2005). However, both Drp1 and Opa1 can prevent apoptosis. A variety of cell death patterns, such as apoptosis, necrosis, phagoptosis, and autophagy, form a complex network with different molecular mechanisms after stroke (Fricker et al., 2018), which suggests that mitochondrial dynamics may play an important role in cell death after stroke. However, in this review we mainly focused on the molecular mechanisms of mitochondrial dynamics in apoptosis after ischemic stroke.

TABLE 1 | Mitochondrial dynamics related proteins.

Mitochondrial dynamics		Proteins	References
Mitochondrial fusion	OMM fusion	Mfn1 Mfn2	Sokoloff et al., 1977; Bruick, 2000; Sowter et al., 2001; Falkowska et al., 2015; Um and Yun, 2017; Cheng et al., 2018; Rodger et al., 2018; Williams and Ding, 2018
	IMM fusion	Opa1	
Mitochondrial fission	Cytoplasm	Drp1	Herrero-Mendez et al., 2009; Belanger et al., 2011; Lunt and Vander Heiden, 2011; Nortley and Attwell, 2017; Magistretti and Allaman, 2018; Bordone et al., 2019
	Mitochondria	Mff MiD49 MiD51 Fis1	

OMM, outer mitochondrial membrane; IMM, inner mitochondrial membrane; Mfn1, mitofusin1; Mfn2, mitofusin2; Opa1, optic atrophy protein 1; Drp1, dynamin-related protein 1; Mff, mitochondrial fission factors; MiD49, mitochondrial kinetic proteins 49; MiD51, mitochondrial kinetic proteins 51; Fis1, mitochondrial fission protein 1.

In addition, mitophagy is a defensive mechanism that selectively removes damaged or unnecessary mitochondria *via* autophagy, which plays an important role in maintaining mitochondrial quality control and homeostasis (Gustafsson and Dorn, 2019). Mitophagy is mediated by autophagy-related proteins. Autophagy-related proteins specifically recognize and bind to functionally defective mitochondria so that they become fused with lysosomes to complete the degradation of damaged organelles and proteins (Gustafsson and Dorn, 2019). Mitophagy is closely associated with many functions and physiological processes in cells, such as cell differentiation and development, cell programing, cell death, and the immune response (Um and Yun, 2017). Molecular mechanisms of mitophagy involve PTEN-induced putative kinase 1(PINK1)/Parkin, BCL2/adenovirus E1B 19kDa-interacting protein 3 (BNIP3)/BCL2/adenovirus E1B 19kDa-interacting protein 3-like (NIX), FUN14 domain containing 1 (FUNDC1), BCL2-like 13(BCL2L13), FK506-Binding Protein 8 (FKBP8), and Cardiolipin (Rodger et al., 2018; Williams and Ding, 2018). BNIP3/NIX is associated with hypoxia-induced mitophagy, and the levels of BNIP3 and NIX are upregulated by hypoxia-inducible factor (HIF-1α) transcription (Bruick, 2000; Sowter et al., 2001), suggesting that this pathway may be involved in the brain

damage that occurs as a result of the hypoxic ischemia that manifests after stroke.

Energy Metabolism in the Brain

Energy Metabolism in the Brain Under Normal Physiological Conditions

The weight of the brain accounts for only 2% of total body weight. However, the brain accounts for 25 and 20% of glucose and oxygen consumption in the body, respectively (Sokoloff et al., 1977). Under aerobic conditions, ATP in brain cells is primarily derived from glucose that is consumed in the TCA cycle occurring in the mitochondria for oxidative phosphorylation. Moreover, the uptake and utilization of glucose by cells in the brain are associated with specific features. This process requires several cell types, which comprise the neurovascular unit, to coordinate and complete it. The neurovascular unit is composed of brain capillary endothelial cells, pericytes, astrocytes, oligodendrocytes, microglia, and neurons (Cheng et al., 2018; **Figure 2**). Glucose enters cells through specific glucose transporters (GLUTs), such as GLUT1, GLUT2, and GLUT7 in astrocytes, GLUT1 in oligodendrocytes, and GLUT3 and GLUT4 in neurons. Additionally, glucose is phosphorylated by hexokinase to produce glucose-6-phosphate (Falkowska et al., 2015). Glucose 6-phosphate can be processed through various metabolic pathways (e.g., glycolysis, pentose phosphate pathway, and glycogenesis). Numerous metabolic intermediates formed by glucose in the brain, such as lactate, pyruvate, glutamate, or acetate, can also be utilized to produce energy (Belanger et al., 2011).

In the brain, different cell types have different metabolic characteristics. There is dynamic regulation between astrocytes and neurons known as the astrocyte–neuron lactate shuttle (Bordone et al., 2019; **Figure 2**). Neurons release glutamate to stimulate astrocytes to take up glucose (Magistretti and Allaman, 2018). Due to the low activity of pyruvate dehydrogenase in astrocytes, it is easier to produce lactic acid *via* aerobic glycolysis in the cytoplasm, which is also known as the Warburg effect in cancer cells (Lunt and Vander Heiden, 2011; Magistretti and Allaman, 2018). Astrocytes play a significant role in regulating the energy supply of the brain, but it remains unclear whether the lactic acid produced by astrocytes is fuel for neurons (Nortley and Attwell, 2017). Neurons lack fructose 6-phosphate-2-kinase/fructose-2,6- bisphosphatase-3(Pfkfb3), thus demonstrating a slower rate of glycolysis than other cells. However, neurons can efficiently utilize lactic acid (Herrero-Mendez et al., 2009; Bolanos, 2016). After glucose is transported through the blood-brain barrier (BBB) and the cell membrane, it is transformed into pyruvate *via* anaerobic glycolysis in the cytoplasm, which leads to the generation of 2 mol of ATP. Each mole of glucose pyruvate is subsequently transported to the mitochondria, and is then converted into acetyl coenzyme A, which then participates in the TCA cycle. During the subsequent steps of the TCA cycle, oxidative phosphorylation produces an additional 30 mol of ATP per mole of glucose. This process is closely associated with the TCA cycle, electron transfer in the

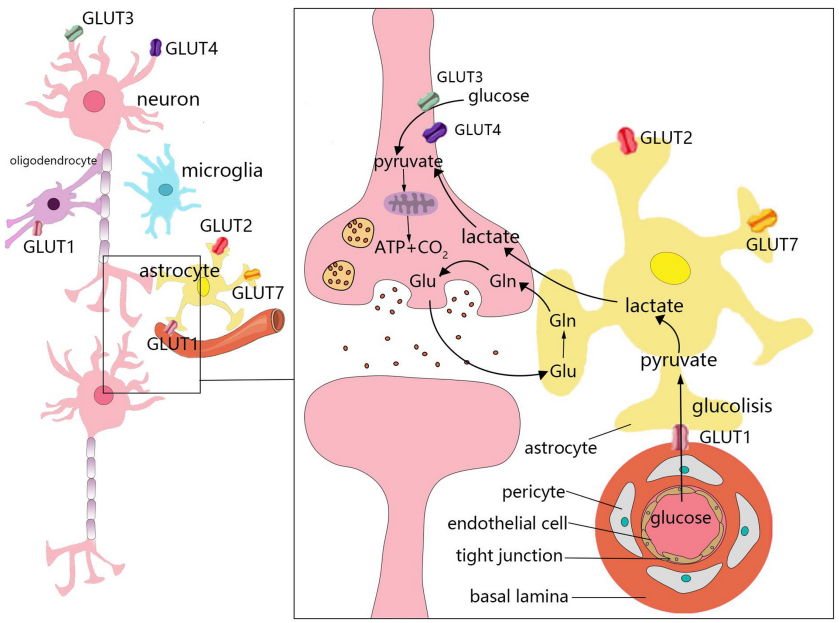

FIGURE 2 | Energy metabolism in the brain. The uptake and utilization of glucose by cells in the brain requires the neurovascular unit, which is composed of brain capillary endothelial cells, pericytes, astrocytes, oligodendrocytes, microglia, and neurons. Glucose enters cells through specific glucose transporters (GLUTs), such as GLUT1, GLUT2, and GLUT7 in astrocytes, GLUT1 in oligodendrocytes, and GLUT3 and GLUT4 in neurons. Numerous metabolic intermediates formed by glucose in the brain can also be oxidized to produce energy, such as lactate, pyruvate, and glutamate. The dynamic regulatory mechanism of lactic acid metabolism between astrocytes and neurons is known as the astrocyte–neuron lactate shuttle. Neurons release glutamate to stimulate glucose uptake by astrocytes. Astrocytes produce lactic acid by aerobic glycolysis in the cytoplasm and then transport to neurons.

respiratory chain, oxygen consumption, and the production of carbon dioxide and water. In addition to basic cell activities, the energy produced by various cells in the brain is mainly used to maintain and restore ion gradients that are dissipated by signaling processes (e.g., postsynaptic and action potentials), as well as participate in the uptake and recycling of neurotransmitters (Attwell and Laughlin, 2001).

Energy Metabolism in the Brain After Ischemic Stroke

Obviously, ischemic hypoxic brain injury after stroke is closely associated with energy metabolism disorder. However, there are various pathophysiological mechanisms involved in brain damage after stroke, such as oxidative stress, mitochondrial dysfunction, excitotoxicity, calcium overload, neuroinflammation, acidosis, neuronal apoptosis, and BBB disruption (Moskowitz et al., 2010; Sekerdag et al., 2018). The normal supply of glucose and oxygen is cut off during cerebral ischemia, although astrocytes can synthesize and store glycogen, as well as metabolize glycogen into lactic acid to provide energy for neurons (Mergenthaler et al., 2013; Falkowska et al., 2015). When the glucose supply is insufficient, ketone bodies and lactic acid can also become substrates for brain energy metabolism (Sokoloff, 1981). In early ischemia, when synaptic activity disappears, adenosine is released to block presynaptic Ca^{2+} influx and inhibit glutamate release (Hofmeijer and van Putten, 2012). This early inhibition of glutamate release prevents glutamate excitotoxicity. However, if the ischemic period is prolonged, neuronal cells cannot maintain the normal transmembrane concentration gradient, which causes neuronal signal impairment. Conversely, synaptic terminal depolarization releases the neurotransmitter glutamate. Furthermore, the reabsorption of glutamate clearance from the synaptic space leads to glutamic acid accumulation, excessive stimulation of N-methyl-D-aspartate (NMDA) receptors, high levels of calcium influx, mitochondrial depolarization, the release of Cyt-c, and neuronal apoptosis (Harris et al., 2012; Campbell et al., 2019).

After stroke, different regions comprising the stroke lesion will exhibit various metabolic characteristics. The location of the stroke lesion can be divided into three regions according to cerebral blood flow (CBF; Pushie et al., 2018). The ischemic core area is the central region of brain tissue infarct. The ischemic periphery region surrounding the core is divided into two components. One is close to the infarct area. Here, there are a large number of cells undergoing oxidative stress due to the reduced blood supply, but timely reperfusion therapy can save this section of tissue, known as the ischemic penumbra. The ischemic peripheral region is relatively far from the infarct area, and the blood circulation is relatively similar to that of normal tissue. The levels of glucose utilization, ATP, lactic acid, creatine phosphate, and pH varies according to CBF changes (Leigh et al., 2018). The ischemic penumbra cannot be rescued and it expands into the infarct area when CBF decreases beyond a certain threshold (Astrup et al., 1981). Currently, it is an important objective in stroke treatment to identify ischemic penumbral tissue based on PET/CT and related brain metabolism (Sarrafzadeh et al., 2010; Zenonos and Kim, 2010), and to treat it in a timely manner. Due to the different metabolic demands of grey matter (GM) and white matter (WM), the CBF and cerebral blood volume (CBV) thresholds of the damaged region are different (An et al., 2015; Leigh et al., 2018). Moreover, GM is more susceptible to ischemia than WM because GM has a higher CBF, CBV, and apparent diffusion coefficient (ADC), as well as a shorter mean transit time (MTT; Bristow et al., 2005). GM mainly includes neuronal cell bodies, dendrites, and axons, which are used for local information, while WM mainly includes axons, oligodendrocytes, and astrocytes. Neuronal apoptosis or necrosis results from excessive free radical production, calcium overload, and excitotoxicity following ischemia and hypoxia (Radak et al., 2017). The decreased blood supply after stroke leads to the destruction of axonal electrophysiological characteristics and nutritional dysfunction in WM. The effect of glutamate metabolism on astrocytes induces excitotoxicity in oligodendrocytes (Wang et al., 2016). After reperfusion, energy metabolism does not immediately return to baseline as expected. The activation of platelets and complement systems, the release of inflammatory mediators, and neuronal mitochondria in the ischemic penumbra overcompensate for ischemic injury by inducing metabolic pathways, which leads to the excessive release of ROS. All of these factors contribute to neuronal death and brain injury after ischemia-reperfusion (Al-Mufti et al., 2018).

THE ROLE OF MITOCHONDRIAL DYNAMICS IN BRAIN INJURY AFTER ISCHEMIC STROKE

The Molecular Mechanisms of Mitochondrial Dynamics in the Ischemic Stroke

The mechanism of mitochondrial division and fusion is complex, and not only affects energy metabolism in cells, but also induces apoptosis. After cerebral ischemia and hypoxia, changes in mitochondrial dynamics also greatly impact the survival of nerve cells. Seventy percent of neuronal energy is used to maintain the sodium and potassium pump on the cell membrane. The ATP supply is insufficient after stroke, which leads to depolarization of the neuronal plasma membrane, release of the excitatory neurotransmitter, glutamate, and causes glutamate excitotoxicity (Doyle et al., 2008). Ischemia induced an increase in glutamate release from neurons and astrocytes, which leads to overstimulation of NMDA and α-amino-3-hydroxy-5-methyl-4-isoxazole-propionic acid (AMPA) receptors. Glutamate excitotoxicity and oxidative stress influence mitochondrial division and fusion, as well as the imbalance in mitochondrial division and fusion, leading to NMDA receptor upregulation and oxidative stress (Nguyen et al., 2011). Next, we will review the molecular mechanisms of mitochondrial dynamics in post-stroke injury (**Figure 3**).

Calcium Overload

Excessive calcium enters cells, activates many calcium-dependent proteases, lipases, and deoxyribonucleases, and leads to cell death (Besancon et al., 2008). The mitochondrial calcium uniporter

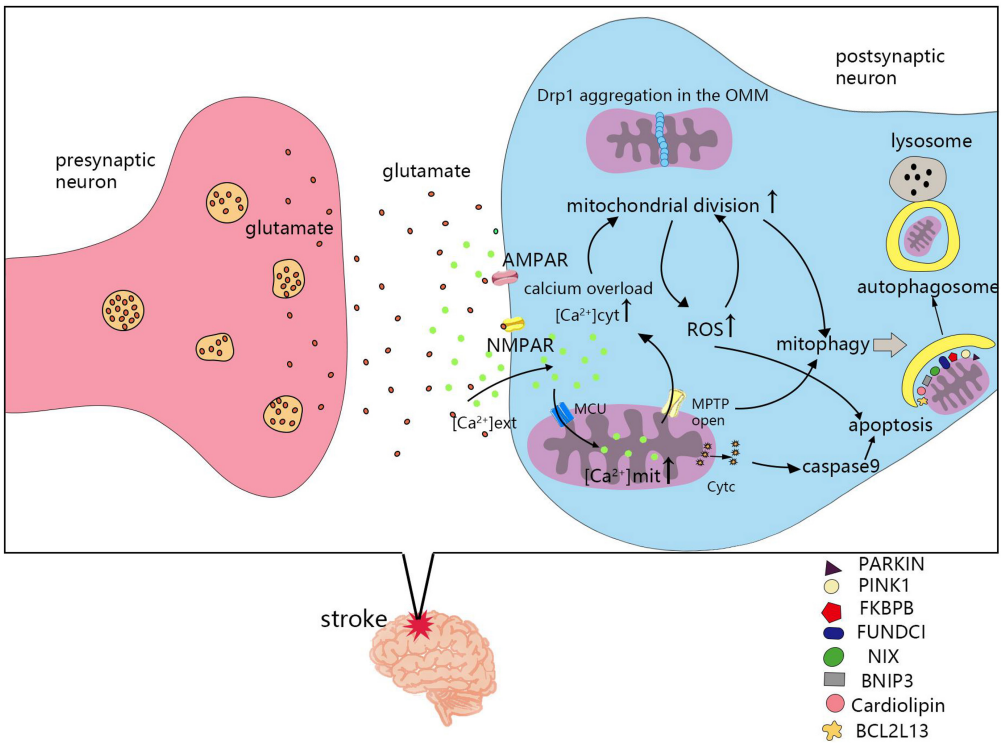

FIGURE 3 | Molecular mechanisms of mitochondrial dynamics in post-ischemic stroke injury. Cerebral ischemia and hypoxia lead to the imbalance of mitochondrial division and fusion, which is related to calcium overload, reactive oxygen species (ROS), mitochondrial permeability transition pores(MPTP), apoptosis, and mitophagy. MCU, mitochondrial calcium uniporter; NMPAR, N-methyl-D-aspartate receptors; AMPAR, α-amino-3-hydroxy-5-methyl-4-isoxazole-propionic acid receptors; [Ca^{2+}] ext, calcium ion concentration in extracellular; [Ca^{2+}] cyt, calcium ion concentration in cytoplasmic; [Ca^{2+}] mit, calcium ion concentration in mitochondria.

(MCU), a calcium transporter in mitochondria, plays a vital role in maintaining intracellular homeostasis by transporting Ca^{2+} from the cytoplasm into the mitochondrial matrix (Zhao et al., 2013; Kwong et al., 2015). Mitochondrial Ca^{2+} controls energy production and metabolism by regulating key enzymes and fatty acid oxidation in the TCA cycle. Calcium overload in the cytoplasm activates calcineurin, and dephosphorylates Drp1 at serine 637, leading to Drp1 accumulation from the cytoplasm to the OMM. Promoting mitochondrial division and ROS production, but inhibiting mitochondrial division by using mitochondrial division inhibitor 1(Mdivi-1), Drp1siRNA, or calcineurin inhibitors shows that mitochondrial morphology is retained, intracellular calcium ions are reduced, and cell death is prevented in cardiac ischemia-reperfusion injury (Sharp et al., 2014). Inhibiting Drp1 can participate in neuroprotection by combating glutamate toxicity *in vitro* and ischemic brain injury *in vitro* (Grohm et al., 2012). Calcium overload also causes mitochondria to release apoptotic factors and induce apoptosis (Pivovarova et al., 2004).

Reactive Oxygen Species

Reactive oxygen species and oxidative stress are important causes of tissue damage during cerebral ischemia (Crack and Taylor, 2005). Mitochondria are thought to be the main origin of intracellular ROS (Bayir and Kagan, 2008). Oxygen-free radicals are highly active and have the ability to destroy cellular components (Droge, 2002). Changes in ROS lead to changes in the expression or activity of proteins associated with mitochondrial dynamics that affect mitochondrial fusion and division (Cid-Castro et al., 2018). In general, elevated ROS levels trigger mitochondrial fission. It is worth mentioning that phosphorylation at different sites of Drp1 differentially affects mitochondrial dynamics. The increase in ROS promotes Drp1 activation through Ser616 phosphorylation, which promotes mitochondrial fission (Cho et al., 2012). However, Drp1 serine 637 phosphorylation inhibits mitochondrial fission. The phosphorylation of Drp1 at tyrosines 266, 368, and 449 leads to mitochondrial division and neuronal death (Zhou et al., 2017). The Drp1-mitochondrial fission ROS cycle may play a role in central nervous system (CNS) diseases (da Rosa et al., 2020). There is an interaction between mitochondrial dynamics and ROS production. On one hand, increased mitochondrial division will increase the production of ROS, but inhibition of mitochondrial division can restore ROS levels to normal (Zhang Y. K. et al., 2020). On the other hand, the increase of ROS will promote the activation of Drp1, leading to increased mitochondrial division (Youle and van der Bliek, 2012; Cid-Castro et al., 2018), thereby further increasing the production of ROS, whereas knocking out Drp1 reduces oxidative stress-induced

mitochondrial fragmentation (Youle and van der Bliek, 2012). This cyclic reaction will aggravate mitochondrial dysfunction after stroke, increase the level of ROS, and increase brain damage after stroke. After inhibiting ROS levels in a mouse model of stroke, mitochondrial dysfunction, obstruction volume, and neurological deficits were reduced (Hwang et al., 2020). From this perspective, interrupting this cycle by reducing ROS levels or inhibiting mitochondrial division is a key part of stroke treatment. Studies have shown that inhibiting excessive mitochondrial division could protect against neurotoxicity (Rappold et al., 2014). Hyperbaric oxygen (HBO) can also reduce brain damage by regulating Drp1 phosphorylation (Ni et al., 2020). ROS can also activate OMA1 to promote the cleavage of L-Opa1 to S-Opa1, resulting in mitochondrial crest remodeling and Cyt-c release, further resulting in increased apoptosis (Zhang K. et al., 2014).

Mitochondrial Permeability Transition Pores

The MPTP is a channel that triggers a sudden increase in the permeability of the mitochondrial inner membrane when there is mitochondrial calcium overload, especially when combined with oxidative or nitrite stress and/or ATP depletion (Bernardi, 1999). When the MPTP is open, it can lead to a rapid increase in the osmotic pressure of the matrix solute, rupture of the OMM, collapse of the mitochondrial membrane potential ($\Delta\Psi m$), and a reduction in intracellular ATP, which eventually leads to necrotic cell death (Kinnally et al., 2011). The MPTP can also be used as a physiological efflux pathway, and can open transiently (Altschuld et al., 1992). In cyclophilin D-knockout mice, transient activation of the MPTP could protect neurons from cytoplasmic Ca^{2+} overload (Barsukova et al., 2011). Mitochondrial matrix calcium overload is the main mechanism of MPTP opening, and plays an important role in regulating the MPTP (Hurst et al., 2017). Moreover, ROS can also regulate the activity of the MPTP (Halestrap et al., 1997). Hence, the opening of the MPTP is involved in the pathophysiological mechanism after stroke. The infarct size after transient occlusion of the artery can be reduced by the cyclosporine A analog, N-methyl-Val-4-cyclosporin A (Me ValCsA), which blocks the MPTP (Matsumoto et al., 1999). Melatonin and atorvastatin can also block the MPTP and the release of Cyt-c from mitochondria, thereby reducing neuronal apoptosis after ischemia-reperfusion (Andrabi et al., 2004; Song et al., 2014). Treatment of HL-1 cells with Drp-1 inhibitors reduces mitochondrial permeability transition pore sensitivity after cardiac ischaemia-reperfusion (Ong et al., 2010). In Mfn-2-deficient mice, MPTP opening is delayed. Therefore, Mfn-2 participates in the regulation of the MPTP and triggers death in cardiomyocytes (Papanicolaou et al., 2011).

Apoptosis

After apoptotic stimulation, apoptotic members of the Bcl-2 protein family, such as Bax and Bak, insert into the mitochondrial outer membrane (Ader et al., 2019) and change the permeability of the OMM, thus mediating the release of apoptosis-related factors, such as Cyt-c, second mitochondria-derived activator of caspases (Smac), and apoptosis-inducing factor (AIF) from mitochondria into the cytoplasmic matrix (Jurgensmeier et al., 1998; Susin et al., 1999; Jeong and Seol, 2008). Apoptosis-related factors in the cytoplasm activate caspase-9, causing cascade reactions, consequently leading to apoptosis (Green and Reed, 1998). However, mitochondrial dynamics is involved in the regulation of apoptosis (Frank et al., 2001). The dominant-negative mutant of Drp1, as well as siRNA-mediated silencing of Drp1, could reduce apoptosis in Q111/0 cells in Huntington's disease (Costa et al., 2010). By inhibiting Drp1 activation, mitochondrial debris and ROS can be reduced, and neuronal damage can be alleviated (Zhou et al., 2020). Using propofol to treat oxidation-injured neurons could reduce the expression of Fis1 and increase the expression of Mfn1, maintaining normal levels of these two proteins, thus reducing the expression of apoptotic proteins in neurons and alleviating neuronal damage induced by hypoxia (Zhang H. S. et al., 2020). Research has shown that inducing mitochondrial fission *via* activation of Drp1 and Mff results in apoptosis in hippocampal neuronal cells (Zhang C. et al., 2020).

Mitophagy

The regulation of mitochondrial autophagy is associated with mitochondrial dynamics (Yoo and Jung, 2018), and is expected to be a new target for ischemic stroke treatment (Guan et al., 2018). In an acute model of mitochondrial damage induced by carbonyl cyanide-m-chlorophenylhydrazone (CCCP), the ubiquitination of mitofusin 1 (Mfn-1) and 2 (Mfn-2) is closely associated with the induction of mitophagy, and the ubiquitination of both proteins is dependent on parkin and PINK1, which play crucial roles in mitophagy (Gegg et al., 2010). In Parkin-null HeLa cells and in HEK293 cells with siRNA-mediated Parkin knockdown, glycoprotein 78 (Gp78) induction of mitophagy was Mfn1-dependent (Fu et al., 2013). In adult cardiac progenitor cells (CPCs), knockdown of either Fundc1 or Bnip3l had no effect on Mfn1/2 protein levels, but led to the activation of DNM1L and the promotion of mitochondrial fission during differentiation (Lampert et al., 2019). In proximal tubule-specific Fundc1-knockout mice, Drp1 is overactivated and leads to mitochondrial division (Wang J. et al., 2020). In traumatic brain injury (TBI) models, the Drp1 inhibitor, Mdivi-1, could inhibit the activation of PTEN-induced putative kinase 1 (PINK1)-Parkin mediated mitophagy (Wu et al., 2018).

Mitochondrial Dynamics in Different Neuronal Cells After Ischemic Stroke

Mitochondrial dynamics play various roles in different cells after stroke. Because of the length of axons and special energy requirements in neurons, the distribution, movement, and timely fusion and repair of mitochondria are particularly important in maintaining normal neuronal function (Mandal and Drerup, 2019). Oxygen-glucose deprivation (OGD) can induce mitochondrial division, leading to autophagy or apoptosis (Wu et al., 2017). Astrocytic endfeet are enriched in mitochondria-ER contact sites. These sites, as well as mitochondrial fusion, can promote vascular remodeling after brain injury (Gobel et al., 2020). After several hours of OGD, the length of the astrocytic endfeet were shortened, mitochondrial fission was delayed, and the mitochondria were lost (O'Donnell et al., 2016). Increased

mitochondrial division in astrocytes during hypoxia may be a possible method of increasing mitochondrial energy production (Quintana et al., 2019). In microglia, the inflammatory response induced by OGD can be improved by inhibiting mitochondrial fission (Zhou et al., 2019b). Mitochondrial division can also promote the production of mitochondrial ROS in microglia by activating NF-κB and mitogen-activated protein kinase (MAPK), and by inducing the expression of proinflammatory mediators (Park et al., 2013). The neurovascular unit is composed of neurons, glial cells, such as astrocytes and microglia, vascular cells, such as endothelial cells and perivascular cells, and basement membrane (Iadecola, 2017). After inducing excessive mitochondrial division, endothelial cell death also increased (Rao et al., 2020). After stroke, changes in mitochondrial dynamics affect the cells of the neurovascular unit, thus destroying the BBB. Using Mdivi-1 to inhibit mitochondrial division can reduce damage to the BBB after TBI (Wu et al., 2018). Oligodendrocytes primarily wrap axons and form insulated myelin structures, which are essential in maximizing the conduction and velocity of the action potential. Unlike neurons, mitochondria are sparsely distributed in oligodendrocytes with poor fluidity, and glutamate activation can promote mitochondrial motility in oligodendrocytes (Rinholm et al., 2016). However, unlike in astrocytes, the use of mitochondrial division inhibitor 1 makes oligodendrocytes sensitive to excitotoxicity and ER stress due to their non-targeted effects, resulting in oxidative stress and apoptosis (Ruiz et al., 2020).

The Role of Mitochondrial Dynamics in Ischemic Stroke

As mentioned previously, the interaction between calcium overload, ROS production, and the MPTP leads to an increase in mitochondrial fission in ischemic stroke. Although increased mitochondrial fission during hypoxia may increase mitochondrial energy production, which is beneficial in the maintenance of neural function after stroke (Quintana et al., 2019), inducing mitochondrial fission is detrimental to neurons (Zhang C. et al., 2020). However, inhibiting Drp1 to restore the balance of mitochondrial fission and fusion could reduce Bax oligomerization and the release of apoptotic factors after ischemic stroke, thereby reducing the volume of cerebral infarction (Zhao et al., 2014). Exercise preconditioning could promote mitochondrial fusion after cerebral ischemia by up-regulating OPA1, thus reducing cerebral edema and improving neurologic function in ischemic stroke (Zhang L. et al., 2014). Mitochondrial fission can clear damaged mitochondria through autophagy, but excessive mitochondrial division affects the normal function of mitochondria so that the production of ATP is reduced (Wai and Langer, 2016; Sprenger and Langer,

TABLE 2 | Drugs targeting mitochondrial dynamics after ischemic stroke.

Target	Treatment	Mechanism	Effect	References
Inhibit mitochondrial fission	Atractylenolide III	Reduce Drp1 phosphorylation and translocation by inhibiting the JAK2/STAT3 pathway	Attenuate cerebral edema and neurological deficits	Zhou et al., 2019a
	AG490			
	miR-7 mimics	Repress α-synuclein, a protein that induces mitochondrial fragmentation	Reduce the post-ischemic lesion volume, accelerate motor function recovery, and ameliorate motor and cognitive deficits in mice	Kim et al., 2018
	Nitric Oxide Synthase 3 (NOS3) inhibition	Regulate Miro-2 levels and prevent mitochondrial division,	Promote axonal functional recovery	Bastian et al., 2018
	peptide P110	Inhibit the interaction between Drp1 and Fis1	Increase neuronal cell viability by reducing apoptosis and autophagic cell death	Qi et al., 2013
	photobiomodulation therapy	Inhibit hypoxic-ischemic-induced mitochondrial fragmentation	Reduce neuronal apoptosis in neonatal hypoxic-ischemic encephalopathy	Tucker et al., 2018
Promote mitochondrial fusion	Melatonin	Upregulate Opa1 expression by activating the Yap-Hippo pathway	Reduce infarct size and cerebral reperfusion stress, inhibit neuronal death	Wei et al., 2019
Restore the balance of mitochondrial dynamics	B355252	Restore Mfn2, p-Drp1, and Fis1 levels	Decrease the mitochondrial membrane potential and ROS, reduce the autophagy induction	Chimeh et al., 2018
	deletion of Nurr1	Inhibit Fis1/Drp1 expression, reverse the levels of Mfn2 and Opa1	Reduce neuronal death	Zhang and Yu, 2018
	subcutaneous injection of G-CSF	Reduce levels of Beclin-1, Bax, Bak, and Drp1, upregulate Opa1	Reduce apoptosis, and protect neurons in cerebral ischemia	Modi et al., 2020
Others	Mitochondrial transplantation	Transfer of exogenous mitochondria through local or systemic intra-arterial injections	Reduce brain damage, cell death, and motor function in MCAO rats	Huang et al., 2016; Chang et al., 2019

B355252: 4-chloro-N-(naphthalen-1-ylmethyl)-5-(3-(piperazin-1-yl) phenoxy) thiophene-2-sulfon-amiden.
NOS, Nitric oxide synthase; G-CSF, granulocyte-colony stimulating factor.

2019). Dysfunction of mitochondrial dynamics can lead to obstacles in mitochondrial distribution and transport in neurons, which can lead to insufficient local energy in neurons (Sheng, 2014). Excessive mitochondrial fission also affects intracellular calcium homeostasis and exacerbates excitotoxicity (Wang et al., 2015). However, mitochondrial fusion can repair damaged mitochondria (Cohen and Tareste, 2018) and produce additional energy by upregulating the activity of ATP synthase through the remodeling of mitochondrial cristae (Gomes et al., 2011). Therefore, inhibiting excessive mitochondrial fission, properly promoting mitochondrial fusion, and restoring the balance of mitochondrial dynamics are beneficial in recovery after ischemic stroke.

TREATMENTS TARGETING MITOCHONDRIAL DYNAMICS AFTER ISCHEMIC STROKE

The clinical treatment of ischemic stroke primarily includes acute stage treatment and subacute stage treatment. The acute stage occurs within 4.5 h. If patients meet admission criteria and have no thrombolytic contraindications, thrombolytic therapy is recommended (Powers et al., 2018). Currently, great progress has been made in endovascular treatment, such as mechanical thrombectomy, which has played a great role in the treatment of stroke (Prabhakaran et al., 2015). However, these treatments still have limitations, such as a strict time window for thrombolytic therapy, and there is a certain risk of complications, such as hemorrhagic transformation (Yaghi et al., 2017). Therefore, it is necessary to find new therapeutic targets and to develop corresponding drugs. The mitochondrial dynamics are closely associated with energy metabolism after stroke and pathophysiological mechanisms, such as ROS, apoptosis, and autophagy. Therefore, the molecular mechanisms associated with mitochondrial dynamics may represent new directions in ischemic stroke treatment. However, the excessive mitochondrial division plays an essential role in ischemic stroke. Therefore, an emphasis should be placed on inhibiting excessive mitochondrial fission and restoring the balance of mitochondrial dynamics when using mitochondrial dynamics as a focal point in the treatment of ischemic stroke (**Table 2**).

Atractylenolide III and AG490 (an inhibitor of jak2) therapy in middle cerebral artery occlusion (MCAO) mice could reduce Drp1 phosphorylation and translocation, as well as and mitochondrial division though the JAK2/STAT3 pathway, thereby attenuating cerebral edema and neurological deficits (Zhou et al., 2019a). Melatonin upregulates Opa1 expression by activating the Yap–Hippo pathway, thereby promoting mitochondrial fusion, reducing infarct size, inhibiting neuronal death, and reducing cerebral reperfusion stress (Wei et al., 2019). Opa1, Mfn2, p-Drp1, and FIS1 were decreased to varying degrees in the mouse model of $CoCl_2$-induced cerebral hypoxia. However, 4-chloro-*N*-(naphthalen-1-ylmethyl)-5-(3-(piperazin-1-yl) phenoxy) thiophene-2-sulfonamide (B355252) treatment could restore Mfn2, p-Drp1, and Fis1 levels, maintain mitochondrial stability, restore mitochondrial membrane potential, and reduce ROS (Chimeh et al., 2018). Injection of miR-7 mimic oligonucleotide after cerebral ischemia could repress α-synuclein, a protein that induces mitochondrial fragmentation, oxidative stress, autophagy, and the promotion of neuronal cell death, thus reducing brain injury after stroke (Kim et al., 2018). Nitric oxide synthase 3 (NOS3) inhibition regulates Miro-2 levels, prevents mitochondrial division, and promotes axonal functional recovery by protecting mitochondrial structure and movement (Bastian et al., 2018). Fis1 and Drp1 are increased, and both Mfn2 and Opa1 are downregulated after cerebral ischemia-reperfusion, indicating that cerebral ischemia-reperfusion induces excessive mitochondrial division and prevents mitochondrial fusion. However, deletion of Nurr1 could inhibit Fis1/Drp1 expression, reverse the levels of Mfn2 and Opa1, correct the imbalance in mitochondrial division and fusion, and reduce neuronal death (Zhang and Yu, 2018). In a mouse model of bilateral common carotid artery occlusion, subcutaneous injection of granulocyte-colony stimulating factor (G-CSF) was used as treatment. G-CSF reportedly reduced the levels of the autophagy marker, Beclin-1, and the proapoptotic proteins, Bax, Bak, and Drp1, but upregulated the mitochondrial fusion protein, Opa1. Therefore, G-CSF can maintain cellular homeostasis by maintaining the stability of mitochondrial dynamics, reducing apoptosis, and protecting neurons in cerebral ischemia (Modi et al., 2020).

However, mitochondrial fission is necessary for maintaining normal cellular function, and it is unrealistic to inhibit mitochondrial fission completely. Some studies have focused on the role of the interaction between Drp1 and its recruitment molecules, such as Mff (Kornfeld et al., 2018) and Fis1 (Qi et al., 2013), in physiological and pathological mitochondrial fission. One study showed that peptide P259-mediated inhibition of the Drp1-Mff interaction could influence normal mitochondrial morphology and basic function under physiological conditions (Kornfeld et al., 2018). The peptide P110 could inhibit the interaction between Drp1 and Fis1, thus reducing excessive mitochondrial fission under pathological conditions without affecting physiological fission (Qi et al., 2013). Moreover, some biomarkers, such as flavin adenine dinucleotide fluorescence (Berndt et al., 2020), can be used as early markers of mitochondrial damage during brain hypoxia, which helps in studying the optimal time to administer drugs targeting mitochondria. There are also some new therapies, such as photobiomodulation therapy, which can inhibit hypoxic-ischemia-induced mitochondrial fragmentation, alleviate mitochondrial dysfunction and oxidative stress, and ultimately reduce neuronal apoptosis in neonatal hypoxic-ischemic encephalopathy (Tucker et al., 2018). Mitochondrial transplantation is also on the rise, and the transfer of exogenous mitochondria through local or systemic intra-arterial injections reduces brain damage, cell death, and motor function in MCAO rats (Huang et al., 2016; Chang et al., 2019).

CONCLUSION AND PERSPECTIVE

Energy metabolism after ischemic stroke is closely associated with mitochondrial dynamics. Targeting mitochondrial

dynamics-related molecular mechanisms and associated processes, such as calcium overload, ROS, MPTP, apoptosis, and mitophagy, can alleviate brain injury after stroke by improving mitochondrial function and its effect on energy metabolism. This review shows that mitochondrial dynamics play essential roles in pathophysiological changes after stroke. However, the related studies of mitochondrial dynamics mainly focus on cardiac ischemia-reperfusion and neurodegenerative diseases. Mitochondrial dynamics should also be studied intensively in ischemic stroke to understand the specific regulatory mechanisms of mitochondrial dynamics on the clinical manifestations and prognosis of stroke. The clinical application and long-term prognosis of stroke patients are also worthy of further study. In addition, most drug-related effects have only been examined in laboratory studies. There have been few studies on clinical applications. Whether mitochondrial dynamics-targeted drugs could improve a stroke patient's condition and prognosis in the clinic is a challenge to be explored in subsequent drug studies.

AUTHOR CONTRIBUTIONS

XZ and YH conceived the main outline. XZ wrote the manuscript. LW and HC made the figures. CL, LL, and YO took charge for the manuscript revision in English. YH participated in the correction and finally reviewed of this manuscript. All authors contributed to the article and approved the submitted version.

ACKNOWLEDGMENTS

We would like to acknowledge the help of all the staff involved in contributing to the manuscript writing, editing, and literature review.

REFERENCES

Abrisch, R. G., Gumbin, S. C., Wisniewski, B. T., Lackner, L. L., and Voeltz, G. K. (2020). Fission and fusion machineries converge at ER contact sites to regulate mitochondrial morphology. *J. Cell Biol.* 219:e201911122. doi: 10.1083/jcb.201911122

Ader, N. R., Hoffmann, P. C., Ganeva, I., Borgeaud, A. C., Wang, C., Youle, R. J., et al. (2019). Molecular and topological reorganizations in mitochondrial architecture interplay during Bax-mediated steps of apoptosis. *eLife* 8:e40712. doi: 10.7554/eLife.40712

Al-Mufti, F., Amuluru, K., Roth, W., Nuoman, R., El-Ghanem, M., and Meyers, P. M. (2018). Cerebral ischemic reperfusion injury following recanalization of large vessel occlusions. *Neurosurgery* 82, 781–789. doi: 10.1093/neuros/nyx341

Altschuld, R. A., Hohl, C. M., Castillo, L. C., Garleb, A. A., Starling, R. C., and Brierley, G. P. (1992). Cyclosporin inhibits mitochondrial calcium efflux in isolated adult rat ventricular cardiomyocytes. *Am. J. Physiol.* 262, H1699–H1704. doi: 10.1152/ajpheart.1992.262.6.H1699

An, H., Ford, A. L., Chen, Y., Zhu, H., Ponisio, R., Kumar, G., et al. (2015). Defining the ischemic penumbra using magnetic resonance oxygen metabolic index. *Stroke* 46, 982–988. doi: 10.1161/Str.0000000000000063

Andrabi, S. A., Sayeed, I., Siemen, D., Wolf, G., and Horn, T. F. (2004). Direct inhibition of the mitochondrial permeability transition pore: a possible mechanism responsible for anti-apoptotic effects of melatonin. *FASEB J.* 18, 869–871. doi: 10.1096/fj.03-1031fje

Astrup, J., Siesjo, B. K., and Symon, L. (1981). Thresholds in cerebral ischemia – the ischemic penumbra. *Stroke* 12, 723–725. doi: 10.1161/01.str.12.6.723

Attwell, D., and Laughlin, S. B. (2001). An energy budget for signaling in the grey matter of the brain. *J. Cereb. Blood Flow Metab.* 21, 1133–1145. doi: 10.1097/00004647-200110000-00001

Barsukova, A., Komarov, A., Hajnoczky, G., Bernardi, P., Bourdette, D., and Forte, M. (2011). Activation of the mitochondrial permeability transition pore modulates Ca2+ responses to physiological stimuli in adult neurons. *Eur. J. Neurosci.* 33, 831–842. doi: 10.1111/j.1460-9568.2010.07576.x

Bastian, C., Zaleski, J., Stahon, K., Parr, B., McCray, A., Day, J., et al. (2018). NOS3 inhibition confers post-ischemic protection to young and aging white matter integrity by conserving mitochondrial dynamics and Miro-2 levels. *J. Neurosci.* 38, 6247–6266. doi: 10.1523/JNEUROSCI.3017-17.2018

Bayir, H., and Kagan, V. E. (2008). Bench-to-bedside review: mitochondrial injury, oxidative stress and apoptosis–there is nothing more practical than a good theory. *Crit. Care* 12:206. doi: 10.1186/cc6779

Belanger, M., Allaman, I., and Magistretti, P. J. (2011). Brain energy metabolism: focus on astrocyte-neuron metabolic cooperation. *Cell Metab.* 14, 724–738. doi: 10.1016/j.cmet.2011.08.016

Bernardi, P. (1999). Mitochondrial transport of cations: channels, exchangers, and permeability transition. *Physiol. Rev.* 79, 1127–1155. doi: 10.1152/physrev.1999.79.4.1127

Berndt, N., Kovacs, R., Rosner, J., Wallach, I., Dreier, J. P., and Liotta, A. (2020). Flavin adenine dinucleotide fluorescence as an early marker of mitochondrial impairment during brain hypoxia. *Int. J. Mol. Sci.* 21:3977. doi: 10.3390/ijms21113977

Besancon, E., Guo, S., Lok, J., Tymianski, M., and Lo, E. H. (2008). Beyond NMDA and AMPA glutamate receptors: emerging mechanisms for ionic imbalance and cell death in stroke. *Trends Pharmacol. Sci.* 29, 268–275. doi: 10.1016/j.tips.2008.02.003

Bolanos, J. P. (2016). Bioenergetics and redox adaptations of astrocytes to neuronal activity. *J. Neurochem.* 139(Suppl. 2), 115–125. doi: 10.1111/jnc.13486

Bordone, M. P., Salman, M. M., Titus, H. E., Amini, E., Andersen, J. V., Chakraborti, B., et al. (2019). The energetic brain – a review from students to students. *J. Neurochem.* 151, 139–165. doi: 10.1111/jnc.14829

Bristow, M. S., Simon, J. E., Brown, R. A., Eliasziw, M., Hill, M. D., Coutts, S. B., et al. (2005). MR perfusion and diffusion in acute ischemic stroke: human gray and white matter have different thresholds for infarction. *J. Cereb. Blood Flow Metab.* 25, 1280–1287. doi: 10.1038/sj.jcbfm.9600135

Bruick, R. K. (2000). Expression of the gene encoding the proapoptotic Nip3 protein is induced by hypoxia. *Proc. Natl. Acad. Sci. U.S.A.* 97, 9082–9087. doi: 10.1073/pnas.97.16.9082

Bueler, H. (2010). Mitochondrial dynamics, cell death and the pathogenesis of Parkinson's disease. *Apoptosis* 15, 1336–1353. doi: 10.1007/s10495-010-0465-0

Campbell, B. C. V., De Silva, D. A., Macleod, M. R., Coutts, S. B., Schwamm, L. H., Davis, S. M., et al. (2019). Ischaemic stroke. *Nat. Rev. Dis. Prim.* 5:70. doi: 10.1038/s41572-019-0118-8

Cardoso, A. R., Queliconi, B. B., and Kowaltowski, A. J. (2010). Mitochondrial ion transport pathways: role in metabolic diseases. *Biochim. Biophys. Acta* 1797, 832–838. doi: 10.1016/j.bbabio.2009.12.017

Chan, D. C. (2020). Mitochondrial dynamics and its involvement in disease. *Annu. Rev. Pathol.* 15, 235–259. doi: 10.1146/annurev-pathmechdis-012419-032711

Chang, C. Y., Liang, M. Z., and Chen, L. (2019). Current progress of mitochondrial transplantation that promotes neuronal regeneration. *Transl. Neurodegener.* 8:17. doi: 10.1186/s40035-019-0158-8

Chen, Y., Liu, Y., and Dorn, G. W. II (2011). Mitochondrial fusion is essential for organelle function and cardiac homeostasis. *Circ. Res.* 109, 1327–1331. doi: 10.1161/CIRCRESAHA.111.258723

Cheng, J., Korte, N., Nortley, R., Sethi, H., Tang, Y., and Attwell, D. (2018). Targeting pericytes for therapeutic approaches to neurological disorders. *Acta Neuropathol.* 136, 507–523. doi: 10.1007/s00401-018-1893-0

Chimeh, U., Zimmerman, M. A., Gilyazova, N., and Li, P. A. (2018). B355252, a novel small molecule, confers neuroprotection against cobalt chloride toxicity

in mouse hippocampal cells through altering mitochondrial dynamics and limiting autophagy induction. *Int. J. Med. Sci.* 15, 1384–1396. doi: 10.7150/ijms.24702

Chiurazzi, M., Di Maro, M., Cozzolino, M., and Colantuoni, A. (2020). Mitochondrial dynamics and microglia as new targets in metabolism regulation. *Int. J. Mol. Sci.* 21:3450. doi: 10.3390/ijms21103450

Cho, M. H., Kim, D. H., Choi, J. E., Chang, E. J., and Seung, Y. (2012). Increased phosphorylation of dynamin-related protein 1 and mitochondrial fission in okadaic acid-treated neurons. *Brain Res.* 1454, 100–110. doi: 10.1016/j.brainres.2012.03.010

Cid-Castro, C., Hernandez-Espinosa, D. R., and Moran, J. (2018). ROS as regulators of mitochondrial dynamics in neurons. *Cell. Mol. Neurobiol.* 38, 995–1007. doi: 10.1007/s10571-018-0584-7

Cohen, M. M., and Tareste, D. (2018). Recent insights into the structure and function of Mitofusins in mitochondrial fusion. *F1000Research* 7:1983. doi: 10.12688/f1000research.16629.1

Costa, V., Giacomello, M., Hudec, R., Lopreiato, R., Ermak, G., Lim, D., et al. (2010). Mitochondrial fission and cristae disruption increase the response of cell models of Huntington's disease to apoptotic stimuli. *EMBO Mol. Med.* 2, 490–503. doi: 10.1002/emmm.201000102

Crack, P. J., and Taylor, J. M. (2005). Reactive oxygen species and the modulation of stroke. *Free Radic. Biol. Med.* 38, 1433–1444. doi: 10.1016/j.freeradbiomed.2005.01.019

da Rosa, M. S., da Rosa-Junior, N. T., Parmeggiani, B., Glanzel, N. M., de MouraAlvorcem, L., Ribeiro, R. T., et al. (2020). 3-Hydroxy-3-methylglutaric acid impairs redox and energy homeostasis, mitochondrial dynamics, and endoplasmic reticulum-mitochondria crosstalk in rat brain. *Neurotox. Res.* 37, 314–325. doi: 10.1007/s12640-019-00122-x

Dorn, G. W. II, and Kitsis, R. N. (2015). The mitochondrial dynamism-mitophagy-cell death interactome: multiple roles performed by members of a mitochondrial molecular ensemble. *Circ. Res.* 116, 167–182. doi: 10.1161/circresaha.116.303554

Doyle, K. P., Simon, R. P., and Stenzel-Poore, M. P. (2008). Mechanisms of ischemic brain damage. *Neuropharmacology* 55, 310–318. doi: 10.1016/j.neuropharm.2008.01.005

Droge, W. (2002). Free radicals in the physiological control of cell function. *Physiol. Rev.* 82, 47–95. doi: 10.1152/physrev.00018.2001

Ducommun, S., Deak, M., Sumpton, D., Ford, R. J., Galindo, A. N., Kussmann, M., et al. (2015). Motif affinity and mass spectrometry proteomic approach for the discovery of cellular AMPK targets: identification of mitochondrial fission factor as a new AMPK substrate. *Cell Signal* 27, 978–988. doi: 10.1016/j.cellsig.2015.02.008

Elmore, S. (2007). Apoptosis: a review of programmed cell death. *Toxicol. Pathol.* 35, 495–516. doi: 10.1080/01926230701320337

Falkowska, A., Gutowska, I., Goschorska, M., Nowacki, P., Chlubek, D., and Baranowska-Bosiacka, I. (2015). Energy metabolism of the brain, including the cooperation between astrocytes and neurons, especially in the context of glycogen metabolism. *Int. J. Mol. Sci.* 16, 25959–25981. doi: 10.3390/ijms161125939

Frank, S., Gaume, B., Bergmann-Leitner, E. S., Leitner, W. W., Robert, E. G., Catez, F., et al. (2001). The role of dynamin-related protein 1, a mediator of mitochondrial fission, in apoptosis. *Dev. Cell* 1, 515–525. doi: 10.1016/s1534-5807(01)00055-7

Fricker, M., Tolkovsky, A. M., Borutaite, V., Coleman, M., and Brown, G. C. (2018). Neuronal cell death. *Physiol. Rev.* 98, 813–880. doi: 10.1152/physrev.00011.2017

Friedman, J. R., Lackner, L. L., West, M., DiBenedetto, J. R., Nunnari, J., and Voeltz, G. K. (2011). ER tubules mark sites of mitochondrial division. *Science* 334, 358–362. doi: 10.1126/science.1207385

Fu, M., St-Pierre, P., Shankar, J., Wang, P. T., Joshi, B., and Nabi, I. R. (2013). Regulation of mitophagy by the Gp78 E3 ubiquitin ligase. *Mol. Biol. Cell* 24, 1153–1162. doi: 10.1091/mbc.E12-08-0607

GBD 2016 Stroke Collaborators (2019). Global, regional, and national burden of stroke, 1990-2016: a systematic analysis for the Global Burden of Disease Study 2016. *Lancet Neurol.* 18, 439–458. doi: 10.1016/S1474-4422(19)30034-1

Gegg, M. E., Cooper, J. M., Chau, K. Y., Rojo, M., Schapira, A. H., and Taanman, J. W. (2010). Mitofusin 1 and mitofusin 2 are ubiquitinated in a PINK1/parkin-dependent manner upon induction of mitophagy. *Hum. Mol. Genet.* 19, 4861–4870. doi: 10.1093/hmg/ddq419

Gobel, J., Engelhardt, E., Pelzer, P., Sakthivelu, V., Jahn, H. M., Jevtic, M., et al. (2020). Mitochondria-endoplasmic reticulum contacts in reactive astrocytes promote vascular remodeling. *Cell Metab.* 31, 791–808.e8. doi: 10.1016/j.cmet.2020.03.005

Gomes, L. C., Di Benedetto, G., and Scorrano, L. (2011). During autophagy mitochondria elongate, are spared from degradation and sustain cell viability. *Nat. Cell Biol.* 13, 589–598. doi: 10.1038/ncb2220

Green, D. R., and Reed, J. C. (1998). Mitochondria and apoptosis. *Science* 281, 1309–1312. doi: 10.1126/science.281.5381.1309

Grohm, J., Kim, S. W., Mamrak, U., Tobaben, S., Cassidy-Stone, A., Nunnari, J., et al. (2012). Inhibition of Drp1 provides neuroprotection in vitro and in vivo. *Cell Death Differ.* 19, 1446–1458. doi: 10.1038/cdd.2012.18

Guan, R. Q., Zou, W., Dai, X. H., Yu, X. P., Liu, H., Chen, Q. X., et al. (2018). Mitophagy, a potential therapeutic target for stroke. *J. Biomed. Sci.* 25:87. doi: 10.1186/s12929-018-0487-4

Guo, Y., Li, D., Zhang, S., Yang, Y., Liu, J. J., Wang, X., et al. (2018). Visualizing intracellular organelle and cytoskeletal interactions at nanoscale resolution on millisecond timescales. *Cell* 175, 1430–1442.e17. doi: 10.1016/j.cell.2018.09.057

Gustafsson, A. B., and Dorn, G. W. (2019). Evolving and expanding the roles of mitophagy as a homeostatic and pathogenic process. *Physiol. Rev.* 99, 853–892. doi: 10.1152/physrev.00005.2018

Halestrap, A. P., Woodfield, K. Y., and Connern, C. P. (1997). Oxidative stress, thiol reagents, and membrane potential modulate the mitochondrial permeability transition by affecting nucleotide binding to the adenine nucleotide translocase. *J. Biol. Chem.* 272, 3346–3354. doi: 10.1074/jbc.272.6.3346

Harris, J. J., Jolivet, R., and Attwell, D. (2012). Synaptic energy use and supply. *Neuron* 75, 762–777. doi: 10.1016/j.neuron.2012.08.019

Herrero-Mendez, A., Almeida, A., Fernandez, E., Maestre, C., Moncada, S., and Bolanos, J. P. (2009). The bioenergetic and antioxidant status of neurons is controlled by continuous degradation of a key glycolytic enzyme by APC/C-Cdh1. *Nat. Cell Biol.* 11, 747–752. doi: 10.1038/ncb1881

Hofmeijer, J., and van Putten, M. J. (2012). Ischemic cerebral damage: an appraisal of synaptic failure. *Stroke* 43, 607–615. doi: 10.1161/STROKEAHA.111.632943

Hoppins, S. (2014). The regulation of mitochondrial dynamics. *Curr. Opin. Cell Biol.* 29, 46–52. doi: 10.1016/j.ceb.2014.03.005

Huang, P. J., Kuo, C. C., Lee, H. C., Shen, C. I., Cheng, F. C., Wu, S. F., et al. (2016). Transferring xenogenic mitochondria provides neural protection against ischemic stress in ischemic rat brains. *Cell Transplant.* 25, 913–927. doi: 10.3727/096368915X689785

Hurst, S., Hoek, J., and Sheu, S. S. (2017). Mitochondrial Ca(2+) and regulation of the permeability transition pore. *J. Bioenerget. Biomembr.* 49, 27–47. doi: 10.1007/s10863-016-9672-x

Hwang, J. A., Shin, N., Shin, H. J., Yin, Y., Kwon, H. H., Park, H., et al. (2020). Protective effects of ShcA protein silencing for photothrombotic cerebral infarction. *Transl. Stroke Res.* doi: 10.1007/s12975-020-00874-1

Iadecola, C. (2017). The neurovascular unit coming of age: a journey through neurovascular coupling in health and disease. *Neuron* 96, 17–42. doi: 10.1016/j.neuron.2017.07.030

Jeong, S. Y., and Seol, D. W. (2008). The role of mitochondria in apoptosis. *BMB Rep.* 41, 11–22. doi: 10.5483/bmbrep.2008.41.1.011

Jurgensmeier, J. M., Xie, Z., Deveraux, Q., Ellerby, L., Bredesen, D., and Reed, J. C. (1998). Bax directly induces release of cytochrome c from isolated mitochondria. *Proc. Natl. Acad. Sci. U.S.A.* 95, 4997–5002. doi: 10.1073/pnas.95.9.4997

Kim, T., Mehta, S. L., Morris-Blanco, K. C., Chokkalla, A. K., Chelluboina, B., Lopez, M., et al. (2018). The microRNA miR-7a-5p ameliorates ischemic brain damage by repressing alpha-synuclein. *Sci. Signal.* 11:eaat4285. doi: 10.1126/scisignal.aat4285

Kinnally, K. W., Peixoto, P. M., Ryu, S. Y., and Dejean, L. M. (2011). Is mPTP the gatekeeper for necrosis, apoptosis, or both? *BBA Mol. Cell Res.* 1813, 616–622. doi: 10.1016/j.bbamcr.2010.09.013

Kornfeld, O. S., Qvit, N., Haileselassie, B., Shamloo, M., Bernardi, P., and Mochly-Rosen, D. (2018). Interaction of mitochondrial fission factor with dynamin

related protein 1 governs physiological mitochondrial function in vivo. *Sci. Rep.* 8:14034. doi: 10.1038/s41598-018-32228-1

Koshiba, T., Detmer, S. A., Kaiser, J. T., Chen, H., McCaffery, J. M., and Chan, D. C. (2004). Structural basis of mitochondrial tethering by mitofusin complexes. *Science* 305, 858–862. doi: 10.1126/science.1099793

Kwong, J. Q., Lu, X., Correll, R. N., Schwanekamp, J. A., Vagnozzi, R. J., Sargent, M. A., et al. (2015). The mitochondrial calcium uniporter selectively matches metabolic output to acute contractile stress in the heart. *Cell Rep.* 12, 15–22. doi: 10.1016/j.celrep.2015.06.002

Lampert, M. A., Orogo, A. M., Najor, R. H., Hammerling, B. C., Leon, L. J., Wang, B. J., et al. (2019). BNIP3L/NIX and FUNDC1-mediated mitophagy is required for mitochondrial network remodeling during cardiac progenitor cell differentiation. *Autophagy* 15, 1182–1198. doi: 10.1080/15548627.2019.1580095

Leigh, R., Knutsson, L., Zhou, J., and van Zijl, P. C. (2018). Imaging the physiological evolution of the ischemic penumbra in acute ischemic stroke. *J. Cereb. Blood Flow Metab.* 38, 1500–1516. doi: 10.1177/0271678X17700913

Lewis, S. C., Uchiyama, L. F., and Nunnari, J. (2016). ER-mitochondria contacts couple mtDNA synthesis with mitochondrial division in human cells. *Science* 353:aaf5549. doi: 10.1126/science.aaf5549

Lindsay, M. P., Norrving, B., Sacco, R. L., Brainin, M., Hacke, W., Martins, S., et al. (2019). World stroke organization (WSO): global stroke fact sheet 2019. *Int. J. Stroke* 14, 806–817. doi: 10.1177/1747493019881353

Lunt, S. Y., and Vander Heiden, M. G. (2011). Aerobic glycolysis: meeting the metabolic requirements of cell proliferation. *Annu. Rev. Cell Dev. Biol.* 27, 441–464. doi: 10.1146/annurev-cellbio-092910-154237

Magistretti, P. J., and Allaman, I. (2018). Lactate in the brain: from metabolic end-product to signalling molecule. *Nat. Rev. Neurosci.* 19, 235–249. doi: 10.1038/nrn.2018.19

Mandal, A., and Drerup, C. M. (2019). Axonal transport and mitochondrial function in neurons. *Front. Cell. Neurosci.* 13:373. doi: 10.3389/fncel.2019.00373

Matsumoto, S., Friberg, H., Ferrand-Drake, M., and Wieloch, T. (1999). Blockade of the mitochondrial permeability transition pore diminishes infarct size in the rat after transient middle cerebral artery occlusion. *J. Cereb. Blood Flow Metab.* 19, 736–741. doi: 10.1097/00004647-199907000-00002

Mergenthaler, P., Lindauer, U., Dienel, G. A., and Meisel, A. (2013). Sugar for the brain: the role of glucose in physiological and pathological brain function. *Trends Neurosci.* 36, 587–597. doi: 10.1016/j.tins.2013.07.001

Modi, J., Menzie-Suderam, J., Xu, H., Trujillo, P., Medley, K., Marshall, M. L., et al. (2020). Mode of action of granulocyte-colony stimulating factor (G-CSF) as a novel therapy for stroke in a mouse model. *J. Biomed. Sci.* 27:19. doi: 10.1186/s12929-019-0597-7

Montessuit, S., Somasekharan, S. P., Terrones, O., Lucken-Ardjomande, S., Herzig, S., Schwarzenbacher, R., et al. (2010). Membrane remodeling induced by the dynamin-related protein Drp1 stimulates Bax oligomerization. *Cell* 142, 889–901. doi: 10.1016/j.cell.2010.08.017

Moskowitz, M. A., Lo, E. H., and Iadecola, C. (2010). The science of stroke: mechanisms in search of treatments. *Neuron* 67, 181–198. doi: 10.1016/j.neuron.2010.07.002

Neuspiel, M., Zunino, R., Gangaraju, S., Rippstein, P., and McBride, H. (2005). Activated mitofusin 2 signals mitochondrial fusion, interferes with Bax activation, and reduces susceptibility to radical induced depolarization. *J. Biol. Chem.* 280, 25060–25070. doi: 10.1074/jbc.M501599200

Nguyen, D., Alavi, M. V., Kim, K. Y., Kang, T., Scott, R. T., Noh, Y. H., et al. (2011). A new vicious cycle involving glutamate excitotoxicity, oxidative stress and mitochondrial dynamics. *Cell Death Dis.* 2:e240. doi: 10.1038/cddis.2011.117

Ni, X. X., Nie, J., Xie, Q. Y., Yu, R. H., Su, L., and Liu, Z. F. (2020). Protective effects of hyperbaric oxygen therapy on brain injury by regulating the phosphorylation of Drp1 through ROS/PKC pathway in heatstroke rats. *Cell. Mol. Neurobiol.* 40, 1253–1269. doi: 10.1007/s10571-020-00811-8

Norbury, C. J., and Hickson, I. D. (2001). Cellular responses to DNA damage. *Annu. Rev. Pharmacol. Toxicol.* 41, 367–401. doi: 10.1146/annurev.pharmtox.41.1.367

Nortley, R., and Attwell, D. (2017). Control of brain energy supply by astrocytes. *Curr. Opin. Neurobiol.* 47, 80–85. doi: 10.1016/j.conb.2017.09.012

Nunnari, J. (2007). The machines that divide and fuse mitochondria. *FASEB J.* 21:A96. doi: 10.1146/annurev.biochem.76.071905.090048

O'Donnell, J. C., Jackson, J. G., and Robinson, M. B. (2016). Transient oxygen/glucose deprivation causes a delayed loss of mitochondria and increases spontaneous calcium signaling in astrocytic processes. *J. Neurosci.* 36, 7109–7127. doi: 10.1523/Jneurosci.4518-15.2016

Ong, S. B., Subrayan, S., Lim, S. Y., Yellon, D. M., Davidson, S. M., and Hausenloy, D. J. (2010). Inhibiting mitochondrial fission protects the heart against ischemia/reperfusion injury. *Circulation* 121, 2012–2022. doi: 10.1161/CIRCULATIONAHA.109.906610

Pagliuso, A., Cossart, P., and Stavru, F. (2018). The ever-growing complexity of the mitochondrial fission machinery. *Cell. Mol. Life Sci.* 75, 355–374. doi: 10.1007/s00018-017-2603-0

Papanicolaou, K. N., Khairallah, R. J., Ngoh, G. A., Chikando, A., Luptak, I., O'Shea, K. M., et al. (2011). Mitofusin-2 maintains mitochondrial structure and contributes to stress-induced permeability transition in cardiac myocytes. *Mol. Cell. Biol.* 31, 1309–1328. doi: 10.1128/MCB.00911-10

Park, J., Choi, H., Min, J. S., Park, S. J., Kim, J. H., Park, H. J., et al. (2013). Mitochondrial dynamics modulate the expression of pro-inflammatory mediators in microglial cells. *J. Neurochem.* 127, 221–232. doi: 10.1111/jnc.12361

Pivovarova, N. B., Nguyen, H. V., Winters, C. A., Brantner, C. A., Smith, C. L., and Andrews, S. B. (2004). Excitotoxic calcium overload in a subpopulation of mitochondria triggers delayed death in hippocampal neurons. *J. Neurosci.* 24, 5611–5622. doi: 10.1523/JNEUROSCI.0531-04.2004

Powers, W. J., Rabinstein, A. A., Ackerson, T., Adeoye, O. M., Bambakidis, N. C., Becker, K., et al. (2018). 2018 Guidelines for the early management of patients with acute ischemic stroke: a guideline for healthcare professionals from the American heart association/American stroke association. *Stroke* 49, e46–e110. doi: 10.1161/STR.0000000000000158

Prabhakaran, S., Ruff, I., and Bernstein, R. A. (2015). Acute stroke intervention: a systematic review. *JAMA* 313, 1451–1462. doi: 10.1001/jama.2015.3058

Pushie, M. J., Crawford, A. M., Sylvain, N. J., Hou, H., Hackett, M. J., George, G. N., et al. (2018). Revealing the penumbra through imaging elemental markers of cellular metabolism in an ischemic stroke model. *ACS Chem. Neurosci.* 9, 886–893. doi: 10.1021/acschemneuro.7b00382

Qi, X., Qvit, N., Su, Y. C., and Mochly-Rosen, D. (2013). A novel Drp1 inhibitor diminishes aberrant mitochondrial fission and neurotoxicity. *J. Cell Sci.* 126, 789–802. doi: 10.1242/jcs.114439

Qin, Y., Li, A., Liu, B., Jiang, W., Gao, M., Tian, X., et al. (2020). Mitochondrial fusion mediated by fusion promotion and fission inhibition directs adult mouse heart function toward a different direction. *FASEB J.* 34, 663–675. doi: 10.1096/fj.201901671R

Quintana, D. D., Garcia, J. A., Sarkar, S. N., Jun, S. J., Engler-Chiurazzi, E. B., Russell, A. E., et al. (2019). Hypoxia-reoxygenation of primary astrocytes results in a redistribution of mitochondrial size and mitophagy. *Mitochondrion* 47, 244–255. doi: 10.1016/j.mito.2018.12.004

Radak, D., Katsiki, N., Resanovic, I., Jovanovic, A., Sudar-Milovanovic, E., Zafirovic, S., et al. (2017). Apoptosis and acute brain ischemia in ischemic stroke. *Curr. Vasc. Pharmacol.* 15, 115–122. doi: 10.2174/1570161115666161104095522

Rao, G., Murphy, B., Dey, A., Dwivedi, S. K. D., Zhang, Y., Roy, R. V., et al. (2020). Cystathionine beta synthase regulates mitochondrial dynamics and function in endothelial cells. *FASEB J.* 34, 9372–9392. doi: 10.1096/fj.202000173R

Rappold, P. M., Cui, M., Grima, J. C., Fan, R. Z., de Mesy-Bentley, K. L., Chen, L., et al. (2014). Drp1 inhibition attenuates neurotoxicity and dopamine release deficits in vivo. *Nat. Commun.* 5:5244. doi: 10.1038/ncomms6244

Rigoulet, M., Bouchez, C. L., Paumard, P., Ransac, S., Cuvellier, S., Duvezin-Caubet, S., et al. (2020). Cell energy metabolism: an update. *Biochim. Biophys. Acta Bioenerget.* 1861:148276. doi: 10.1016/j.bbabio.2020.148276

Rinholm, J. E., Vervaeke, K., Tadross, M. R., Tkachuk, A. N., Kopek, B. G., Brown, T. A., et al. (2016). Movement and structure of mitochondria in oligodendrocytes and their myelin sheaths. *Glia* 64, 810–825. doi: 10.1002/glia.22965

Rodger, C. E., McWilliams, T. G., and Ganley, I. G. (2018). Mammalian mitophagy – from in vitro molecules to in vivo models. *FEBS J.* 285, 1185–1202. doi: 10.1111/febs.14336

Roy, M., Reddy, P. H., Iijima, M., and Sesaki, H. (2015). Mitochondrial division and fusion in metabolism. *Curr. Opin. Cell Biol.* 33, 111–118. doi: 10.1016/j.ceb.2015.02.001

Ruiz, A., Quintela-López, T., Sánchez-Gómez, M. V., Gaminde-Blasco, A., Alberdi, E., and Matute, C. (2020). Mitochondrial division inhibitor 1 disrupts oligodendrocyte Ca(2+)homeostasis and mitochondrial function. *Glia* 68, 1743–1756. doi: 10.1002/glia.23802

Sarrafzadeh, A. S., Nagel, A., Czabanka, M., Denecke, T., Vajkoczy, P., and Plotkin, M. (2010). Imaging of hypoxic-ischemic penumbra with F-18-fluoromisonidazole PET/CT and measurement of related cerebral metabolism in aneurysmal subarachnoid hemorrhage. *J. Cereb. Blood Flow Metab.* 30, 36–45. doi: 10.1038/jcbfm.2009.199

Scheffler, I. E. (2001). Mitochondria make a come back. *Adv. Drug Deliv. Rev.* 49, 3–26. doi: 10.1016/S0169-409x(01)00123-5

Sekerdag, E., Solaroglu, I., and Gursoy-Ozdemir, Y. (2018). Cell death mechanisms in stroke and novel molecular and cellular treatment options. *Curr. Neuropharmacol.* 16, 1396–1415. doi: 10.2174/1570159X16666180302115544

Sharp, W. W., Fang, Y. H., Han, M., Zhang, H. J., Hong, Z., Banathy, A., et al. (2014). Dynamin-related protein 1 (Drp1)-mediated diastolic dysfunction in myocardial ischemia-reperfusion injury: therapeutic benefits of Drp1 inhibition to reduce mitochondrial fission. *FASEB J.* 28, 316–326. doi: 10.1096/fj.12-226225

Sheng, Z. H. (2014). Mitochondrial trafficking and anchoring in neurons: new insight and implications. *J. Cell Biol.* 204, 1087–1098. doi: 10.1083/jcb.201312123

Sokoloff, L. (1981). Localization of functional activity in the central nervous system by measurement of glucose utilization with radioactive deoxyglucose. *J. Cereb. Blood Flow Metab.* 1, 7–36. doi: 10.1038/jcbfm.1981.4

Sokoloff, L., Reivich, M., Kennedy, C., Des Rosiers, M. H., Patlak, C. S., Pettigrew, K. D., et al. (1977). The [14C]deoxyglucose method for the measurement of local cerebral glucose utilization: theory, procedure, and normal values in the conscious and anesthetized albino rat. *J. Neurochem.* 28, 897–916. doi: 10.1111/j.1471-4159.1977.tb10649.x

Song, T., Liu, J., Tao, X., and Deng, J. G. (2014). Protection effect of atorvastatin in cerebral ischemia-reperfusion injury rats by blocking the mitochondrial permeability transition pore. *Genet. Mol. Res.* 13, 10632–10642. doi: 10.4238/2014.December.18.5

Song, Z., Chen, H., Fiket, M., Alexander, C., and Chan, D. C. (2007). OPA1 processing controls mitochondrial fusion and is regulated by mRNA splicing, membrane potential, and Yme1L. *J. Cell Biol.* 178, 749–755. doi: 10.1083/jcb.200704110

Sowter, H. M., Ratcliffe, P. J., Watson, P., Greenberg, A. H., and Harris, A. L. (2001). HIF-1-dependent regulation of hypoxic induction of the cell death factors BNIP3 and NIX in human tumors. *Cancer Res.* 61, 6669–6673.

Sprenger, H. G., and Langer, T. (2019). The good and the bad of mitochondrial breakups. *Trends Cell Biol.* 29, 888–900. doi: 10.1016/j.tcb.2019.08.003

Susin, S. A., Lorenzo, H. K., Zamzami, N., Marzo, I., Snow, B. E., Brothers, G. M., et al. (1999). Molecular characterization of mitochondrial apoptosis-inducing factor. *Nature* 397, 441–446. doi: 10.1038/17135

Tilokani, L., Nagashima, S., Paupe, V., and Prudent, J. (2018). Mitochondrial dynamics: overview of molecular mechanisms. *Essays Biochem.* 62, 341–360. doi: 10.1042/EBC20170104

Toyama, E. Q., Herzig, S., Courchet, J., Lewis, T. L., Loson, O. C., Hellberg, K., et al. (2016). AMP-activated protein kinase mediates mitochondrial fission in response to energy stress. *Science* 351, 275–281. doi: 10.1126/science.aab4138

Tucker, L. D., Lu, Y., Dong, Y., Yang, L., Li, Y., Zhao, N., et al. (2018). Photobiomodulation therapy attenuates hypoxic-ischemic injury in a neonatal rat model. *J. Mol. Neurosci.* 65, 514–526. doi: 10.1007/s12031-018-1121-3

Um, J. H., and Yun, J. (2017). Emerging role of mitophagy in human diseases and physiology. *BMB Rep.* 50, 299–307. doi: 10.5483/BMBRep.2017.50.6.056

Varanita, T., Soriano, M. E., Romanello, V., Zaglia, T., Quintana-Cabrera, R., Semenzato, M., et al. (2015). The Opa1-dependent mitochondrial cristae remodeling pathway controls atrophic, apoptotic, and ischemic tissue damage. *Cell Metab.* 21, 834–844. doi: 10.1016/j.cmet.2015.05.007

Wai, T., and Langer, T. (2016). Mitochondrial dynamics and metabolic regulation. *Trends Endocrinol. Metab.* 27, 105–117. doi: 10.1016/j.tem.2015.12.001

Wang, J., Zhu, P., Li, R., Ren, J., and Zhou, H. (2020). Fundc1-dependent mitophagy is obligatory to ischemic preconditioning-conferred renoprotection in ischemic AKI via suppression of Drp1-mediated mitochondrial fission. *Redox Biol.* 30:101415. doi: 10.1016/j.redox.2019.101415

Wang, W. Z., Zhang, F., Li, L., Tang, F. Q., Siedlak, S. L., Fujioka, H., et al. (2015). MFN2 couples glutamate excitotoxicity and mitochondrial dysfunction in motor neurons. *J. Biol. Chem.* 290, 168–182. doi: 10.1074/jbc.M114.617167

Wang, Y., Liu, G., Hong, D. D., Chen, F. H., Ji, X. M., and Cao, G. D. (2016). White matter injury in ischemic stroke. *Prog. Neurobiol.* 141, 45–60. doi: 10.1016/j.pneurobio.2016.04.00

Wang, Y., Zhou, L., Guo, J., Wang, Y., Yang, Y., Peng, Q., et al. (2020). Secular trends of stroke incidence and mortality in China, 1990 to 2016: the global burden of disease study 2016. *J. Stroke Cerebrovasc. Dis.* 29:104959. doi: 10.1016/j.jstrokecerebrovasdis.2020.104959

Wang, Z. G., Jiang, H., Chen, S., Du, F. H., and Wang, X. D. (2012). The mitochondrial phosphatase PGAM5 functions at the convergence point of multiple necrotic death pathways. *Cell* 148, 228–243. doi: 10.1016/j.cell.2011.11.030

Wei, N., Pu, Y., Yang, Z., Pan, Y., and Liu, L. (2019). Therapeutic effects of melatonin on cerebral ischemia reperfusion injury: role of Yap-OPA1 signaling pathway and mitochondrial fusion. *Biomed. Pharmacother.* 110, 203–212. doi: 10.1016/j.biopha.2018.11.060

Westermann, B. (2010). Mitochondrial fusion and fission in cell life and death. *Nat. Rev. Mol. Cell Biol.* 11, 872–884. doi: 10.1038/nrm3013

White, K. E., Davies, V. J., Hogan, V. E., Piechota, M. J., Nichols, P. P., Turnbull, D. M., et al. (2009). OPA1 deficiency associated with increased autophagy in retinal ganglion cells in a murine model of dominant optic atrophy. *Invest. Ophth. Vis. Sci.* 50, 2567–2571. doi: 10.1167/iovs.08-2913

Williams, J. A., and Ding, W. X. (2018). Mechanisms, pathophysiological roles and methods for analyzing mitophagy – recent insights. *Biol. Chem.* 399, 147–178. doi: 10.1515/hsz-2017-0228

Wu, B., Luo, H., Zhou, X., Cheng, C. Y., Lin, L., Liu, B. L., et al. (2017). Succinate-induced neuronal mitochondrial fission and hexokinase II malfunction in ischemic stroke: therapeutical effects of kaempferol. *BBA Mol. Basis Dis.* 1863, 2307–2318. doi: 10.1016/j.bbadis.2017.06.011

Wu, Q., Gao, C., Wang, H., Zhang, X., Li, Q., Gu, Z., et al. (2018). Mdivi-1 alleviates blood-brain barrier disruption and cell death in experimental traumatic brain injury by mitigating autophagy dysfunction and mitophagy activation. *Int. J. Biochem. Cell Biol.* 94, 44–55. doi: 10.1016/j.biocel.2017.11.007

Xie, L. L., Shi, F., Tan, Z., Li, Y., Bode, A. M., and Cao, Y. (2018). Mitochondrial network structure homeostasis and cell death. *Cancer Sci.* 109, 3686–3694. doi: 10.1111/cas.13830

Yaghi, S., Willey, J. Z., Cucchiara, B., Goldstein, J. N., Gonzales, N. R., Khatri, P., et al. (2017). Treatment and outcome of hemorrhagic transformation after intravenous alteplase in acute ischemic stroke: a scientific statement for healthcare professionals from the American heart association/American stroke association. *Stroke* 48, e343–e361. doi: 10.1161/STR.0000000000000152

Yoo, S. M., and Jung, Y. K. (2018). A molecular approach to mitophagy and mitochondrial dynamics. *Mol. Cells* 41, 18–26. doi: 10.14348/molcells.2018.2277

Youle, R. J., and van der Bliek, A. M. (2012). Mitochondrial fission, fusion, and stress. *Science* 337, 1062–1065. doi: 10.1126/science.1219855

Yu, B., Ma, J., Li, J., Wang, D. Z., Wang, Z. G., and Wang, S. S. (2020). Mitochondrial phosphatase PGAM5 modulates cellular senescence by regulating mitochondrial dynamics. *Nat. Commun.* 11:2549. doi: 10.1038/s41467-020-16312-7

Zenonos, G., and Kim, J. E. (2010). 18F-fluoromisonidazole PET/CT and related gauges of cerebral metabolism identify salvageable tissue in ischemic penumbra following aneurysmal subarachnoid hemorrhage. *Neurosurgery* 66, N13–N15. doi: 10.1227/01.neu.0000367839.75141.e6

Zhang, C., Wang, J., Zhu, J., Chen, Y., and Han, X. (2020). Microcystin-leucine-arginine induced neurotoxicity by initiating mitochondrial fission in hippocampal neurons. *Sci. Total Environ.* 703:134702. doi: 10.1016/j.scitotenv.2019.134702

Zhang, H. S., Liu, C. D., Zheng, M. C., Zhao, H. T., and Liu, X. J. (2020). Propofol alleviates hypoxic neuronal injury by inhibiting high levels of mitochondrial fusion and fission. *Eur. Rev. Med. Pharmacol. Sci.* 24, 9650–9657. doi: 10.26355/eurrev_202009_23054

Zhang, K., Li, H., and Song, Z. (2014). Membrane depolarization activates the mitochondrial protease OMA1 by stimulating self-cleavage. *EMBO Rep.* 15, 576–585. doi: 10.1002/embr.201338240

Zhang, L., He, Z., Zhang, Q., Wu, Y., Yang, X., Niu, W., et al. (2014). Exercise pretreatment promotes mitochondrial dynamic protein OPA1 expression after cerebral ischemia in rats. *Int. J. Mol. Sci.* 15, 4453–4463. doi: 10.3390/ijms15034453

Zhang, Y. K., Sun, R. J., Li, X. L., and Fang, W. H. (2020). Porcine circovirus 2 induction of ROS is responsible for mitophagy in PK-15 cells via activation of Drp1 phosphorylation. *Viruses Basel* 12:289. doi: 10.3390/v12030289

Zhang, Z., and Yu, J. (2018). Nurr1 exacerbates cerebral ischemia-reperfusion injury via modulating YAP-INF2-mitochondrial fission pathways. *Int. J. Biochem. Cell Biol.* 104, 149–160. doi: 10.1016/j.biocel.2018.09.014

Zhao, Q., Wang, S., Li, Y., Wang, P., Li, S., Guo, Y., et al. (2013). The role of the mitochondrial calcium uniporter in cerebral ischemia/reperfusion injury in rats involves regulation of mitochondrial energy metabolism. *Mol. Med. Rep.* 7, 1073–1080. doi: 10.3892/mmr.2013.1321

Zhao, Y. X., Cui, M., Chen, S. F., Dong, Q., and Liu, X. Y. (2014). Amelioration of ischemic mitochondrial injury and Bax-dependent outer membrane permeabilization by Mdivi-1. *CNS Neurosci. Ther.* 20, 528–538. doi: 10.1111/cns.12266

Zhou, K., Chen, J., Wu, J., Wu, Q., Jia, C., Xu, Y. X. Z., et al. (2019a). Atractylenolide III ameliorates cerebral ischemic injury and neuroinflammation associated with inhibiting JAK2/STAT3/Drp1-dependent mitochondrial fission in microglia. *Phytomedicine* 59:152922. doi: 10.1016/j.phymed.2019.152922

Zhou, K., Wu, J. Y., Chen, J., Zhou, Y., Chen, X. L., Wu, Q. Y., et al. (2019b). Schaftoside ameliorates oxygen glucose deprivation-induced inflammation associated with the TLR4/Myd88/Drp1-related mitochondrial fission in BV2 microglia cells. *J. Pharmacol. Sci.* 139, 15–22. doi: 10.1016/j.jphs.2018.10.012

Zhou, L., Zhang, Q., Zhang, P., Sun, L., Peng, C., Yuan, Z., et al. (2017). c-Abl-mediated Drp1 phosphorylation promotes oxidative stress-induced mitochondrial fragmentation and neuronal cell death. *Cell Death Dis.* 8:e3117. doi: 10.1038/cddis.2017.524

Zhou, L. Y., Yao, M., Tian, Z. R., Liu, S. F., Song, Y. J., Ye, J., et al. (2020). Muscone suppresses inflammatory responses and neuronal damage in a rat model of cervical spondylotic myelopathy by regulating Drp1-dependent mitochondrial fission. *J. Neurochem.* 155, 154–176. doi: 10.1111/jnc.15011

Conflict of Interest: The authors declare that the research was conducted in the absence of any commercial or financial relationships that could be construed as a potential conflict of interest.

Publisher's Note: All claims expressed in this article are solely those of the authors and do not necessarily represent those of their affiliated organizations, or those of the publisher, the editors and the reviewers. Any product that may be evaluated in this article, or claim that may be made by its manufacturer, is not guaranteed or endorsed by the publisher.

frontiers in Aging Neuroscience

ORIGINAL RESEARCH
published: 20 October 2021
doi: 10.3389/fnagi.2021.666301

Disrupted Brain Connectivity Networks in Aphasia Revealed by Resting-State fMRI

Xiaoyun Chen[1†], Liting Chen[2†], Senning Zheng[3†], Hong Wang[1], Yanhong Dai[1], Zhuoming Chen[1] and Ruiwang Huang[3*]*

[1] Department of Rehabilitation, The First Affiliated Hospital of Jinan University, Guangzhou, China, [2] Medical Imaging Center, First Affiliated Hospital of Jinan University, Guangzhou, China, [3] Key Laboratory of Mental Health and Cognitive Science of Guangdong, Center for the Study of Applied Psychology and MRI Center, School of Psychology, Institute of Brain Research and Rehabilitation (IBRR), South China Normal University, Guangzhou, China

Aphasia is characterized by the disability of spontaneous conversation, listening, understanding, retelling, naming, reading, or writing. However, the neural mechanisms of language damage after stroke are still under discussion. This study aimed to investigate the global and nodal characterization of the functional networks in patients with aphasic stroke based on resting-state functional MRI (fMRI). Twenty-four right-handed patients with aphasia after stroke and 19 healthy controls (HC) underwent a 3-TfMRI scan. A whole-brain large-scale functional connectivity network was then constructed based on Power's atlas of 264 functional regions of interest, and the global and nodal topological properties of these networks were analyzed using graph theory approaches. The results showed that patients with aphasia had decreased in small-worldness (sigma), normalized clustering coefficient (gamma), and local efficiency (E_{loc}) values. Furthermore, E_{loc} was positively correlated with language ability, retelling, naming, and listening comprehension in patients with aphasia. Patients with aphasia also had decreased nodal degree and decreased nodal efficiency in the left postcentral gyrus, central opercular cortex, and insular cortex. Our results suggest that the global and local topology attributes were altered by injury in patients with aphasic stroke. We argue that the local efficiency of brain networks might be used as a potential indicator of basic speech function in patients with aphasia.

Keywords: aphasia, cognitive impairment, topological properties, functional MRI, stroke

OPEN ACCESS

Edited by:
Feng Yan,
Zhejiang University, China

Reviewed by:
Henning U. Voss,
Cornell University, United States
Ljun Bai,
Xi'an Jiaotong University, China

***Correspondence:**
Zhuoming Chen
czmxy2020@163.com
Ruiwang Huang
ruiwang.huang@gmail.com

† These authors have contributed equally to this work

Received: *10 February 2021*
Accepted: *15 September 2021*
Published: *20 October 2021*

Citation:
Chen X, Chen L, Zheng S, Wang H, Dai Y, Chen Z and Huang R (2021) Disrupted Brain Connectivity Networks in Aphasia Revealed by Resting-State fMRI. Front. Aging Neurosci. 13:666301. doi: 10.3389/fnagi.2021.666301

INTRODUCTION

Aphasia, disruption of cognitive processes underlying language, manifests as impairments in spontaneous conversation, auditory comprehension, retelling, naming, reading, or writing. Notably, aphasia is closely associated with higher morbidity, mortality, and societal costs. Stroke is the most common cause of aphasia (especially in occlusion within the middle cerebral artery territory), and about 20–40% of strokes leading to acute aphasia (Engelter et al., 2006).

For a long time, one of the important models to help us understand the pathological mechanism of aphasia is the Wernicke-Lichtheim model (Lichteim, 1885; Wernicke, 1984), which includes Broca's and Wernicke's areas, and white matter fiber bundles (arcuate bundle) connecting these two brain regions. This model asserts that each of these brain regions has specialized functions, that neuroanatomical pathways support communication between them, and that this can be used to

understand the interpretation of language or early clinical symptoms. It is particularly useful in the neurobiological study; however, with increased understanding of and research into the structure and function of the brain, the limitations of this early classical model of language have become increasingly prominent.

With the development of research technology, a new language model, the dual-stream model (Hickok and Poeppel, 2004, 2007) has gradually emerged. This model pays more attention to the connection between the cortex, and it mainly describes two large-scale processing streams: the ventral and dorsal streams. The ventral flow supports auditory-to-semantic information processing and listening comprehension. This area is mainly located in the lateral temporal lobe, extending into the posterior-inferior frontal gyrus pars orbitalis *via* the uncinate fasciculus. The dorsal stream, which processes information from hearing to pronunciation, is located at the junction between the left frontal language area and the temporal parietal area. It mainly provides auditory and proprioceptive feedback, which is important for fluent speech. The major brain regions involved are frontoparietal regions, including the pars opercularis, pars triangularis, pre- and postcentral regions, and portions of the parietal lobe. Although the dorsal and nerve streams provide the crucial organizational framework for human communication, they are not equally important for language processing and speech. For instance, damage to the cerebral cortex, angular gyrus, or posterior cortex is generally more harmful to speech and language processing than damage to other regions based on region-wise lesion-symptom mapping (Fridriksson et al., 2018). Additionally, there are symptomatic differences between injuries to brain areas associated with producing increasingly complex word combinations and areas associated with producing syntactically accurate connected speech. Inability to produce complicated language structure is associated with damage to the posterior temporal cortex and the angular gyrus of the inferior parietal lobe. In contrast, defects in syntactic accuracy are associated with damage to the left inferior frontal gyrus, insular, postcentral gyrus, precentral gyrus, and supramarginal gyrus of the inferior parietal lobe (Fridriksson et al., 2018).

The graph theory analysis method is centrally important to understanding the structure and function of networked brain systems, including their architecture, development, and evolution. Based on the strong influence of the dual stream model, we used a graph theory analysis method to explore the local and global topological properties of brain functional networks in patients with aphasia and explore the relationships between these indicators and aphasia symptoms. An increasing number of studies have used graph theory in conjunction with functional connectivity (FC) to investigate the topological properties of brain functional networks and the effects of focal damage on functional brain networks (Baliki et al., 2018; Tao and Rapp, 2019; Johnson et al., 2020). Tao and Rapp (2019) investigated the properties of functional networks in aphasia, and their investigation revealed that more modular networks with higher local integration resulted in a greater response to treatment and were associated with lower deficit severity; both global network modularity and local integration increased after treatment, especially within intact ventral occipital-temporal regions of the spelling network. Johnson et al. (2020) also used graph analysis to examine a network of regions linked to semantic processing in aphasia who went on to receive naming treatment. They found that aphasia with higher pre-treatment graph metrics responded better to treatment than those with lower network measures. They accordingly suggested that higher global efficiency and strength in the semantic network might be favorable prognostic indicators for improvement from semantic naming treatment. In addition, Baliki et al. (2018) used graph theory analysis to investigate the influence of baseline anatomical and functional brain properties in response to intensive comprehensive aphasia treatment based on resting-state functional MRI (fMRI). They found that baseline resting-state FC (rsFC) properties in aphasia were strongly associated with treatment outcomes, and that large-scale properties, such as global efficiency and interhemispheric connectivity, were related to improved language and visual attention performances, respectively. They also found that the connectivity between the default mode network and the auditory regions was highly related to improved language, while connectivity between the salience network and visual regions was related to increasing visual attention performance. Above all, these previous studies have reflected that network topology indicators can well-predict the effectiveness of comprehensive speech therapy for patients with aphasia. Although this early study identified specific rsFC properties that predict outcomes in aphasia following treatment, the powers of these studies are usually suffered from a small sampling problem, which makes their results difficult to generalize. Thus, our study aims to extend the results of a previous study by exploring the topological properties of functional networks in patients with aphasia before comprehensive speech therapy.

Based on the dual stream model and the neuropsychological dual dissociation of structural damage and functional networks,

TABLE 1 | Demographic and clinical data comparisons between the patients with aphasia and healthy controls.

Characteristic	Patients with aphasia ($n = 24$)	Healthy controls ($n = 19$)	χ^2/*t*-value	*p*-value
Age	48.39 ± 10.66	53.70 ± 9.34	−1.71	0.094[a]
Sex (M:F)	16:8	10:9	0.48	0.490[b]
Duration (month)	5.16 ± 5.58	—	—	—
ABC (spontaneous speech)	53.08 ± 18.86	98.53 ± 1.12	−10.46	0.000*
ABC (auditory comprehension)	76.00 ± 18.24	99.95 ± 0.23	−6.43	0.000*
ABC (repetition)	74.08 ± 21.07	99.89 ± 1.12	−6.00	0.000*
ABC (naming)	54.42 ± 28.40	99.74 ± 0.57	−7.81	0.000*
language ability[c]	64.39 ± 19.20	99.53 ± 0.42	−8.96	0.000*
MMSE	14.42 ± 6.86	29.21 ± 0.98	−10.43	0.000*
MoCA	10.46 ± 6.16	28.57 ± 1.01	−14.18	0.000*

[a]*independent-samples t-test;* [b]*chi-square test;* [c]*the mean value of all sub-measures in ABC.* $*p < 0.05$*, the difference is statistically significant.*

we aim to explore changes in the whole brain functional network in aphasia after stroke. We examined the relationships between abnormal topological properties of the whole brain functional network and language behavior and cognition in aphasia after stroke. To address this issue, we used quantitative evaluations of the global and nodal characteristics of the brain functional networks and examined the relationships between these topological metrics and the aphasia battery of Chinese (ABC) (Gao, 1992), mini-mental state examination (MMSE) (Byrne et al., 2000), and the Montreal Cognitive Assessment (MoCA) (Nasreddine et al., 2005) scores.

MATERIALS AND METHODS

Subjects

Twenty-four patients with aphasia after stroke and 19 healthy controls (HC) matched for age, sex, and years of education were recruited from the center for diagnosis and treatment of language disorders, First Affiliated Hospital of Jinan University, Guangzhou, China, from January 2016 to February 2019. All HCs and patients were right-handed and aged more than 18 years and <70 years. Inclusion criteria for the aphasia group were the following: (1) at the first onset of stroke, the lesion was confirmed to be located in the left hemisphere by cranial CT or MRI; (2) patients had received no treatment for speech recovery; (3) the duration of aphasia was 1–24 months; (3) motor aphasia diagnosis was determined by the ABC (Gao, 1992); (4) the education level of the patient was elementary school or above; and (5) they were right-handed. The exclusion criteria for all the participants were the following: (1) speech, reading, or writing impairment due to severe damage to sensory and motor organs, such as hearing, vision, articulation, and writing; (2) congenital or early childhood illnesses causing language learning difficulties and resulting in language function deficits; (3) subjects who were unconscious and unable to cooperate with examination and treatment, or who were unable to complete the scale assessment; (4) those with a history of neurological or psychiatric disorders (e.g., Alzheimer's disease, epilepsy, depression); (5) combined epilepsy, severe cardiac, hepatic, or renal dysfunction, or other serious physical illness; (6) bilateral stroke; (7) contraindications for MRI, for instance, metallic implants. The demographic and clinical information of the patients (8 women, 16 men; mean age, 51.16 $\pm$ 9.48 years) and HC (9 women, 10 men; mean age, 48.39 $\pm$ 10.66 years) is detailed in **Table 1**. This study was approved by the Medical Research Ethics Committee of the First Affiliated Hospital of Jinan University. Informed consent was obtained from all the subjects prior to the study.

Neuropsychological Assessments

The neuropsychological status of each patient was examined using the following scales: the ABC, the MMSE, and the MoCA (Chinese version) The ABC (Gao, 1992), which is the Chinese-standardized adaptation of the western aphasia battery, and this was applied to assess the language abilities of the patients, including spontaneous speech, auditory comprehension, repetition, and naming. The MMSE (Li et al., 2016) and MoCA (Nasreddine et al., 2005), which are widely used to systematically assess cognitive impairment. The MMSE questionnaire contains 11 indexes to measure five areas of cognitive function (attention, calculation, orientation, recall, registration, and language). The maximum MMSE score is 30, with a score <23, indicating cognitive impairment. The MoCA has eight cognitive items, including language, memory, abstraction, naming, attention, executive function, calculation, and orientation. The maximum MoCA score is 30, and a score of 26 or lower is indicative of cognitive impairment. When the number of years in education is <12, one point should be added to adjust for educational deviations (Nasreddine et al., 2005).

MRI Data Acquisition

All MRI data were collected on a GE Discovery MR750 3.0T System equipped with an eight-channel head coil at the radiology department of the First Affiliated Hospital of Jinan University. Foam pads were used to restrict head movement, and earplugs were used to minimize scanner noise. First, conventional T1-weighted images and T2-weighted images were collected to observe brain lesions. Resting-state functional images were acquired using a gradient-recalled echo-planar imaging sequence. The sequence parameters were as follows: repetition time = 2,100 ms, echo time = 30 ms, thickness = 3.0 mm, gap = 0.6 mm, voxel size = 3.125 × 3.125 × 3.6 mm^3, flip angle = 90°, matrix = 64 × 64, number of volumes = 160, number of slices = 42. Finally, high-resolution T1-weighted brain structural magnetic resonance images were obtained using a three-dimensional (3D) brain volume imaging (3D-BRAVO) sequence (repetition time = 4,500 ms, echo time = 3.22 ms, thickness = 1.0 mm, gap = 0.5 mm, field of view = 240 mm × 240 mm, flip angle = 15°, voxel size = 0.47 × 0.47 × 1.0 mm^3, slices = 164).

Image Preprocessing

The preprocessing was carried out using Data Processing and Analysis Assistant for Resting-State Brain Imaging (DPABI_V5.1) based on Statistical Parametric Mapping (SPM12) in the MATLAB 2014a platform (The MathWorks Inc., Natick, MA, US). The first 10 images of each rs-fMRI dataset were discarded, and the remaining 150 images were slice timing corrected. Then, 3D head motion correction was conducted for small head movements, which also provided a record of the head motion for image quality control. The subject whose head motion of maximum rotation was more than 3°, or maximum displacement in any direction was >3 mm, was excluded from analyses. Two imaging physicians with more than 5 years of work experience drew the 3D contours of lesions in each subject based on T1-weighted structural images, and these were used as lesion masks for normalization (see below Brett et al., 2001; Andersen et al., 2010). The T1 structural images were segmented into white matter, gray matter, and cerebrospinal fluid. For the patients, this procedure was conducted using the Clinical Toolbox (https://www.nitrc.org/projects/clinicaltbx/) supported by SPM12. Notably, as many of the subjects included in this study had large unilateral brain lesions, we used the enantiomorphic

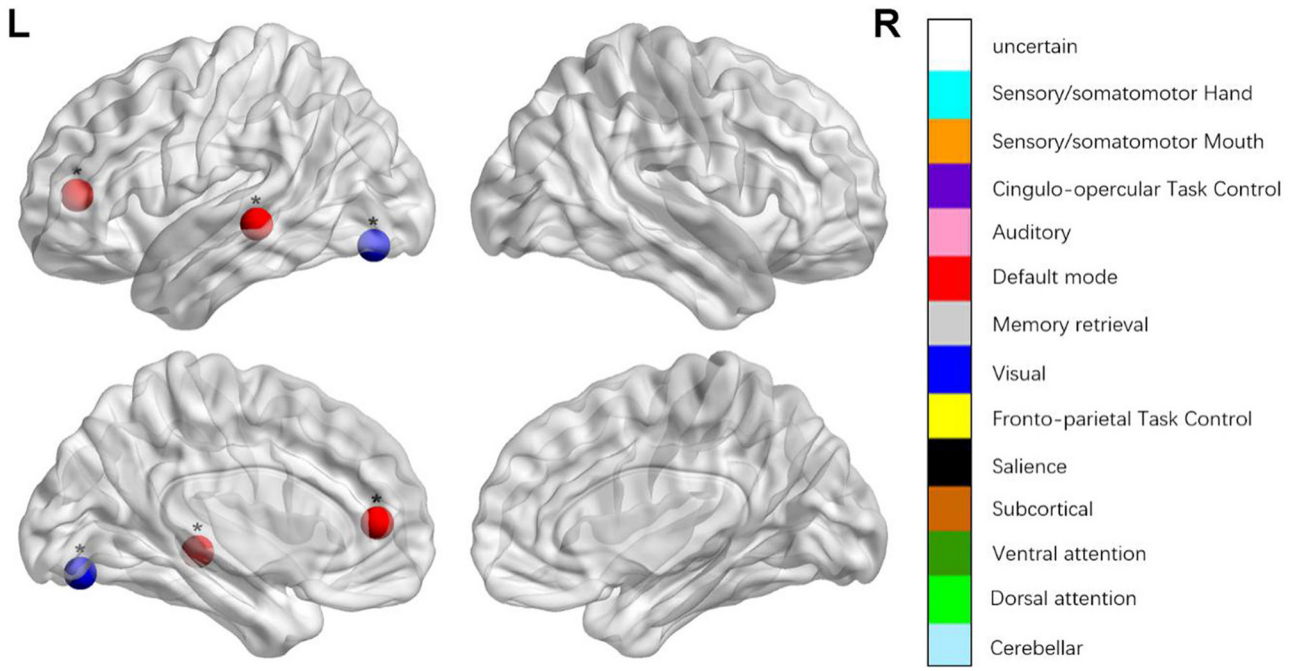

FIGURE 1 | Regions were considered abnormal nodal betweenness in patients with aphasia if they exhibited significant between-group differences. *$p < 0.000189$, Bonferroni correction (i.e., 1/264).

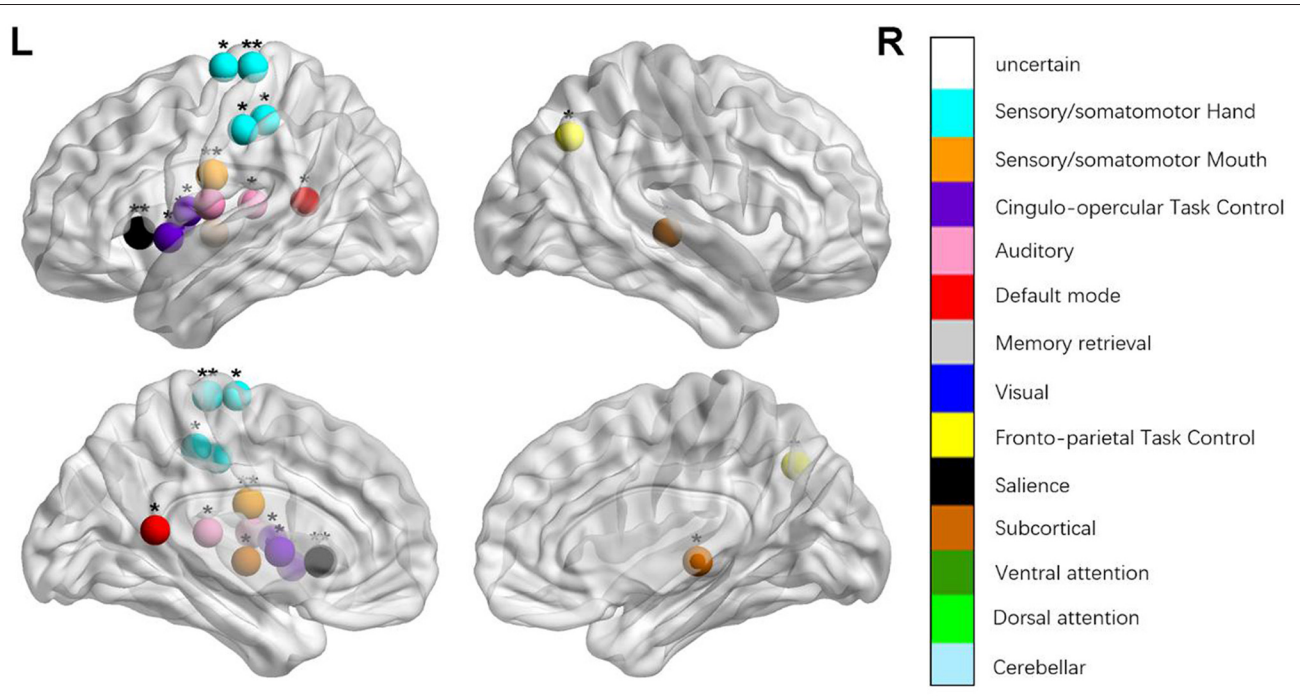

FIGURE 2 | Regions were considered an abnormal nodal degree in patients with aphasia if they exhibited significant between-group differences. *$p < 0.003787$, Bonferroni correction (i.e., 1/264). **$p < 0.000189$, Bonferroni correction (i.e., 0.05/264).

normalization with a 6-tissue parameter rather than traditional lesion-masked normalization (Rorden et al., 2012) to get a better result. For the controls, the common SPM New Segment was used. The results of segmentation were visually checked by the authors to ensure their correctness. Then, all resting-state functional images for each individual were co-registered to the

T1-weighted structural images that were used for segmentation. These realigned functional images were normalized into the Montreal Neurological Institute (MNI) space with 3 × 3 × 3 resolution. The nuisance covariates (including the global signal, white matter, and cerebrospinal fluid signals, and the Friston-24-parameter model of head motions) were then removed from the functional data through linear regression to reduce the effects of confounding factors. Finally, all the standard MNI space functional images were smoothed with an 8-mm full width at half maximum Gaussian kernel, and temporal band-pass filtering (0.01–0.08 Hz) was performed.

Functional Network Construction and Analysis

In the current study, we used the Graph Theoretical Network Analysis (GRETNA) (Wang et al., 2015) toolbox (https://www.nitrc.org/projects/gretna/) to construct the large-scale brain network. The Power-264 atlas (Power et al., 2011), a high-resolution parcellation scheme based on the results of a large meta-analysis was selected to define the nodes (i.e., functional areas) in the brain network. This atlas includes 264 putative functional areas, and its robustness for network construction has been proved by many studies (Power et al., 2013). We first extracted the time series in each node by averaging the time series of all voxels in the same nodal areas. Then, we calculated the Pearson correlation coefficient between the time series of each possible node pair. Thus, a 264 × 264 functional correlation matrix was generated for each subject. To improve the normality of the correlation coefficient, a Fisher's *r*-to-*z* transformation was applied to the correlation matrices.

A general approach to determining the available edges in a matrix is to binarize the whole matrix using a thresholding method (Achard and Bullmore, 2007). As there is no consensus in regard to the setting of functional-network-threshold to date, we employed a wide range of sparsity thresholds (0.05–0.40 with an interval of 0.05) to all the correlation matrices for the following reasons. First, we chose to threshold the functional matrix by using the network sparsity rather than the value of the matrix elements, because the latter approach will cause the extraction of different numbers of edges across subjects, which might confound group comparisons in network topology. Also, the network sparsity approach can ensure that no isolated nodes existed in any threshold point under our chosen threshold band. Second, as suggested by previous studies (Chen et al., 2019), the lower sparsity of 0.05 still ensures that the average degree is greater than the natural logarithm of the number of nodes in the Power-264 atlas, and the upper sparsity of 0.40 also does not exceed the 50% network density. Finally, as the meaning of negative correlations in the functional network is still controversial, we only included positive correlations for later network analyses.

Functional Network Analysis

For the network analyses, we calculated both global and regional network metrics at each sparsity threshold and the area under the curve (AUC) over the sparsity range. The AUC metric provides a summarized scalar for the topological properties of brain networks that is independent of the threshold, and this is sensitive for detecting the topological alterations of brain disorders (Zhang et al., 2011; Chen et al., 2018). The global metrics included the small-world properties and network efficiency properties. Specifically, the small-world properties included five sub-measures (Watts and Strogatz, 1998): small-worldness (*sigma*), normalized clustering coefficient (*gamma*), normalized characteristic path length (*lambda*), clustering coefficient (*Cp*), and characteristic path length (*Lp*) [for the details of these sub-measures, please refer to the study of Chen et al. (2019)]. In addition, consistent with previous studies (Latora and Marchiori, 2001), we also computed the global and local network efficiencies (E_{glob}/E_{loc}) to overcome the shortcomings of the clustering coefficient (ignorance of indirect connections) and the shortest path length (misjudgment of isolated nodes).

In comparison to global metrics, regional metrics are better at quantitatively characterizing the nodal dynamics of brain networks (Rubinov and Sporns, 2010). In this study, we included the three node-based metrics: the nodal degree, nodal efficiency, and nodal betweenness (Achard and Bullmore, 2007; Rubinov and Sporns, 2010). The nodal degree is the original and most important measure for describing the nodal characteristics of a graph. The nodal efficiency measures the efficiency of the communication among the first neighbors of a node when it is removed, and it is very suitable for describing the local functional state in aphasia with brain injury. The nodal betweenness is defined as the fraction of all shortest paths in the network that pass through a given node, and this is suggested as a sensitive measure to detect important anatomical or functional connections (Rubinov and Sporns, 2010).

Statistical Analysis

We used the IBM Statistical Package for the Social Sciences 20.0 software (IBM SPSS Inc., Chicago, IL, USA; https://www.ibm.com/products/spss-statistics) to compare the statistical differences in demographic and clinical data between the aphasia and the HC groups. More specifically, we used two-sample *t*-tests to detect the group differences in age, sex, duration, ABC score, MMSE score, and MoCA score, and we used chi-square tests to examine any significant sex distribution difference and duration distribution differences.

To determine whether there existed significant between-group differences in the global and the regional network metrics, we perform several two-sample *t*-tests on the AUC of each network measure (small-world metrics: *sigma*, *gamma*, *lambda*, *Cp*, *Lp*, and network efficiency metrics: E_{glob}, E_{loc}) between the patients with aphasia and the HC. To avoid misuse of statistical methods (e.g., when the data do not obey normal distribution), we also conducted the non-parametric permutation tests that randomly shuffle the group distribution 5,000 times to confirm the results of group comparisons. If any significant between-group differences in the network metrics were identified in the network metrics, we will further extract the AUC values of these topological properties and evaluate their relationships with the clinical

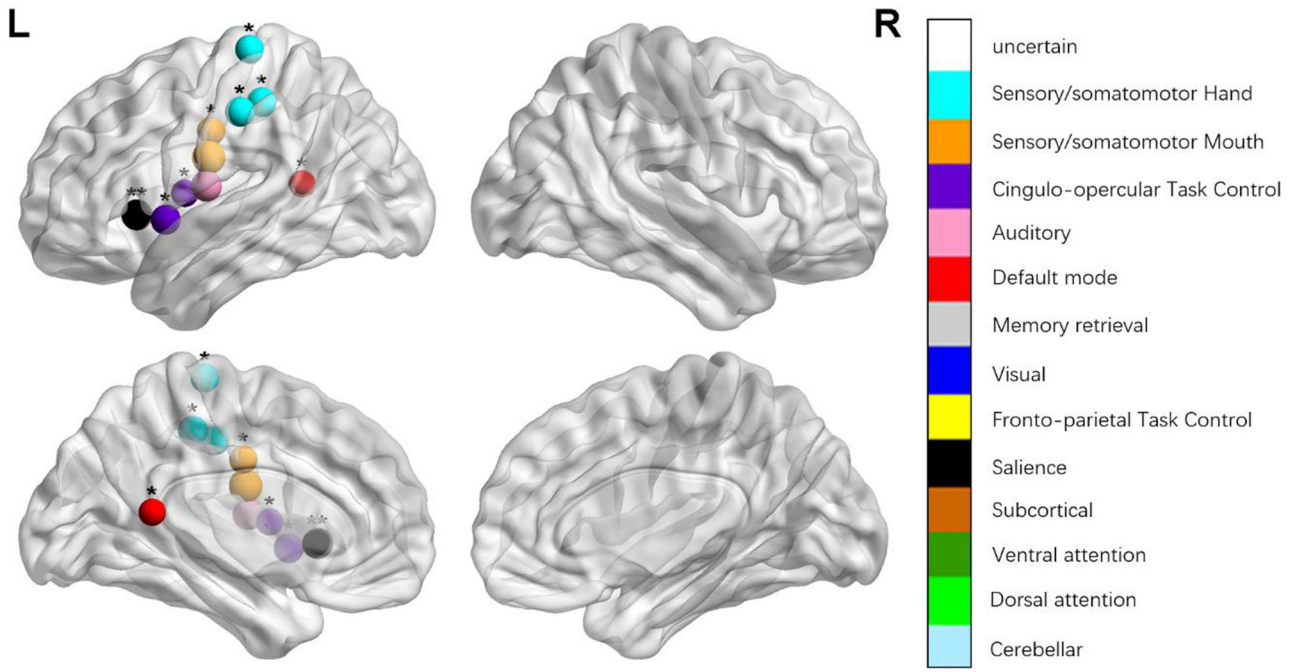

FIGURE 3 | Regions were considered abnormal nodal efficiency in patients with aphasia if they exhibited significant between-group differences. *$p < 0.003787$, Bonferroni correction (i.e., 1/264). **$p < 0.000189$, Bonferroni correction (i.e., 0.05/264).

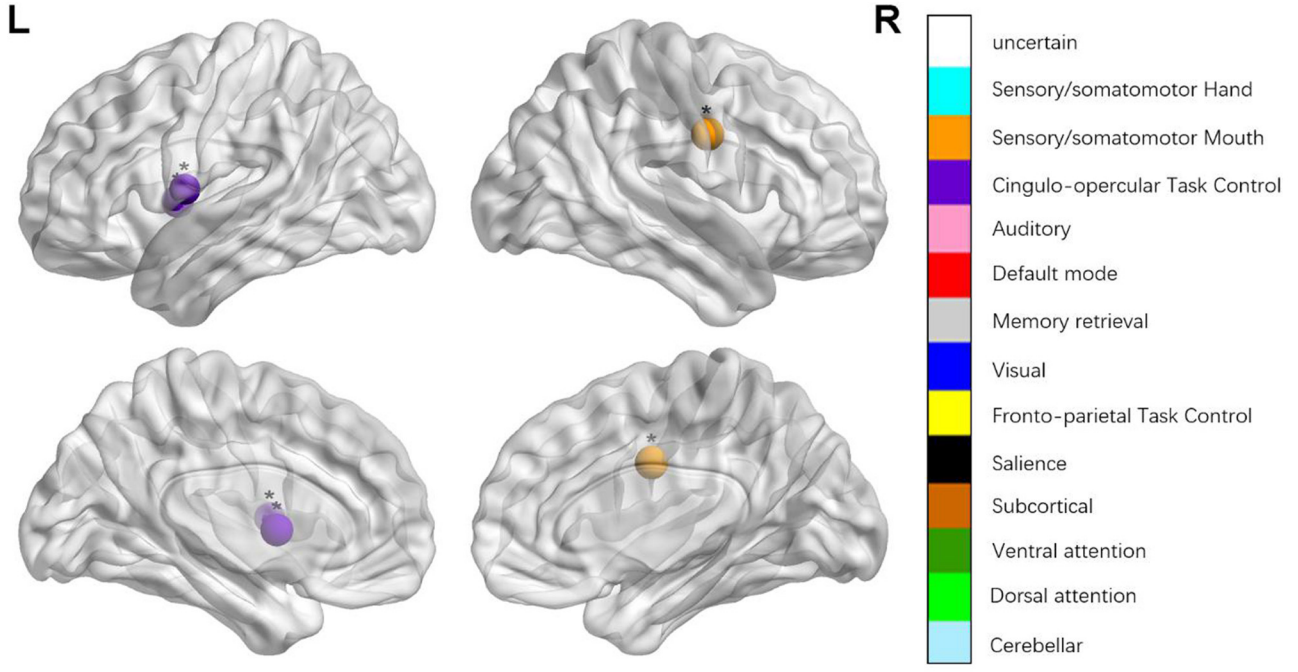

FIGURE 4 | Regions were considered abnormal nodal local efficiency in patients with aphasia if they exhibited significant between-group differences. *$p < 0.003787$, Bonferroni correction (i.e., 1/264). **$p < 0.000189$, Bonferroni correction (i.e., 0.05/264).

data (i.e., the ABC, MMSE, and MoCA scores) in the aphasic group by using Pearson correlations. Note that as the AUC values (instead of the topological value under each threshold point) were used for statistical analyses, the potential risk of false-positive rates yielded by multiple comparisons was alleviated. Therefore, the significance level

for the above analyses (the group differences in demographic and clinical data, the group differences in global network metrics, and the correlations between global network metrics and clinical data) was set at $p < 0.05$ without multiple comparison correction.

Finally, for the regional metrics (the nodal degree, nodal efficiency, and nodal betweenness), we performed two-sample *t*-tests between the patients with aphasia and the HC in each node. The Bonferroni method was used to correct the issue of multiple comparisons. In this study, given that the number of nodes was 264, the significant level for each node was set at $p < 0.000189$ (i.e., 0.05/264). However, for the exploratory purpose, we also reported the node with a more liberal threshold, which is $p < 0.0038$ (i.e., 1/264).

RESULTS

Demographic and Clinical Comparisons

The demographic and clinical data from 24 patients with aphasia and the 19 HC subjects are summarized in **Table 1**. There were significant between-group differences in spontaneous speech, auditory comprehension, repetition, naming, language ability, MMSE, and MoCA between the patients with aphasia and healthy controls. There were no significant differences in age ($p = 0.094$) or sex ($p = 0.49$) between the patients with aphasia and healthy controls.

Global Topological Metrics of Brain Functional Networks

In the defined threshold range (from 0.05 to 0.40, step = 0.05), we used the AUC of each global metric as an independent variable in the between-group statistical comparisons. Compared with the HC group, patients with aphasia showed significant decreased in *sigma* ($t = -3.5065$, $p = 0.001$), *gamma* ($t = -3.637$, $p = 0.001$), and E_{loc}($t = -2.444$, $p < 0.019$). No significant between-group differences were identified in the *Cp* ($t = -1.876$, $p = 0.068$), *Lp* ($t = -0.848$, $p = 0.402$), E_{glob} ($t = 1.093$, $p = 0.281$) and *Lambda* ($t = -1.139$, $p = 0.261$). In addition, we also calculated the difference of AUC values of all parameters in the threshold range (from.05 to.40, step = 0.01). Our results showed that, when choosing network sparsity, 0.01 as a step size or 0.05 as a step size did not significantly affect the pattern of the results (**Supplementary Table 1**). In addition to the two-sample *t*-test, we also used the non-parametric test (Mann-Whitney U-test) and permutation to compare the differences of topological properties; our results showed that the results pattern were basically the same, which indicated that the results of the *t*-test comparison between the groups in this study were reliable (**Supplementary Tables 2, 3**).

Regional Topological Metrics of the Brain Functional Networks

We identified the brain regions that showed a between-group difference in the regional topological organization ($^*p < 0.000189$, i.e., 1/264). Compared with the HC group, aphasia showed a decreased nodal degree in the left postcentral gyrus, central opercular cortex, and insular cortex. We also found that patients with aphasia showed decreased nodal efficiency in the left postcentral gyrus, central opercular cortex, and insular cortex (**Figures 1–4** and **Table 2**).

Brain-Behavior Correlation Analysis

Then, we used Pearson correlation to evaluate the relationships between the AUCs of sigma, gamma, and E_{loc}, and the clinical variables in the aphasia group in the threshold range (from 0.05 to 0.40, step = 0.05). We found that the AUC of E_{loc} was positively correlated with the language ability ($r = 0.5013$, $p = 0.0126$), retelling ($r = 0.4054$, $p = 0.0494$), naming ($r = 0.4054$, $p = 0.0076$), listening comprehension ($r = 0.4389$, $p = 0.0319$) in patients. This pattern of correlations is not affected by the choosing network sparsity (i.e., 0.01 step or 0.05 step; see the details in **Supplementary Tables 4, 5**). In addition, to further ensure that the correlations are not systematically confounded by other extraneous variables, we also conducted a partial correlation between *Eloc* and clinical measures that controlled for age, sex, head motion, and the duration of the disease. The results of partial correlation confirm that Eloc was still significantly correlated with naming, listening comprehension, and language ability (**Supplementary Table 6**). Finally, similar correlation results were also attained by the permutation correlation procedure (**Supplementary Table 7**).

DISCUSSION

In the present study, graph-theoretical approaches were applied to assess the topological properties of brain functional networks in patients with aphasia using resting-state fMRI based on the Power-264 atlas. The results showed that patients with aphasia had a decreased sigma, gamma, and E_{loc}. Moreover, patients with aphasia had decreased nodal degree and decreased nodal efficiency in the left postcentral gyrus, central opercular cortex, and insular cortex. Furthermore, E_{loc} was positively correlated with language ability, retelling, naming, and listening comprehension in patients with aphasia. Our study shows that the local efficiency of the brain network might be used as a potential indicator of basic speech function in patients with aphasia.

The dual-stream model includes a dorsal stream and a ventral stream, and these promote grammar processing and support speech production and comprehension. In contrast to the symptom–lesion view, this model envisages that the entire brain is used to process language. Following this rationale, our study considered the brain functional network as a whole and explored the changes in topological properties. In the graph theory, small-worldness is a fascinating parameter for the description of complex brain networks; it attains a much higher clustering coefficient and a similar characteristic path length and facilitates an energy-efficient balance between local specialization and global integration (Achard and Bullmore, 2007; Rubinov and Sporns, 2010). Compared with the normal

TABLE 2 | Between-group differences in nodal characteristics in patients with aphasia and healthy controls.

Name	*t*	*p*	Power_NO	MNI	Anatomy (Harvardy)
BC	−3.206	0.003	111	−11 45 8	Paracingulate grus (L)
	−3.098	0.004	118	−58 −30 −4	Posterior middle temporal gyrus (L)
	3.101	0.004	172	−33 −79 −13	Occipital fusiform gyrus (L)
DC	−5.537	0.000*	45	−53 −10 24	Postcentral gyrus (L)
	−4.798	0.000*	70	−55 −9 12	Central opercular cortex (L)
	−6.14	0.000*	208	−35 20 0	Insular cortex (L)
NEg	−5.185	0.000*	45	−53 −10 24	Postcentral gyrus (L)
	−4.347	0.000*	70	−55 −9 12	Central opercular cortex (L)
	−4.31	0.000*	208	−35 20 0	Insular cortex (L)
NEloc	−3.462	0.001	42	−49 −11 35	Precentral gyrus (L)
	−4.038	0.000	58	−51 8 −2	Superior temporal gyrus (L)
	3.109	0.003	91	−3 −49 13	Posterior cingulate gyrus (L)
	−3.748	0.001	44	51 −6 32	Precentral gyrus (R)
	−3.109	0.003	55	−45 0 9	Central opercular cortex (L)
	−3.595	0.001	57	−34 3 4	Insular cortex (L)

*$p < 0.05$, the difference is statistically significant. *$p < 0.000189$, Bonferroni correction (i.e., 1/264); BC, betweenness centrality; DC, degree centrality; NEg, nodal efficiency; NEloc, local efficiency.*

control group, the patients with aphasia showed a decrease in sigma, gamma, and E_{loc}. The decrease in sigma might suggest that the stroke patients with aphasia had less local specialization and global integration and that highly specialized and integrated information processing may be impaired in the brain functional network. The parameter gamma is often interpreted as an index of the strength of network segregation or specialization (Rubinov and Sporns, 2010). The decrease of gamma in stroke patients with aphasia was considered to indicate altered short-distance functional connections between adjacent regions.

The parameter E_{loc} is a metric that quantifies the capacity for transmitting information over local networks and the fault tolerance of a network (Rubinov and Sporns, 2010). Therefore, our results that patients with aphasia exhibited decreased E_{loc} might suggest that the capacity for information exchange and regional information processing have been disrupted, and it may result from the sparse or damaged functional connections. Moreover, E_{loc} was positively correlated with language ability, spontaneous expression, retelling, naming, and listening comprehension. However, there were no significant differences in the correlations between sigma, gamma, and clinical symptoms. It further illustrated that disrupted local efficiency influences cognitive impairments, information exchange and processing, and language competence in patients with aphasia. These results indicated that the topological properties of small world network had been injured in patients with aphasia, which may be caused by the impairment of language understanding and expression, memory, executive function and attention, and the local efficiency of brain networks can be a potential indicator of basic speech function in patients with aphasia. Agosta et al. (2014) found that patients with aphasia were characterized by a lower network degree, clustering coefficient, and global efficiency, as well as a longer characteristic path length and higher assortativity; and the reduced nodal degree in the inferior and ventral temporal regions and occipital cortices and the local network analysis showed that patients with aphasia were associated with a functional degradation in the "pan-modal" inferior and/or ventral temporal regions, and the "modality-specific" visual cortical origin of the ventral processing pathway. Baliki et al. (2018) used graph theory analysis to investigate the influence of anatomical and functional brain properties in response to intensive comprehensive aphasia treatment, and they found that the rsFC properties in aphasia were strongly associated with treatment outcomes instead of lesion location or size, and global efficiency and interhemispheric connectivity were related to improved language and visual attention performances, respectively. Combined with these previous studies, our results further illustrated that the network theory approach is feasible for accurate and informative mapping of brain functional networks in patients with aphasia, and that network theory might provide a more sensitive measure of brain dysfunction than those measures evaluating the properties of individual brain regions. The E_{loc} of brain network can be a potential indicator of basic speech function in patients with aphasia.

The classical framework for the study and treatment of aphasia is based on the symptom-lesion view, which considers specific behavioral and clinical symptoms in aphasia were caused by specific brain regions with particular functional specialization. Thus, the speech and language impairments that result from a stroke should be somewhat predictable (Dronkers et al., 2004). This study also explored the topological changes of each focal brain region from the local node attributes. The nodal degree is designated as the number of

edges of a node that connects with the remaining nodes, evaluating the strength of a node and indicating the impact of a particular node on the overall functional network. The nodal local efficiency can be defined as a measure of the fault tolerance of a network, indicating how well each subgraph exchanges information when the node is eliminated (Sporns, 2011). Compared with the HCs, patients with aphasia showed changed nodal degree and nodal local efficiency in the left insular cortex, postcentral gyrus, and central opercular cortex.

The insular cortex is an important part of the language center, and it is involved in the formation and expression of language, as well as explicit and implicit learning of grammar. It is closely associated with language comprehension (Wernicke area), language repetition (superior gyrus), language production (Broca area), and other language-related areas (Jakab et al., 2012). Patients with aphasia showed lower nodal degree and lower nodal local efficiency in the insular cortex, which may be the reason for their lower language fluency, language comprehension, and language repetition. Peter et al. conducted a positron emission tomography study and found that several regions, including the left anterior insula/prefrontal lobe, showed low metabolism in aphasia, which indicated that the decreased language fluency was due to the defect of a motor pronunciation plan (apraxia of speech) caused by the defects of the insula (Nestor et al., 2003). Patients with aphasia also showed changed nodal degree and nodal local efficiency in the left postcentral gyrus, central opercular cortex, which is the part of the dorsal stream (Hickok and Poeppel, 2007; Fridriksson et al., 2016). The dorsal stream (involving the fronto-parietal regions, including the pars opercularis, pars triangularis, pre- and post-central regions, and portions of the parietal lobe (Fridriksson et al., 2016) processes auditory-to-articulation information, including the feedback necessary for predicting the spoken output and online error detection and modification of speech output, and it provides *ad hoc* auditory and proprioceptive feedback that is crucial for producing fluent speech (Hickok and Poeppel, 2007; Fridriksson et al., 2016). The decreased nodal degree and nodal efficiency in the left postcentral gyrus and central opercular cortex region, indicate the damage to the dorsal stream and the impaired motor speech production functions, leading to the production of non-fluent speech. We maintain that the decreased nodal properties of local brain regions can further explain the motor speech and comprehension impairment.

There are some limitations to our study. First, the course of disease of the subjects varied greatly, and future studies should select more rigorous samples and have a larger sample size to verify the results of this study. Second, to further explore the link between network attributes and the mechanisms of aphasia, future studies should include longitudinal comparisons of treatments. Third, only one network template (Power-264) was calculated in this study, and future studies should compare whether the results of different network templates are different and whether there are more closely related clinical indicators in the process and network template selection.

CONCLUSION

In our study, graph-based theoretical approaches were applied to assessing the altered topological properties of brain functional networks in patients with aphasia using resting-state fMRI. The results show that patients with aphasia had decreased sigma, gamma, and E_{loc}. Notably, the E_{loc}were positively correlated with language ability, retelling, naming, and listening comprehension in patients with aphasia. Moreover, patients with aphasia had decreased nodal degree and nodal efficiency in the left postcentral gyrus, central opercular cortex, and insular cortex. We argue that the local efficiency of the brain network might be used as a potential indicator of basic speech function in patients with aphasia.

DATA AVAILABILITY STATEMENT

The raw data supporting the conclusions of this article will be made available by the authors, without undue reservation.

ETHICS STATEMENT

The studies involving human participants were reviewed and approved by the Medical Research Ethics Committee of The First Affiliated Hospital of Jinan University. The patients/participants provided their written informed consent to participate in this study.

AUTHOR CONTRIBUTIONS

XC contributed to the study design, execution, methodology, analysis, manuscript drafting, writing—review, and editing. LC and SZ contributed to methodology, software analysis, manuscript drafting and writing, review, and editing. XC, HW, and YD contributed to the execution of the study and reviewed the article. ZC and RH were involved in the conceptualization, funding acquisition, project administration, resources, and supervision. All authors read and approved the final manuscript.

FUNDING

This work was co-funded by the Medical Science and Technology Research Fund of Guangdong Province, China, Grant Nos. A2019407, A2021113 and the Project of Administration of Traditional Chinese Medicine of Guangdong Province of China, Grant No. 20201080.

SUPPLEMENTARY MATERIAL

The Supplementary Material for this article can be found online at: https://www.frontiersin.org/articles/10.3389/fnagi.2021.666301/full#supplementary-material

REFERENCES

Achard, S., and Bullmore, E. (2007). Efficiency and cost of economical brain functional networks. *PLoS Comput. Biol.* 3:e17. doi: 10.1371/journal.pcbi.0030017

Agosta, F., Galantucci, S., Valsasina, P., Canu, E., Meani, A., Marcone, A., et al. (2014). Disrupted brain connectome in semantic variant of primary progressive aphasia. *Neurobiol. Aging* 35, 2646–2655. doi: 10.1016/j.neurobiolaging.2014.05.017

Andersen, S. M., Rapcsak, S. Z., and Beeson, P. M. (2010). Cost function masking during normalization of brains with focal lesions: still a necessity? *Neuroimage* 53, 78–84. doi: 10.1016/j.neuroimage.2010.06.003

Baliki, M. N., Babbitt, E. M., and Cherney, L. R. (2018). Brain network topology influences response to intensive comprehensive aphasia treatment. *NeuroRehabilitation* 43, 63–76. doi: 10.3233/NRE-182428

Brett, M., Leff, A. P., Rorden, C., and Ashburner, J. (2001). Spatial normalization of brain images with focal lesions using cost function masking. *Neuroimage* 14, 486–500. doi: 10.1006/nimg.2001.0845

Byrne, L., Bucks, R. S., and Wilcock, G. K. (2000). Mini mental state examination. *Lancet* 355, 314–315. doi: 10.1016/S0140-6736(05)72308-4

Chen, L., Fan, X., Li, H., Ye, C., Yu, H., Gong, H., et al. (2018). Topological reorganization of the default mode network in severe male obstructive sleep apnea. *Front. Neurol.* 9:363. doi: 10.3389/fneur.2018.00363

Chen, Z., Hu, X., Chen, Q., and Feng, T. (2019). Altered structural and functional brain network overall organization predict human intertemporal decision-making. *Hum. Brain Mapp.* 40, 306–328. doi: 10.1002/hbm.24374

Dronkers, N. F., Wilkins, D. P., Van Valin, R. D., Redfern, B. B., and Jaeger, J. J. (2004). Lesion analysis of the brain areas involved in language comprehension. *Cognition* 92, 145–177. doi: 10.1016/j.cognition.2003.11.002

Engelter, S. T., Gostynski, M., Papa, S., Frei, M., Born, C., Ajdacic-Gross, V., et al. (2006). Epidemiology of aphasia attributable to first ischemic stroke: incidence, severity, fluency, etiology, and thrombolysis. *Stroke* 37, 1379–1384. doi: 10.1161/01.STR.0000221815.64093.8c

Fridriksson, J., den Ouden, D. B., Hillis, A. E., Hickok, G., Rorden, C., Basilakos, A., et al. (2018). Anatomy of aphasia revisited. *Brain* 141, 848–862. doi: 10.1093/brain/awx363

Fridriksson, J., Yourganov, G., Bonilha, L., Basilakos, A., Den Ouden, D. B., and Rorden, C. (2016). Revealing the dual streams of speech processing. *Proc. Natl. Acad. Sci. U.S.A.* 113, 15108–15113. doi: 10.1073/pnas.1614038114

Gao, S. (1992). Standardized Aphasia Battery of Chinese. *Chin. Mental Health J.* 6, 125–128.

Hickok, G., and Poeppel, D. (2004). Dorsal and ventral streams: a framework for understanding aspects of the functional anatomy of language. *Cognition* 92, 67–99. doi: 10.1016/j.cognition.2003.10.011

Hickok, G., and Poeppel, D. (2007). The cortical organization of speech processing. *Nat. Rev. Neurosci.* 8, 393–402. doi: 10.1038/nrn2113

Jakab, A., Molnár, P. P., Bogner, P., Béres, M., and Berényi, E. L. (2012). Connectivity-based parcellation reveals interhemispheric differences in the insula. *Brain Topogr.* 25, 264–271. doi: 10.1007/s10548-011-0205-y

Johnson, J. P., Meier, E. L., Pan, Y., and Kiran, S. (2020). Pre-treatment graph measures of a functional semantic network are associated with naming therapy outcomes in chronic aphasia. *Brain Lang.* 207:104809. doi: 10.1016/j.bandl.2020.104809

Latora, V., and Marchiori, M. (2001). Efficient behavior of small-world networks. *Phys. Rev. Lett.* 87:198701. doi: 10.1103/PhysRevLett.87.198701

Li, H., Jia, J., and Yang, Z. (2016). Mini-mental state examination in elderly Chinese: a population-based normative study. *J. Alzheimers. Dis.* 53, 487–496. doi: 10.3233/JAD-160119

Lichteim, L. (1885). On aphasia. *Brain* 7, 433–484. doi: 10.1093/brain/7.4.433

Nasreddine, Z. S., Phillips, N. A., Bédirian, V., Charbonneau, S., Whitehead, V., Collin, I., et al. (2005). The Montreal Cognitive Assessment, MoCA: a brief screening tool for mild cognitive impairment. *J. Am. Geriatr. Soc.* 53, 695–699. doi: 10.1111/j.1532-5415.2005.53221.x

Nestor, P. J., Graham, N. L., Fryer, T. D., Williams, G. B., Patterson, K., and Hodges, J. R. (2003). Progressive non-fluent aphasia is associated with hypometabolism centred on the left anterior insula. *Brain* 126, 2406–2418. doi: 10.1093/brain/awg240

Power, J. D., Cohen, A. L., Nelson, S. M., Wig, G. S., Barnes, K. A., Church, J. A., et al. (2011). Functional network organization of the human brain. *Neuron* 72, 665–678. doi: 10.1016/j.neuron.2011.09.006

Power, J. D., Schlaggar, B. L., Lessov-Schlaggar, C. N., and Petersen, S. E. (2013). Evidence for hubs in human functional brain networks. *Neuron* 79, 798–813. doi: 10.1016/j.neuron.2013.07.035

Rorden, C., Bonilha, L., Fridriksson, J., Bender, B., and Karnath, H. O. (2012). Age-specific CT and MRI templates for spatial normalization. *Neuroimage* 61, 957–965. doi: 10.1016/j.neuroimage.2012.03.020

Rubinov, M., and Sporns, O. (2010). Complex network measures of brain connectivity: uses and interpretations. *Neuroimage* 52, 1059–1069. doi: 10.1016/j.neuroimage.2009.10.003

Sporns, O. (2011). The non-random brain: efficiency, economy, and complex dynamics. *Front. Comput. Neurosci.* 5:5. doi: 10.3389/fncom.2011.00005

Tao, Y., and Rapp, B. (2019). The effects of lesion and treatment-related recovery on functional network modularity in post-stroke dysgraphia. *Neuroimage Clin.* 23:101865. doi: 10.1016/j.nicl.2019.101865

Wang, J., Wang, X., Xia, M., Liao, X., Evans, A., and He, Y. (2015). GRETNA: a graph theoretical network analysis toolbox for imaging connectomics. *Front. Hum. Neurosci.* 9:386. doi: 10.3389/fnhum.2015.00458

Watts, D. J., and Strogatz, S. H. (1998). Collective dynamics of "small-world" networks. *Nature* 393, 440–442. doi: 10.1038/30918

Wernicke, C. (1984). *Der Aphasische Symptomencomplex: Eine Psychologische Studie Auf Anatomischer Basis*. Breslau: M. Cohn und Weigert. doi: 10.1007/978-3-642-65950-8

Zhang, J., Wang, J., Wu, Q., Kuang, W., Huang, X., Yong, H., et al. (2011). Disrupted brain connectivity networks in drug-naive, first-episode major depressive disorder. *Biol. Psychiat.* 70, 334–342.

Conflict of Interest: The authors declare that the research was conducted in the absence of any commercial or financial relationships that could be construed as a potential conflict of interest.

frontiers in Aging Neuroscience

ORIGINAL RESEARCH
published: 20 December 2021
doi: 10.3389/fnagi.2021.718631

Scalp Acupuncture Attenuates Brain Damage After Intracerebral Hemorrhage Through Enhanced Mitophagy and Reduced Apoptosis in Rats

Peng Liu[1], Xinyang Yu[1,2], Xiaohong Dai[1], Wei Zou[1,2], Xueping Yu[1], Mingming Niu[3], Qiuxin Chen[1], Wei Teng[1], Ying Kong[4], Ruiqiao Guan[5] and Xiaoying Liu[1]*

[1] First Affiliated Hospital, Heilongjiang University of Chinese Medicine, Harbin, China, [2] Clinical Key Laboratory of Integrated Traditional Chinese and Western Medicine, Heilongjiang University of Chinese Medicine, Harbin, China, [3] Structural Biology and Developmental Neurobiology, St. Jude Children's Research Hospital, Memphis, TN, United States, [4] Second Affiliated Hospital, Heilongjiang University of Chinese Medicine, Harbin, China, [5] Integrated Chinese and Western Medicine, Zhongshan Hospital, Fudan University, Shanghai, China

OPEN ACCESS

Edited by:
John Zhang,
Loma Linda University, United States

Reviewed by:
Qingyi MA,
Loma Linda University, United States
Zhong Wang,
Soochow University, China
Anatol Manaenko,
Innsbruck Medical University, Austria

***Correspondence:**
Wei Zou
zouwei@hljucm.net

Specialty section:
This article was submitted to Neuroinflammation and Neuropathy, a section of the journal Frontiers in Aging Neuroscience

Received: 23 June 2021
Accepted: 18 November 2021
Published: 20 December 2021

Citation:
Liu P, Yu X, Dai X, Zou W, Yu X, Niu M, Chen Q, Teng W, Kong Y, Guan R and Liu X (2021) Scalp Acupuncture Attenuates Brain Damage After Intracerebral Hemorrhage Through Enhanced Mitophagy and Reduced Apoptosis in Rats. Front. Aging Neurosci. 13:718631. doi: 10.3389/fnagi.2021.718631

To study the effect of scalp acupuncture (SA) on the mitophagy signaling pathway in the caudate nucleus of Sprague-Dawley rats following intracerebral hemorrhage (ICH). An ICH model was established by injecting autologous arterial blood into the caudate nucleus in 200 male Sprague-Dawley rats, which were divided into five groups: sham, ICH, 3-methyladenine group (3-MA, 30 mg/kg), SA, and SA+3-MA. Animals were analyzed at 6 and 24 h as well as at 3 and 7 days. Composite neurological scale score was significantly higher in the SA group than in the ICH group. Transmission electron microscopy showed less structural damage and more autophagic vacuoles within brain in the SA group than in the ICH group. SA group showed higher levels of Beclin1, Parkin, PINK1, NIX protein, and a lower level of Caspase-9 in brain tissue. These animals consequently showed less neural cell apoptosis. Compared with the SA group, however, the neural function score and levels of mitophagy protein in the SA+3-MA group were decreased, neural cell apoptosis was increased with more severe structural damage, which suggested that 3-MA may antagonize the protective effect of SA on brain in rats with ICH. SA may mitigate the neurologic impairment after ICH by enhancing mitophagy and reducing apoptosis.

Keywords: scalp acupuncture, intracerebral hemorrhage, mitophagy, apoptosis, Baihui, Qubin

INTRODUCTION

Intracerebral hemorrhage (ICH) remains the most serious and intractable type of stroke in the world. Approximately two million people are affected each year (Keep et al., 2012), one in three dies within one month of the event (Krishnamurthi et al., 2013). Most patients are left with severe nerve defects and reduced quality of life. Primary brain damage after ICH includes physical damage such as hematoma, which can lead to secondary brain damage that is propagated by mitochondrial dysfunction, activation of microglia, and release of neurotransmitters and inflammatory mediators

(Fan et al., 2019). Ultimately, these responses lead to apoptosis and necrosis of the brain tissue, two strong determinants of neurological deterioration and poor prognosis (Bobinger et al., 2018).

Autophagy is involved in ICH pathophysiology (Niu et al., 2017) and is essential for homeostasis, including in the nervous system, but its detailed effects in physiology and pathophysiology are still poorly understood, limiting its usefulness as a therapeutic target. For example, one study showed that inhibiting autophagy helped reduce the severity of brain damage after iron-induced ICH (Chen et al., 2012), whereas another study showed that promoting autophagy decreased early brain injury in subarachnoid hemorrhage (Jing et al., 2012).

Intracerebral hemorrhage disturbs energy metabolism (Liu et al., 2018a) and so may involve a specific form of autophagy called mitophagy, which promotes mitochondrial renewal, maintains mitochondrial homeostasis, and removes damaged mitochondria (Ozden et al., 2011). It is possible that ICH involves the same mitophagy pathways as Parkinson's disease, which is attributed to mitochondrial dysfunction (Nunnari and Suomalainen, 2012). Insights from mitophagy proteins in Parkinson's may provide candidates for research in ICH. In Parkinson's, the PTEN-induced putative kinase protein 1 (PINK1)/PARK2 gene-encoded E3 ubiquitin ligase (Parkin) signaling cascade activates mitophagy (Chang et al., 2017). In hypoxic Parkinson's brain tissue, PINK1 can bind and stabilize the mitochondrial membrane after mitochondrial depolarization. PINK1 recruits the E3 ubiquitin ligase Parkin from the cytosol, and Parkin forms complexes with p62 and histone deacetylase (HDAC)6 to ubiquitinate proteins on the mitochondrial surface. These complexes interact with LC3, promoting formation and recruitment of mitochondrial autophagosomes (Geisler et al., 2010). Beclin1 can also participate in the translocation of Parkin to the mitochondrial membrane, thus promoting its interaction with mitophagy initiating factors (Choubey et al., 2014). NIX/BINP3L is a mitophagic receptor that helps clear mitochondria during mammalian reticulocyte maturation (Schweers et al., 2007), and it can bind to Atg8 autophagy family proteins to initiate mitophagy. NIX can also compete with Beclin1 for binding to Bcl-2, resulting in free Beclin1 that induces autophagy (Maiuri et al., 2007).

Autophagy can be stimulated by scalp acupuncture (SA) after ICH (Liu et al., 2019). SA has been widely used in China for thousands of years and has become a widespread complementary treatment for epilepsy, Parkinson's disease, and stroke (Liao et al., 2012). SA can stimulate the release of several neurochemicals and promote cerebral microcirculation, normal metabolism, neurogenesis, angiogenesis, and neuronal activity (Weng et al., 2016), but the exact mechanism has not yet been elucidated. In this work, we examined whether SA may activate autophagy, specifically mitophagy, after ICH in rats.

MATERIALS AND METHODS

Animals

This study involved 200 male Sprague-Dawley rats (6–7 weeks old, 250 ± 30 g) from the Animal Experiment Center of Heilongjiang University of Chinese Medicine (certificate SCXK(Heilongjiang) 2017-018). Animals were housed in a pathogen-free facility maintained at 45–65% ambient humidity, temperature of 23 ± 2°C, and 12-h day-night cycles. Food and water were provided *ad libitum*.

Prior to experiments, animals were deprived of food and water for 12 h, then they were allocated into the following five groups (n = 40 each): sham, ICH, 3-methyladenine (3-MA), SA, and SA+3-MA. These groups were treated as described below. Each group was divided into four subgroups and evaluated at 6 h, 24 h, 3 days, and 7 days after treatment. 3-MA is an autophagy inhibitor that reduces the occurrence of autophagy in subarachnoid hemorrhage without affecting the extent of bleeding (Jing et al., 2012).

ICH Induction

Intracerebral hemorrhage was achieved through blood autotransfusion, as described by Hua et al. (2002) in 3-MA, SA, and SA+3-MA groups. Rats were anesthetized intraperitoneally with pentobarbital (34.62 mg/kg, Selleck, Shanghai, China). Animals were immobilized in the prone position using a stereotaxic device (STW-3X, Chengdu Instrument Factory, Chengdu, China) to ensure that the anterior and posterior fontanelles remained on an even plane. After hair removal and disinfection, a 1-cm median incision was made in the scalp. The periosteum was pulled away to expose the bregma and the coronal suture of the cranium. A dental drill was placed 3.5 mm to the right of the bregma and 0.2 mm posterior to it (**Figure 1**). Then a circular opening with a diameter of 1 mm was bored with a dental drill down to the dura mater surface (Yang et al., 2018). The tail was disinfected, 2 cm was cut off from the end, and blood (50 μL) was collected using a microsyringe. The same microsyringe was inserted through the drill hole to the depth of the caudate putamen (∼6 mm). The blood from the tail was injected into the caudate putamen at 25 μL/min, and the needle was maintained in position for ∼2 min. Then the microsyringe was slowly removed, the skull opening was sealed with dental cement, and the skin was sutured and sterilized. Rats from the sham group underwent sham surgery without receiving blood, but received an injection of equal dose of saline. In the process of modeling, we placed rats on a thermostatic water blanket to keep their rectal temperature at about 37.5°C. When rats woke up and ate freely, the blanket was removed. According to Bederson' s scale, the model was successful if the score was 1–3 at 2 h after modeling (Bederson et al., 1986).

SA and 3-MA Treatment

At 6 h after ICH surgery, SA and SA+3-MA rats underwent SA intervention twice daily using no. 28 needles (Φ 0.35 × 40 mm, HuaTuo Brand, Suzhou Medical Appliance, Suzhou, China), which penetrated the DU20 (Baihui) acupoint for 1.5 cm through to the GB7 (Qubin) acupoint on the lesion side of the brain. Each treatment session was for 30 min. For each 30-min session, needling at 180–200 rpm was performed for three sessions, each lasting for 5 min (**Figure 2**). Rats were treated with acupuncture one time, two times, six times, and 14 times for 6 h, 24 h, 3 days, and 7 days, respectively. At 30 min before ICH, 3-MA (20 mg/ml

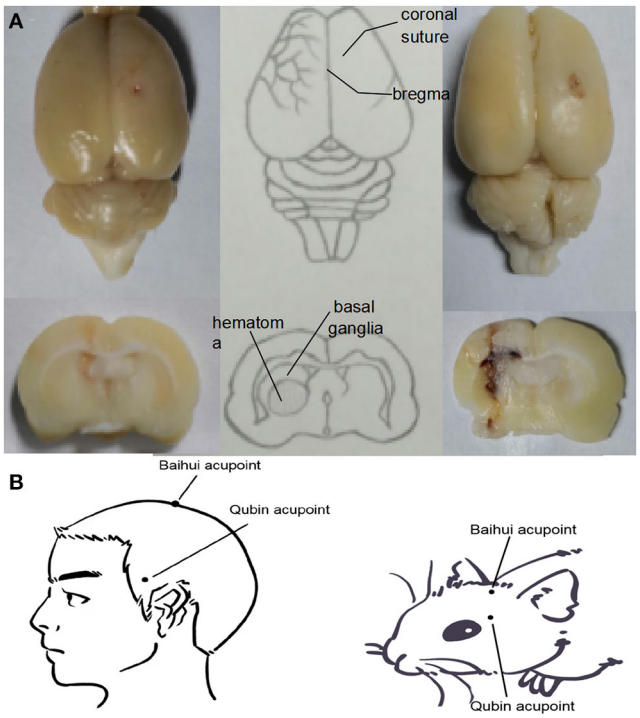

FIGURE 1 | (A) Location of the ICH hematoma. Schematic showing the position of the blood transfusion into the caudate putamen. **(B)** Location of Baihui acupoint and Qubin acupoint in human and rats. Baihui acupoint is located at the midpoint of the line between the double ear tips on the parietal bone, and Qubin acupoint is located at 2/3 of the line from the orbital margin to the external ear hole.

in saline) was injected intracranially at 30 mg/kg (Duan et al., 2017) into 3-MA and SA+3-MA animals.

Neural Function Assessment

At 6 h after all interventions, neural function was evaluated using the composite neurological scale score described by Garcia (Garcia et al., 1995). This composite contains a battery of tests to examine the following spontaneous activity, symmetry of limb movement, lateral rotation, forelimb movement, axial sensation, tentacle proprioception, and crawling. Animals were scored on a scale from 3 (lowest) to 21 (highest) points. Lower score indicates greater severity of neurological defects.

Histopathology

At 3 days after ICH, rats were injected intraperitoneally with pentobarbital (60 mg/kg) and then perfused with 4% paraformaldehyde. Brain tissue was removed, stained with hematoxylin for 5 min, destained with 1% hydrochloric acid-ethanol for 5 s, soaked in ammonia for 10 s, and sliced into 4-micron sections. Sections were counter-stained with eosin for 3 min, rinsed, coverslipped, and sealed with neutral gum. Images were captured using a light microscope (BX53; Olympus, Tokyo, Japan) at 400× magnification.

Transmission Electron Microscopy

Following sedation and perfusion as described for histopathology, brains were collected and placed in 2.5% glutaraldehyde buffer (pH 7.4). Five sections ($1 \times 1 \times 1$ mm^3) were excised from the lateral margin of the hematoma and fixed with 1% osmium. Samples were dehydrated through an ethanol gradient and embedded in epoxy resin. Sections were sliced to a thickness of 0.5 μm with an ultramicrotome (UC6; Leica, Wetzlar, Germany) at room temperature and stained with saturated uranium acetate. Sections were analyzed at 100,000× magnification using a transmission electron microscope (CM 100; Philips, Amsterdam, Netherlands), and digital images were taken using an ORCA-HR camera (Hamamatsu, Shizuoka, Japan).

Immunohistochemistry

Brain tissue (5 μm) were cut and fixed in formalin buffer after being paraffin-embedded. Paraffin-embedded sections of brain tissue were first deparaffinized and dehydrated. Slides were incubated with 0.3% H_2O_2 for 10 min and washed with ddH_2O three times, 3 min each time. Antigen retrieval was undertaken in a pressure cooker for 10 min with 0.01 M citrate buffer and washed with phosphate-buffered saline (PBS) three times, 5 min each time. Five percent bovine serum albumin (BSA) was applied to the specimen sections to block nonspecific protein for 20 min at room temperature. The primary antibodies, which were rabbit antibodies against Beclin1 (bs-1353R, Bioss, China), Parkin (bs-23687R, Bioss, China), PINK1 (6946, CST, USA), or BNIP3L/NIX (12396, CST, USA), were incubated for 2 h at 37°C and washed with PBS three times, each time 3 min. After washing, slides were washed and then incubated with secondary antibody, goat anti-rabbit IgG (ab7090, Abcam, UK), at 37°C for 30 min and washed with PBS three times, 3 min each time. The sections were stained with diaminobenzidine for ∼5–10 min. Five nonoverlapping visual fields at 400×magnification were analyzed from each sample using a Moticam 3000 (Hong Kong Special Administrative Region, China) microphotography system. The mean number of positive cells was calculated using Image-Pro Plus 6.0 software (Xue et al., 2014).

Terminal Deoxynucleotidyl Transferase (TdT)-Mediated DUTP Nick end Labeling (TUNEL)

Paraffin sections of brain tissue were dewaxed, rehydrated in water, and permeabilized at room temperature for 30 min in 10 mM Tris/HCl (pH 7.4-8.0) containing pepsin K (20 μg/ml). Sections were rinsed two times with phosphate-buffered saline (PBS), incubated with 50 μL TUNEL reaction mixture for 1 h at 37°C, rinsed three times with PBS, incubated with 50 μL of inverter-POD for 30 min at 37°C, and again rinsed three times with PBS. Sections were incubated with DAB at room temperature for 10 min, thoroughly rinsed with distilled water, and counterstained with hematoxylin for 1 min. Coverslips were sealed with neutral gum sealant. Three slices of each rat brain tissue were selected for observation, and five nonoverlapping visual fields around the hematoma were selected

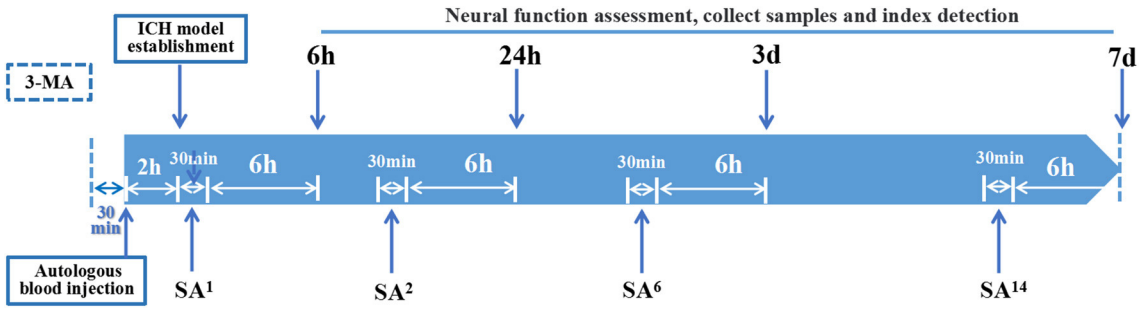

FIGURE 2 | Time axis: At 30 min before establishing ICH model, 3-MA was injected into the lateral ventricle of rats in 3-MA and SA+3-MA group. The success rate of ICH model establishment was evaluated 2 h after autologous blood injection. All established rat models were given acupuncture for the first time. Rats were treated with SA once, twice, 6 times, and 14 times for 6-h, 24-h, 3-day, and 7-day models, respectively. Each treatment takes 30 min. Neurological function, sampling and target detection were evaluated at 6 h, 24 h, 3 days, and 7 days after SA treatment respectively.

for each slice. The images were taken from penumbra region. Visual fields were captured at 400e magnification using the Motic3000 system. Mean positivity was calculated using Image-Pro Plus 6.0.

Western Blot Assay

We selected the striatum in brain tissue for sampling. The striatum is the prone site of intracerebral hemorrhage. We used a stereotactic instrument to accurately inject autologous blood into the rat brain. We take brain tissue and preserve the tissue with a thickness of about 6 mm centered on the injection point. Brain tissues were homogenized in lysis buffer and centrifuged, and the supernatant (50 g total protein) was fractionated by SDS-PAGE. Proteins were transferred to a polyvinylidene fluoride membrane and blocked in 5% skim milk for one hour at room temperature. Membranes were incubated at 4°C overnight with rabbit primary antibodies against Beclin1 (Bioss, China), Parkin (Bioss, China), PINK1 (CST, USA), BNIP3L (CST, USA), or Caspase-9 (bs-0049R, Bioss, China). Blots were incubated with rabbit anti-β-actin (bs-0061R, Bioss, China) as a loading control. After three times of washing every 10 min with PBST, membranes were incubated with goat anti-rabbit IgG (Abcam, UK) for 2 h at room temperature. Protein signal was detected using a 3,3′-diaminobenzidine (DAB) electrochemiluminescence system (Beyotime, Jiangsu, China). Optical density was measured using ImageJ software (NIH, Bethesda, MD, USA).

Data Analysis

Data were expressed as mean ± SD and analyzed using SPSS 22.0 (IBM, Armonk, NY, USA). Intergroup differences in neural function defect score were assessed for significance using one-way ANOVA and the Student-Newman-Keuls test. Intergroup differences in results for immunohistochemistry, Western blotting, or TUNEL assay were assessed for significance using one-way ANOVA and Tukey's *post hoc* test. The value $p < 0.05$ was considered statistically significant.

RESULTS

SA Improves Neural Function Score After ICH in Rats

To measure the severity of neural function defects after ICH, we used a composite neurological scale score based on seven physical functions. The sham group showed a similar score across the different time points (**Figure 3**). The ICH group scored significantly lower than the sham group at all time points. Compared with the ICH group, the SA group scored significantly higher, while the 3-MA group scored significantly lower at all time points. These results suggest that SA can mitigate ICH-related damage to improve neural function.

SA Can Attenuate ICH-Related Brain Histopathology and Neural Cell Apoptosis

Next, we examined structural effects of ICH on brain tissue to determine whether SA could attenuate ICH-induced secondary brain damage and apoptosis. At 3 days after sham or ICH surgery, brain tissue was isolated and stained with hematoxylin–eosin (**Figure 4**) and TUNEL assay (**Figure 6**). Brain tissue from sham-operated animals showed normal morphology and structure, including tight arrangement of cells and uniform chromatin without obvious damage or inflammatory infiltration, the minimum number of apoptotic cells. In contrast, brain tissue from the ICH group showed noticeable damage to neural structures around the hemorrhage, swollen and deformed cells, and vacuoles of various sizes among intercellular space. Tissue from the SA group showed less severe cell injury-edema, inflammatory infiltration, and apoptotic cells than tissue from the ICH group. Conversely, 3-MA exacerbated ICH-induced cell damage, the maximum apoptotic cells number in the 3-MA group. SA+3-MA group showed less severe structural damage than the 3-MA group, suggesting that SA can mitigate the effects of 3-MA. The SA+3-MA group displayed more apoptosis than the ICH group and far more than the SA group. These findings by TUNEL assay were confirmed in Western blotting of brain tissue (**Figure 7**).

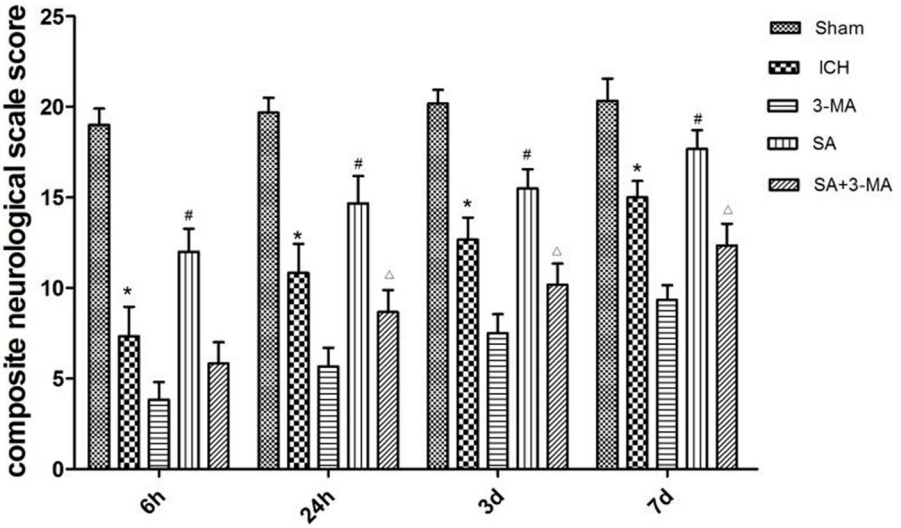

FIGURE 3 | Effect of SA on composite neurological scale score in a rat model of ICH. The results show that SA improves neural function score after ICH in rats. Neuronal function was analyzed in seven behavioral tests. Animals were scored on a scale of 3–21, where lower score indicated more severe neural defect. Data are mean ± SD ($n = 6$). Intergroup differences were analyzed using one-way ANOVA and the Student-Newman-Keuls test. $^{*}p < 0.05$, vs. sham; $^{\#}p < 0.05$, vs. ICH; $^{\triangle}p < 0.01$ vs. SA. ICH, intracerebral hemorrhage; SA, scalp acupuncture; 3-MA, 3-methyladenine.

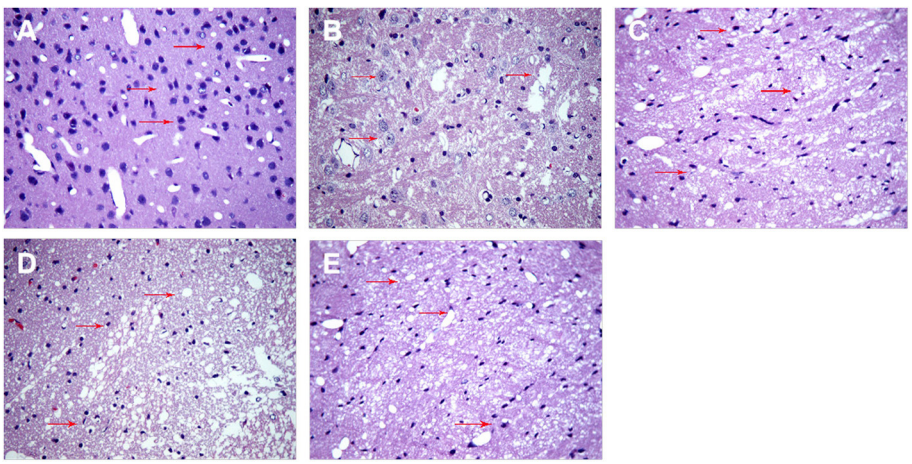

FIGURE 4 | SA mitigates cell injury-edema, inflammatory infiltration in the peri hemorrhagic penumbra of rats with ICH. Brain tissue structure was analyzed at 3 days after sham or ICH surgery by hematoxylin-eosin staining. Representative images are shown from the **(A)** sham, **(B)** ICH, **(C)** 3-MA, **(D)** SA, and **(E)** SA + 3-MA groups. Red arrows indicate inflammatory cells and necrotic cells at the site of injury. Magnification: 400×. ICH, intracerebral hemorrhage; SA, scalp acupuncture; 3-MA, 3-methyladenine.

SA Promotes Mitophagy After ICH

Intracerebral hemorrhage -induced cellular damage can activate mitophagy as a way to replace damaged mitochondria. We examined neural cells by transmission electron microscopy at 3 days after sham or ICH surgery to determine whether SA can activate mitophagy (**Figure 5**). In the sham group, the nuclei of neurons were large and round, the nucleoli were clear, and the organelles in the cytoplasm looked normal. Most importantly, mitochondria were abundant and both the inner and outer membranes were clearly visible. In contrast, in the ICH group, the mitochondria were swollen and deformed, the mitochondrial crest was blurred, and it even disappeared completely in some cases. Autolysosomes were observed, suggesting that autophagy was occurring. The 3-MA group showed loose, elongated mitochondria, and a few autophagosomes containing damaged mitochondria. In contrast, the SA group showed less swelling of nerve cells, damage of the cellular and nuclear membrane, and the damage of mitochondrial than that of ICH group. What's more, more autophagosomes and autolysosomes were detected within cells among the SA group. The SA+3-MA group

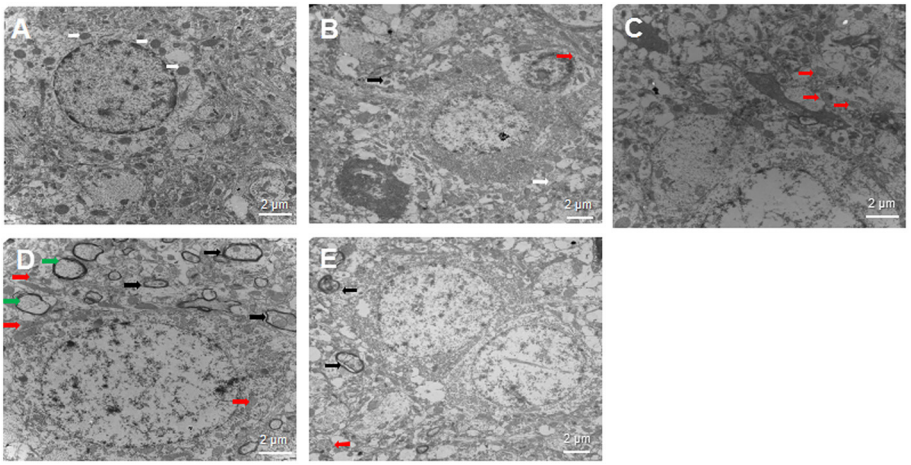

FIGURE 5 | Effect of SA on neural cell ultrastructure after ICH. Autophagy is activated following ICH. Brain samples were isolated from rats at 3 days after sham or ICH surgery and analyzed by transmission electron microscopy. Representative sections are shown from the **(A)** sham, **(B)** ICH, **(C)** 3-MA, **(D)** SA, and **(E)** SA+3-MA groups. Magnification, 10000× **(A, C, D)**, 8000× **(B)** or 7000× **(E)**. White arrows indicate healthy mitochondria; red arrows, damaged mitochondria; black arrows, autophagosome; and green arrows, autolysosomes. Scale bars, 2 μm. ICH, intracerebral hemorrhage.

showed more loose mitochondria and autophagosomes than the SA group.

SA Upregulates Mitophagy Markers in Neural Cells After ICH

To confirm mitophagy activation in neural cells after ICH, we examined specific protein markers by immunohistochemistry and Western blot. Brain sections from all the five groups were probed for the presence of PINK1, Parkin, Beclin1, and NIX (**Figure 6**). Immunohistochemistry revealed significantly higher levels of all proteins in the SA group than the other groups at all time points. Levels of all proteins significantly increased at 3 days and remained stable for up to 7 days after treatment. The 3-MA group showed lower protein levels than the ICH group in the Beclin1, whereas the others tended to show lower levels than the ICH group, although the difference failed to reach statistical significance. These findings by immunohistochemistry were confirmed in Western blotting of brain tissue (**Figure 7**).

DISCUSSION

The pathology of ICH is quite complex. Brain injuries caused by hemorrhage can be classified as primary and secondary injuries. Hematoma reduces local tissue blood supply and initiates secondary ischemia reperfusion injury, which involves mitochondrial damage, ultimately leading to neural cell apoptosis through death receptor signaling and endoplasmic reticulum stress signals (Shimada et al., 2012). Mitochondrial impairment induced by the hematoma is a major factor leading to secondary damage. If mitochondria can be preserved through the specific form of autophagy called mitophagy, this secondary damage may be ameliorated. The inflammatory reaction and coagulation cascade caused by hematoma can lead to edema of the surrounding brain tissue, which causes the more serious and lasting damage, and has a negative impact on the prognosis of intracerebral hemorrhage. Our previous studies have shown that SA can reduce the water content of brain tissue in rats with ICH to alleviate the secondary injury of brain edema. Further study found that SA could reduce inflammatory injury and brain edema by regulating the Mincle/Syk pathway (Liu et al., 2018b). SA could reduce neuronal death and inflammation and alleviate brain edema after intracerebral hemorrhage by downregulating miR-23a-3p (Kong et al., 2021). Research has confirmed that acupuncture may enhance mitochondrial respiratory chain enzyme activity and improve mitochondrial dysfunction (Zhang et al., 2014). Previous studies in our team have indicated that SA may preserve neuronal structure and neural function after ICH through inhibition of cell apoptosis by Sonic hedgehog pathway and activation of autophagy (Zhang et al., 2018; Liu et al., 2019). In this work, we induced ICH in male rats through the injection of autologous blood, and then we examined the possibility that SA protected against neuronal apoptosis and brain tissue damage through eliminating damaged mitochondria by mitophagy pathway. The mechanism elucidated in this work might be conducive to providing a new direction for the clinical application and basic research of SA treatment for ICH.

In this study, we found that SA could improve neural function score, reduce the number of apoptotic cells, alleviate mitochondrial damage, and significantly promote expression of mitophagy-related proteins in our rat model of ICH. Using transmission electron microscopy, immunohistochemistry, and Western blotting, we found that not only ICH but also SA activated mitophagy through the PI3KIII, PINK1/Parkin, and NIX pathways in brain tissue. More importantly, the extent of increased mitophagy was higher in SA group than in ICH group, while mitochondrial damage, neuronal apoptosis, and brain injury in ICH group were significantly higher than

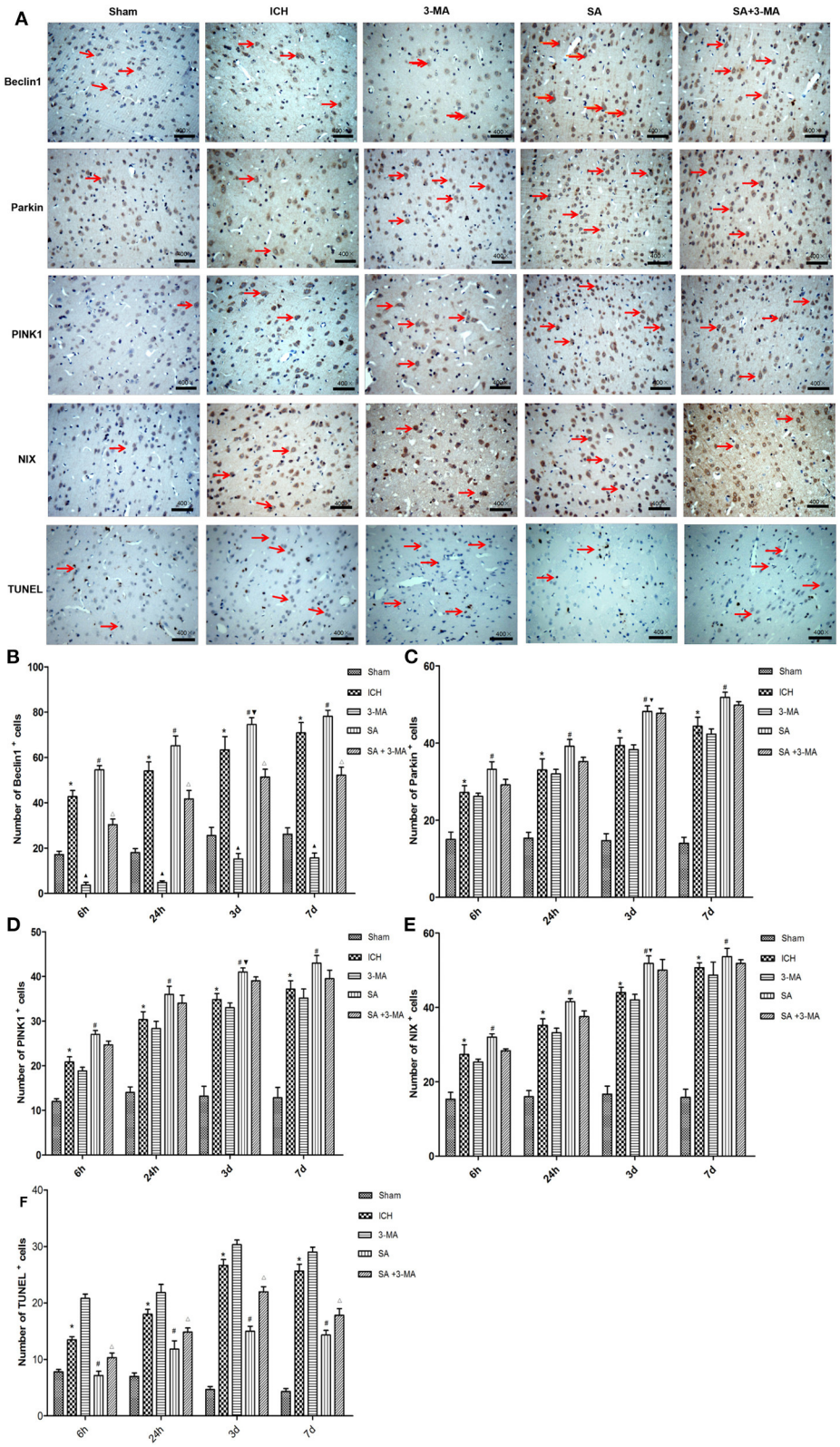

FIGURE 6 | Immunohistochemistry: SA upregulates mitophagy-related proteins and decrease the number of TUNEL positive cells after ICH. **(A)** Immunohistochemistry and TUNEL of brain tissue. Arrows mark positive cells. Magnification, 400×. Scale bars, 50 μm. **(B–F)** Quantitation of numbers of cells positive *(Continued)*

FIGURE 6 | for Beclin1, PINK1, Parkin, NIX and apoptotic cells in fields of view at 400× magnification. Data are mean ± SD ($n = 6$). Significance was assessed by one-way ANOVA, followed by Tukey's *post hoc* test. $^{*}P < 0.05$, *vs*. sham; $^{\#}P < 0.05$, *vs*. ICH; $^{\blacktriangle}P < 0.05$, *vs*. ICH; $^{\triangle}P < 0.05$, *vs*. SA; $^{\blacktriangledown}P < 0.05$, *vs*. 24h SA group. ICH, intracerebral hemorrhage; SA, scalp acupuncture; 3-MA, 3-methyladenine.

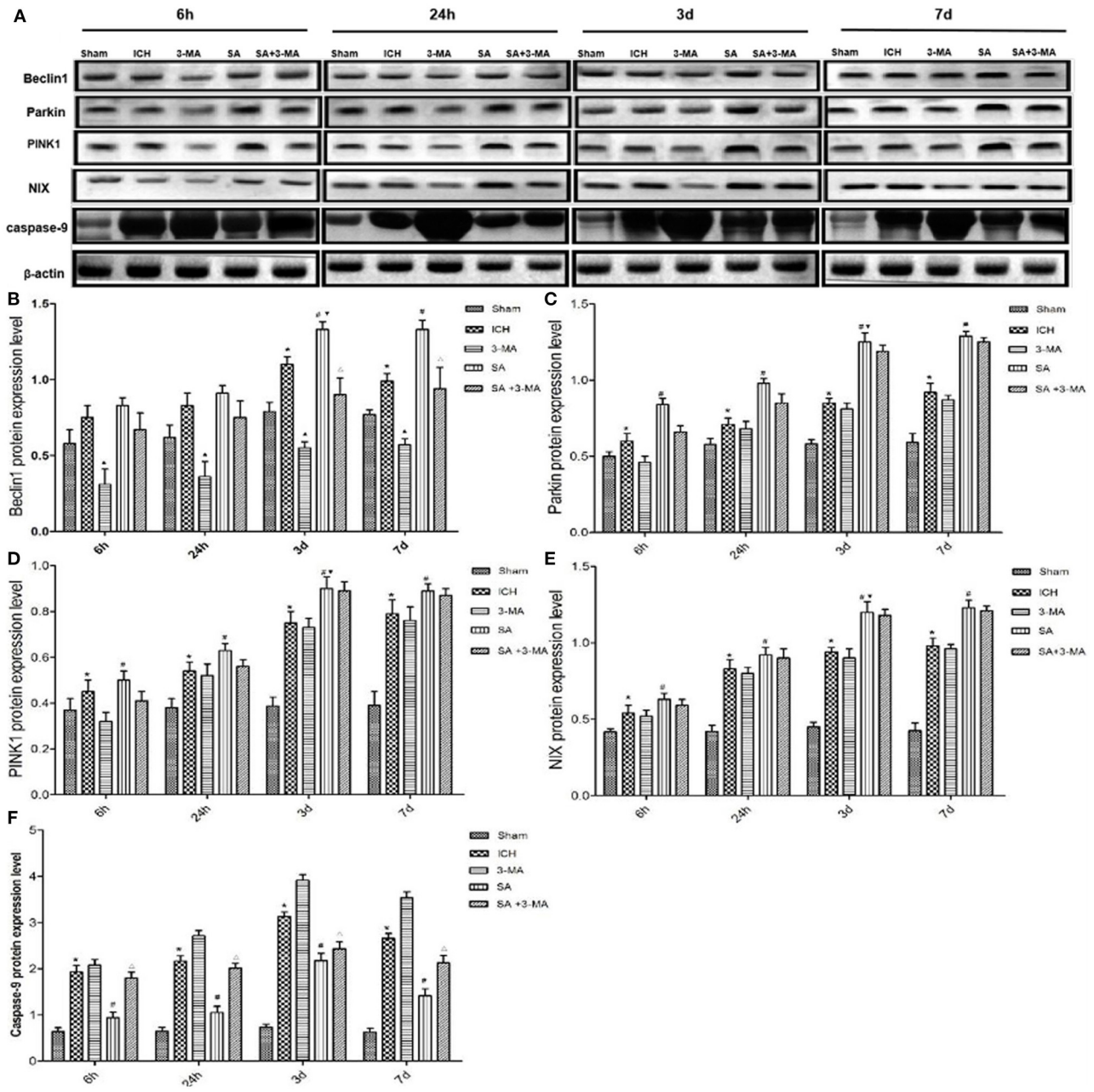

FIGURE 7 | Western blotting: SA upregulates mitophagy-related proteins and decrease the apoptosis-related protein after ICH. **(A)** Western blotting of proteins relevant to mitophagy activation in rat brain tissue after ICH. Protein levels were normalized to levels of β-actin as loading control. **(B–F)** Quantitation of levels of Beclin1, Parkin, PINK1, NIX and Caspase-9. Data are mean ± SD ($n = 6$). Significance was assessed using one-way ANOVA, followed by Tukey's *post hoc* test. $^{*}P < 0.05$, vs. sham; $^{\#}P < 0.05$, *vs*. ICH; $^{\blacktriangle}P < 0.05$, *vs*. ICH; $^{\triangle}P < 0.05$, *vs*. SA; $^{\blacktriangledown}P < 0.05$, *vs*. 24h SA group. ICH, intracerebral hemorrhage; SA, scalp acupuncture; 3-MA, 3-methyladenine.

the SA group. Accordingly, we speculated that SA might attenuate brain damage after ICH through enhanced mitophagy, a consequence of reduced apoptosis. Further, we applied 3-MA to inhibit autophagy by blocking autophagosome formation *via*

the inhibition of class III PI3K (Castino et al., 2010). Compared with SA group, we found that the score, structural damage, and expression of mitophagy proteins in the SA+3-MA group were decreased, especially of Beclin1, but the level of Caspase-9 was increased in our rat model of ICH. It was found that 3-MA exacerbated hypoxic-ischemic brain damage in neonatal rats by inhibiting mitophagy, resulting in infarct expansion (Liu et al., 2017). Together, we provided evidence that SA might prevent the brain tissue impairment from ICH injury through enhanced mitophagy, thus reducing apoptosis.

Physiological activation of autophagy can eliminate the accumulation of damaged organelles and abnormal proteins, inhibiting the expansion of harmful signals and the death of neurons (Liu et al., 2010). Autophagy promotes cell survival under stress conditions such as starvation, hypoxia, and infection (He et al., 2012; Choi et al., 2013; Green and Levine, 2014). Studies have shown that enhancing autophagy plays a protective role in nervous system diseases. In a model of subarachnoid hemorrhage in rats, activation of autophagic pathways could reduce early brain injury (Jing et al., 2012). Research reported that electroacupuncture might strengthen autophagy *via* mTOR signaling pathway, reducing the early impairment in cerebral ischemia rats (Wu et al., 2016). It is consistent with our current results.

Whether autophagy exerts profitable or detrimental effection remains controversial. It is suggested that activation of autophagy could aggravate brain injury in ICH model, which may be relevant to regulation of NF-kB pathway, thus promoting inflammatory response and apoptosis (Shen et al., 2016). The reasons for the contradiction between the results above and that of our work may be involved in different methods of modeling animal species and intervention methods. Whether there exists appropriate, overactivated, or defective autophagy in the course of this disease deserves further investigation.

Scalp penetration acupuncture therapy for ICH has been proved to be clinically effective (Zheng et al., 2011). It can ameliorate patient neurological defects, make it easier to obtain the sense of "Deqi," and reduce the effect of pain, achieving a better prognosis (Wang et al., 2016). The inhibitory effects of acupuncture on apoptosis in brain tissue after ICH have been confirmed. Previous studies have shown that acupuncture can inhibit the apoptosis of brain tissue cells in ICH model rats by upregulating the level of Bcl-2 mRNA and downregulating the level of Bax mRNA (Li et al., 2017). Acupuncture can reduce apoptosis through endoplasmic reticulum stress (Sun et al., 2020), oxidative stress (Li et al., 2018), and PI3K/Akt signaling (Wang et al., 2019). Both acupuncture and electroacupuncture are considered as nondrug treatments for ICH. Electroacupuncture can also increase Bcl-2 and reduce Caspase-3, Bax, and p53 in the brain tissue of rats with ICH (Zhu et al., 2017; Guan et al., 2021). However, electroacupuncture and acupuncture are two different stimulation methods. Electroacupuncture relies on electric current to stimulate tissue. Acupuncture we use achieved the purpose of stimulation through mechanical actions such as lifting, inserting, twisting, and turning. The effect of electroacupuncture on organisms cannot be completely equal to that of acupuncture. In this study, we focused on the selective autophagy pathway-mitophagy. The results showed that acupuncture could reduce the apoptosis of brain cells by enhancing mitophagy, and then improve neurological function. This finding has rarely been reported in previous studies. However, this study did not explore the mechanism regulating autophagy and apoptosis by SA. Our study provided some insights so far into the relationship between mitophagy and post-ICH neural repair, which might implicate the PI3KIII, PINK1-Parkin, and NIX signaling pathways. These pathways are unlikely to be the only ones involved after ICH, since mitophagy can also occur in mice lacking Parkin and NIX (Yuan et al., 2017). In future, we will explore the role of other mitochondrial pathways in ICH model and realize the mechanism of SA for mitophagy enhancement and apoptosis attenuation.

DATA AVAILABILITY STATEMENT

The raw data supporting the conclusions of this article will be made available by the authors, without undue reservation.

ETHICS STATEMENT

The animal study was reviewed and approved by Animal Experiment Center of Heilongjiang University of Chinese Medicine.

AUTHOR CONTRIBUTIONS

PL, WZ, and X-PY: designed the study. PL: wrote the manuscript. X-YY and X-HD: conducted most of the experiments and collected the data. MN, QC, WT, YK, X-YL, and R-QG participated in the discussion and helped with the experiment. All authors have read and approved the final.

FUNDING

This study was funded by the National Natural Science Foundation of China (No. 81774416). Heilongjiang University of Chinese Medicine Graduate Innovation Fund Project (No. 2017yjscx005).

ACKNOWLEDGMENTS

We thank the First Affiliated Hospital of Heilongjiang University of Chinese Medicine for providing funding and necessary facilities to complete this project.

REFERENCES

Bederson, J. B., Pitts, L. H., Tsuji, M., Nishimura, M. C., Davis, R. L., and Bartkowski, H. (1986). Rat middle cerebral artery occlusion: evaluation of the model and development of a neurologic examination. *Stroke*. 17, 472–476. doi: 10.1161/01.STR.17.3.472

Bobinger, T., Burkardt, P., Huttner, B., and Manaenko, A. (2018). Programmed Cell Death after intracerebral hemorrhage. *Curr.*

Neuropharmacol. 16, 1267–1281. doi: 10.2174/1570159X15666170602112851

Castino, R., Bellio, N., Follo, C., Murphy, D., and Isidoro, C. (2010). Inhibition of PI3k class III-dependent autophagy prevents apoptosis and necrosis by oxidative stress in dopaminergic neuroblastoma cells. *Toxicol Sci.* 117, 152–162. doi: 10.1093/toxsci/kfq170

Chang, J. Y., Yi, H. S., Kim, H. W., and Shong, M. (2017). Dysregulation of mitophagy in carcinogenesis and tumor progression. *Biochim. Biophys. Acta Bioenerg.* 1858, 633–640. doi: 10.1016/j.bbabio.2016.12.008

Chen, C. W., Chen, T. Y., Tsai, K. L., Lin, C. L., Yokoyama, K. K., Lee, W. S., et al. (2012). Inhibition of autophagy as a therapeutic strategy of iron-induced brain injury after hemorrhage. *Autophagy*. 8, 1510–1520. doi: 10.4161/auto.21289

Choi, A. M., Ryter, S. W., and Levine, B. (2013). Autophagy in human health and disease. *N. Engl. J. Med*. 368, 651–662. doi: 10.1056/NEJMra1205406

Choubey, V., Cagalinec, M., Liiv, J., Safiulina, D., Hickey, M. A., Kuum, M., et al. (2014). BECN1 is involved in the initiation of mitophagy: it facilitates PARK2 translocation to mitochondria. *Autophagy*. 10, 1105–1119. doi: 10.4161/auto.28615

Duan, X. C., Wang, W., Feng, D. X., Yin, J., Zuo, G., Chen, D. D., et al. (2017). Roles of autophagy and endoplasmic reticulum stress in intracerebral hemorrhage induced secondary brain injury in rats. *CNS Neurosci. Ther.* 23, 554–566. doi: 10.1111/cns.12703

Fan, W., Zhang, X., Li, D., Shen, H., Liu, Y., and Chen, G. (2019). Detrimental role of miRNA-144-3p in intracerebral hemorrhage induced secondary brain injury is mediated by formyl peptide receptor 2 downregulation both *in vivo* and *in vitro*. *Cell Transplant*. 28, 723–738. doi: 10.1177/0963689718817219

Garcia, J. H., Wagner, S., Liu, K. F., and Hu, X. J. (1995). Neurological deficit and extent of neuronal necrosis attributable to middle cerebral artery occlusion in rats. *Statistic. Valid. Stroke*. 26, 627–634. doi: 10.1161/01.STR.26.4.627

Geisler, S., Holmström, K. M., Skujat, D., Fiesel, F. C., Rothfuss, O. C., Kahle, P. J., et al. (2010). PINK1/Parkin-mediated mitophagy is dependent on VDAC1 and p62/SQSTM1. *Nat. Cell. Biol.* 2, 119–131. doi: 10.1038/ncb2012

Green, D. R., and Levine, B. (2014). To be or not to be? How selective autophagy and cell death govern cell fate. *Cell*. 157, 65–75. doi: 10.1016/j.cell.2014.02.049

Guan, R., Li, Z., Dai, X., Zou, W., Yu, X., Liu, H., et al. (2021). Electroacupuncture at GV20- GB7 regulates mitophagy to protect against neurological deficits following intracerebral hemorrhage via inhibition of apoptosis. *Mol. Med. Rep.* 24:492. doi: 10.3892/mmr.2021.12131

He, C., Bassik, M. C., Moresi, V., Sun, K., Wei, Y., Zou, Z., et al. (2012). Exercise-induced BCL2-regulated autophagy is required for muscle glucose homeostasis. *Nature*. 481, 511–515. doi: 10.1038/nature10758

Hua, Y., Schallert, T., Keep, R. F., Wu, J., Hoff, J. T., Behavioral, X., et al. (2002). Behavioral tests after intracerebral hemorrhage in the rat. *Stroke.* 33, 2478–2484. doi: 10.1161/01.STR.0000032302.91894.0F

Jing, C. H., Wang, L., Liu, P. P., Wu, C., Ruan, D., and Chen, G. (2012). Autophagy activation is associated with neuroprotection against apoptosis via a mitochondrial pathway in a rat model of subarachnoid hemorrhage. *Neuroscience.* 201, 144–53. doi: 10.1016/j.neuroscience.2012.03.055

Keep, R. F., Hua, Y., and Intracerebral, X. I. G. (2012). Haemorrhage: mechanisms of injury and therapeutic targets. *Lancet Neurol.* 11, 720–731. doi: 10.1016/S1474-4422(12)70104-7

Kong, Y., Li, S., Zhang, M., Xu, W., Chen, Q., Zheng, L., et al. (2021). Acupuncture ameliorates neuronal cell death, inflammation, and ferroptosis and Downregulated miR-23a-3p after intracerebral hemorrhage in rats. *J Mol Neurosci*. 71:1863–1875. doi: 10.1007/s12031-020-01770-x

Krishnamurthi, R. V., Feigin, V. L., Forouzanfar, M. H., Mensah, G. A., Connor, M., Bennett, D. A., et al. (2013). Global burden of diseases, injuries, risk factors study 2010 (Gbd 2010); GBD stroke experts group. global and regional burden of first-ever ischaemic and haemorrhagic stroke during 1990–2010: findings from the global burden of disease Study 2010. *Lancet Glob. Health*. 1:e259–81. doi: 10.1016/S2214-109X(13)70089-5

Li, S., Bao, L., Si, L., Wang, X., Bo, A. (2018). Research on roles of mongolian medical warm acupuncture in inhibiting p38 MAPK activation and apoptosis of nucleus pulposus cells. *Evid Based Complement Alternat Med*. 9:6571320. doi: 10.1155/2018/6571320

Li, Z., Zheng, X., Li, P., Itoua, E. S., Moukassa, D., Ndinga, A. F. (2017). Effects of acupuncture on mRNA Levels of apoptotic factors in perihematomal brain tissue during the acute phase of cerebral Hemorrhage. *Med Sci Monit*. 23:1522–1532. doi: 10.12659/msm.897689

Liao, C. C., Lin, J. G., Tsai, C. C., Lane, H. L., Su, T. C., Wang, H. H., et al. (2012). An investigation of the use of traditional chinese medicine in stroke patients in taiwan. *Evid Based Complem. Alternat. Med*. 2012:387164. doi: 10.1155/2012/387164

Liu, C., Gao, Y., Barrett, J., and Hu, B. (2010). Autophagy and protein aggregation after brain ischemia. *J. Neurochem*. 115, 68–78. doi: 10.1111/j.1471-4159.2010.06905.x

Liu, H., Sun, X., Zou, W., Leng, M., Zhang, B., Kang, X., et al. (2017). Scalp acupuncture attenuates neurological deficits in a rat model of hemorrhagic stroke. *Complem. Ther. Med*. 32, 85–90. doi: 10.1016/j.ctim.2017.03.014

Liu, H., Zhang, B., Li, X. W., Feng, P. P., Du, J., Lou, K. L., et al. (2019). Penetrative needling improves neurological function by up-regulating expression of autophagy related protein LC3 in rats with hemorrhagic stroke. *Zhen Ci Yan Jiu*. 44, 637–642. doi: 10.13702/j.1000-0607.180860

Liu, T., Zhou, J., Cui, H., Li, P., Li, H., Wang, Y., et al. (2018a). Quantitative proteomic analysis of intracerebral hemorrhage in rats with a focus on brain energy metabolism. *Brain Behav.* 8:e01130. doi: 10.1002/brb3.1130

Liu, X. Y., Dai, X. H., Zou, W., Yu, X. P., Teng, W., Wang, Y., et al. (2018b). Acupuncture through Baihui (DU20) to Qubin (GB7) mitigates neurological impairment after intracerebral hemorrhage. *Neural. Regen. Res.* 13, 1425–1432. doi: 10.4103/1673-5374.235298

Maiuri, M. C., Le Toumelin, G., Criollo, A., Rain, J. C., Gautier, F., Juin, P., et al. (2007). Functional and physical interaction between Bcl-X(L) and a BH3-like domain in Beclin-1. *EMBO J*. 26, 2527–2539. doi: 10.1038/sj.emboj.7601689

Niu, M., Dai, X., Zou, W., Yu, X., Teng, W., Chen, Q., et al. (2017). Autophagy, endoplasmic reticulum stress and the unfolded protein response in intracerebral hemorrhage. *Transl. Neurosci.* 8, 37–48. doi: 10.1515/tnsci-2017-0008

Nunnari, J., and Suomalainen, A. (2012). Mitochondria: in sickness and in health. *Cell*. 148, 1145–1159. doi: 10.1016/j.cell.2012.02.035

Ozden, O., Park, S. H., Kim, H. S., Jiang, H., Coleman, M. C., Spitz, D. R., et al. (2011). Acetylation of MnSOD directs enzymatic activity responding to cellular nutrient status or oxidative stress. *Aging* 3, 102–107. doi: 10.18632/aging.100291

Schweers, R. L., Zhang, J., Randall, M. S., Loyd, M. R., Li, W., Dorsey, F. C., et al. (2007). NIX is required for programmed mitochondrial clearance during reticulocyte maturation. *Proc. Natl. Acad. Sci.* 104, 19500–19505. doi: 10.1073/pnas.0708818104

Shen, X., Ma, L., Dong, W., Wu, Q., Gao, Y., Luo, C., et al. (2016). Autophagy regulates intracerebral hemorrhage induced neural damage via apoptosis and NF-κB pathway. *Neurochem. Int*. 96, 100–112. doi: 10.1016/j.neuint.2016.03.004

Shimada, K., Crother, T. R., Karlin, J., Dagvadorj, J., Chiba, N., Chen, S., et al. (2012). Oxidized mitochondrial DNA activates the NLRP3 inflammasome during apoptosis. *Immunity* 36, 401–414. doi: 10.1016/j.immuni.2012.01.009

Sun, X., Liu, H., Sun, Z., Zhang, B., Wang, X., Liu, T., et al. (2020). Acupuncture protects against cerebral ischemia-reperfusion injury via suppressing endoplasmic reticulum stress-mediated autophagy and apoptosis. *Mol. Med.* 26:105. doi: 10.1186/s10020-020-00236-5

Wang, H. Q., Bao, C. L., Jiao, Z. H., and Dong, G. R. (2016). Efficacy and safety of penetration acupuncture on head for acute intracerebral hemorrhage: a randomized controlled study. *Medicine* 95:e5562. doi: 10.1097/MD.0000000000005562

Wang, S., Lin, S., Zhu, M., Li, C., Chen, S., Pu, L., et al. (2019). Granulosa cells in rats with premature ovarian failure via restoring the pi3k/akt signaling pathway. *Int. J. Mol. Sci*. 20, 6311. doi: 10.3390/ijms20246311

Weng, S. W., Liao, C. C., Yeh, C. C., Chen, T. L., Lane, H. L., Lin, J. G., et al. (2016). Risk of epilepsy in stroke patients receiving acupuncture treatment: a nationwide retrospective matched-cohort study. *BMJ Open*. 6:e010539. doi: 10.1136/bmjopen-2015-010539

Wu, Z. Q., Cui, S. Y., Zhu, L., and Zou, Z. Q. (2016). Study on the mechanism of mtor-mediated autophagy during electroacupuncture pretreatment against cerebral ischemic injury. *Evid Based Complem. Alternat Med.* 2016:9121597. doi: 10.1155/2016/9121597

Xue, X., You, Y., Tao, J., Ye, X., Huang, J., Yang, S., et al. (2014). Electroacupuncture at points of Zusanli and Quchi exerts anti-apoptotic effect through the modulation of PI3K/Akt signaling pathway. *Neurosci. Lett*. 558, 14–19. doi: 10.1016/j.neulet.2013.10.029

Yang, P., Wang, Z., Zhang, Z., Liu, D., Manolios, E. N., Chen, C., et al. (2018). The extended application of the rat brain in stereotaxic coordinates in rats of various body weight. *J. Neurosci. Methods*. 307, 60–69. doi: 10.1016/j.jneumeth.2018.06.026

Yuan, Y., Zheng, Y., Zhang, X., Chen, Y., Wu, X., Wu, J., et al. (2017). BNIP3L/NIX-mediated mitophagy protects against ischemic brain injury independent of PARK2. *Autophagy*. 13, 1754–1766. doi: 10.1080/15548627.2017.1357792

Zhang, H., Gao, J., Wang, M., Lv, Y., Udi, X., Deng, X., et al. (2018). Effects of scalp electroacupuncture on the PI3K/Akt signalling pathway and apoptosis of hippocampal neurons in a rat model of cerebral palsy. *Acupunct. Med.* 36, 96–102. doi: 10.1136/acupmed-2016-011335

Zhang, X., Wu, B., Nie, K., Jia, Y., and Yu, J. (2014). Effects of acupuncture on declined cerebral blood flow, impaired mitochondrial respiratory function and oxidative stress in multi-infarct dementia rats. *Neurochem. Int.* 65, 23–29. doi: 10.1016/j.neuint.2013.12.004

Zheng, G. Q., Zhao, Z. M., Wang, Y., Gu, Y., Chen, L., et al. (2011). Meta-analysis of scalp acupuncture for acute hypertensive intracerebral hemorrhage. *J. Altern. Complem. Med*. 17, 293–299. doi: 10.1089/acm.2010.0156

Zhu, Y., Deng, L., Tang, H., Gao, X., Wang, Y., Guo, K., et al. (2017). Electroacupuncture improves neurobehavioral function and brain injury in rat model of intracerebral hemorrhage. *Brain Res. Bull*. 131, 123–132. doi: 10.1016/j.brainresbull.2017.04.003

Conflict of Interest: The authors declare that the research was conducted in the absence of any commercial or financial relationships that could be construed as a potential conflict of interest.

Publisher's Note: All claims expressed in this article are solely those of the authors and do not necessarily represent those of their affiliated organizations, or those of the publisher, the editors and the reviewers. Any product that may be evaluated in this article, or claim that may be made by its manufacturer, is not guaranteed or endorsed by the publisher.

frontiers in Aging Neuroscience

ORIGINAL RESEARCH
published: 10 February 2022
doi: 10.3389/fnagi.2021.808094

The Predictive Value of Dynamic Intrinsic Local Metrics in Transient Ischemic Attack

Huibin Ma[1,2†], Guofeng Huang[1†], Mengting Li[3†], Yu Han[4,5], Jiawei Sun[1], Linlin Zhan[6], Qianqian Wang[7], Xize Jia[8], Xiujie Han[5], Huayun Li[7], Yulin Song[5] and Yating Lv[8]**

[1] School of Information and Electronics Technology, Jiamusi University, Jiamusi, China, [2] Integrated Medical School, Jiamusi University, Jiamusi, China, [3] Key Laboratory of Intelligent Education Technology and Application of Zhejiang Province, Zhejiang Normal University, Jinhua, China, [4] Department of Neurology, The First Affiliated Hospital, Dalian Medical University, Dalian, China, [5] Department of Neurology, Anshan Changda Hospital, Anshan, China, [6] Faculty of Western Languages, Heilongjiang University, Harbin, China, [7] School of Teacher Education, Zhejiang Normal University, Jinhua, China, [8] Center for Cognition and Brain Disorders, The Affiliated Hospital of Hangzhou Normal University, Hangzhou, China

OPEN ACCESS

Edited by:
Feng Yan,
Zhejiang University, China

Reviewed by:
Xin Huang,
Renmin Hospital of Wuhan University, China
Xiaofen Ma,
Guangdong Second Provincial General Hospital, China

***Correspondence:**
Yulin Song
yulinsong1969@sina.com
Yating Lv
lvyating@hznu.edu.cn

[†] These authors have contributed equally to this work and share first authorship

Specialty section:
This article was submitted to Neuroinflammation and Neuropathy, a section of the journal Frontiers in Aging Neuroscience

Received: 03 November 2021
Accepted: 30 December 2021
Published: 10 February 2022

Citation:
Ma H, Huang G, Li M, Han Y, Sun J, Zhan L, Wang Q, Jia X, Han X, Li H, Song Y and Lv Y (2022) The Predictive Value of Dynamic Intrinsic Local Metrics in Transient Ischemic Attack. Front. Aging Neurosci. 13:808094. doi: 10.3389/fnagi.2021.808094

Background: Transient ischemic attack (TIA) is known as "small stroke." However, the diagnosis of TIA is currently difficult due to the transient symptoms. Therefore, objective and reliable biomarkers are urgently needed in clinical practice.

Objective: The purpose of this study was to investigate whether dynamic alterations in resting-state local metrics could differentiate patients with TIA from healthy controls (HCs) using the support-vector machine (SVM) classification method.

Methods: By analyzing resting-state functional MRI (rs-fMRI) data from 48 patients with and 41 demographically matched HCs, we compared the group differences in three dynamic local metrics: dynamic amplitude of low-frequency fluctuation (d-ALFF), dynamic fractional amplitude of low-frequency fluctuation (d-fALFF), and dynamic regional homogeneity (d-ReHo). Furthermore, we selected the observed alterations in three dynamic local metrics as classification features to distinguish patients with TIA from HCs through SVM classifier.

Results: We found that TIA was associated with disruptions in dynamic local intrinsic brain activities. Compared with HCs, the patients with TIA exhibited increased d-fALFF, d-fALFF, and d-ReHo in vermis, right calcarine, right middle temporal gyrus, opercular part of right inferior frontal gyrus, left calcarine, left occipital, and left temporal and cerebellum. These alternations in the dynamic local metrics exhibited an accuracy of 80.90%, sensitivity of 77.08%, specificity of 85.37%, precision of 86.05%, and area under curve of 0.8501 for distinguishing the patients from HCs.

Conclusion: Our findings may provide important evidence for understanding the neuropathology underlying TIA and strong support for the hypothesis that these local metrics have potential value in clinical diagnosis.

Keywords: resting-state fMRI, dynamic local metric, machine learning, support-vector machine, transient ischemic attack

INTRODUCTION

Transient ischemic attack (TIA) is a transient neurological dysfunction triggered by focal brain, medulla spinalis, or retinal ischemia, also known as "small stroke" (Easton et al., 2009). As the problem of population aging becomes more and more serious, the death rate due to stroke is constantly increasing. Preventing the social harm caused by stroke is very important (On et al., 2021). Evidence presented in previous studies has demonstrated a fact that TIA can be regarded as one of the main, under-recognized, and modifiable risk factors for stroke (Rothwell and Warlow, 2005; Turner et al., 2019). Given up to 80% of strokes after TIA are preventable (Coutts, 2017), accurate diagnosis of TIA is valuable and meaningful from the perspective of offering the greatest opportunity for the early intervention of stroke. However, the transient symptoms make the diagnosis of TIA hard and difficult. Therefore, objective and reliable biomarkers are urgently needed in clinical practice.

Resting-state functional magnetic resonance imaging (rs-fMRI), which measures the changes in the blood oxygen level-dependent (BOLD) signals, is a promising tool to explore the functional alterations of human brain (Biswal et al., 1995; Fox and Raichle, 2007). Several methods have been proposed and proven to be effective in characterizing the local features of the brain function, such as the amplitude of low-frequency fluctuations (ALFF), which measures signal strength in low-frequency oscillations (LFOs) of local spontaneous neural activity (Zang et al., 2007); fractional ALFF (fALFF), which characterizes the relative contribution of a specific LFO to the entire frequency range (Zou et al., 2008); and regional homogeneity (ReHo), which reflects the coherence of local neural activity among spatially neighboring regions (Zang et al., 2004). These three methods can reveal local brain activity from different perspectives and have been widely applied to localize the functional abnormalities in brain disorders (Zang et al., 2007; Gupta et al., 2020; Li et al., 2021). With regard to TIA, it has been shown that TIA is associated with the reductions of ReHo in the right dorsolateral prefrontal cortex, inferior prefrontal cortex, ventral anterior cingulate cortex, and dorsal posterior cingulate cortex (Guo et al., 2014) and decreased ALFF in the left middle temporal gyrus (Lv et al., 2019). These studies indicated that local metrics are promising to locate abnormal brain areas for TIA; however, only one value for each metric was calculated for the entire rs-fMRI scan, which ignored the characteristics of the dynamic brain variation or time-varying process of the BOLD signal along the course during fMRI scanning (Liao et al., 2015; Deng et al., 2016). In fact, previous studies have suggested that brain activity exhibits dynamic characteristics over time-varying process (Sporns, 2011; Abrams et al., 2013; Yin et al., 2013; Bassett and Sporns, 2017). Brain dynamics are thought to reflect the functional capacity of the neural system and could offer physiological neuromarker in many neurological and psychiatric diseases (Damaraju et al., 2014; Liao et al., 2014). Thus, it is of great importance to explore the dynamic changes in these local metrics. Moreover, the traditional identification of TIA, which was mainly judged from subjective evaluation of the symptoms, is time-consuming and labor-intensive with relatively low accuracy rate. Therefore, whether these local abnormalities could serve as objective and reliable biomarkers for TIA is still need to be clarified.

The support-vector machine (SVM) is a supervised machine learning algorithm that aims to maximize the margin so as to classify data points between classes in a high-dimensional space (Pereira et al., 2009) and has been widely used to assist diagnosis of neurological disorders. For example, Bu et al. (2019) selected the optimal features from the ALFF, fALFF, ReHo, and degree centrality of different brain regions and applied SVM to differentiate patients with obsessive-compulsive disorder from healthy controls (HCs). In a previous study, excellent performance with an accuracy of 95.37% was achieved when ALFF maps were employed, followed by ReHo, fALFF, and DC. Ma X. et al. (2020) chose 54 amyotrophic lateral sclerosis participants and used ALFF and d-ALFF as the SVM classification feature, and the classification accuracy was 79.63%. From what have been listed above, a reliable conclusion can be drawn that SVM has relatively high accuracy compared with traditional methods to differentiate the patients from healthy subjects. Hence, we used SVM to examine whether local abnormalities can be used as diagnostic and prognostic indicators for TIA.

In this study, we first employed sliding window approaches (Chen et al., 2018; Duncan and Small, 2018) to investigate the dynamic changes of three resting-state local metrics: dynamic ALFF (d-ALFF), dynamic fALFF (d-fALFF), and dynamic ReHo (d-ReHo) in patients with TIA. By using the SVM classification method, we further examined whether these dynamic local abnormalities could differentiate patients from HCs. We used two hypotheses in this study: (i) patients with TIA would exhibit significant temporal variability compared with HCs and (ii) the d-ALFF, d-fALFF, and d-ReHo values could be sensitive biomarkers to distinguish patients with TIA from HCs.

MATERIALS AND METHODS

Participants

Data were obtained from 51 suspected patients with TIA from the Department of Neurology, Anshan Changda Hospital from April 2015 to June 2016. The patients with transient neurological symptoms had been evaluated to have a possible vascular etiology judged by recruited clinical neurologists. Patients who have history of hemorrhage, leukoaraiosis, migraine, epilepsy, or psychiatric diseases were excluded in this study. Information about each participant was recorded as follows: (Easton et al., 2009) history of TIA and stroke; (On et al., 2021) previous risk factors, such as hypertension, diabetes mellitus, coronary artery disease, current smoking, and drinking behavior; (Turner et al., 2019) medications used ahead of the MRI scanning; (Qiu and Xu, 2020) in hospital evaluation of arterial stenosis (carotid duplex ultrasound and MR angiography), atrial fibrillation (ECG), and brain infarcts (diffusion-weighted imaging and T2-FLAIR); and (Rothwell and Warlow, 2005) 1-year telephone follow-up of stroke and/or TIA attack. In addition, four patients dropped out during the 1-year follow-up period. The risk of each patient for subsequent stroke was evaluated by age, blood pressure, clinical

features, duration of symptoms, and history of diabetes (ABCD2) (Johnston et al., 2007) score.

Besides, the study involves forty-one age- and sex-matched HCs with no physical diseases or history of psychiatric or neurological disorders from local community through advertising.

Finally, three patients were excluded because of unacceptable image quality of multimodal MRI data (incomplete coverage of the whole brain in rs-fMRI scan or missing 3D T1 image), leaving 48 patients with TIA and 41 HCs in the final analysis. Of the 48 patients, 25 patients suffered TIA (not first-time attack) and 4 patients suffered stroke. Detailed demographic and clinical information of all participants are displayed in **Table 1**.

Physiological and Biochemical Tests

All participants completed blood systolic pressure, blood diastolic pressure, blood sugar level, total cholesterol, triglycerides, high-density lipoprotein cholesterol (HDL-C), and low-density lipoprotein cholesterol (LDL-C) physiological/biochemical tests within 24 h before the MRI data acquisition. Additionally, all participants underwent the mini-mental state examination (MMSE) (Mingyuan, 1998) to evaluate global cognition.

Data Acquisition

GE MR-750 3.0 T scanner (GE Medical Systems, Inc., Waukesha, WI, United States) was used. The time interval between the latest TIA attack and subsequent MRI scanning was 0.25–16 days for the patients. During the resting state scanning, all participants were instructed to refrain from any cognitive task (Biswal et al., 1995). Specifically, all participants were required to keep relaxed, to close their eyes but not fall asleep, not to think systematically, and to remain motionless.

BOLD-fMRI EPI (echo planar imaging) scan parameters included TE (echo time) = 30 ms, TR (repetition time) = 2,000 ms, FA (flip angle) = 60°, matrix size = 64 × 64, thickness/gap = 3.2/0 mm, slices = 43, time = 8 min. A total of 240 scans were collected.

The high-resolution anatomic 3D T1 sequence had the following parameters: 176 sagittal slice, TR = 8,100 ms, TE = 3.1 ms, matrix = 256 × 256, voxel size = 1 mm × 1 mm × 1 mm, thickness/gap = 1/0 mm. This session lasted for about 5 min.

TABLE 1 | Demographic and clinical information.

	TIA (n = 48)	HCs (n = 41)	p value
Age (year, mean ± SD)	57.6 ± 9.8	55.0 ± 8.0	0.182[t]
Gender (male/female)	37/11	30/11	0.670[χ]
FD (mean ± SD)	0.06 ± 0.03	0.06 ± 0.05	0.961[t]
MMSE (mean ± SD)	29.2 ± 2.6	28.6 ± 1.7	0.222[t]
Blood systolic pressure (mmHg, mean ± SD)	145.5 ± 20.8	126.9 ± 19.8[a]	<0.001[t]
Blood diastolic pressure (mmHg, mean ± SD)	86.7 ± 10.4	80.0 ± 10.9[a]	0.007[t]
Blood sugar level (mmol/L, mean ± SD)	6.3 ± 2.1	5.2 ± 0.7[a]	<0.001[t]
Total cholesterol (mmol/L, mean ± SD)	5.3 ± 1.2	4.8 ± 1.0[a]	0.037[t]
Triglycerides (mmol/L, mean ± SD)	1.6 ± 0.9	1.9 ± 1.3[a]	0.234[t]
HDL-C (mmol/L, mean ± SD)	1.1 ± 0.2	1.1 ± 0.3[a]	0.311[t]
LDL-C (mmol/L, mean ± SD)	3.3 ± 1.0	2.7 ± 0.9[a]	0.004[t]
ABCD2 scores (median)	4 (2–6)		

[t]Data were obtained using two-sample two-side t-tests; [χ] Data were obtained using Pearson's chi-square tests; [a]Data were missing for 6 controls; TIA, transient ischemic attack; HCs, healthy controls; MMSE, mini-mental state examination; HDL-C, high-density lipoprotein cholesterol; LDL-C, low-density lipoprotein cholesterol; DWI, diffusion-weighted imaging; FD, frame-wise displacement.

Data Preprocessing

Resting-state fMRI images and structural images were preprocessed using the Temporal Dynamic Analysis (TDA) toolbox based on RESTplus version 1.24 (Jia et al., 2019)[1] running on Matlab2014a (MathWorks, Natick, MA, United States) and included the following steps: (Easton et al., 2009) the first 10 time points were removed to make the initial MRI signal reach steady state and to permit the participants to adapt to the scanning environment, and the remaining 230 consecutive volumes were used for data analyses; (On et al., 2021) slice timing and head motion were done in the left volumes of images, and no participant had a head movement bigger than 3 mm or rotation larger than 3°; (Turner et al., 2019) spatial normalization to the Montreal Neurological Institute space *via* the deformation fields derived from tissue segmentation of structural images was performed, and all images were then resampled into 3 mm × 3 mm × 3 mm voxels; (Qiu and Xu, 2020) for the dynamic ALFF and fALFF calculations, spatial smoothing (4 mm isotropic Gaussian kernel) was performed; (Rothwell and Warlow, 2005) detrending was used to correct the signal drift in real time; (Coutts, 2017) nuisance covariate regression (head motion effect using Friston 24 parameter model) from fMRI data (Friston et al., 1996) was calculated; and (Biswal et al., 1995) for the dynamic ReHo calculations, band-pass filtering (0.01–0.08 Hz) was applied to reduce low-frequency drift and high-frequency noise. The band-pass filter was applied only in ReHo.

Dynamic Measurements

Dynamic local metrics analysis was performed using TDA toolkits based on RESTplus (Jia et al., 2019) (see text footnote 1). The dynamic metrics was calculated using a sliding window method, and it is sensitive in detecting time-dependent variations and examining metrics variability over the whole brain (Hindriks et al., 2016; Yan et al., 2017; Fu et al., 2018; Ma M. et al., 2020). The most important parameter in resting-state dynamic computation is window length. Previous studies have demonstrated that the minimum window length should be larger than 1/fmin (where fmin is the minimum frequency of time series) so that the spurious fluctuations could be excluded (Leonardi and Van De Ville, 2015). Therefore, we applied a sliding window length of 50 TR (100 s) and a shifting step size of 1 TR (2 s). This procedure produced a total of 180 windows for each participant. Based on these sliding windows, we proposed three local metrics, namely, d-ALFF, d-fALFF, and d-ReHo (Liao et al., 2018; Yu et al., 2019; Tian et al., 2021).

[1]http://www.restfmri.net

d-ALFF Calculation

The time courses for each individual voxel were subject to a fast Fourier transformation to the frequency domain, and the power spectrum was determined. The square root of this spectrum was calculated for each frequency and then averaged across 0.01–0.08 Hz. This averaged square root was used as an ALFF index (Zang et al., 2007). After calculating ALFF of all voxels in time windows, each participant will get several window-based ALFF maps. Then, we computed the mean and SD of each voxel in all window-based ALFF maps for each participant and further got the corresponding coefficient of variation (CV = SD/mean). The CV maps were prepared for further statistical analysis.

d-fALFF Calculation

The fALFF was calculated as the ratio of the amplitude within the low-frequency range (0.01–0.08 Hz) to the total amplitude over the full frequency range (0–0.25 Hz). It indicates the relative contribution of oscillations in the low-frequency range to the signal variations over the whole frequency range (Zou et al., 2008). Then, we computed the CV of each voxel in all window-based fALFF maps for each participant. The CV maps were used for further statistical analysis.

d-ReHo Calculation

Individual ReHo maps were generated by calculating the Kendall coefficient of concordance (KCC) of the time courses of a given voxel with those of its neighbors (26 voxels) in a voxel-wise manner (Zang et al., 2004). Then, we computed the CV of each voxel in all window-based ReHo maps for each participant. Finally, the CV maps were spatially smoothed with an isotropic Gaussian kernel of 4 mm full-width-at-half-maximum (FWHM). The spatially smoothed CV maps were used for further statistical analyses.

Statistical Analyses

To detect the group differences in demographic variables between patients with TIA and HCs, two-sample *t*-tests and chi-square analyses were performed using Statistical Package for the Social Sciences (SPSS) software (SPSS Inc., Chicago, IL, United States). Age and clinical/physiological/biochemical characteristics between patients with TIA and HCs were compared using two-sample *t*-test. Sex difference was obtained with the Pearson's chi-square test.

The dynamic metrics (d-ALFF, d-fALFF, and d-ReHo) of regional brain activity between patients with TIA and HCs were compared using two-sample *t*-tests on each voxel to examine the between-group differences in RESTplus software (Jia et al., 2019) (see text footnote 1). Multiple comparison correction was performed based on Gaussian random field theory (GRF, voxel-wise $p < 0.005$, cluster-wise $p < 0.05$, two-tailed).

Feature Extraction and SVM Model Training

To evaluate whether the alterations of three dynamic metrics could serve as potential diagnostic indices for TIA, we performed machine learning analyses using SVM algorithm with the average dynamic metric values of all clusters showing significant among-group differences as the features.

Mapping non-linear data to a high dimensional feature space and finding a linear separating hyperplane to separate the two-group data are the core idea of the SVM algorithm. In this study, we used the Gaussian radial basis function kernel SVMs (RBF-SVM) (Cristianini and Shawe-Taylor, 2000), a implement in the LIBSVM software package (Pereira et al., 2009)[2], to investigate the potential diagnostic indices of the dynamic metrics. We used gird search optimization algorithm to obtain the parameters that enable SVM to achieve optimal performance. The grid search method is the most basic parameter optimization algorithm. In essence, it divides the parameters to be searched into a grid of the same length in a certain space range according to the proposed coordinate system. Each point in the coordinate system represents a set of parameters. The C (last parameter C = 1) in the SVM was set to 2^N (N from -4 to 4), and radial basis function kernel parameter γ (last parameter $\gamma = 0.125$) was optimized among the values of 2^N (N from -4 to 4). These points are brought into the SVM system to verify its performance, and the point that makes the performance of the entire system the best is called the optimal parameter. In addition, a leave-one-out cross-validation (LOOCV) was applied to validate the performance of our proposed approach. It involved excluding a participant from each group for test and training the classifier using the remaining participants. This procedure was repeated for each participant to assess the overall accuracy of the SVM. To quantify the performance of classification methods, accuracy, sensitivity, and specificity were reported.

Validation Analysis

To further test the reliability of our results for three dynamic local metrics, we reanalyzed the rs-fMRI data with three additional window lengths (25, 32, and 75 TRs) and 6 mm isotropic Gaussian kernel for spatial smoothing.

To explore the effects of head motion, we reanalyzed between-group differences of three dynamic metrics by treating mean framewise displacement (FD) (Jenkinson et al., 2002) as a covariate of no interest. To further test the effects of age and gender on our results, we also reanalyzed between-group differences with regressing age and gender out.

Correlation Between Local Metrics and Clinical/Physiological/Biochemical Characteristics

Relationships with symptom severity were examined by extracting d-ALFF, d-fALFF, and d-ReHo values from the regions showing group differences and by correlating these values with blood systolic pressure, blood diastolic pressure, blood sugar level, total cholesterol, triglycerides HDL-C, LDL-C, MMSE, and duration time from the last TIA to MRI scanning. The correlations were considered significant at a threshold of $p < 0.05$.

[2]http://www.csie.ntu.edu.tw/∼cjlin/libsvm/

RESULTS

Clinical Data

Demographic and clinical information for the final 48 patients with TIA and 41 HCs is summarized in **Table 1**. The patients with TIA and HCs were matched in age ($p = 0.182$) and sex ($p = 0.670$). Compared with HCs, patients with TIA showed significantly higher systolic pressure ($p < 0.001$), diastolic pressure ($p = 0.007$), blood sugar level ($p < 0.001$), total cholesterol ($p = 0.037$), and LDL-C ($p = 0.004$). The median ABCD2 score for the patients with TIA was 4 (Coutts, 2017; On et al., 2021). Detailed demographics and the psychological characteristics of the two groups are shown in **Table 1**.

Differences in d-ALFF, d-fALFF, and d-ReHo

As shown in **Figure 1A**, for d-ALFF, TIA increased in vermis, right calcarine, and right middle temporal gyrus. The significant differences in d-ALFF between the two groups are shown in **Table 2** and **Figure 1A**. Compared with HCs, the patients with TIA exhibited increased d-fALFF in the opercular part of right inferior frontal gyrus and left calcarine as shown in **Table 2** and **Figure 1B**. The cerebellum, left inferior occipital gyrus, and left inferior temporal gyrus showed increased d-ReHo in patients with TIA compared with HCs described in **Table 2** and **Figure 1C**.

Classification Accuracy

To evaluate the classification ability of the SVM model, the accuracy, sensitivity, specificity and precision were calculated, and the receiver operating characteristic (ROC) curve of the classifier is shown in **Figure 2**. The curve was drawn using Receiver Operating Characteristic Assistant software (Wang et al., 2021). The performance of the classifier achieved an accuracy of 80.90%, sensitivity of 77.08%, specificity of 85.37%, precision of 86.05%, and area under curve (AUC) of 0.8501 for TIA vs. HCs.

Validation Results

The validation analyses indicated that the TIA-related dynamic alterations in the three local metrics were consistent with the main results when using different window lengths and smooth kernels. From this perspective, smooth kernels and window lengths in our study have changed, respectively, under the condition of keeping the other calculation parameters the same, so as to fairly compare all the results and to enrich our data analysis. When the smooth kernel is 4 mm, the results of different window lengths are shown in **Supplementary Tables 1–3** and **Supplementary Figures 1–3**, respectively. When the smooth

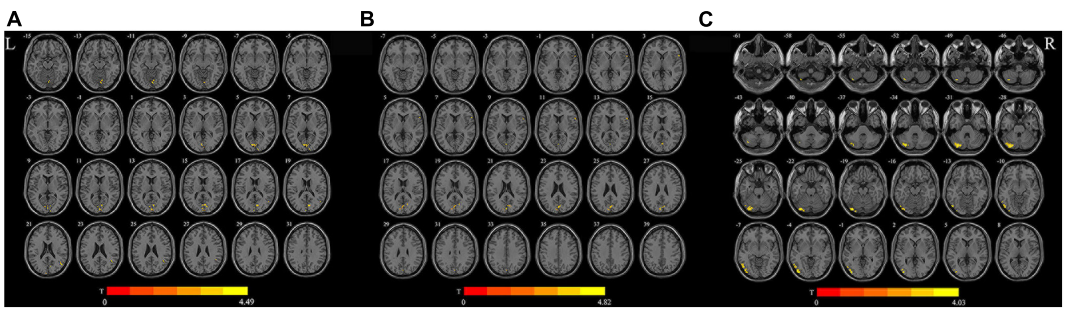

FIGURE 1 | Brain regions with significant differences in d-ALFF **(A)**, d-fALFF **(B)**, and d-ReHo **(C)** between the TIA group and the HC group (after GRF correction; voxel-wise $p < 0.005$, cluster-wise $p < 0.05$, two-tailed). The color bar indicates the *T*-value. L, left; R, right; d-ALFF, dynamic amplitude of low-frequency fluctuations; d-fALFF, dynamic fractional amplitude of low-frequency fluctuations; d-ReHo, dynamic regional homogeneity.

TABLE 2 | Regions showing abnormal d-ALFF, d-fALFF, and d-ReHo in patients with TIA compared with HCs.

Metrics	Voxels	Peak MNI Coordinate (mm)			Peak T value	Effect size	Brian Regions (AAL)
		x	y	z			
d-ALFF	12	3	−78	−15	3.4067	0.7328	Cerebelum Vermis_6
	56	6	−75	15	4.4887	0.9655	Calcarine_R
	11	48	−66	21	4.2192	0.9075	Temporal_Middle_R
d-fALFF	12	60	12	12	4.8197	1.0367	Frontal_Inferior_Opercular_R
	47	−3	−75	9	4.3218	0.9296	Calcarine_L
d-ReHo	265	−33	−81	−30	4.0296	0.8661	Cerebellum-crus1_L
							Occipital_Inf_L
							Temporal_Inf_L

d-ALFF, dynamic amplitude of low-frequency fluctuations; d-fALFF, dynamic fractional amplitude of low-frequency fluctuations; d-ReHo, dynamic regional homogeneity; MNI, Montreal Neurological Institute; AAL, Anatomical Automatic Labeling; L, left; R, right.

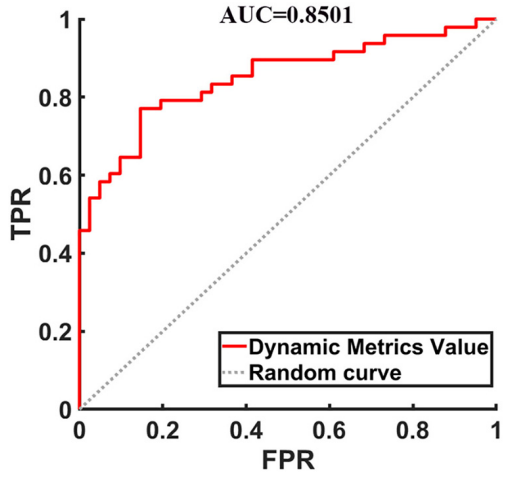

FIGURE 2 | The receiver operating characteristic curve of dynamic metrics. The image of ROC was displayed using MATLAB software. FPR, false positivity rate; TPR, true positivity rate; AUC, area under the receiver operating characteristic curve.

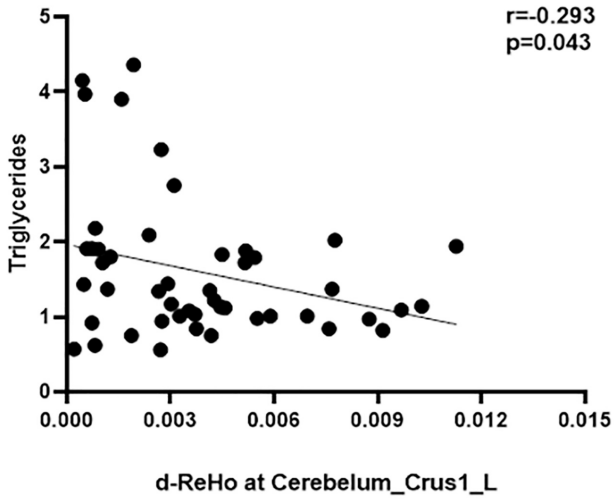

FIGURE 3 | Correlation between d-ReHo variability of the Cerebelum_Crus1_L and the triglycerides score.

kernel is 6 mm, the results of different window lengths are shown in **Supplementary Tables 4–6** and **Supplementary Figures 4–6**, respectively. They are provided in the **Supplementary Material**.

Transient ischemic attack-related alterations in the dynamic local metrics were consistent with the main results after correcting for head motion (FD), age, and gender (refer to **Supplementary Figures 7–12**).

To reveal the stability of the results, SVM was also performed based on the three datasets: training set, validation set, and test set to distinguish TIA from HCs (refer to **Supplementary Figure 13**).

Correlational Analysis

To avoid the influence of extreme value (value beyond 3 SD), all the correlation analyses were conducted after removing the extreme values from our data. No correlations between d-ALFF and d-fALFF different region values and clinical measures reached significance (uncorrected $p < 0.05$). The d-ReHo variability in the cerebellum was negatively correlated with the triglycerides scores of the patients with TIA ($r = -0.2931$, $p = 0.0432$, uncorrected $p < 0.05$, **Figure 3**). All results of correlation between dynamic local values and clinical data are described in **Supplementary Tables 7–9**, and they are provided in the **Supplementary Material**. Here only shows the significantly related ones. There was no correlation between brain dynamic values and duration time from the last attack to scanning (refer to **Supplementary Table 10** for details).

DISCUSSION

In this study, we used three rs-fMRI local dynamic metrics to investigate the alterations of intrinsic brain activity in patients with TIA. Compared with the HCs, the patients with TIA showed increased d-ALFF value in the cerebellum, right calcarine, and right middle temporal gyrus. Patients with TIA also exhibited increased d-fALFF value in the opercular part of the right inferior frontal gyrus and left calcarine. In addition, an increased d-ReHo value was observed in the cerebellum, left inferior occipital gyrus, and left inferior temporal gyrus. The values of d-ALFF, d-fALFF, and d-ReHo in regions that showed abnormal brain dynamics served as classification features, and the SVM classification achieved a total accuracy of 80.90%, sensitivity of 77.08%, specificity of 85.37%, precision of 86.05%, and AUC of 0.8501. Overall, these findings provide evidence for the local abnormalities in TIA, which may help to understand the neurophysiological basis and to establish objective biomarkers for TIA.

The ALFF reflects the power within the effective frequency range (0.01–0.08 Hz) and is considered as an dependable approach to detect the regional intensity of spontaneous fluctuations and to present spontaneous brain activity of the brain (Zang et al., 2007), and d-ALFF characterizes the dynamic alterations of ALFF over time (Chen et al., 2018). In this study, we found increased d-ALFF in cerebellar vermis, right calcarine, and right middle temporal gyrus in patients with TIA. Growing evidence indicates that the cerebellar vermis may contribute significantly to cognitive and global functioning in clinical populations (Steinlin, 2007; Bernard et al., 2015). Middle temporal gyrus plays an essential role in language, semantic memory processing, along with visual perception (Soderfeldt et al., 1997; Bonilha et al., 2017). The calcarine is connected with blurred visual (Yu et al., 2020). Thus, we speculated that the increased d-ALFF in these three regions was associated with the difficulties in language processing, disturbance of consciousness, and vision in patients with TIA (Lavallee and Amarenco, 2007). Notably, the abnormalities were also observed in stroke patients. For example, Chen et al. (2015) found that stroke patients exhibited larger ALFF in the right middle temporal gyrus. Jiang et al. (2019) reported

decreased degree centrality in the calcarine in stroke patients. Being important risk factors for stroke, these TIA-related abnormalities already existed in the early stage of stroke according to our study.

The fALFF measures the relative spontaneous neural activity within the effective frequency range to the whole detectable frequency range, and it is calculated as the ratio of the power spectrum of the low-frequency range to that of the entire frequency range (Zou et al., 2008). Compared with ALFF, it could effectively suppress the physiological noise (Zou et al., 2008; Zuo et al., 2010), and d-fALFF examined the temporal variability of power of intrinsic brain activity and the regional features of low-frequency oscillation changes in TIA (Chen et al., 2018). In this study, the opercular part of right inferior frontal gyrus and left calcarine of patients with TIA show increased d-fALFF. A previous study has indicated that the opercular part of right inferior frontal gyrus is vital to the implementation of multicomponent behavior (Dippel and Beste, 2015). Since calcarine is related to the visual center, the damage of which also suggests the possibility of early visual center disturbance in patients with TIA (Gupta et al., 2016; Liang et al., 2020; Yu et al., 2020). The abnormality in behavior processing and disturbed vision in patients with TIA may be relevant to the increased d-fALFF in these regions (Lavallee and Amarenco, 2007). These findings indicate that the alterations of fALFF changes over time in the opercular part of right inferior frontal gyrus and left calcarine may at least partially lead to behavior impairments and visual dysfunction in patients with TIA. The speculation could be examined in future studies.

The ReHo reflects the local synchronization of spontaneous BOLD signal (Zang et al., 2004). The d-ReHo represents the change of similarity between the time series of a given voxel and its nearest neighbors (Yin et al., 2013; Avena-Koenigsberger et al., 2017). In this study, the left cerebellum-crus1, left occipital, and the left temporal showed increased d-ReHo in patients with TIA. The cerebellum is related to sensorimotor (Kansal et al., 2017) and cognitive-emotional processing (Adamaszek et al., 2017; Beckinghausen and Sillitoe, 2018). Besides, it influences motor and cognitive functions *via* cerebello-thalamocortical circuits (Middleton and Strick, 2001). The occipital lobe damage leads to visual-field loss (Tohid et al., 2015). As naming function is a critical function of temporal lobe, damage to which will result in language impairment (Trimmel et al., 2018). This result echoed the symptoms of sudden dizziness or loss of balance and coordination in patients with TIA (Lavallee and Amarenco, 2007; Easton et al., 2009; Bonilha et al., 2017). Notably, a previous study has shown decreased functional connectivity (FC) in left middle temporal gyrus within the default mode network (DMN) in patients with TIA (Li et al., 2013), decreased FC in the left middle temporal gyrus, the medial prefrontal cortex and the posterior cingulate cortex/precuneus in patients with TIA (Zhu et al., 2019), and decreased ALFF in the left middle temporal gyrus of patients with TIA (Lv et al., 2019). The decreased FC in the left middle of occipital with visual network (VN) was reported (Li et al., 2013). Taken together with these findings, it provided further evidence for the existence of impaired brain region in TIA patients, which may help to understand the pathophysiological underpinnings in patients with TIA.

Considering dynamic indicators and static indicators are bond with each other closely and these dynamic results are not reported in static results before, doing dynamic indicators within patients with TIA are urgently needed in this study, which further proved the necessity of this study. As traditional TIA diagnosis methods were subjective and lacked of clear objective standards, we used machine learning algorithms, data-driven methods used to obtain diagnostic criteria, to acquire higher reliability. Researching the algorithms of machine learning to search for the diagnosis biomarker of TIA can alleviate the contradiction between supply and demand between the limited psychiatrists with professional diagnostic qualifications and the increasing number of patients with TIA and can improve the accuracy of diagnosis and the precision of treatment at the same time. Although the application of artificial intelligence in the medical field is still in the initial stage, with more in-depth development of machine learning technology, it will become a general trend for doctors to use artificial intelligence to diagnose and manage the health of the patients in the future. SVM has been widely applied in various diseases and achieved great classification performance (Chan et al., 2019; Gui et al., 2021). Using the SVM classifier, the patients with TIA could be differentiated from HCs by dynamic local metrics. In addition, high identification accuracy of 80.90% between the TIA and HCs was achieved in this study. The results may indicate the potential value of the dynamic local metrics in the clinical diagnosis of TIA.

This is the first study to explore the dynamic characteristics of patients with TIA. In addition, the temporal brain dynamics could distinguish the patients with TIA from HCs. The results of our study are of great importance to investigate the underlying mechanism of TIA. However, considering the heterogeneity of patients, the results should be cautious when applied to the whole patients with TIA. Further studies are encouraged to pay more attention to the TIA-specific brain dynamic alterations based on this study.

This study has several potential limitations. First, although the findings were encouraging, the sample size was relatively small. The results that there were no significant correlations between TIA-related brain dynamics and clinical variables may be due to the sample size, which was demonstrated to result in low statistical power (Button et al., 2013). Accordingly, our findings should be interpreted with caution regarding the observed brain dynamic alterations as sensitive biomarkers for TIA, and further studies are required to expand the sample size to improve the statistical power. Second, although the correlation analysis revealed there was no significant correlation between TIA-related brain dynamics and clinical variables, the mismatch between two groups in clinical variables results in a heterogeneity of the sample. Third, the medications were used ahead of the MRI scanning, and it might have impact on the brain dynamics, which would be controlled in the future. Fourth, due to the lack of the TIA attack times, we could not evaluate the extent to which our findings are dependent on the attack frequency of the patients. In further studies, we would like to combine larger sample and reduce heterogeneity among participants to confirm our findings.

CONCLUSION

Our results demonstrate that TIA is associated with spontaneous brain activity accompanied by dynamic characteristics, and it may provide important evidence for understanding the neuropathology underlying TIA and strong support for the hypothesis that these local metrics have a potential value in clinical diagnosis.

DATA AVAILABILITY STATEMENT

The raw data supporting the conclusions of this article will be made available by the authors, without undue reservation.

ETHICS STATEMENT

The studies involving human participants were reviewed and approved by the Ethics Committee of the Center for Cognition and Brain Disorders, Hangzhou Normal University. The patients/participants provided their written informed consent to participate in this study.

AUTHOR CONTRIBUTIONS

HM, GH, ML, YS, and YL conceived and designed the experiments. GH, ML, YH, JS, QW, XH, and HL performed the experiments. HM, GH, and ML analyzed the data. HM, GH, ML, YH, LZ, and XJ participated in the completion of the manuscript. All authors have made significant scientific contributions to this manuscript and reviewed the manuscript.

FUNDING

This work was supported by grants from the National Key R&D Program of China (No. 2017YFC1310000), the National Natural Science Foundation of China (Nos. 81771911 and 82001898), the cultivation project of the province leveled preponderant characteristic discipline in the College of Education of Hangzhou Normal University (No. 20JYXK026), and the Zhejiang Medical and Health Science and Technology Project (No. 2021KY249).

ACKNOWLEDGMENTS

We would like to thank the Center for Cognition and Brain Disorders, The Affiliated Hospital of Hangzhou Normal University, Hangzhou, China, for assistance with MRI data acquisition.

SUPPLEMENTARY MATERIAL

The Supplementary Material for this article can be found online at: https://www.frontiersin.org/articles/10.3389/fnagi.2021.808094/full#supplementary-material

REFERENCES

Abrams, D. A., Lynch, C. J., Cheng, K. M., Phillips, J., Supekar, K., Ryali, S., et al. (2013). Underconnectivity between voice-selective cortex and reward circuitry in children with autism. *Proc. Natl. Acad. Sci. U.S.A.* 110, 12060–12065. doi: 10.1073/pnas.1302982110

Adamaszek, M., D'Agata, F., Ferrucci, R., Habas, C., Keulen, S., Kirkby, K. C., et al. (2017). Consensus Paper: cerebellum and Emotion. *Cerebellum* 16, 552–576. doi: 10.1007/s12311-016-0815-8

Avena-Koenigsberger, A., Misic, B., and Sporns, O. (2017). Communication dynamics in complex brain networks. *Nat. Rev. Neurosci.* 19, 17–33. doi: 10.1038/nrn.2017.149

Bassett, D. S., and Sporns, O. (2017). Network neuroscience. *Nat. Neurosci.* 20, 353–364. doi: 10.1038/nn.4502

Beckinghausen, J., and Sillitoe, R. V. (2018). Insights into cerebellar development and connectivity. *Neurosci. Lett.* 688, 2–13. doi: 10.1016/j.neulet.2018.05.013

Bernard, J. A., Leopold, D. R., Calhoun, V. D., and Mittal, V. A. (2015). Regional cerebellar volume and cognitive function from adolescence to late middle age. *Hum. Brain Mapp.* 36, 1102–1120. doi: 10.1002/hbm.22690

Biswal, B., Yetkin, F. Z., Haughton, V. M., and Hyde, J. S. (1995). Functional Connectivity in the Motor Cortex of Resting Human Brain Using Echo-Planar MRI. *Magn. Reson. Med.* 34, 537–541. doi: 10.1002/mrm.1910340409

Bonilha, L., Hillis, A. E., Hickok, G., den Ouden, D. B., Rorden, C., and Fridriksson, J. (2017). Temporal lobe networks supporting the comprehension of spoken words. *Brain* 140, 2370–2380. doi: 10.1093/brain/awx169

Bu, X., Hu, X., Zhang, L., Li, B., Zhou, M., Lu, L., et al. (2019). Investigating the predictive value of different resting-state functional MRI parameters in obsessive-compulsive disorder. *Transl. Psychiatry* 9:17. doi: 10.1038/s41398-018-0362-9

Button, K. S., Ioannidis, J. P., Mokrysz, C., Nosek, B. A., Flint, J., Robinson, E. S., et al. (2013). Power failure: why small sample size undermines the reliability of neuroscience. *Nat. Rev. Neurosci.* 14, 365–376. doi: 10.1038/nrn3475

Chan, K. L., Leng, X., Zhang, W., Dong, W., Qiu, Q., Yang, J., et al. (2019). Early Identification of High-Risk TIA or Minor Stroke Using Artificial Neural Network. *Front. Neurol.* 10:171. doi: 10.3389/fneur.2019.00171

Chen, J., Sun, D., Shi, Y., Jin, W., Wang, Y., Xi, Q., et al. (2018). Dynamic Alterations in Spontaneous Neural Activity in Multiple Brain Networks in Subacute Stroke Patients: a Resting-State fMRI Study. *Front. Neurosci.* 12:994. doi: 10.3389/fnins.2018.00994

Chen, Y. C., Xia, W., Luo, B., Muthaiah, V. P., Xiong, Z., Zhang, J., et al. (2015). Frequency-specific alternations in the amplitude of low-frequency fluctuations in chronic tinnitus. *Front. Neural. Circuits* 9:67. doi: 10.3389/fncir.2015.00067

Coutts, S. B. (2017). Diagnosis and Management of Transient Ischemic Attack. *Continuum* 23, 82–92.

Cristianini, N., and Shawe-Taylor, J. (2000). *An Introduction to Support Vector Machines and Other Kernel-Based Learning Methods*. Cambridge: Cambridge University Press.

Damaraju, E., Allen, E. A., Belger, A., Ford, J. M., McEwen, S., Mathalon, D. H., et al. (2014). Dynamic functional connectivity analysis reveals transient states of dysconnectivity in schizophrenia. *Neuroimage Clin.* 5, 298–308. doi: 10.1016/j.nicl.2014.07.003

Deng, L., Sun, J., Cheng, L., and Tong, S. (2016). Characterizing dynamic local functional connectivity in the human brain. *Sci. Rep.* 6:26976. doi: 10.1038/srep26976

Dippel, G., and Beste, C. (2015). A causal role of the right inferior frontal cortex in implementing strategies for multi-component behaviour. *Nat. Commun.* 6:6587. doi: 10.1038/ncomms7587

Duncan, E. S., and Small, S. L. (2018). Changes in dynamic resting state network connectivity following aphasia therapy. *Brain Imaging Behav.* 12, 1141–1149.

Easton, J. D., Saver, J. L., Albers, G. W., Alberts, M. J., Chaturvedi, S., Feldmann, E., et al. (2009). Definition and evaluation of transient ischemic attack: a scientific statement for healthcare professionals from the American Heart Association/American Stroke Association Stroke Council; Council on Cardiovascular Surgery and Anesthesia; Council on Cardiovascular Radiology and Intervention; Council on Cardiovascular Nursing; and the Interdisciplinary Council on Peripheral Vascular Disease. The American Academy of Neurology affirms the value of this statement as an educational tool for neurologists. *Stroke* 40, 2276–2293. doi: 10.1161/STROKEAHA.108.192218

Fox, M. D., and Raichle, M. E. (2007). Spontaneous fluctuations in brain activity observed with functional magnetic resonance imaging. *Nat. Rev. Neurosci.* 8, 700–711. doi: 10.1038/nrn2201

Friston, K. J., Williams, S., Howard, R., Frackowiak, R. S., and Turner, R. (1996). Movement-Related Effects in fMRI Time-Series. *Magn. Reson. Med.* 35, 346–355. doi: 10.1002/mrm.1910350312

Fu, Z., Tu, Y., Di, X., Du, Y., Pearlson, G. D., Turner, J. A., et al. (2018). Characterizing dynamic amplitude of low-frequency fluctuation and its relationship with dynamic functional connectivity: an application to schizophrenia. *Neuroimage* 180, 619–631. doi: 10.1016/j.neuroimage.2017.09.035

Gui, S. G., Chen, R. B., Zhong, Y. L., and Huang, X. (2021). Machine Learning Analysis Reveals Abnormal Static and Dynamic Low-Frequency Oscillations Indicative of Long-Term Menstrual Pain in Primary Dysmenorrhea Patients. *J. Pain Res.* 14, 3377–3386. doi: 10.2147/JPR.S332224

Guo, J., Chen, N., Li, R., Wu, Q., Chen, H., Gong, Q., et al. (2014). Regional homogeneity abnormalities in patients with transient ischaemic attack: a resting-state fMRI study. *Clin. Neurophysiol.* 125, 520–525. doi: 10.1016/j.clinph.2013.08.010

Gupta, S., Kumaran, S. S., Saxena, R., Gudwani, S., Menon, V., and Sharma, P. (2016). BOLD fMRI and DTI in strabismic amblyopes following occlusion therapy. *Int. Ophthalmol.* 36, 557–568. doi: 10.1007/s10792-015-0159-2

Gupta, Y., Kim, J. I., Kim, B. C., and Kwon, G. R. (2020). Classification and Graphical Analysis of Alzheimer's Disease and Its Prodromal Stage Using Multimodal Features From Structural, Diffusion, and Functional Neuroimaging Data and the APOE Genotype. *Front. Aging Neurosci.* 12:238. doi: 10.3389/fnagi.2020.00238

Hindriks, R., Adhikari, M. H., Murayama, Y., Ganzetti, M., Mantini, D., Logothetis, N. K., et al. (2016). Can sliding-window correlations reveal dynamic functional connectivity in resting-state fMRI? *Neuroimage* 127, 242–256. doi: 10.1016/j.neuroimage.2015.11.055

Jenkinson, M., Bannister, P., Brady, M., and Smith, S. (2002). Improved Optimization for the Robust and Accurate Linear Registration and Motion Correction of Brain Images. *Neuroimage* 17, 825–841. doi: 10.1016/s1053-8119(02)91132-8

Jia, X.-Z., Wang, J., Sun, H.-Y., Zhang, H., Liao, W., Wang, Z., et al. (2019). RESTplus: an improved toolkit for resting-state functional magnetic resonance imaging data processing. *Sci. Bull.* 64, 953–954. doi: 10.1016/j.scib.2019.05.008

Jiang, C.-X., Cai, S., Zhang, L. (2019). Ischemic stroke in pontine and corona radiata: location specific impairment of neural network investigated with resting state fmri. *Front. Neurol.* 10, 1–8. doi: 10.3389/fneur.2019.00575

Johnston, S. C., Rothwell, P. M., Nguyen-Huynh, M. N., Giles, M. F., Elkins, J. S., Bernstein, A. L., et al. (2007). Validation and refinement of scores to predict very early stroke risk after transient ischaemic attack. *Lancet* 369, 283–292. doi: 10.1016/s0140-6736(07)60150-0

Kansal, K., Yang, Z., Fishman, A. M., Sair, H. I., Ying, S. H., Jedynak, B. M., et al. (2017). Structural cerebellar correlates of cognitive and motor dysfunctions in cerebellar degeneration. *Brain* 140, 707–720. doi: 10.1093/brain/aww327

Lavallee, P., and Amarenco, P. (2007). Transient ischemic attacks. *Presse Med.* 36, 134–141. doi: 10.1016/j.lpm.2006.10.021

Leonardi, N., and Van De Ville, D. (2015). On spurious and real fluctuations of dynamic functional connectivity during rest. *Neuroimage* 104, 430–436. doi: 10.1016/j.neuroimage.2014.09.007

Li, R., Wang, S., Zhu, L., Guo, J., Zeng, L., Gong, Q., et al. (2013). Aberrant functional connectivity of resting state networks in transient ischemic attack. *PLoS One* 8:e71009. doi: 10.1371/journal.pone.0071009

Li, Y. T., Chang, C. Y., Hsu, Y. C., Fuh, J. L., Kuo, W. J., Yeh, J. T., et al. (2021). Impact of physiological noise in characterizing the functional MRI default-mode network in Alzheimer's disease. *J. Cereb. Blood Flow Metab.* 41, 166–181. doi: 10.1177/0271678X19897442

Liang, S., Xue, K., Wang, W., Yu, W., Ma, X., Luo, S., et al. (2020). Altered brain function and clinical features in patients with first-episode, drug naive major depressive disorder: a resting-state fMRI study. *Psychiatry Res. Neuroimaging* 303:111134. doi: 10.1016/j.pscychresns.2020.111134

Liao, W., Li, J., Duan, X., Cui, Q., Chen, H., and Chen, H. (2018). Static and dynamic connectomics differentiate between depressed patients with and without suicidal ideation. *Hum. Brain Mapp.* 39, 4105–4118. doi: 10.1002/hbm.24235

Liao, W., Zhang, Z., Mantini, D., Xu, Q., Ji, G. J., Zhang, H., et al. (2014). Dynamical intrinsic functional architecture of the brain during absence seizures. *Brain Struct. Funct.* 219, 2001–2015. doi: 10.1007/s00429-013-0619-2

Liao, X., Yuan, L., Zhao, T., Dai, Z., Shu, N., Xia, M., et al. (2015). Spontaneous functional network dynamics and associated structural substrates in the human brain. *Front. Hum. Neurosci.* 9:478. doi: 10.3389/fnhum.2015.00478

Lv, Y., Li, L., Song, Y., Han, Y., Zhou, C., Zhou, D., et al. (2019). The Local Brain Abnormalities in Patients With Transient Ischemic Attack: a Resting-State fMRI Study. *Front. Neurosci.* 13:24. doi: 10.3389/fnins.2019.00024

Ma, M., Zhang, H., Liu, R., Liu, H., Yang, X., Yin, X., et al. (2020). Static and Dynamic Changes of Amplitude of Low-Frequency Fluctuations in Cervical Discogenic Pain. *Front. Neurosci.* 14:733. doi: 10.3389/fnins.2020.00733

Ma, X., Lu, F., Chen, H., Hu, C., Wang, J., Zhang, S., et al. (2020). Static and dynamic alterations in the amplitude of low-frequency fluctuation in patients with amyotrophic lateral sclerosis. *PeerJ* 8:e10052. doi: 10.7717/peerj.10052

Middleton, F. A., and Strick, P. L. (2001). Cerebellar projections to the prefrontal cortex of the primate. *J. Neurosci.* 21, 700–712. doi: 10.1523/JNEUROSCI.21-02-00700.2001

Mingyuan, Z. (1998). *Handbook of Psychiatric Rating Scale*. China: Hunan science & technology press.

On, B. I., Vidal, X., Berger, U., Sabate, M., Ballarin, E., Maisterra, O., et al. (2021). Antidepressant use and stroke or mortality risk in the elderly. *Eur. J. Neurol.* [Epub Online ahead of print]. doi: 10.1111/ene.15137

Pereira, F., Mitchell, T., and Botvinick, M. (2009). Machine learning classifiers and fMRI: a tutorial overview. *Neuroimage* 45, S199–S209. doi: 10.1016/j.neuroimage.2008.11.007

Qiu, S., and Xu, Y. (2020). Guidelines for Acute Ischemic Stroke Treatment. *Neurosci. Bull.* 36, 1229–1232. doi: 10.1007/s12264-020-00534-2

Rothwell, P. M., and Warlow, C. P. (2005). Timing of TIAs preceding stroke: time window for prevention is very short. *Neurology* 64, 817–820. doi: 10.1212/01.WNL.0000152985.32732.EE

Soderfeldt, B., Ingvar, M., Ronnberg, J., Eriksson, L., Serrander, M., and Stone-Elander, S. (1997). Signed and spoken language perception studied by positron emission tomography. *Neurology* 49, 82–87. doi: 10.1212/wnl.49.1.82

Sporns, O. (2011). The non-random brain: efficiency, economy, and complex dynamics. *Front. Comput. Neurosci.* 5:5. doi: 10.3389/fncom.2011.00005

Steinlin, M. (2007). The cerebellum in cognitive processes: supporting studies in children. *Cerebellum* 6, 237–241. doi: 10.1080/14734220701344507

Tian, S., Zhu, R., Chattun, M. R., Wang, H., Chen, Z., Zhang, S., et al. (2021). Temporal dynamics alterations of spontaneous neuronal activity in anterior cingulate cortex predict suicidal risk in bipolar II patients. *Brain Imaging Behav.* 15, 2481–2491. doi: 10.1007/s11682-020-00448-7

Tohid, H., Faizan, M., and Faizan, U. (2015). Alterations of the occipital lobe in schizophrenia. *Neurosciences* 20, 213–224. doi: 10.17712/nsj.2015.3.20140757

Trimmel, K., van Graan, A. L., Caciagli, L., Haag, A., Koepp, M. J., Thompson, P. J., et al. (2018). Left temporal lobe language network connectivity in temporal lobe epilepsy. *Brain* 141, 2406–2418. doi: 10.1093/brain/awy164

Turner, G. M., McMullan, C., Atkins, L., Foy, R., Mant, J., and Calvert, M. (2019). TIA and minor stroke: a qualitative study of long-term impact and experiences of follow-up care. *BMC Fam. Pract.* 20:176. doi: 10.1186/s12875-019-1057-x

Wang, L., Feng, Q., Wang, M., Zhu, T., Yu, E., Niu, J., et al. (2021). An Effective Brain Imaging Biomarker for AD and aMCI: ALFF in Slow-5 Frequency Band. *Curr. Alzheimer. Res.* [Epub Online ahead of print]. doi: 10.2174/1567205018666210324130502

Yan, C. G., Yang, Z., Colcombe, S. J., Zuo, X. N., and Milham, M. P. (2017). Concordance among indices of intrinsic brain function: insights from inter-individual variation and temporal dynamics. *Sci. Bull.* 62, 1572–1584. doi: 10.1016/j.scib.2017.09.015

Yin, D., Luo, Y., Song, F., Xu, D., Peterson, B. S., Sun, L., et al. (2013). Functional reorganization associated with outcome in hand function after stroke revealed by regional homogeneity. *Neuroradiology* 55, 761–770. doi: 10.1007/s00234-013-1146-9

Yu, Y., Lan, D. Y., Tang, L. Y., Su, T., Li, B., Jiang, N., et al. (2020). Intrinsic functional connectivity alterations of the primary visual cortex in patients with proliferative diabetic retinopathy: a seed-based resting-state fMRI study. *Ther. Adv. Endocrinol. Metab.* 11:2042018820960296.

Yu, Y., Li, Z., Lin, Y., Yu, J., Peng, G., Zhang, K., et al. (2019). Depression Affects Intrinsic Brain Activity in Patients With Mild Cognitive Impairment. *Front. Neurosci.* 13:1333. doi: 10.3389/fnins.2019.01333

Zang, Y., Jiang, T., Lu, Y., He, Y., and Tian, L. (2004). Regional homogeneity approach to fMRI data analysis. *Neuroimage* 22, 394–400. doi: 10.1016/j.neuroimage.2003.12.030

Zang, Y. F., He, Y., Zhu, C. Z., Cao, Q. J., Sui, M. Q., Liang, M., et al. (2007). Altered baseline brain activity in children with ADHD revealed by resting-state functional MRI. *Brain. Dev.* 29, 83–91. doi: 10.1016/j.braindev.2006.07.002

Zhu, T., Li, L., Song, Y., Han, Y., Zhou, C., Zhou, D., et al. (2019). Altered Functional Connectivity within Default Mode Network in Patients with Transient Ischemic Attack: a Resting-State Functional Magnetic Resonance Imaging Study. *Cerebrovasc. Dis.* 48, 61–69. doi: 10.1159/000502884

Zou, Q. H., Zhu, C. Z., Yang, Y., Zuo, X. N., Long, X. Y., Cao, Q. J., et al. (2008). An improved approach to detection of amplitude of low-frequency fluctuation (ALFF) for resting-state fMRI: fractional ALFF. *J. Neurosci. Methods* 172, 137–141. doi: 10.1016/j.jneumeth.2008.04.012

Zuo, X. N., Di Martino, A., Kelly, C., Shehzad, Z. E., Gee, D. G., Klein, D. F., et al. (2010). The oscillating brain: complex and reliable. *Neuroimage* 49, 1432–1445. doi: 10.1016/j.neuroimage.2009.09.037

Conflict of Interest: The authors declare that the research was conducted in the absence of any commercial or financial relationships that could be construed as a potential conflict of interest.

Publisher's Note: All claims expressed in this article are solely those of the authors and do not necessarily represent those of their affiliated organizations, or those of the publisher, the editors and the reviewers. Any product that may be evaluated in this article, or claim that may be made by its manufacturer, is not guaranteed or endorsed by the publisher.

frontiers in Aging Neuroscience

ORIGINAL RESEARCH
published: 03 March 2022
doi: 10.3389/fnagi.2022.785761

Neurons Release Injured Mitochondria as "Help-Me" Signaling After Ischemic Stroke

Li Gao[1,2†], Fan Liu[3†], Pin-Pin Hou[1], Anatol Manaenko[4], Zhi-Peng Xiao[2], Fei Wang[2], Tian-Le Xu[3] and Qin Hu[1*]*

[1] Central Laboratory, Ren Ji Hospital, Shanghai Jiao Tong University School of Medicine, Shanghai, China, [2] Cerebrovascular Disease Center, Ren Ji Hospital, Shanghai Jiao Tong University School of Medicine, Shanghai, China, [3] Department of Anatomy and Physiology, Collaborative Innovation Center for Brain Science, Shanghai Jiao Tong University School of Medicine, Shanghai, China, [4] Department of Neurology, The First Affiliated Hospital of Chongqing Medical University, Chongqing, China

OPEN ACCESS

Edited by:
Hailiang Tang,
Fudan University, China

Reviewed by:
Xinchun Jin,
Capital Medical University, China
Arturo Hernandez-Cruz,
National Autonomous University of Mexico, Mexico

***Correspondence:**
Tian-Le Xu
xu-happiness@shsmu.edu.cn
Qin Hu
huqinle20010709@126.com

† These authors have contributed equally to this work

Specialty section:
This article was submitted to Cellular and Molecular Mechanisms of Brain-aging, a section of the journal Frontiers in Aging Neuroscience

Received: *29 September 2021*
Accepted: *17 January 2022*
Published: *03 March 2022*

Citation:
Gao L, Liu F, Hou P-P, Manaenko A, Xiao Z-P, Wang F, Xu T-L and Hu Q (2022) Neurons Release Injured Mitochondria as "Help-Me" Signaling After Ischemic Stroke. Front. Aging Neurosci. 14:785761. doi: 10.3389/fnagi.2022.785761

Mitochondrial dysfunction has been regarded as one of the major contributors of ischemic neuronal death after stroke. Recently, intercellular mitochondrial transfer between different cell types has been widely studied and suggested as a potential therapeutic approach. However, whether mitochondria are involved in the neuron-glia cross-talk following ischemic stroke and the underlying mechanisms have not been explored yet. In this study, we demonstrated that under physiological condition, neurons release few mitochondria into the extracellular space, and the mitochondrial release increased when subjected to the challenges of acidosis, hydrogen peroxide (H_2O_2), *N*-methyl-D-aspartate (NMDA), or glutamate. Acidosis reduced the mitochondrial basal respiration and lowered the membrane potential in primary-cultured mouse cortical neurons. These defective mitochondria were prone to be expelled to the extracellular space by the injured neurons, and were engulfed by adjacent astrocytes, leading to increased astrocytic expressions of mitochondrial Rho GTPase 1 (Miro 1) and mitochondrial transcription factor A (TFAM) at mRNA level. In mice subjected to transient focal cerebral ischemia, the number of defective mitochondria in the cerebrospinal fluid increased. Our results suggested that the neuron-derived mitochondria may serve as a "help-me" signaling and mediate the neuron-astrocyte cross-talk following ischemic stroke. Promoting the intercellular mitochondrial transfer by accelerating the neuronal releasing or astrocytic engulfing might be a potential and attractive therapeutic strategy for the treatment of ischemic stroke in the future.

Keywords: ischemic stroke, metabolic stress, mitochondrial release, neuron-glial crosstalk, mitochondrial biogenesis

INTRODUCTION

Stroke is one of the major causes of death and permanent disability worldwide, and ischemic stroke accounts for approximately 80% of stroke incidences (Powers et al., 2019). Recombinant tissue plasminogen activator (rt-PA)-mediated thrombolysis is clinically effective after acute ischemic stroke. However, the narrow therapeutic window and the risk of hemorrhagic transformation

limit its clinical application (Gao et al., 2020). Therefore, exploring the molecular mechanisms underlying endogenous neuroprotection and finding a novel therapeutic strategy are of great significance for the treatment of ischemic stroke.

Mitochondrial dysfunction is the most immediate response to glucose and oxygen deprivation after ischemia and is closely associated with the early events following ischemic stroke, including reactive oxygen species (ROS)-mediated oxidative stress, acidosis, and *N*-methyl-D-aspartate (NMDA), and glutamate-induced excitotoxicity (Liu et al., 2018; Chen et al., 2020). Numerous studies have evidenced that maintaining the mitochondrial function is essential for the neuronal activity and survival (Huang and Jiang, 2019; Chen et al., 2020). Therefore, mitochondria might be a promising neuroprotective target for the treatment of ischemic stroke.

Recently, intercellular mitochondrial transfer between different cell types, such as mesenchymal stem cell (MSC) and pulmonary alveoli, astrocyte and neuron, and MSC and cardiomyocyte, has been demonstrated and attracted great interest (Plotnikov et al., 2008; Islam et al., 2012; English et al., 2020). Under mitochondrial stress, damaged mitochondria are transported into migrasomes and released to the periphery to facilitate mitocytosis (Jiao et al., 2021). The released mitochondria can also be taken up and reprogrammed by adjacent cells to activate signals for cell survival, highlighting an innovative pathway mediating the pathogenesis of many diseases. The intercellular mitochondrial transfer has also been documented in the cardiovascular injury model and experimental stroke models (Han et al., 2016; Hayakawa et al., 2016; Huang et al., 2016; Liu et al., 2019; Maeda et al., 2020). In ischemic mice, the astrocytes were able to produce functional mitochondria and transfer them into the neurons to promote cell survival and attenuate neurological deficits (Hayakawa et al., 2016) that indicates the existence of a crosstalk between glial cells and neurons during ischemic stroke. However, whether and how the mitochondria of neurons are involved in the neuron-glia cross-talk during ischemic insult has not been explored yet.

MATERIALS AND METHODS

Cell Cultures

Primary neuronal cell cultures were prepared from 1-day-old C57BL/6 pups as described before (Wang et al., 2015). In brief, the cerebral cortex was dissociated and digested with 0.05% trypsin-ethylene diamine tetraacetic acid (trypsin-EDTA) (#E5134, Sigma-Aldrich, St. Louis, MO, USA) for 15 min at 37°C, followed by trituration with fire-polished glass pipettes, and plated in poly-D-lysine-coated culture dishes or 24-well plates. Neurons were cultured with neurobasal medium (#21103049, Thermo Fisher Scientific, Waltham, MA, USA) containing B27% (#17504044, Thermo Fisher Scientific, Waltham, MA, USA) and maintained at 37°C in a humidified 5% carbon dioxide (CO_2) atmosphere incubator. Cell culture medium (CM) was changed every 3 days and used 10–14 days after seeding. The collected neuronal CM was treated by spin cell debris down with centrifuging at 2,000 rpm for 10 min or by filtrating through a 0.2 μm sterile filter as described previously (Hayakawa et al., 2016) for further experiments.

Primary astrocyte cultures were prepared from the cortex of 16-day-old embryos of C57BL/6 mice. The dissociated cortical cells were seeded on uncoated T75 culture flasks in Dulbecco's modified eagle medium (DMEM) (#01-055-1A, Biological Industries, Kibbutz Beit Haemek, Israel) supplemented with 10% (v/v) fetal bovine serum (FBS; #SH30070.03, Hyclone Life Science, Logan, UT, USA). After 14 days, the flasks were shaken to remove microglia and passaged with trypsin to reduce the presence of other types of cells. The astrocytes were then detached by trypsinization and plated in six-well plates at a density of 1×10^6 cells/ml.

The Chinese hamster ovary (CHO) cell line was purchased from the Cell Bank/Stem Cell bank (#ACSP-507, Shanghai Chinese Academy of Sciences, Shanghai, China). The cells were cultured in DMEM/nutrient mixture F-12 (#11320-033, Gibco, NY, USA) supplemented with 1% penicillin/streptomycin (#03-031-1B, Biological Industries, Kibbutz Beit Haemek, Israel) and 10% FBS at 37°C in a humidified 5% CO_2 incubator as described previously (Wu et al., 2018). Cells were grown to 70–80% confluence in 100 mm diameter dishes, and the medium was exchanged every 2 days. The CM was collected, and the mitochondria-depleted CM (mdCM) was obtained by passing the CM through the 0.2 μm sterile filter.

Establishment of Cerebral Ischemia/Reperfusion Cell Model

Acidosis, ROS-mediated oxidative stress, and excitotoxicity are major events following ischemic stroke. To mimic the cerebral ischemia/reperfusion (I/R) injury *in vitro*, the cultured neurons were exposed to acidosis, hydrogen peroxide (H_2O_2), NMDA, and glutamate, respectively. In brief, the neurons were cultured in six-well plates at a density of 1×10^6 cells per well in the neurobasal medium for 10–14 days and used for the subsequent experiments.

The acidosis was stimulated as we reported before (Wang et al., 2020). First, cells were washed three times with a pH 6.5 solution [150 mM sodium chloride (NaCl), 5 mM potassium chloride (KCl), 1 mM magnesium chloride ($MgCl_2$), 2 mM calcium chloride ($CaCl_2$), and 10 mM glucose, buffered to the desired pH value with 10 mM 4-[2-hydroxyethyl]-1-piperazineethanesulfonic acid (HEPES)] within 5 min at room temperature (22–25°C) and then incubated at 37°C for 1 h. Afterward, the solution was replaced with the normal pH CM and the culture resumed at 37°C for 24 h.

Oxidative stress was induced by H_2O_2 stimulation as described previously (Luo et al., 2021). The cells were treated with H_2O_2 (#7722-84-1, Sigma-Aldrich, St. Louis, MO, USA) at a concentration of 20 or 50 μM for 1 h. Thereafter, the CM was replaced with normal neurobasal medium for 24 h as restoration.

The NMDA- and glutamate-mediated neurotoxicity was induced as described earlier (Sabogal-Guáqueta et al., 2019). The neurons were challenged to 50 μM NMDA (#M3262, Sigma-Aldrich, St. Louis, MO, USA) or 100 μM glutamate (#G1626, Sigma-Aldrich, St. Louis, MO, USA) for 30 min, and then the original feeding medium was restored for 24 h.

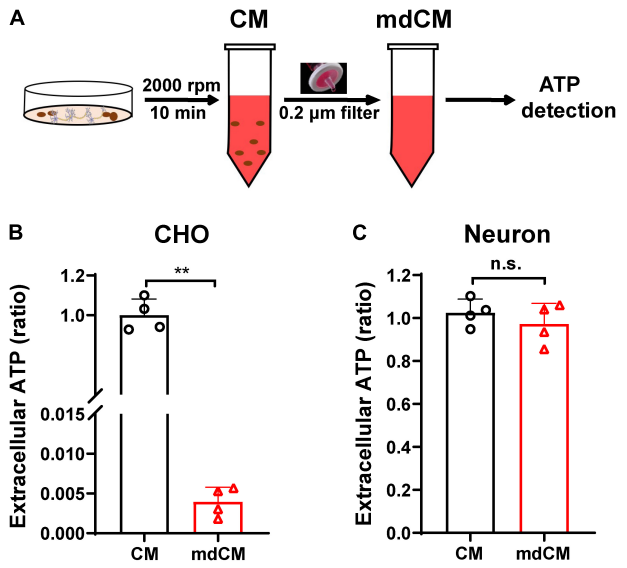

FIGURE 1 | Extracellular ATP detected in the CM and mdCM of CHO cells and neurons. **(A)** The CM was collected by spin cell debris down with centrifuging at 2,000 rpm for 10 min, and the mdCM was collected by passing the CM through the 0.2 μm sterile filter. **(B)** Significant decrease of extracellular ATP concentration in CHO cells was observed after removing mitochondria from the CM of CHO cells. **(C)** No changes in extracellular ATP concentration were observed after removing mitochondria from the CM of neurons. $n = 4$. $^{**}p < 0.01$ vs. CM. CM, culture medium; mdCM, mitochondria-depleted CM; n.s., not significant.

Mouse Focal Cerebral Ischemia Model

All the experimental protocols were approved by the Animal Care and Use Committee of the Shanghai Jiao Tong University School of Medicine, Shanghai, China. First, 12–14-week-old male C57BL/6 mice (Jiesijie, Shanghai, China) were anesthetized with 1.5–2% isoflurane, and rectal temperatures and cerebral blood flow (CBF) were monitored. Transient middle cerebral artery occlusion (tMCAO) was induced using intraluminal suture as described before (Zuo et al., 2019). A midline neck incision was made, and the left common carotid artery (CCA), external carotid artery (ECA), and internal carotid artery (ICA) were isolated. The ECA was ligated with 5-0 silk suture, and a 6-0 nylon monofilament coated with silicon resin (6023PK, Doccol Corp., Redlands, CA, USA) was inserted from ECA to occlude the MCA. The reduction of the CBF was confirmed by a laser-Doppler flowmeter (moorVMS-LDF-2, Moor Instruments, Devon, UK). Only animals with CBF lower than 20% of baseline were admitted in this study. One hour after occlusion, the suture was gently removed to allow reperfusion. Mice in the Sham group received the same surgical procedure without filament insertion. Body temperature was regularly monitored and maintained at 37 ± 0.5°C with a heating pad. All animals were allowed *ad libitum* access to water and food after surgery.

Cerebrospinal Fluid Collection and Mitochondrial Tracking

For the collection of cerebrospinal fluid (CSF) (25–50 μl per mice), mice were anesthetized with 2% isoflurane at 24 h post-reperfusion. CSF samples were collected by puncture of the cisterna magna with an A-100 insulin syringe and then stored at -80°C for the detection of mitochondria. For mitochondrial tracking, the CSF was prepared after centrifugation at 2,000 rpm for 10 min. Then, the MitoTracker Green (15 ng/ml, #M7514, Thermo Fisher Scientific, Waltham, MA, USA) was added to the CSF samples (25 μl CSF per mice was diluted with 75 μl PBS) for 1 h at room temperature and then fluorescence-activated cell sorter analysis was performed.

Adenosine Triphosphate Measurement

Extracellular adenosine triphosphate (ATP) was determined by CellTiter-Glo luminescence (#G7570, Promega, Madison, WI, USA), which can perform cell lysis and generate a luminescent signal that is proportional to the amount of ATP present. Basically, opaque-walled 96-well plates with CM (50 μl) or mdCM (50 μl) were prepared. Then, 50 μl CellTiter-Glo luminescence test solution was added and incubated for 30 min at room temperature. Luminescent signal was recorded using a luminescence microplate reader (BioTek Instruments, Winooski, VT, USA). Since mitochondria produce and restore most of the cellular ATP, the number of released mitochondria in the CM can be estimated by evaluating the extracellular ATP.

Flow Cytometry

Flow cytometric analysis was performed by the BD LSR II flow cytometer (BD Biosciences, Franklin Lakes, NJ, USA) after the neurons were treated with pH 6.5 and 7.4 solutions for 1 h and reperfusion for 24 h. The CMs were collected from cortical neurons and labeled with MitoTracker Green (#M7514, Thermo Fisher Scientific, Waltham, MA, USA) for 1 h. After being centrifuged at 2,000 rpm for 10 min, the supernatants were used to sort the labeled mitochondria fraction by FACS AriaII cell sorter.

Mitochondrial Membrane Potential Measurement

For monitoring the health status of mitochondria, JC-1 dye (#T3168, Thermo Fisher Scientific, Waltham, MA, USA) was used, and mitochondrial membrane potential ($\Delta\psi m$) was assessed. The CM and mdCM of cortical neurons and CSF of mice were collected and incubated with JC-1 (5 or 2 μM) for 30 min at 37°C. JC-1 dye exhibits potential-dependent accumulation in mitochondria, indicated by fluorescence emission shift from green (Ex 485 nm/Em 516 nm) to red (Ex 579 nm/Em 599 nm). $\Delta\psi m$ was determined by the red/green fluorescence intensity ratio with Synergy H1 Hybrid Multi-Mode Reader (BioTek Instruments, Winooski, VT, USA).

Oxygen Consumption Rate Analysis

The neurons were cultured in poly-D-lysine-coated 24-well seahorse plates (#100777-004, Agilent, Palo Alto, CA, USA) and exposed to pH 6.5 or 7.4 solution for 1 h. After 24-h restoration, oxygen consumption rate (OCR) was measured according to the vendor recommendation. In brief, neurons were washed twice with XF calibrant solution (#100840-000, Agilent, Palo Alto, CA, USA) and then placed in fresh assay medium. The basal, maximal, and ATP-coupled respiration was monitored after the addition of

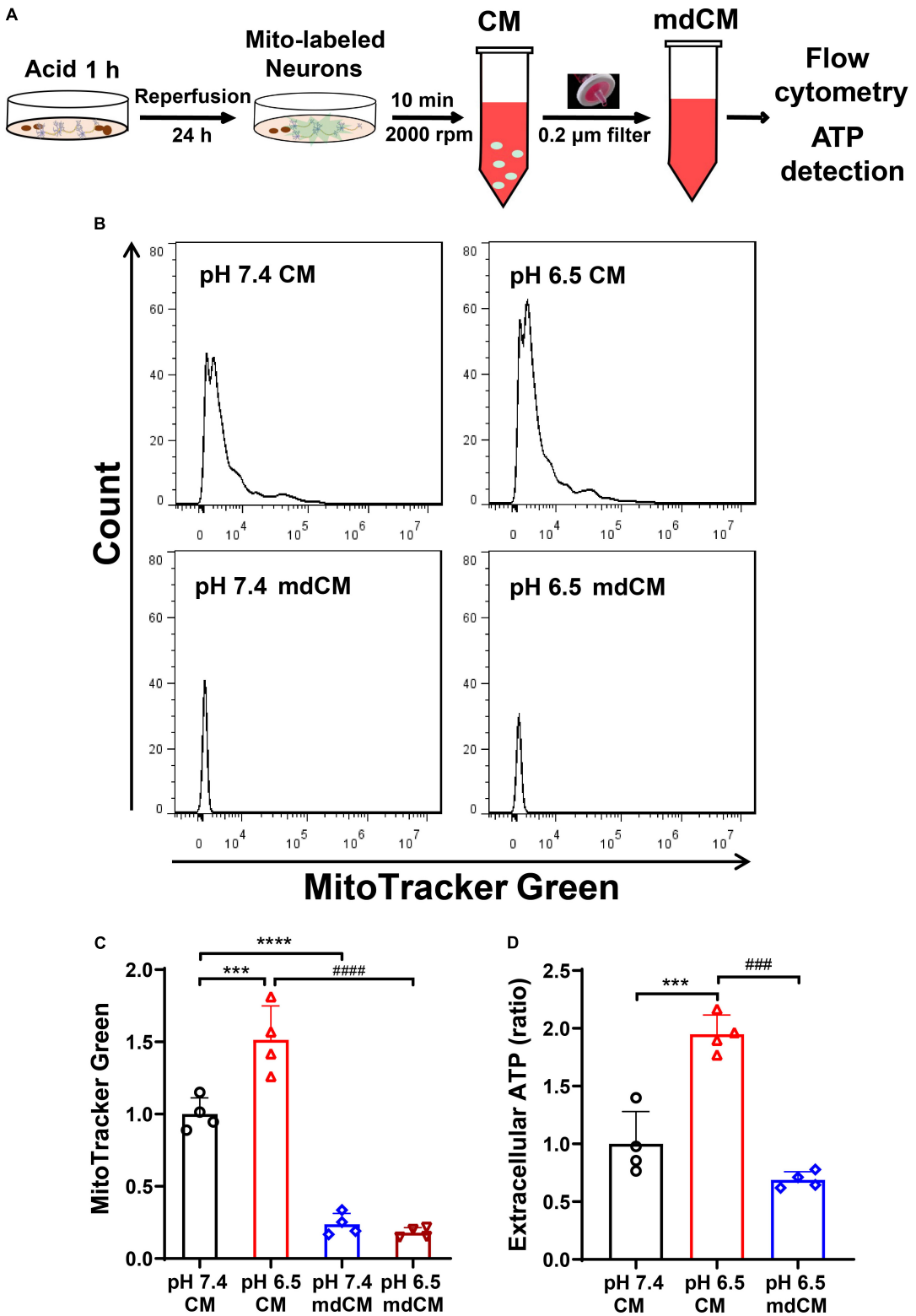

FIGURE 2 | Neurons released mitochondria under the acidosis. **(A)** Schematic diagram describing the experimental procedure. **(B)** The presence of neuronal mitochondria in culture medium (CM) and mitochondria-depleted culture medium (mdCM) in both groups was analyzed by flow cytometry. **(C)** The neuronal mitochondria labeled with MitoTracker Green increased in CM treated with a pH 6.5 solution when compared with the pH 7.4 group, but decreased significantly in mdCM in both pH 7.4 and 6.5 groups. **(D)** The extracellular ATP increased significantly in CM after pH 6.5 treatment, but the ATP concentration decreased dramatically in mdCM after pH 6.5 treatment. $n = 4$. $^{***}p < 0.001$, $^{****}p < 0.0001$ vs. pH 7.4 CM; $^{\#\#\#}p < 0.001$, $^{\#\#\#\#}p < 0.0001$ vs. pH 6.5 CM.

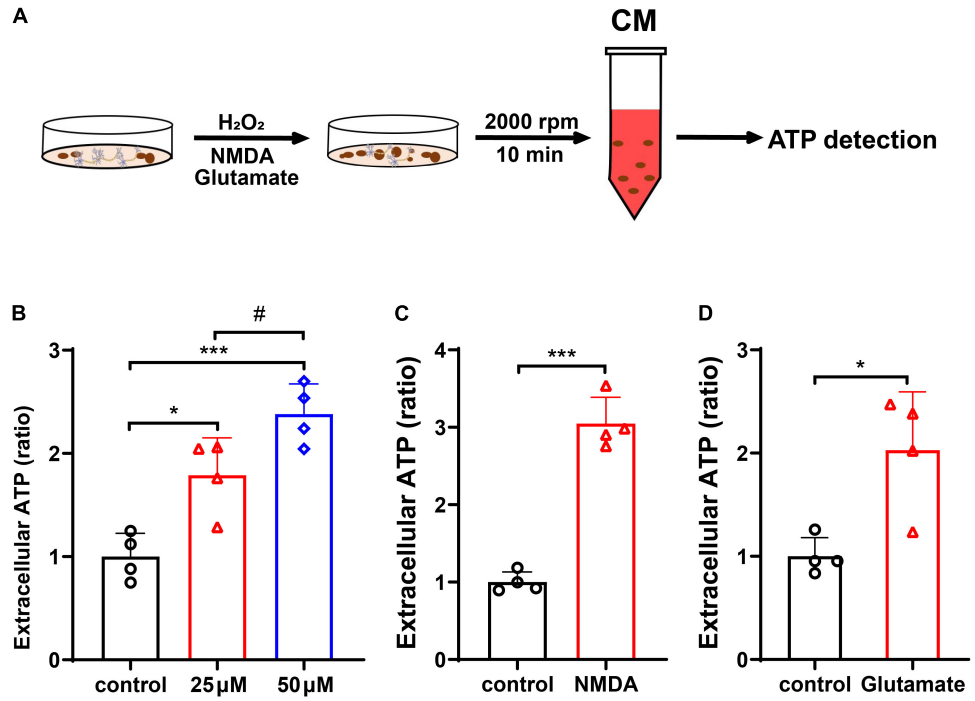

FIGURE 3 | Neurons released mitochondria under hydrogen peroxide (H_2O_2)-mediated oxidative stress and glutamate- and *N*-methyl-D-aspartate (NMDA)-induced excitotoxicity. **(A)** The experimental procedure. **(B)** The extracellular ATP increased dose-dependently in CM after H_2O_2 treatment. **(C,D)** The extracellular ATP increased significantly after treatment with NMDA (50 μM) or glutamate (100 μM). $n = 4$. $^{*}p < 0.05$, $^{***}p < 0.001$ vs. control, $^{\#}p < 0.05$ vs. 25 μM H_2O_2.

oligomycin (1 μM, #75351, Sigma-Aldrich, St. Louis, MO, USA), carbonyl cyanide 4-(trifluoromethoxy)phenylhydrazone (FCCP) (1 μM, #2920, Sigma-Aldrich, St. Louis, MO, USA) + sodium pyruvate (5 mM, #P2256, Sigma-Aldrich, St. Louis, MO, USA), antimycin A (4 μM, #A8674, Sigma-Aldrich, St. Louis, MO, USA), and rotenone (1 μM, #R8875, Sigma-Aldrich, St. Louis, MO, USA) as described previously (Savic Azoulay et al., 2020). The assay was performed using Seahorse Bioscience XF96 extracellular flux analyzer (Agilent, Palo Alto, CA, USA), and the statistics were exported from Wave Desktop 2.4 software (Agilent, Palo Alto, CA, USA).

Immunofluorescence Staining

To investigate the role of the released mitochondria in neuron-glia cross-talk, we labeled the neurons with MitoTracker Red CMXRos (#M22425, Thermo Fisher Scientific, Waltham, MA, USA) and incubated for 1 h. After being washed three times with CM, the neurons were treated with pH 6.5 or 7.4 solution for 1 h. After 24 h, the CM or mdCM was collected and added to the glial fibrillary acidic protein (GFAP)-labeled astrocytes and incubated for 24 h. Then, the astrocytes were washed three times with PBS. The mdCM from neurons was filtered with a 0.2 μm filter and served as control. The astrocytes were fixed with absolute methanol for 10 min on ice and imaged using a fluorescence microscope (Leica, Wetzlar, Germany).

Real-Time Quantitative-PCR

Total RNA was extracted using TRIzol Reagent (#15596018, Thermo Fisher Scientific, Waltham, MA, USA), and PrimeScript§ RT Reagent Kit (#RR037Q, Takara Bio, Tokyo, Japan) was used to obtain cDNA according to the instructions of the manufacturer. The levels of β-actin mRNA were served as an internal reference. The primers used were as follows: mitochondrial Rho GTPase 1 (Miro1) forward: CAAATGAAAGCGGCTGGATAAC; Miro1 reverse: AGCCTAG ATAGCCCAGATACTC; mitochondrial transcription factor A (TFAM) forward: TCCACAGAACAGCTACCCAA; TFAM reverse: CCACAGGGCTGCAATTTTCC; β-actin forward: CCTGGCACCCAGCACAAT; and β-actin reverse: GGGCCGGACTCGTCATAC. All the experiments were performed for six times, and the gene expression was analyzed with the $2^{-\Delta\Delta Ct}$ method.

Statistical Analysis

Results were expressed as mean ± SD. The *t*-test (normally distributed data) or the Mann-Whitney *U* test (non-normally distributed data) was used to determine the differences between the two groups. One-way ANOVA followed by the Tukey's Kramer test was used to analyze multiple comparisons. The *p*-value < 0.05 was considered to be statistically significant.

RESULTS

Neurons Release Mitochondria Under the Stimulation of Acidosis, Oxidative Stress, and Excitotoxicity

To assess whether cells release mitochondria into the extracellular space under physiological condition, the CM from CHO cells and

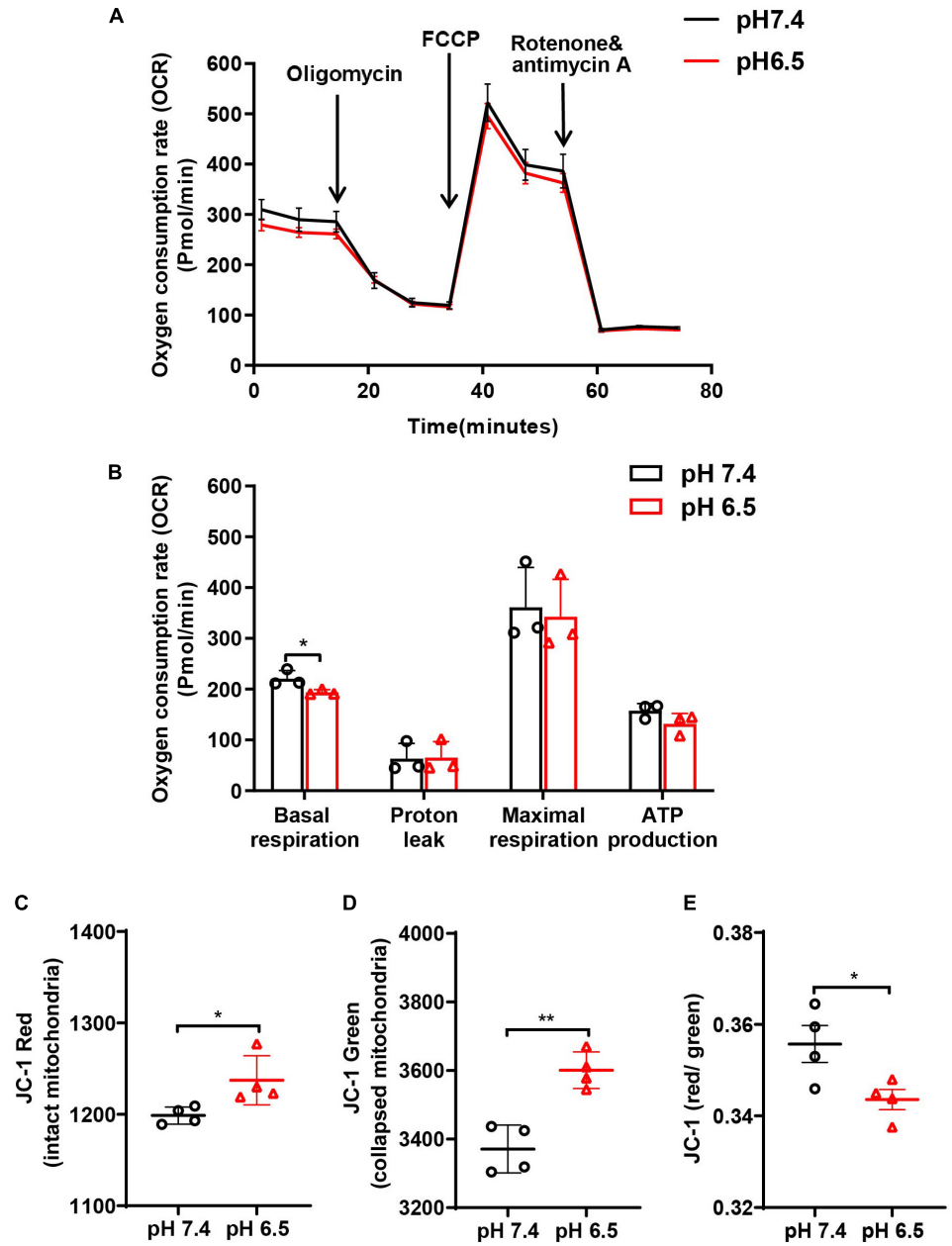

FIGURE 4 | Oxygen consumption rate (OCR) and mitochondrial membrane potential ($\Delta\psi m$; JC-1 red/green ratio) were performed to examine the function of neuronal mitochondria following acidosis. **(A)** Representative OCR traces ± SD measured in neurons treated with pH 6.5 and 7.4 solutions. **(B)** Quantification of basal, "leak," "maximal" state, and ATP production for pH 6.5- and 7.4-treated neurons. **(C–E)** The JC-1 staining in neurons showed that both JC-1 red and JC-1 green increased after pH 6.5 treatment, but JC-1 red/green ratio decreased significantly. $n = 4$. $^*p < 0.05$, $^{**}p < 0.01$ vs. pH 7.4.

neurons were collected. The ATP concentration was measured before or after removing the mitochondria with a 0.2 μm filter (**Figure 1A**). In CHO cells, the extracellular ATP decreased dramatically after removing mitochondria (**Figure 1B**, $p < 0.01$ vs. CM). Unlike the CHO cells, there were no significant changes in the extracellular ATP in neurons between before and after being filtered (**Figure 1C**, $p = 0.3991$).

To investigate whether the neurons release mitochondria under stress, the neurons were labeled with MitoTracker Green and subjected to acidosis with a pH 6.5 solution for 1 h. After restoring for 24 h, the mitochondria in CM and mdCM were examined by flow cytometry (**Figure 2A**). Treatment with pH 6.5 induced an increase of mitochondria (MitoTracker Green positive) in the CM when compared with the pH 7.4 group. However, the number of mitochondria (MitoTracker Green positive) decreased significantly in mdCM in both groups (**Figures 2B,C**, $p < 0.001$, $p < 0.0001$ vs. pH 7.4 CM, and $p < 0.0001$ vs. pH 6.5 CM). Consistently,

pH 6.5 treatment increased the extracellular ATP in primary-cultured neurons (**Figure 2D**, $p < 0.001$ vs. pH 7.4 CM), and filtrating through a 0.2 μm filter greatly decreased the ATP level in the pH 6.5 group (**Figure 2D** $p < 0.001$ vs. pH 6.5 CM).

To verify that neurons release mitochondria under oxidative stress, we assessed the extracellular ATP level in the neuronal CM after H_2O_2 treatment. Treatment with H_2O_2 at 25 μM dramatically elevated the level of ATP in neuronal CM when compared with control (**Figures 3A,B**, $p < 0.05$ vs. control); and H_2O_2 at 50 μM further increased the release of ATP (**Figure 3B**, $p < 0.001$ vs. control, $p < 0.05$ vs. 25 μM H_2O_2). The effect of glutamate and NMDA excitotoxicity in ATP release was also examined. As shown, exposure of neurons to the NMDA (50 μM) or glutamate (100 μM) resulted in a significant increase of extracellular ATP (**Figure 3C**, for NMDA, $p < 0.001$ vs. control; and **Figure 3D**, for glutamate, $p < 0.05$ vs. control).

Neurons Release Impaired Mitochondria Under Acidosis Stress

To analyze whether acidosis compromises mitochondrial respiratory function in neurons, cellular OCR was measured using Seahorse Metabolic Kit. We found that pH 6.5 treatment decreased the basal respiration at 24 h after reperfusion (**Figures 4A,B**, $p < 0.05$ vs. pH 7.4 group). Then, the mitochondrial respiratory capacity was measured by adding FCCP, which dissipates the $\Delta\psi m$ and pushes mitochondria toward their maximal respiration rate. The data showed no difference in the "leak" OCR between the two groups (**Figure 4B**, $p = 0.9393$). Although the "maximal" OCR respiration and ATP production showed a declining trend after exposing the neurons to pH 6.5 solution, no significant difference was observed when compared to the pH 7.4 group (**Figure 4B**, for maximal respiration, $p = 0.7754$, and for ATP production, $p = 0.1458$).

To determine the status of the extracellular mitochondria, we monitored $\Delta\psi m$ using cationic JC-1 dye. In healthy cells with a normal $\Delta\psi m$, JC-1 is present in the negatively charged interior of mitochondrion to form red fluorescent J-aggregates. In unhealthy or apoptotic cells, due to the decreased $\Delta\psi m$, JC-1 remains monomeric and exhibits green fluorescence. Quantitative analysis showed that after treatment with pH 6.5, both JC-1 red and JC-1 green-labeled mitochondria increased in the CM (**Figure 4C**, for JC-1 red, $p < 0.05$ vs. pH 7.4; **Figure 4D**, for JC-1 green, $p < 0.01$ vs. pH 7.4), supporting that acidosis induced mitochondria release. In addition, the ratio of red to green decreased significantly when compared with the pH 7.4 group (**Figure 4E**, $p < 0.05$).

Astrocytes Take Up the Neuron-Released Mitochondria

To determine whether the neuron-released mitochondria are involved in neuron-glia cross-talk after acidosis, the neurons were labeled by MitoTracker Red CMXRos and the astrocytes were labeled with GFAP (green). The neuronal CM from pH 7.4 or 6.5 and mdCM from the pH 6.5 group were collected and cultured with astrocytes for 24 h (**Figure 5A**). There were few MitoTracker Red CMXRos detected within the astrocytes after co-culture with CM from pH 7.4-treated neurons. However, the presence of MitoTracker Red CMXRos were observed in the astrocytes co-culture with CM from pH 6.5-treated neurons, and removing the mitochondria with a 0.2 μm filter from the neuronal CM reduced the MitoTracker Red CMXRos in the astrocytes (**Figure 5B**).

The Enveloped Neuronal Mitochondria Promotes Mitochondrial Biogenesis in Astrocyte

To explore the mitochondrial biogenesis in astrocytes after engulfing the neuronal mitochondria, the mRNA expressions of Miro1, and TFAM in the astrocytes were determined. The level of Miro1 mRNA and TFAM mRNA increased significantly in the astrocytes cultured with CM from pH 6.5-treated neurons when compared to CM from the pH 7.4 group (**Figures 6A,B**, $p < 0.05$, $p < 0.001$ vs. pH 7.4 CM). However, the mRNA expressions of Miro1 and TFAM decreased significantly in the mitochondria depleted (md) pH 6.5-treated group (**Figures 6A,B**, $p < 0.001$ vs. pH 6.5 CM).

The Damaged Mitochondria Increased in Cerebrospinal Fluid After Middle Cerebral Artery Occlusion in Mice

To investigate whether neurons release mitochondria after ischemic stroke *in vivo*, the MCAO model was established in mice. After being labeled with MitoTracker Green, the content of mitochondria in CSF was detected by flow cytometry. The data showed that when compared with animals in the Sham group, MCAO induced a great increase of mitochondria (MitoTracker Green) in the CSF at 24-h post-reperfusion (**Figure 7A**, $p < 0.05$ vs. Sham group), suggesting that ischemic stroke-induced massive death of brain cells leading to the release of mitochondria in extracellular space and CSF.

To determine the status of the released mitochondria in CSF, JC-1 dye was used to monitor $\Delta\psi m$. MCAO did not increase the JC-1 red mitochondria in CSF when compared with the Sham group (**Figure 7B**, $p = 0.1320$ vs. Sham group). However, the JC-1 green mitochondria increased significantly after MCAO (**Figure 7C**, $p < 0.05$ vs. Sham group), indicating that ischemic stroke increased the mitochondria release. Furthermore, the ratio of red to green decreased significantly when compared with the Sham group (**Figure 7D**, $p < 0.05$ vs. Sham group), suggesting that the damaged mitochondria were more easily to be released after MCAO.

DISCUSSION

In this study, we investigated the neuronal mitochondria release under hypoxia/ischemia insult and the mitochondria-mediated cross-talk between neurons and astrocytes. We found that compared to CHO cells, neurons under physiological condition seldom release mitochondria. Neurons were, however, prone to release the defective mitochondria when challenged with acidosis,

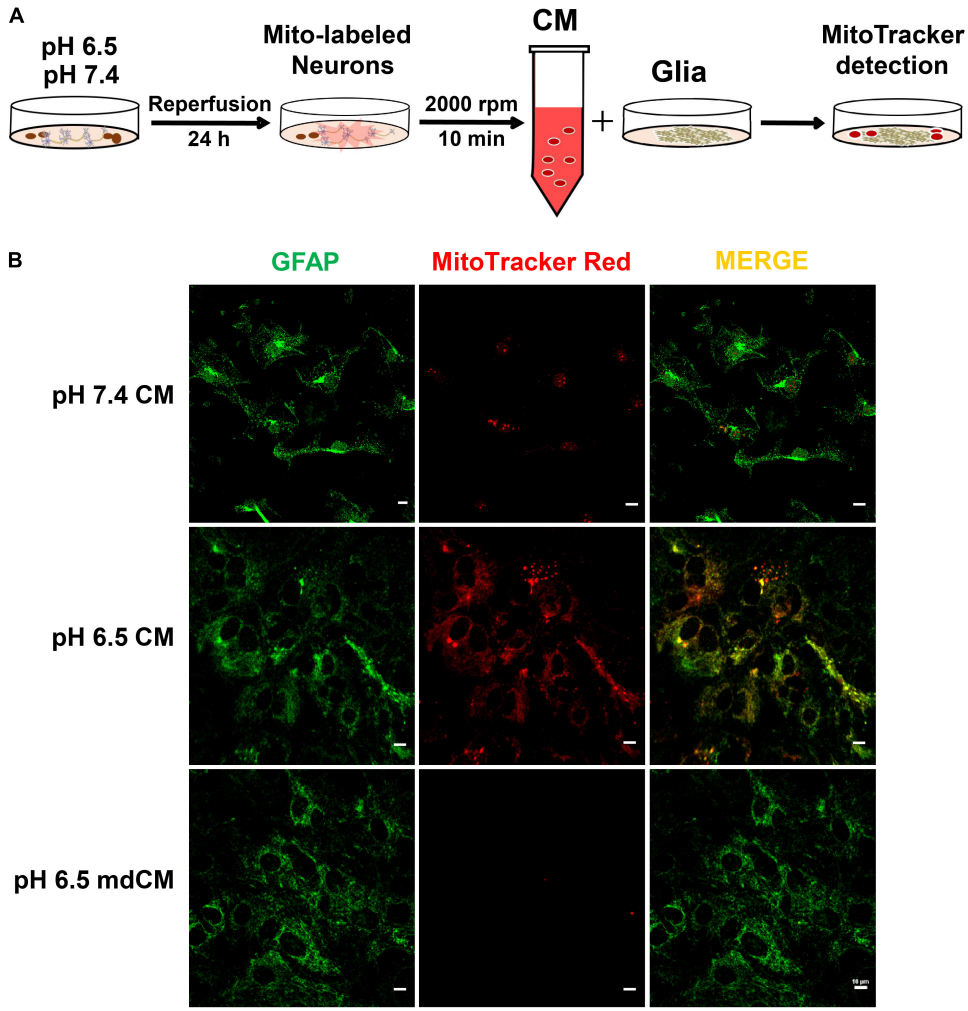

FIGURE 5 | The mitochondria released from neurons were taken up by astrocytes. **(A)** Experimental schematic to detect the cross-talk between neurons and astrocytes after treatment with pH 7.4 and 6.5 solutions. The neurons were labeled by MitoTracker Red CMXRos, and the astrocytes were labeled with GFAP. **(B)** The mitochondria with MitoTracker Red CMXRos were rarely detected within the astrocytes after co-culture with CM from pH 7.4-treated neurons. However, the co-localization of MitoTracker Red CMXRos with GFAP was increased when co-culture with CM from pH 6.5-treated neurons, and the increase was abolished by removing the mitochondria with a 0.2 μm filter.

H_2O_2-induced oxidative stress, or glutamate- and NMDA-induced excitotoxicity. In MCAO mice, increased mitochondria were observed in the CSF. In addition, we found that the damaged mitochondria can be engulfed by the astrocytes and induced the increase of Miro1 and TFAM at the mRNA level, suggesting the activation of mitochondrial biogenesis in the astrocytes. We concluded that when confronting with metabolic stresses, neurons might release the defective mitochondria to act as a "help-me" signaling and recruit the adjacent astrocytes for energy support by promoting astrocytic mitochondrial biogenesis (**Figure 8**). Our findings suggested that facilitating the defective mitochondrial releasing and astrocytic mitochondrial engulfing might be a potential therapeutic strategy for the neuroprotection in ischemic stroke.

Due to the high energetic demand, neurons are particularly susceptible to hypoxic and ischemic insult. Following ischemic stroke, the depletion of oxygen and glucose compromises the mitochondrial metabolism and depolarized mitochondrial membranes, leading to excessive calcium accumulation, overproduction of ROS, and activation of programmed cell death (Liu et al., 2018; Chen et al., 2020). Clearance of the dysfunctional mitochondria is critical for maintaining the viability of neurons and, subsequently, for neurological function recovery after ischemic stroke. Recently, accumulating evidence has demonstrated that intercellular mitochondrial transfer occurs in physiological condition and diseases (Davis et al., 2014; Liu et al., 2014; Hayakawa et al., 2016; Jiao et al., 2021). The extracellular mitochondria can be taken up by adjacent cells, which leads to the reprogramming of the cell metabolism and to relaying the signals for cell survival. Therefore, mitochondria itself may act as transducers undertaking metabolic cross-talk between injured cells and healthy cells. In this study, we found that CHO cells released mitochondria into the extracellular space. Compared with CHO cells, neurons under physiological

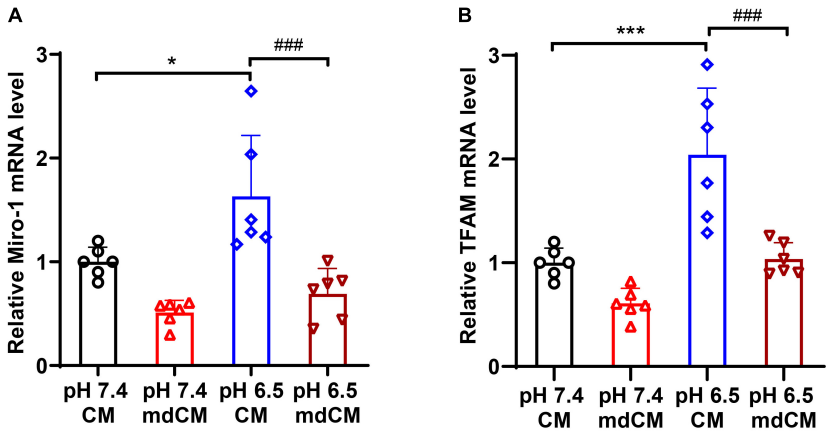

FIGURE 6 | The mRNA expressions of Miro1 and TFAM in astrocytes co-cultured with CM and mdCM from pH 7.4- and 6.5-treated neurons. The mRNA level of Miro1 **(A)** and TFAM **(B)** increased significantly in the CM from pH 6.5-treated group but no significant difference in the mdCM group. $n = 6$. $^{*}p < 0.05$, $^{***}p < 0.001$ vs. pH7.4 CM; $^{\#\#\#}p < 0.001$ vs. pH 6.5 mdCM. CM, culture medium; mdCM, mitochondria-depleted CM; Miro-1, mitochondrial Rho GTPase 1; TFAM, mitochondrial transcription factor A.

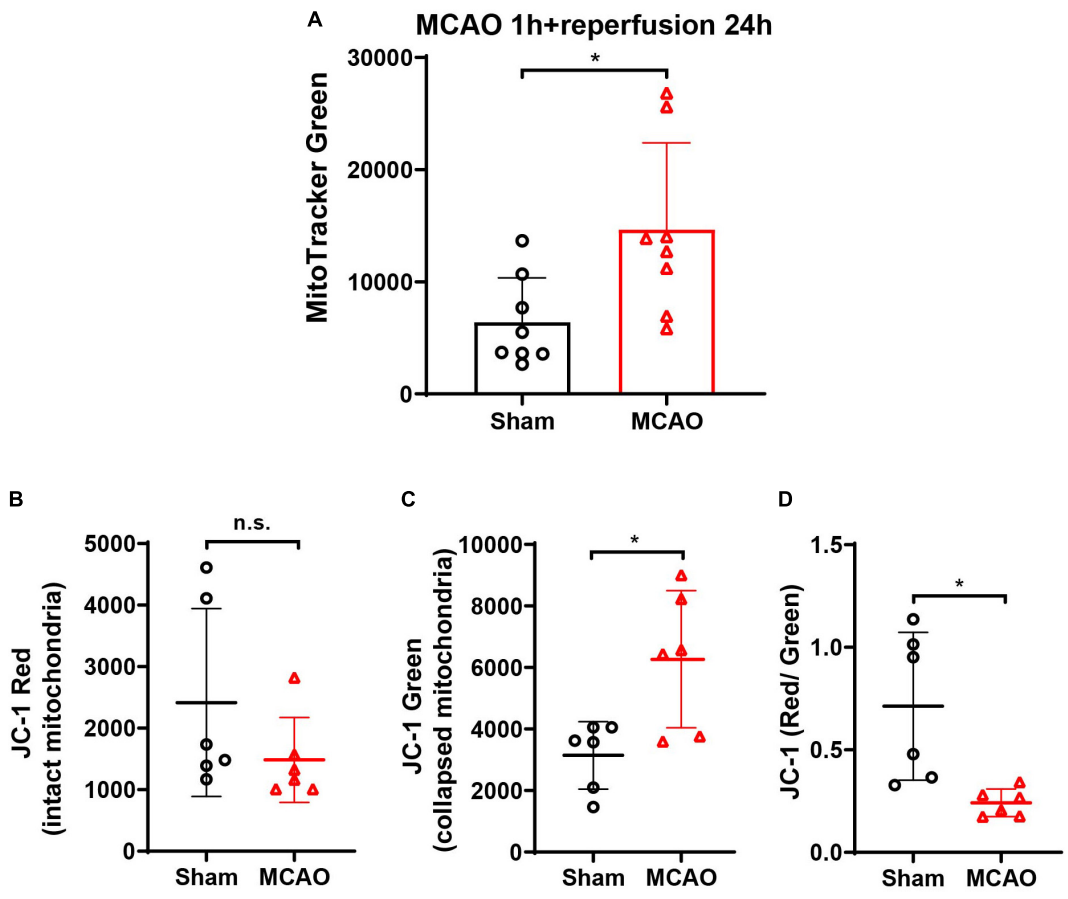

FIGURE 7 | The detection of mitochondria and $\Delta\psi m$ (JC-1 red/green ratio) in the CSF of MCAO mice. **(A)** After cerebral ischemia, the MitoTracker Green-labeled mitochondria elevated significantly in CSF at 24-h post-reperfusion. $n = 8$. $^{*}p < 0.05$ vs. Sham. **(B)** The JC-1 staining in CSF showed no significant difference of JC-1 red between the Sham and MCAO groups. **(C)** JC-1 green increased significantly in the CSF after MCAO when compared with the Sham group. **(D)** JC-1 red/green ratio decreased significantly in the CSF after MCAO. $n = 6$. $^{*}p < 0.05$ vs. Sham. CSF, cerebrospinal fluid; MCAO, middle cerebral artery occlusion; n.s., not significant.

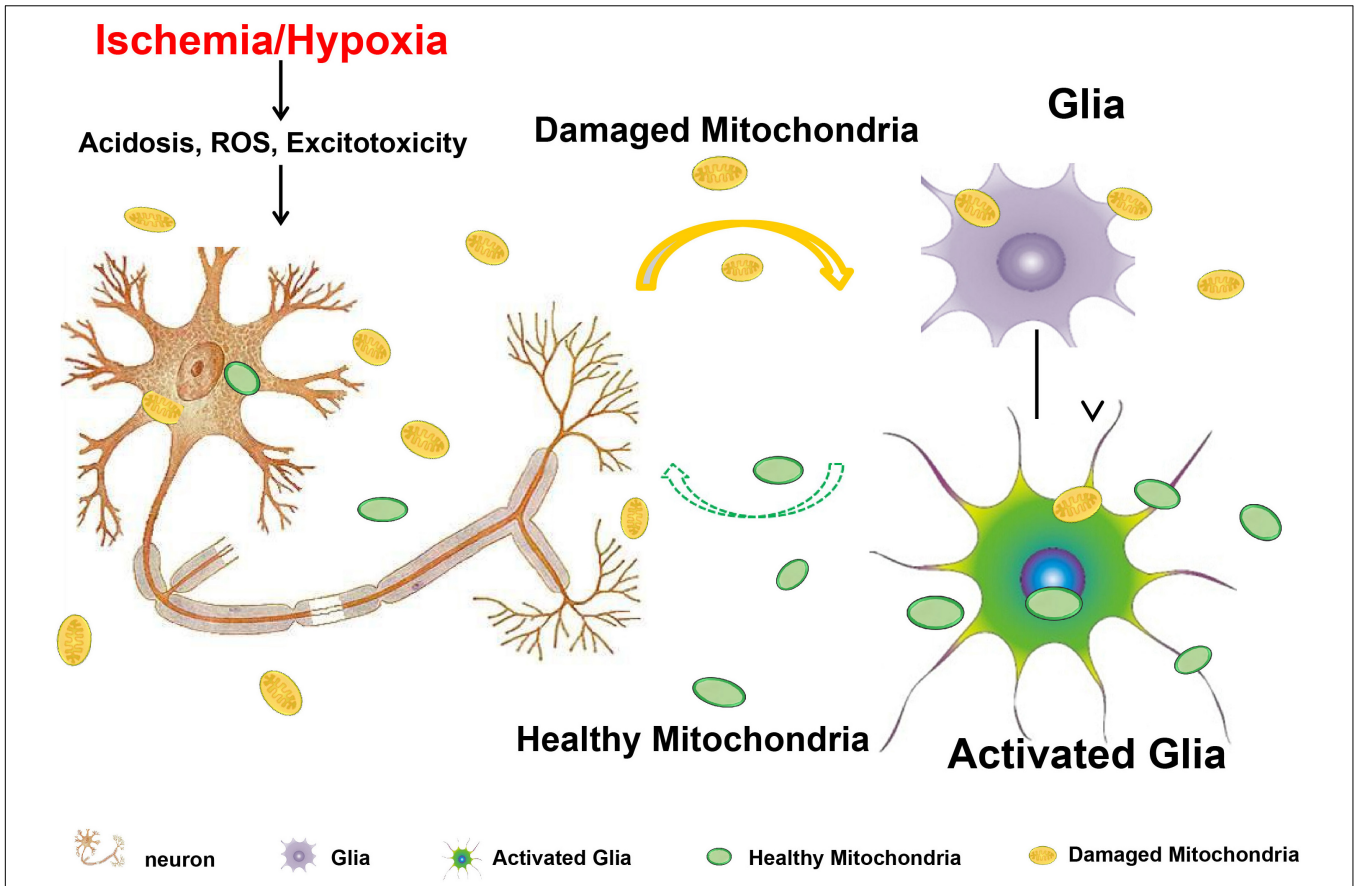

FIGURE 8 | Acidosis, oxidative stress, and excitotoxicity are closely associated with mitochondrial dysfunction and are the major culprits that contribute to the ischemic neuronal death after stroke. When neurons are confronting with these harmful challenges, they might release the defective mitochondria to act as a "help-me" signaling, and recruit the adjacent astrocytes for energy support by promoting astrocytic mitochondrial biogenesis. Solid arrow indicates the confirmed results from this study, and dashed arrow indicates the assumption from previously published studies.

condition release fewer mitochondria, probably because neurons are high energy consuming and depend more on mitochondria for energy production. When the neurons were exposed to acidosis, H_2O_2, glutamate, or NMDA excitotoxicity, the neuronal mitochondria decreased the level of basal respiration and lowered the membrane potential. Neurons dispose these defective mitochondria by releasing them into the CM. It is known that healthy mitochondria are crucial for cell viability. In contrast to the events referred to those characterised for damaged mitochondria such as cytochrome *c* release and caspase activators, changes in electron transport, and/or loss of mitochondrial transmembrane potential result in activation of programmed cell death pathways. We suggested, therefore, that under toxic stresses, neurons may be prone to expel the damaged mitochondria to sustain cell viability. This observation is in line with the recent study that under mitochondrial stress, mitochondria with low $\Delta\psi m$ were shed off from the cell body by migrasomes (Jiao et al., 2021).

It has been demonstrated that mitochondria are critical players in intercellular communications. Cells secrete mitochondrial proteins and mtDNA into their environment and interact with adjacent cells to participate in metabolic regulation or immune system stimulation (Todkar et al., 2021). Mitochondrial DNA, *N*-formyl peptides, and membrane component cardiolipin are important damage-associated molecular patterns and induce innate immune responses (West et al., 2011; Riley and Tait, 2020). Therefore, discarding the damaged mitochondria extracellularly is not a desirable solution. Interestingly, Davis et al. (2014) reported that retinal neurons could release damaged mitochondria and transfer them to astrocytes for disposal and recycling in the optic nerve head. Mahrouf-Yorgov et al. (2017) demonstrated that mitochondria from injured endothelial cells can be engulfed and degraded by MSCs, which lead to the activation of cytoprotective enzyme, i.e., heme oxygenase-1 and promotion of mitochondrial biogenesis. These two studies suggested that the damaged mitochondria released from dying cells not only serve as a disposal but also as a key rescue signal that recruiting the adjacent cells as well as recycling the mitochondria for quickly counteracting the energy deficits. Mitochondrial transfer has also been demonstrated between neurons and astrocytes to promote neuroprotection and neural recovery following ischemic stroke. Under the ischemic condition, astrocytes transferred functional mitochondria into the neighboring neurons and provided endogenous neuroprotective effects *in vivo* and *in vitro* (Hayakawa et al., 2016). Inhibition of astrocytic

mitochondrial function suppressed their ability to protect neurons against excitotoxicity and make neurons vulnerable to ischemia (Voloboueva et al., 2007). Here, we presented that after being subjected to harmful stimulus, neurons released the defective mitochondria into extracellular space. The released mitochondria could be taken up by adjacent astrocytes that would explain the increased expressions of Miro1 and TFAM at mRNA level in astrocytes, which was observed in our publication. Therefore, we hypothesized that the neuron-released mitochondria serve as a "help-me" signaling and mediate the neuron-astrocyte cross-talk following ischemic stroke (**Figure 8**).

We observed that mitochondria with low membrane potential were upregulated in CSF of the mice subjected to focal cerebral ischemia, which was in accordance with previous publications (Hayakawa et al., 2016). The extracellular mitochondria were also detected in CSF with decreased $\Delta\psi$ms in subarachnoid hemorrhage (SAH) rats (Chou et al., 2017). In the clinical studies, extracellular mitochondria were also found in the CSF from patients with SAH, and the higher $\Delta\psi$m was correlated with good clinical recovery (Chou et al., 2017). Extracellular mitochondria in CSF may be a potential biomarker for the diagnosis and prognosis of acute stroke.

CONCLUSION

We presented that when subjected to harmful stimulus, neurons release the defective mitochondria into extracellular space. The released mitochondria could be taken up by adjacent astrocytes to activate the mitochondrial biogenesis. Our findings suggested that neurons may release the defective mitochondria as a "help-me" signaling to mediate the neuron-astrocyte cross-talk following ischemic stroke. Boosting the recycling of endogenous mitochondria between neurons and astrocytes might be a potential therapeutic strategy to counteract the energy deficiency in acute ischemic stroke.

DATA AVAILABILITY STATEMENT

The original contributions presented in the study are included in the article/**Supplementary Material**, further inquiries can be directed to the corresponding authors.

ETHICS STATEMENT

The animal study was reviewed and approved by the Animal Care and Use Committee of Shanghai Jiao Tong University School of Medicine, Shanghai, China.

AUTHOR CONTRIBUTIONS

LG, FL, T-LX, and QH conceived, designed, and coordinated this study. LG, FL, and P-PH performed the experiments and analyzed the data. Z-PX and FW helped with cell culture and performed the RT-qPCR. LG, AM, T-LX, and QH wrote, revised, and checked the data analysis. All the authors revised and approved the final version of the manuscript.

FUNDING

This work was supported by grants from the National Natural Science Foundation of China (82071283 and 81801298) and the NSFC Promotion Program of Renji Hospital affiliated to Shanghai Jiao Tong University School of Medicine (RJTJ22-MS-011).

SUPPLEMENTARY MATERIAL

The Supplementary Material for this article can be found online at: https://www.frontiersin.org/articles/10.3389/fnagi.2022.785761/full#supplementary-material

REFERENCES

Chen, W., Huang, J., Hu, Y., Khoshnam, S. E., and Sarkaki, A. (2020). Mitochondrial transfer as a therapeutic strategy against ischemic stroke. *Transl. Stroke Res.* 11, 1214–1228. doi: 10.1007/s12975-020-00828-7

Chou, S. H. Y., Lan, J., Esposito, E., Ning, M., Balaj, L., Ji, X., et al. (2017). Extracellular mitochondria in cerebrospinal fluid and neurological recovery after subarachnoid hemorrhage. *Stroke* 48, 2231–2237. doi: 10.1161/STROKEAHA.117.017758

Davis, C.-H. O., Kim, K.-Y., Bushong, E. A., Mills, E. A., Boassa, D., Shih, T., et al. (2014). Transcellular degradation of axonal mitochondria. *Proc. Natl. Acad. Sci. U. S. A.* 111, 9633–9638. doi: 10.1073/pnas.1404651111

English, K., Shepherd, A., Uzor, N.-E., Trinh, R., Kavelaars, A., and Heijnen, C. J. (2020). Astrocytes rescue neuronal health after cisplatin treatment through mitochondrial transfer. *Acta Neuropathol. Commun.* 8:36. doi: 10.1186/s40478-020-00897-7

Gao, L., Song, Z., Mi, J., Hou, P., Xie, C., Shi, J., et al. (2020). The effects and underlying mechanisms of cell therapy on blood-brain barrier integrity after ischemic stroke. *Curr. Neuropharmacol.* 18, 1213–1226. doi: 10.2174/1570159X18666200914162013

Han, H., Hu, J., Yan, Q., Zhu, J., Zhu, Z., Chen, Y., et al. (2016). Bone marrow-derived mesenchymal stem cells rescue injured H9c2 cells via transferring intact mitochondria through tunneling nanotubes in an in vitro simulated ischemia/reperfusion model. *Mol. Med. Rep.* 13, 1517–1524. doi: 10.3892/mmr.2015.4726

Hayakawa, K., Esposito, E., Wang, X., Terasaki, Y., Liu, Y., Xing, C., et al. (2016). Transfer of mitochondria from astrocytes to neurons after stroke. *Nature* 535, 551–555. doi: 10.1038/nature18928

Huang, J., and Jiang, Q. (2019). Dexmedetomidine protects against neurological dysfunction in a mouse intracerebral hemorrhage model by inhibiting mitochondrial dysfunction-derived oxidative stress. *J. Stroke Cerebrovasc. Dis.* 28, 1281–1289. doi: 10.1016/j.jstrokecerebrovasdis.2019.01.016

Huang, P.-J., Kuo, C.-C., Lee, H.-C., Shen, C.-I., Cheng, F.-C., Wu, S.-F., et al. (2016). Transferring xenogenic mitochondria provides neural protection against ischemic stress in ischemic rat brains. *Cell Transpl.* 25, 913–927. doi: 10.3727/096368915X689785

Islam, M. N., Das, S. R., Emin, M. T., Wei, M., Sun, L., Westphalen, K., et al. (2012). Mitochondrial transfer from bone-marrow-derived stromal cells to pulmonary alveoli protects against acute lung injury. *Nat. Med.* 18, 759–765. doi: 10.1038/nm.2736

Jiao, H., Jiang, D., Hu, X., Du, W., Ji, L., Yang, Y., et al. (2021). Mitocytosis, a migrasome-mediated mitochondrial quality-control process. *Cell* 184, 2896–2910.e13. doi: 10.1016/j.cell.2021.04.027

Liu, F., Lu, J., Manaenko, A., Tang, J., and Hu, Q. (2018). Mitochondria in ischemic stroke: new insight and implications. *Aging Dis.* 9, 924–937. doi: 10.14336/ad.2017.1126

Liu, K., Guo, L., Zhou, Z., Pan, M., and Yan, C. (2019). Mesenchymal stem cells transfer mitochondria into cerebral microvasculature and promote recovery from ischemic stroke. *Microvasc. Res.* 123, 74–80. doi: 10.1016/j.mvr.2019.01.001

Liu, K., Ji, K., Guo, L., Wu, W., Lu, H., Shan, P., et al. (2014). Mesenchymal stem cells rescue injured endothelial cells in an in vitro ischemia-reperfusion model via tunneling nanotube like structure-mediated mitochondrial transfer. *Microvasc. Res.* 92, 10–18. doi: 10.1016/j.mvr.2014.01.008

Luo, Q., Xian, P., Wang, T., Wu, S., Sun, T., Wang, W., et al. (2021). Antioxidant activity of mesenchymal stem cell-derived extracellular vesicles restores hippocampal neurons following seizure damage. *Theranostics* 11, 5986–6005. doi: 10.7150/thno.58632

Maeda, H., Kami, D., Maeda, R., Murata, Y., Jo, J.-I., Kitani, T., et al. (2020). TAT-dextran-mediated mitochondrial transfer enhances recovery from models of reperfusion injury in cultured cardiomyocytes. *J. Cell. Mol. Med.* 24, 5007–5020. doi: 10.1111/jcmm.15120

Mahrouf-Yorgov, M., Augeul, L., Da Silva, C. C., Jourdan, M., Rigolet, M., Manin, S., et al. (2017). Mesenchymal stem cells sense mitochondria released from damaged cells as danger signals to activate their rescue properties. *Cell Death Differ.* 24, 1224–1238. doi: 10.1038/cdd.2017.51

Plotnikov, E. Y., Khryapenkova, T. G., Vasileva, A. K., Marey, M. V., Galkina, S. I., Isaev, N. K., et al. (2008). Cell-to-cell cross-talk between mesenchymal stem cells and cardiomyocytes in co-culture. *J. Cell. Mol. Med.* 12, 1622–1631. doi: 10.1111/j.1582-4934.2007.00205.x

Powers, W. J., Rabinstein, A. A., Ackerson, T., Adeoye, O. M., Bambakidis, N. C., Becker, K., et al. (2019). Guidelines for the early management of patients with acute ischemic stroke: 2019 update to the 2018 guidelines for the early management of acute ischemic stroke: a guideline for healthcare professionals from the American Heart Association/American Stroke Association. *Stroke* 50, e344–e418. doi: 10.1161/str.0000000000000211

Riley, J. S., and Tait, S. W. (2020). Mitochondrial DNA in inflammation and immunity. *EMBO Rep.* 21:e49799. doi: 10.15252/embr.201949799

Sabogal-Guáqueta, A. M., Hobbie, F., Keerthi, A., Oun, A., Kortholt, A., Boddeke, E., et al. (2019). Linalool attenuates oxidative stress and mitochondrial dysfunction mediated by glutamate and NMDA toxicity. *Biomed. Pharmacother.* 118:109295. doi: 10.1016/j.biopha.2019.109295

Savic Azoulay, I., Liu, F., Hu, Q., Rozenfeld, M., Ben Kasus Nissim, T., Zhu, M. X., et al. (2020). ASIC1a channels regulate mitochondrial ion signaling and energy homeostasis in neurons. *J. Neurochem.* 153, 203–215. doi: 10.1111/jnc.14971

Todkar, K., Chikhi, L., Desjardins, V., El-Mortada, F., Pépin, G., and Germain, M. (2021). Selective packaging of mitochondrial proteins into extracellular vesicles prevents the release of mitochondrial DAMPs. *Nat. Commun.* 12:1971. doi: 10.1038/s41467-021-21984-w

Volobouеva, L. A., Suh, S. W., Swanson, R. A., and Giffard, R. G. (2007). Inhibition of mitochondrial function in astrocytes: implications for neuroprotection. *J. Neurochem.* 102, 1383–1394. doi: 10.1111/j.1471-4159.2007.04634.x

Wang, J.-J., Liu, F., Yang, F., Wang, Y.-Z., Qi, X., Li, Y., et al. (2020). Disruption of auto-inhibition underlies conformational signaling of ASIC1a to induce neuronal necroptosis. *Nat. Commun.* 11:475. doi: 10.1038/s41467-019-13873-0

Wang, Y.-Z., Wang, J.-J., Huang, Y., Liu, F., Zeng, W.-Z., Li, Y., et al. (2015). Tissue acidosis induces neuronal necroptosis via ASIC1a channel independent of its ionic conduction. *Elife* 4:e05682. doi: 10.7554/eLife.05682

West, A. P., Shadel, G. S., and Ghosh, S. (2011). Mitochondria in innate immune responses. *Nat. Rev. Immunol.* 11, 389–402. doi: 10.1038/nri2975

Wu, B., Yu, L., Hu, P., Lu, Y., Li, J., Wei, Y., et al. (2018). GRP78 protects CHO cells from ribosylation. *Biochim. Biophys. Acta Mol. Cell Res.* 1865, 629–637. doi: 10.1016/j.bbamcr.2018.02.001

Zuo, X., Lu, J., Manaenko, A., Qi, X., Tang, J., Mei, Q., et al. (2019). MicroRNA-132 attenuates cerebral injury by protecting blood-brain-barrier in MCAO mice. *Exp. Neurol.* 316, 12–19. doi: 10.1016/j.expneurol.2019.03.017

Conflict of Interest: The authors declare that the research was conducted in the absence of any commercial or financial relationships that could be construed as a potential conflict of interest.

Publisher's Note: All claims expressed in this article are solely those of the authors and do not necessarily represent those of their affiliated organizations, or those of the publisher, the editors and the reviewers. Any product that may be evaluated in this article, or claim that may be made by its manufacturer, is not guaranteed or endorsed by the publisher.

Advantages of publishing in Frontiers

OPEN ACCESS
Articles are free to read for greatest visibility and readership

FAST PUBLICATION
Around 90 days from submission to decision

HIGH QUALITY PEER-REVIEW
Rigorous, collaborative, and constructive peer-review

TRANSPARENT PEER-REVIEW
Editors and reviewers acknowledged by name on published articles

Frontiers
Avenue du Tribunal-Fédéral 34
1005 Lausanne | Switzerland

Visit us: www.frontiersin.org
Contact us: frontiersin.org/about/contact

REPRODUCIBILITY OF RESEARCH
Support open data and methods to enhance research reproducibility

DIGITAL PUBLISHING
Articles designed for optimal readership across devices

FOLLOW US
@frontiersin

IMPACT METRICS
Advanced article metrics track visibility across digital media

EXTENSIVE PROMOTION
Marketing and promotion of impactful research

LOOP RESEARCH NETWORK
Our network increases your article's readership